PHOTOSYNTHESIS, CALCIFICATION, AND PHOTOADAPTATION, IN REEF-BUILDING CRUSTOSE CORALLINE ALGAE ON THE GREAT BARRIER REEF

Thesis submitted
by John R.M. Chisholm, BSc Hons (St. Andrews)
in
March 1988

for the degree of Doctor of Philosophy in
the Botany Department, School of Biological Sciences
at James Cook University of North Queensland

DECLARATION

The studies presented in this dissertation were completed by the author while a post-graduate student in the Department of Botany, School of Biological Sciences, James Cook University, Townsville, Queensland, Australia. I certify that the work presented in this thesis has been carried out by myself, except where otherwise stated. I declare the results are original and have not previously been submitted for any other degree.

March 1988

....

STATEMENT OF ACCESS

I, the undersigned, the author of this thesis, understand that the following restriction placed by me on access to this thesis will not extend beyond three years from the date on which the thesis is submitted to the University.

> I wish to restrict access to this thesis for a period of three years to the individuals named in the Acknowledgements, and to people who seek and obtain my written approval.

After this period has elapsed I understand that the James Cook University of North Queensland will make it available for use within the University Library and, by microfilm or other photographic means, allow access to users in other approved libraries. All users consulting this thesis will have to sign the following statement:

> "In consulting this thesis I agree not to copy or closely paraphrase it in whole or in part without the written consent of the author; and to make proper written acknowledgement for any assistance which I have obtained from it."

March 1988

....

ABSTRACT

In situ rates of photosynthesis and calcification were determined for four species of reef-building crustose coralline algae on the windward crest and slope of a coral reef at Lizard Island, in the northern region of the Great Barrier Reef (GBR). The species studied were *Porolithon onkodes* (Heydrich) Foslie, *Neogoniolithon fosliei* (Heydrich) Setchell & Mason, *Hydrolithon reinboldii* (Weber-van Bosse & Foslie) Foslie, and *Paragoniolithon conicum* (Dawson) Adey, Townsend & Boykins. Rates were measured with an underwater respirometer incorporating oxygen, pH, light and temperature probes located within an ultra-violet transparent incubation chamber. Measurements of photosynthesis were also made in the laboratory using a 'Clark' type oxygen electrode and a specially constructed acrylic cell. The photosynthetic quotients (*PQ*) of the four species were determined from *in situ* measurements of oxygen, pH, and total alkalinity, with corrections for changes in seawater temperature over the period of incubation. Light-saturation curves for photosynthesis (*P-I* curves) and calcification (*C-I* curves) were constructed from each set of *in situ* and laboratory measurements using non-linear, least squares regression analysis. The curves were examined for evidence of photoadaptation and for estimation of the rates of maximal gross photosynthesis, absolute dark respiration, maximal light-enhanced calcification, and dark calcification.

Individuals from selected habitats at depths of between 0 and 18 m were studied both *in situ* and in the laboratory. The specimens received from 85 to 2% of surface irradiance as measured in units of photosynthetic photon flux density (PPFD) between 400 and 700 nm.

Light-saturation curves. *In situ* data were modelled by the hyperbolic tangent function. The less variable laboratory data revealed subtle differences in the shapes of the light-saturation curves of different species and were modelled by one of four related mathematical functions. The functions tested for accuracy of fit were the hyperbolic tangent, a simple exponential, a general exponential, and the right rectangular hyperbola. Specimens collected from 0 m exhibited slow rates of transition from light-limited to light-saturated photosynthesis. Many of these individuals were not entirely saturated at irradiance levels above those naturally occurring in the field. Rates of photosynthesis were generally lower in the laboratory than *in situ*. Specimens measured *in situ* at depths representing the lower limits of the species distributions

were found to exhibit light-response curves which did not indicate saturated levels of photosynthesis or calcification.

Photoadaptation. Adaptive changes were observed in the photokinetic parameters describing the shapes of the light-saturation curves of all species under both laboratory and *in situ* conditions as the quantity of irradiance diminished. Compensation points (I_c), 95% saturation levels ($I_{0.95}$), and intercepts between the initial slopes of the curves and the horizontal asymptotes (I_k) decreased. Rates of respiration (R), maximal gross photosynthesis (P^g_m), and light-enhanced calcification (C_{light}) based on real surface area also tended to fall. The initial slopes of the curves (α) for photosynthesis (based on projected or real surface area) and calcification (based on total protein content) increased with decreasing irradiance. The ratios of gross photosynthesis to respiration ($P^g_m/-R$) increased marginally with decreasing irradiance. The rates of dark calcification (C_{dark}) and light-enhanced calcification expressed on the basis of total protein content were variable and did not vary predictably with diminishing irradiance.

The natural logarithms (*ln*) of I_c, I_k, and $I_{0.95}$ were directly proportional to the natural logarithms of the percentages of surface irradiance (*ln* %SI) transmitted to the depths at which the algae were growing. Similar double logarithmic relationships were observed between P^g_m, R, C_{light} (based on real surface area) and *ln* %SI for some species. The natural logarithms of α for photosynthesis normalised on the basis of real surface area, and for calcification normalised on the basis of total protein content, were inversely proportional to *ln* %SI for all species. Similar double logarithmic relationships were observed between $P^g_m/-R$ and *ln* %SI for some species.

Primary production. Photosynthetic quotients (PQ) were determined for each species. Mean PQ values for *P. onkodes*, *N. fosliei*, and *H. reinboldii* ranged from 1.21 to 1.33. The mean PQ for *P. conicum* was 1.07. Mean rates of maximal net organic carbon production per hour ranged from 0.083 to 0.168 g C m^{-2} (real surface area) *in situ*, and from 0.068 to 0.148g C m^{-2} in the laboratory. Mean rates of net carbon production integrated over the course of a 24 hour day ranged from 0.180 to 1.352 g C m^{-2}(real surface area) *in situ*, and from 0.123 to 1.206 g C m^{-2} in the laboratory. Rates of gross primary production or consumption per day were directly proportional to peak noon irradiance. The rate of carbon production per day could thus be estimated for any amount of irradiance on a cloudless day.

Calcification. Using an adaptation of the alkalinity anomaly technique, the precipitation or solution of calcium carbonate was estimated by subtracting the calculated change in pH resulting from photosynthesis and respiration from the measured change in pH. Mean maximal rates of *in situ* calcification per hour ranged from 0.156 to 0.923 g $CaCO_3$ m^{-2} (real surface area). Mean rates of calcification integrated over a 24 hour day ranged from 0.87 to 9.86 g $CaCO_3$ m^{-2} (real surface area). Rates of calcification per day were directly proportional to peak noon irradiance for all species except *H. reinboldii*.

The rate of calcification per unit of surface area decreased with increasing depth and decreasing irradiance. Calcification rates were always considerably higher in the light than in the dark. Dark rates of calcification were highly variable. In several cases solution of $CaCO_3$ was observed in the dark.

Relationships between calcification and irradiance, and photosynthesis and irradiance, were similar but not identical. In shallow water, greater irradiance was required for the saturation of calcification than for saturation of photosynthesis. These data suggest that calcification is largely controlled by photosynthesis but is probably influenced by other factors, among them tissue biomass.

Conclusions. Crustose coralline algae are highly significant producers of organic and inorganic carbon on coral reefs. Their rates of photosynthesis may have been underestimated by the use of semi-artificial procedures. Their rates of calcification are comparable with corals and in certain reef zones their great abundance may result in overall calcification rates which exceed that of 98-99% of the rest of the reef. As expected crustose coralline algae photoadapt and their ability to do so influences but does not necessarily control their distributions on the reef.

ACKNOWLEDGEMENTS

I hope this thesis is a worthy tribute to the many people who have made it possible.

I am indebted to my supervisors Dr. Ian Price, Dr. Bruce Chalker, and Dr. David Barnes who provided inspiration, encouragement, logistical support, and the priceless wisdom of their own scientific labours. All contributed vastly to this project and willingly suffered the painful task of having to read and criticise a rapidly written draft of the manuscript. To Barry Goldman and Lois Wilson (ex Director and Secretary of the Lizard Island Research Station), Jean-Claude and Claudia Collingwood, Monty Devereux, and Eric Gill, I express my deepest gratitude. These people astounded me with their kindness and generosity, powers of innovation and technical expertise, and singular efforts to help me reach this goal. Geoffrey Smith and Roland Pitcher spent long periods with me at Lizard island providing friendship, scientific stimulus, and much needed assistance on several occasions both in the field and with computing. The people named above have made outstanding contributions to this research.

In addition, I thank Jamie Oliver, Professor Dilwyn Griffiths, Associate Professor Peter Brownell, Jim Luong-Van, Don Kinsey, Peter Doherty, Yuri Sorokin, Terry Done, David Bellwood, and many others too numerous to mention for useful discussions on various aspects of this research. Bill Woelkerling was a valuable correspondent in the early stages of the project, and Walter Adey confirmed the identities of the algal species studied. Nick Holland provided sound advice and histological preparations of material gathered during the study. My three supervisors, Monty Devereux, Jim Luong-Van, Dilwyn Griffiths, Walter Dunlap, Anita Murray, Savita Francis, and Warren Shipton loaned several important items of laboratory equipment, and in many instances taught me how to use them. Walter Dunlap and Mike Susic instructed me in the use of the HPLC. Monty Devereux, Anita Murray, Savita Francis, Jane Wu Won and Alan Nott saved the day on several occasions when rapid logistical or technical assistance was needed. Jean-Claude Collingwood, Eric Gill, Peter Pini (who taught me how to use a lathe at Lizard island), John Small, Ken Carr, Dave White, Don Ross, Zolly Florian, Mike Beecher, and the JCU Engineering Workshop staff were of invaluable assistance in the construction of experimental equipment. Among the last-named people, the first four gave many hours of their own

time, sometimes late into the night or even the early hours of the morning, assisting with the construction of the underwater respirometer described in the thesis. John Hardman kindly tested the underwater equipment for leaks in the A.I.M.S. recompression chamber before field deployment.

David Barnes, Barry Goldman, Alan Mitchell, Roland Pitcher, Eric Gill, Jamie Oliver, Bette Willis, Trevor Cox, Barry Durose, Geoffrey Smith, Malcolm McKenzie, Nick Harcock, Barry Tobin, Peter Isdale, Derek Burrage, Mark McCormack, Bridget Kerrigan, Brian King, Andrew Stevens, Rob Van Woesik, Luisha Kayrooz, Bob McDonald, Coral Graham, Ross Alford, and Professor Howard Choat provided assistance with computing, either with programming, running application software, or by making facilities available to me. Bruce Chalker and Dave Barnes helped with various mathematical problems.

Barry Goldman and Peter Pini's combined skills and abilities to find ways of doing things others would not have thought of, and Lois Wilson's great administrative and practical capabilities contributed greatly to the success of the work carried out at Lizard Island. Lois also provided field assistance towards the conclusion of the fieldwork. These people and Peter's wife Gwen showed me great kindness while staying at the Research Station.

Secretarial assistance in the School of Biological Sciences at JCU was provided by Di McNamara, Bev Gordy, Jan Nugent and Ann Sharp. Lyn Campbell-Ryder and Howard Choat were of great support in an administrative capacity during the writing up period, as was Dilwyn Griffiths throughout the project. Paul Aldridge and other members of the Research Division of the JCU Administration were helpful at all times on matters of funding. Pat Hutchings acted officially as liaison officer in the administration of my Lizard Island Doctoral Fellowship and unofficially as a source of advice on various subjects.

I am grateful to Michael Cuthill who performed the tedious task of reproducing and printing all of the photographic plates presented in the eight copies of the thesis and for supplying two of the photographs. Peter Isdale very generously met the costs. Richard Bogus produced the superbly drawn plan/section view of the *in situ* incubation chamber shown in Fig. 5A.

In the latter stages of the write up almost everybody I spoke to offered assistance. Some of these people made exceptional contributions. Alan Dartnall, Alan Mitchell, Marietta Thyssen, and Rosalie Buck helped with graphics. Lois Wilson assisted with the preparation of the bibliography and illustrative material, and sporadically took measures to prevent a case of malnutrition. Leanne Fernandes doggedly read through the manuscript and chased down vital information necessary for completion of the thesis. Inara Bush, Bronwyn Betts, Suzie Davies, and the staff of the JCU library were of great help uncovering relevant literature. Malcolm McKenzie gave me a crash course in converting a thesis originally written using Wordstar into a Mass 11 document. Frances Conn went to great lengths to show me how to overcome the problems associated with producing horrendously complicated tables in a proportionally spaced font. Sue Steel devoted an enormous amount of her time, after working all day and week, helping me convert the manuscript into Mass 11 and printing the document out. To these people I am extremely grateful.

I wish to thank the Australian Museum in Sydney for access to the Lizard Island Research Station (LIRS), and the donors of the LIRS Doctoral Fellowship who provided funds for much of the field reasearch. The Australian Institute of Marine Science was extraordinarily generous with its facilities and expertise and I am grateful to the many staff there who made my life pleasurable and productive. James Cook University similarly provided many facilities, assistance when requested, and significant funding throughout the project. Cadillac Plastics Pty. Ltd. kindly donated all the perspex used in the construction of the underwater respirometer and associated items. The research was additionally supported by funds from the Great Barrier Reef Marine Park Authority's Augmentative Award scheme, and from the Australian Coral Reef Society. The Australian Government was instrumental in permitting me the opportunity to carry out post-graduate study in Australia under the Commonwealth Scholarship and Fellowship Plan Award scheme.

Finally, on a personal note I wish to express my sincere thanks to Dr. Des Griffin, Director of the Australian Museum, who was largely responsible for negotiating a successful and unprecedented further extension to my CSFP award in Australia; and to Dr. John Bunt and Dr Joe Baker, the past and present Directors of the Australian Institute of Marine Science, for the opportunity to work at the Institute.

To my sisters and friends

TABLE OF CONTENTS

LIST OF FIGURES

LIST OF PLATES

LIST OF TABLES

LIST OF APPENDICES

CHAPTER 1

GENERAL INTRODUCTION

1. 1. INTRODUCTION

The non-articulate (crustose) coralline algae are a biologically and geologically important group of calcareous marine plants. This group of red algae within the family Corallinaceae (Corallinales, Rhodophyta) evolved during the Jurassic, probably from the Solenoporaceae and a family loosely known as the "ancestral corallines" which existed during the late Palaeozoic (Wray 1971). Since the Cretaceous period, when members of modern day genera began appearing in large numbers (Wray 1971), crustose coralline algae have played a critical role in the development of coral reefs. Coral reefs are massive geological structures which develop in warm tropical seas from the continuous deposition of calcium carbonate by hermatypic corals and calcareous algae. Although corals are often the most conspicuous organisms, crustose corallines are the vital cementing agents which bind together the various structural elements which constitute the framework of the reef (e.g., David *et al.* 1904; Finckh 1904; Howe 1912; Glock 1923; Setchell 1926, 1930; Dawson 1961; Goreau 1963; Marsh 1970; Wray 1971; Littler 1972, 1973a). The result is a rigid structure which resists erosion by the sea and supports a diverse array of calcareous and non-calcareous organisms. A coral reef is thus a complex ecosystem which depends upon coralline algae for the maintenance of a wave-resistant front (e.g., Tracey *et al.* 1948; Lee 1967; Maxwell 1968, 1969; Doty 1974; Adey 1975, 1978a,b; Adey & Burke 1976; Ginsburg & Schroeder 1975; Littler & Doty 1975), and also for the production of organic materials upon which numerous grazers feed (e.g., Doty & Morrison 1954; Van den Hoek 1969; Adey 1975; Adey & Vassar 1975; Van den Hoek *et al.* 1975; Bak 1976; Hunter 1977; Ogden & Lobel 1978; Hawkins & Lewis 1982).

The importance of crustose coralline algae on coral reefs has been recognised for over a century (Agassiz 1889). However, information on their rates of organic production is scanty, and data on their rates of inorganic production (i.e., calcification) is almost non-existent. Estimates of organic carbon production are available for a limited number of species. However, all of these estimates have arisen

from laboratory or 'simulated' *in situ* studies and most pertain to populations existing in shallow water (<3 m). There have been no estimates of the inorganic production rates of specific groups of dominant reef-building coralline algae. The only *in situ* data on their rates of calcification have come from metabolic studies of entire communities within which crustose corallines were the dominant components (Sargent & Austin 1949, 1954; Sournia 1976).

The lack of information on crustose coralline rates of production has made quantitative assessment of their biological role in coral reef environments impossible. Biologists have attempted to resolve the issue by measuring standing crop while geologists have concentrated upon sediment production (Littler 1972). What has been missing is a production rate parameter (Goreau 1963). Estimates of standing crop bear little relation to "the skeletal components which remain after such events as grazing, export, and resolution [solution] have occurred" (Littler 1972, p. 339), and geological estimates of upward reef growth do not correlate with the instantaneous rate of $CaCO_3$ deposition (Buddemeier *et al.* 1975). Long term rates of net accretion and quantitative measures of standing crop do not account for losses in the system and therefore provide poor estimates of overall reef productivity. The carbon budgets of coral reef systems cannot be properly assessed without detailed information on the rates of organic and inorganic carbon production by dominant groups of reef organisms.

Littler (1972) attributed the paucity of detailed information on crustose coralline physiology to a lack of suitable techniques with which to measure their metabolic processes. Over the last 15 years new techniques have been developed and improvements have been made to existing ones which facilitate more detailed analysis of physiological processes. With suitable manipulation and a degree of innovation many of these techniques can be adapted for the study of crustose coralline physiology. This thesis describes the application of modern methods and the development of new experimental equipment and procedures to the study of crustose coralline photosynthesis and calcification. It presents detailed analyses of the relationships between irradiance and photosynthesis, irradiance and calcification, and examines aspects of photoadaptation in four dominant species of reef-building crustose coralline algae on the Great Barrier Reef (GBR).

Further details of the objectives of this research and the reasons why they were considered important are provided in the introductory sections to Chapters 2 and 3.

The research was divided into two sections:

(1) Photosynthesis based on

(i) laboratory studies,

(ii) *in situ* studies, and

(2) Calcification based on *in situ* studies.

1. 2. SELECTION OF STUDY SITES

Lizard Island (Fig. 1) was chosen as the base for the fieldwork. The Lizard Island Research Station, a facility of the Australian Museum (Sydney), is an excellent, well-equipped field station which provides access to a variety of nearby reef environments. The island is situated approximately 20 nautical miles off the mainland coast of northeast Australia and 9 nautical miles landward of the ribbon reefs on the outer edge of the continental shelf (14°40'S:145°27'E). The island is largely surrounded by fringing reefs and is connected to two smaller, nearby islands by a well developed reef system which encloses a lagoon with a maximum depth of 10 m.

Study sites were selected along the windward (southeast) margin of the main Lizard Island Reef, between Bird Islet and South Island (see Fig. 1), where crustose coralline algae perform their vital role in creating a wave-resistant front. The reef at this location typically experiences strong tradewinds (18-30 knots) and heavy seas (to 3 m) between the months of April and September, and occasionally much more severe conditions during cyclonic activity in the period from December to March. Calmer weather generally prevails during October, November, and early December. Seawater temperature records for Lizard Island range from a minimum of 22.5°C to a maximum of 29°C (L. Goldman, Secretary of the Lizard Island Research Station - personal communication; and personal observations).

Transects were established at 3 sites which were considered representative of well-developed forereef habitats. The sites did not include anomalous features such as sand and rubble channels and were reasonably uniform with respect to horizontal

Fig. 1. Map of Lizard Island reef complex showing location of study sites (1, 2, 3) on the southeast-facing (i.e., windward) reef. Also reduced scale maps showing reef complex in relation to Lizard Island, and Lizard Island in relation to northeast Australia.

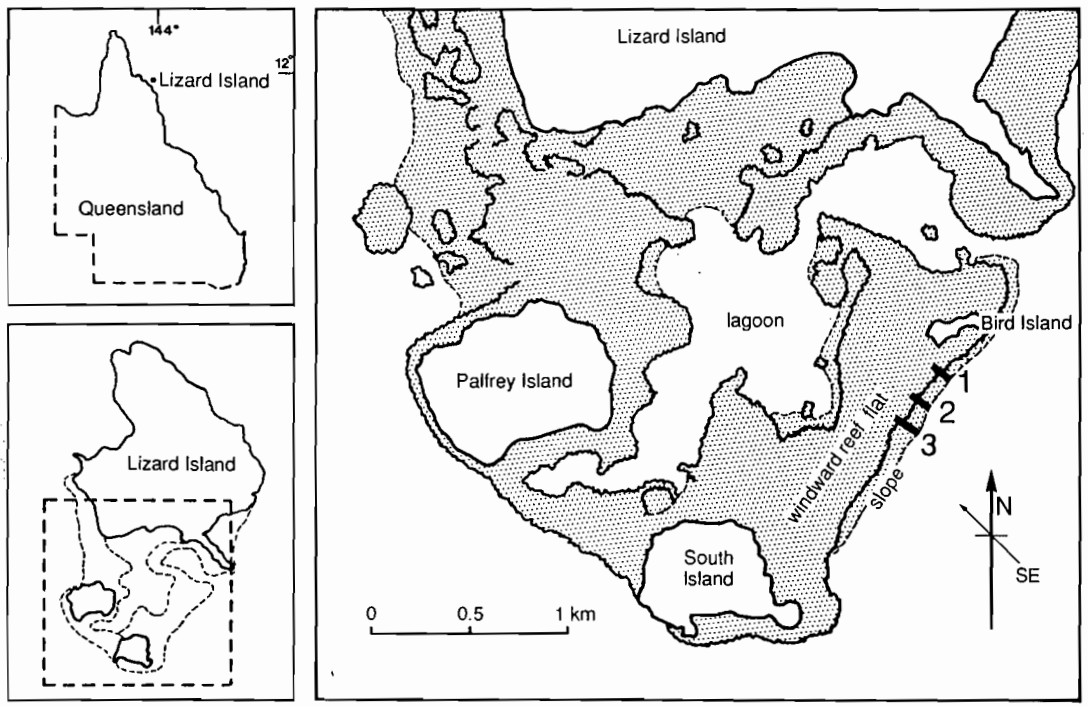
144°
12°
Lizard Island
Queensland
Lizard Island
Lizard Island
lagoon
Bird Island
Pallrey Island
1
2
3
windward reef flat
slope
South
Island
0
0.5
1 km
N
SE

and vertical reef profile. The transects ran in a south-easterly direction (that of the prevailing tradewinds) from the reef crest at 0 m to the foot of the consolidated windward reef slope at 18 m (Fig. 1). The three transects provided lines of reference for the sampling procedures. All depths were standardised against the Low Water Datum (LWD) of predictions at the nearest standard port of Cairns (Official Tide Tables, Coast of Queensland, Department of Harbours and Marine, Queensland 1984).

To facilitate underwater research on the windward reef slope, permanent moorings were constructed in the following manner. Large reinforced concrete blocks were cast with a projecting loop of 3/8″ stainless steel rod. Concrete was poured into well-moistened plastic-lined moulds dug in the sand at Lizard Island. Each of the blocks possessed a concave base to create suction and weighed approximately 200 kg. In each case 10 m of 3/8″ galvanised chain was fitted to the stainless steel loop and to this was added 25 m of 3/4″ nylon rope with two surface buoys spliced in tandem at the free end. The moorings were deployed in deep water (>20 m) near each of the transects to provide safe moorings for the small boat used in the field studies. The purpose of the two surface buoys in tandem was to facilitate the gathering of one tension-free buoy in particularly rough seas.

The Lizard Island Research Station provided the base for the *in situ* and laboratory studies of photosynthesis and calcification. Preliminary construction of some of the equipment used during the study and certain analytical procedures were carried out at the Australian Institute of Marine Science, near Townsville, Queensland, Australia. Other research was undertaken in the Department of Botany of the James Cook University of North Queensland, Townsville.

1. 3. SELECTION AND IDENTIFICATION OF SPECIES

Very few species of crustose coralline algae grow at all depths on the windward reef slope at Lizard Island. However, four of the dominant reef-building species on the GBR overlap in their individual depth distributions at Lizard Island. By comparing the physiological attributes of the species and by measuring changes occurring within each species with depth, bathymetric photoadaptation could be examined over the entire reef profile. A small number of species, such as *Paragoniolithon conicum*, do occur at all depths, but these species typically occupy

shaded niches in shallow water and relatively well illuminated surfaces in deep water. As Adey & MacIntyre (1973) have suggested, researchers examining the distributions of coralline algae with depth should give precedence to the quantity of submarine irradiance rather than to the depth of sampling. In this research, four species were selected which appeared optimally suited to different irradiance levels.

The species selected for study were *Porolithon onkodes* (Heydrich) Foslie 1909, *Neogoniolithon fosliei* (Heydrich) Setchell & Mason 1943, *Hydrolithon reinboldii* (Weber-van Bosse & Foslie) Foslie 1909, and *Paragoniolithon conicum* (Dawson) Adey, Townsend & Boykins 1960. These four species are dominant reef-building elements in the northern GBR (personal observations) and throughout the tropical Indo-Pacific (Adey *et al.* 1982). Their vertical distributions on the windward reef slope at Lizard Island are shown in Fig. 2.

Species were identified using the monograph on Hawaiian crustose coralline algae published by Adey *et al.* (1982). This is the only detailed and modern taxonomic treatment of tropical species of the group. The identifications were confirmed by Dr. Walter H. Adey of the Smithsonian Institution, Washington, U.S.A. (personal communication). Dr. William J. Woelkerling of the Department of Botany, LaTrobe University, Melbourne, Australia, who is currently engaged in taxonomic studies of the crustose Corallinaceae, has suggested that the names applied to some of these species may require revision (personal communication)*.

1. 4. ECOLOGY OF SPECIES AT LIZARD ISLAND

Only a brief summary of the distributions of the four species on the windward crest and slope of the reef at Lizard Island is presented here. Descriptions of the ecology of *Porolithon* and *Neogoniolithon* on reefs of the Marshall Islands have

* During preparation of the manuscript Woelkerling (1987) published amendments to the taxonomic treatment provided by Adey, Townsend & Boykins (1982). He suggests that *Paragoniolithon conicum* should be included in the genus *Neogoniolithon* as originally proposed by Dawson (1960). However, *Paragoniolithon conicum* is clearly distinct from *Neogoniolithon fosliei* and bears greater similarity to *Porolithon onkodes* in terms of pigment composition. For the purposes of this thesis the name *Paragoniolithon conicum* is retained.

Fig. 2. Typical reef profile in the study area. Columns show approximate vertical distributions of the species, and their depths of maximum abundance.

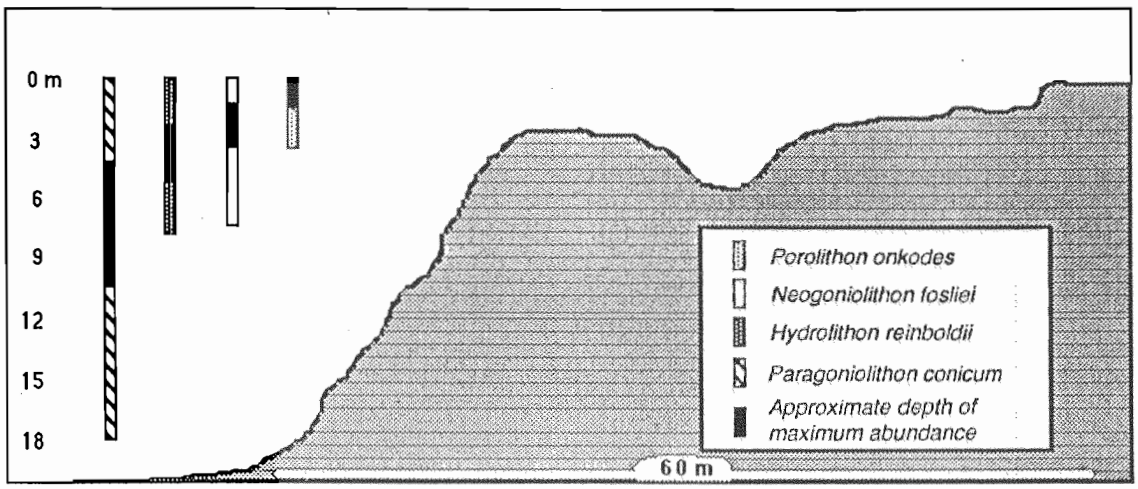
0 m
3
6
9
12
15
18
60 m
Porolithon onkodes
Neogoniolithon fosliei
Hydrolithon reinboldii
Paragoniolithon conicum
Approximate depth of maximum abundance

been provided by Lee (1967), and ecological treatments of the same genera and of the species *Hydrolithon reinboldii* have been provided for reefs of the Hawaiian Islands by Littler (1973a) and Littler & Doty (1975).

Porolithon onkodes is the dominant crustose coralline alga on the windward reef margin to a depth of approximately 1.5 m. It reaches maximum abundance at the junction between the reef flat and the forereef (≡ reef crest) at a depth of 0 m (Fig. 2) where surf action is most vigorous. *P. onkodes* is not commonly found at depths greater than 3 or 4 m on the windward reef slope but does occur in shaded habitats at shallower depths in areas of strong water motion or high grazing pressure.

Neogoniolithon fosliei reaches maximum abundance on the windward reef shoulder and shallow forereef (1.5-4 m)(Fig. 2). The species rarely grows at depths greater than 6 to 8 m and while fairly common in areas of intense illumination is more abundant where irradiance is high to moderate.

Hydrolithon reinboldii occurs on the exposed margin of the reef flat, usually in lightly shaded areas and on surfaces inclined away from direct irradiance. It reaches maximum abundance on the reef shoulder and at moderate depths (2.5-5 m) on the reef slope (Fig. 2), but is rarely found below 7 or 8 m. It appears to be reasonably well adapted to low irradiance but is most abundant where irradiance is moderate.

Paragoniolithon conicum occurs at all depths on the reef slope at Lizard Island with a rather poorly defined region of maximum abundance between approximately 5 and 8 m (Fig. 2), where irradiance is moderate to low. The species does occur in very shallow water on the exposed margin of the reef flat, but usually only in shaded areas and on vertical or steeply inclined surfaces.

CHAPTER 2

PHOTOSYNTHESIS

2. 1. INTRODUCTION

Primary production.

Charles Darwin (1842) was the first to marvel at the immense diversity of life-forms on coral reefs and to question how this might occur in waters so blue and clear and obviously low in nutrients. Sargent & Austin (1949) answered this question by demonstrating that coral reefs have extremely high rates of primary production even though their surrounding waters are largely devoid of productive life. The productivity of coral reefs is due to the thin veneer of algal life which covers their upper surfaces. Coral reefs do not generally support large populations of fleshy macroalgae and the primary fixation of carbon is carried out by the endosymbionts of corals (zooxanthellae), filamentous turf algae, endolithic algae, and the calcareous red and green algae. The survival of non-photosynthetic reef organisms depends either directly or indirectly upon the organic materials produced by these algal groups. Coralline algae are important producers of organic carbon but their rates of production are generally considered to be below those of other primary producers on the reef (Lewis 1977). Nevertheless, because they are extremely abundant on coral reefs which typically have high surface relief (Dahl 1973), their contribution to overall reef production may be of very great significance (Larkum 1983).

The biological contribution of crustose coralline algae to reef production has not been extensively studied (Lewis 1977). Existing information suggests that irradiance is the most important factor affecting both their rates of production and species distributions (Adey 1966, 1971; Adey & Adey 1973; Adey & MacIntyre 1973; Littler 1973a,b,c; Littler & Doty 1975). Since irradiance changes greatly with depth (Jerlov 1976) and shading, accurate information cannot be gathered about the rates of production without establishing the relationship between irradiance and photosynthesis. No previous studies have determined how the photosynthetic rates of particular species change with depth and irradiance. Furthermore, there have been no previous studies of crustose coralline *in situ* primary production. As a result it has not

so far been possible to evaluate the relevancy of laboratory and simulated *in situ* measurements to rates of primary production in the field.

The primary objectives of this research were therefore to:
(i) develop suitable apparatus for the *in situ* measurement of photosynthesis and irradiance,
(ii) to establish the natural photosynthetic rates of dominant species of crustose coralline algae sampled from a variety of depths and over a gradient of irradiance,
(iii) to establish the photosynthetic rates of individuals obtained from the same field populations under laboratory conditions,
(iv) to compare the rates of photosynthesis *in situ* with the rates in the laboratory,
(v) to integrate rates of primary production per hour with the changes in irradiance known to occur over the course of a cloudless day,
(vi) to obtain estimates of consumption (i.e. respiration) per day and to integrate these with estimates of gross primary production to determine the primary production per day.

By meeting these objectives it was hoped to determine:
(vii) to what extent laboratory rates of photosynthesis provide an accurate estimate of rates in the field,
(viii) if there are differences in the photosynthetic rates of different species of crustose coralline algae,
(ix) to what extent depth and ambient submarine irradiance affect their rates of photosynthesis, and
(x) if regression models could be established which would enable prediction of the rates of gross primary production, net primary production, and consumption per day for any measured amount of irradiance at noon-time on a cloudless day.

The most convenient method of estimating rates of photosynthesis and respiration is to measure oxygen liberation in the light and oxygen consumption in the dark. Rates of oxygen evolution cannot be accurately translated into estimates of carbon production without knowledge of the relationship which exists between the amount of oxygen evolved and the amount of carbon dioxide consumed during photosynthesis. The relationship is defined by the photosynthetic quotient ($PQ = \Delta O_2/\Delta CO_2$), where PQ is actually net PQ because respiration continues in the light. In the dark, the fluxes of oxygen and carbon dioxide are reversed and the relationship is defined by the respiratory quotient ($RQ = \Delta CO_2/\Delta O_2$). In the absence

of better estimates, most investigators (e.g., Littler 1973a,c; Littler & Doty 1975; Wanders 1976; Vooren 1981; Hawkins and Lewis 1982; Littler *et al.* 1986) have assumed that coralline algae have a *PQ* of 1.0. One mole of O_2 is liberated for each mole of CO_2 reduced to organic carbon (Ryther 1956). The value of *PQ* thus indicates the reduction level of the carbon compounds produced during photosynthesis. A *PQ* of 1.0 indicates that the sole product of photosynthesis is carbohydrate. A value greater than 1.0 indicates that more reduced compounds are produced such as fats and proteins. The values assigned to *PQ* and *RQ* significantly affect estimates of carbon production and consumption. For this reason it is important to determine appropriate values for these quotients for individual species.

Until now there have been no determinations of the metabolic quotients of crustose coralline algae. Studies were therefore undertaken to determine the values of *PQ* and *RQ* for the four species examined in this study. The methods employed were more directly associated with the studies of calcification and are thus described fully in the following chapter. Nevertheless, the results of these determinations were necessary for calculations of the rates of organic carbon production and are thus included in this chapter.

Finally, studies of photosynthesis were undertaken to gain information about the calcification process. Light-enhanced calcification is intimately associated with photosynthesis (Kawaguti & Sakamuto 1948; Goreau 1963; Okazaki *et al.* 1970; Pentecost 1978; Borowitzka 1979). The association probably involves the metabolic uptake of carbon dioxide during photosyntheis which shifts the carbonate equilibrium in favour of the precipitation of calcium carbonate (Goreau 1959; and see reviews by Borowitzka 1982a and Barnes & Chalker in press). Photosynthesis may also supply energy (Goreau 1959; Okazaki 1977) for the active transport of ions, or organic materials for the development of an organic matrix (Borowitzka 1977), both of which may facilitate the precipitation of calcium carbonate. Whatever the exact role of photosynthesis in calcification, its importance in stimulating reef growth is obvious. However, the degree to which photosynthesis stimulates calcification in algae (and corals) remains a matter of some debate. There have been only three studies which have attempted to measure simultaneously the rates of photosynthesis and calcification by coralline algae (Littler 1973c; Pentecost 1978; Borowitzka 1981). The data which have resulted have generated almost as many questions as they have answers, largely because radioisotopes have been employed in the measurement of calcification.

In this study, photosynthesis and calcification were measured simultaneously by methods which did not involve radioisotopes. This area of research was undertaken to:
(i) investigate possible relationships between the rates of photosynthesis and calcification, and
(ii) to compare how both processes simultaneously respond to irradiance.

The results of these comparative studies will be discussed in the concluding section (Section 3. 4) of Chapter 3.

Photoadaptation

Crustose coralline algae are frequently dominant organisms in the shallow, wave-exposed parts of coral reefs (e.g., Finckh 1904; Setchell 1926b; Taylor 1950; Tracy *et al.* 1950; Doty 1954; Lee 1967; Wray 1971; Littler 1973a; Adey & Vassar 1975; Littler & Doty 1975; Wanders 1976; Van den Hoek *et al.* 1978; Sheveiko 1981; Atkinson & Grigg 1984). They are also abundant in very deep water where irradiance is reduced to only a small fraction of that at the surface. Living representatives have been discovered at depths of up to 268 m in the Bahamas (Littler *et al.* 1985) which is well below the depth considered to be the photic limit for photosynthesis (*ca* 200 m - Humm 1956). The crustose Corallinaceae therefore possess extraordinary abilities to colonise both the most intensely illuminated marine habitats and those experiencing as little as .0005 percent (0.015-0.025 μEinsteins m^{-2} s^{-1}) of surface irradiance (Littler *et al.* 1985).

Given the extreme range of irradiance levels over which crustose coralline algae can grow it seems likely that they must photoadapt. If photoadaptation does occur, rates of carbon production may remain similar over significant changes in irradiance. If this is the case, then estimates of carbon production over the entire depth of a reef slope are likely to be higher than if estimates are based on the photosynthetic efficiencies of shallow water populations.

One effective method of examining photoadaptation is to construct light-saturation curves for photosynthesis (*P-I* curves). These curves describe the relationship between irradiance (*I*) and photosynthesis (*P*). *P-I* curves are prepared by illuminating specimens with a sequence of irradiance levels up to and beyond the point

at which a further increase in irradiance does not cause a measurable change in photosynthetic rate (defined as the photosynthetic capacity). Changes in photosynthetic rate are measured most easily and reliably in a closed water system using an oxygen electrode.

Under low light the rate of photosynthesis is nearly proportional to irradiance. As saturating levels of irradiance are approached the relationship becomes non-linear. The transition from light-limited to light-saturated photosynthesis can occur with varying rate, although most published *P-I* curves show the transition to be rapid. Over this interval the curve tends toward a horizontal asymptote. The plot of irradiance versus photosynthesis has been simulated by several mathematical functions all of which describe *P-I* curves on the basis of a small number of physiologically significant parameters (Jassby & Platt 1976; Chalker 1980). These parameters include the angle of the initial slope (α), the irradiance at which the initial slope intercepts the horizontal asymptote (I_k- Talling 1957), the rate of dark respiration (R), and the maximal rate of gross photosynthesis (P^g_m), which is the summation of net photosynthesis (P_n) and dark respiration. The various functions which have been used to simulate *P-I* curves will be described in detail in Section 2. 2. 2. The appropriateness of these functions in the context of coralline algal photosynthesis will be discussed in Section 2. 4. 3.

P-I curves have been constructed for crustose coralline algae on only three previous occasions (Marsh 1970; Wanders 1976; Vooren 1981). When accurately modelled, such curves provide considerable information about photoadaption and are valuable for standardising estimates of the maximal rates of gross photosynthesis (P^g_m) and dark respiration (R). How the shapes of coralline *P-I* curves change with depth or irradiance has not been previously investigated. Moreover, a consistent approach has not been taken in the analysis of crustose coralline *P-I* data. Proper comparisons can only be made if mathematical models are developed which remove observer bias in the estimation of P^g_m and I_k, and permit statistical analysis of the descriptive parameters.

The objectives of this area of research were therefore:
(i) to measure the rates of photosynthesis by the four crustose coralline species under different levels of irradiance,
(ii) to obtain a satisfactory model, or models, with which to simulate the *P-I* data,
(iii) to construct light-saturation curves from the laboratory and *in situ* data,

(iv) to determine if crustose coralline algae photoadapt, and if so,
(v) do they photoadapt in a similar manner to other photosynthetic reef organisms,
(vi) do certain species photoadapt to a greater degree than others, and
(vii) to what extent does the ability to photoadapt determine the distribution of the species?

2. 2. LABORATORY STUDIES

2. 2. 1. MATERIALS AND METHODS

Collection of crustose coralline algal samples

Samples of the four selected species of crustose coralline algae were collected by SCUBA diving from the transects described in Section 1. 2, during August and September, 1985.

A minimum of four replicates were chosen for each species at each of three depths. These were as follows: *Porolithon onkodes* - 0, 1.5 (shaded), and 3 m; *Neogoniolithon fosliei* - 0, 3, and 6 m; *Hydrolithon reinboldii* - 0, 3, and 6 m; *Paragoniolithon conicum* - 0, 6, and 18 m. These depths were consistent with the upper, mid, and lower limits of the vertical distribution of the species (see Fig. 2). The percentages of surface irradiance transmitted to the depths of collection were measured around noon on a calm, cloudless day in early September. Near simultaneous measurements of surface and underwater irradiance were made using Li-Cor Quantum sensors Li-190SB and Li-192SB, and a Li-188B Integrating Quantum Radiometer/Photometer (Li-Cor, inc./Ltd.).

Disks of coralline algae of fixed diameter (17 mm) were obtained by drilling through *in situ* crusts with a diamond-tipped core drill (Ashworth's Jewellers Pty. Ltd., Home Hill, Queensland, Australia). The core barrel was driven at approximately 600 rpm by a Stenair heavy duty drill (Model GKN 520). The drill was powered by compressed air, fed through an auxillary hose from the diver's SCUBA tank. The disks were left attached to the underlying substrate for one week prior to experimentation to allow the specimens to renew growth along their damaged

margins. Microscopic examination of specimens treated in this manner confirmed that one week was quite sufficient for complete regrowth of a new margin.

On the day of experimentation, the disks were gently dislodged from the reef surface with a small screwdriver. As much of the underlying substrate and the lower non-living portion of the coralline crust as could be removed without damage to the living tissue was carefully ground away using small abrasive grinding stones fitted to the chuck of the air-drill. Specimens treated in this manner were transported to the laboratory in a specially designed acrylic tray (Plate 1) submerged in a large container of seawater.

Before measurement, the disks were washed briefly in running seawater and then acclimatised for 30 min in filtered seawater (0.45 µm Millipore filter). The antibiotics Penicillin G and Streptomycin (Commonwealth Serum Laboratories [CSL], Melbourne, Australia) were added to the seawater to produce working concentrations of 60 µg ml^{-1} and 100 µg ml^{-1} respectively to prevent bacterial activity. These concentrations are recommended by the CSL for routine cover during cell culture.

Experimental apparatus

A modified electrode cell, for use with a Rank Brothers (Bottisham, Cambridge, England) 'Clark'-type oxygen electrode, was designed and built at the Lizard Island Research Station. The cell was similar in certain respects to the cell which Rank Brothers market in conjunction with their electrode. The Rank Brothers cell was not suitable for this study for the following reasons. The cell was designed for use with isolated chloroplasts or phytoplankton whereby samples could be placed in the cell and circulated in suspension during illumination. The coralline disks, by contrast, needed to be mounted securely so that they would not fall onto the electrode during stirring and so that their living surfaces could be orientated towards a horizontal beam of light. Also, because the samples were circular disks of 17 mm diam., the sample compartment needed to have a larger diameter to length ratio than the Rank Brothers cell. Additionally, the Rank Brothers cell does not permit measurement of the incubation water temperature during illumination and it must be assumed that the temperature is the same as that of the water flowing through the surrounding jacket.

Plate 1. Form of acrylic tray for transporting crustose coralline samples from the field to the laboratory.

A

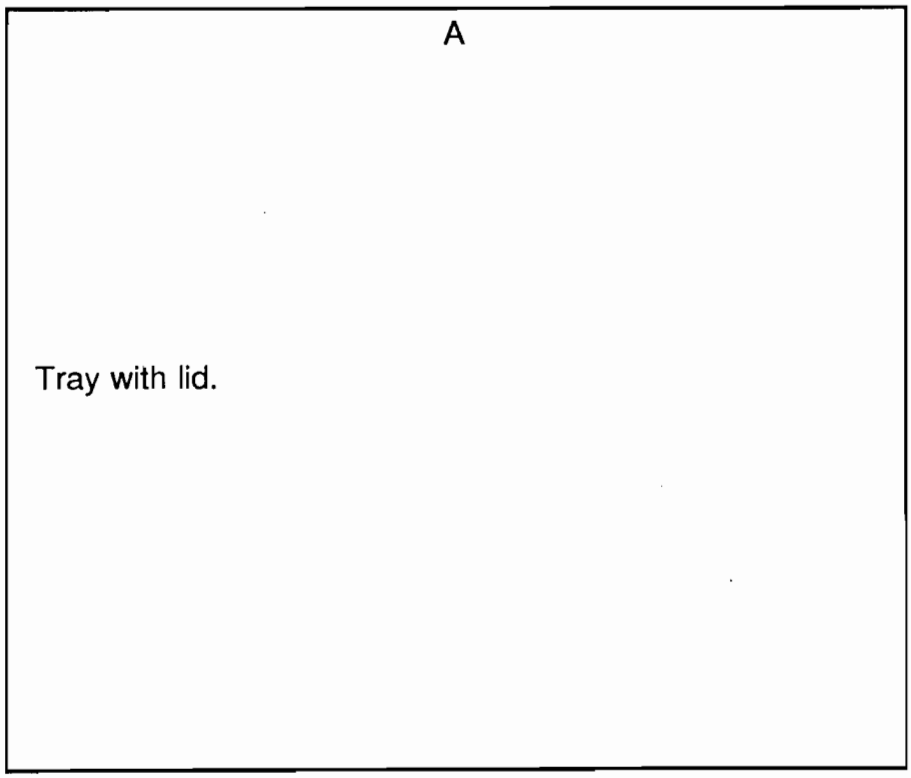

Tray with lid.

B

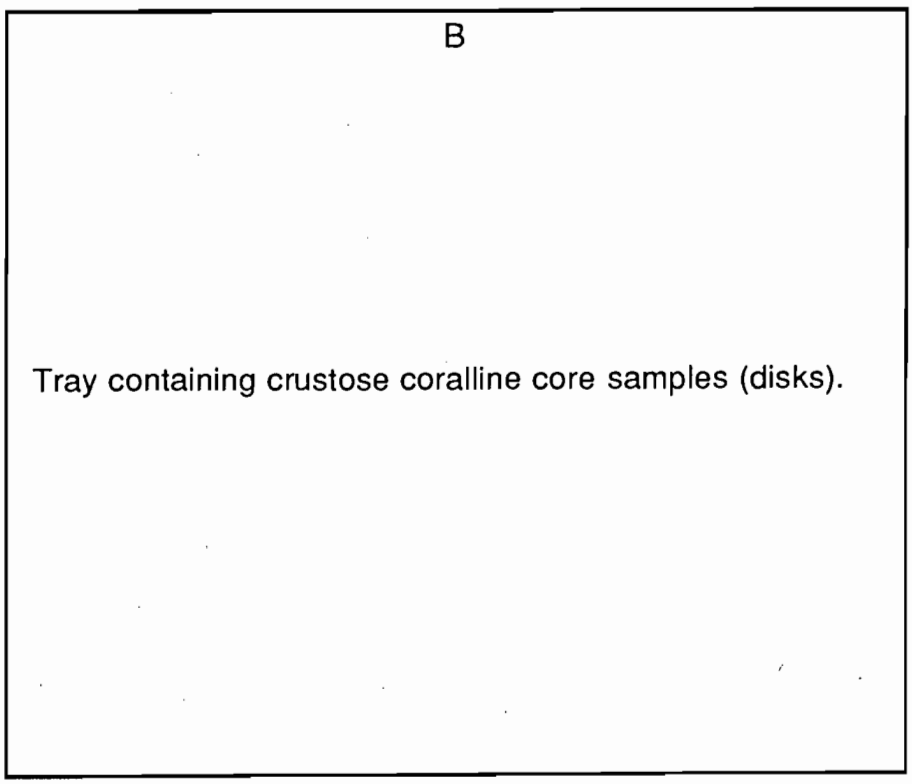

Tray containing crustose coralline core samples (disks).

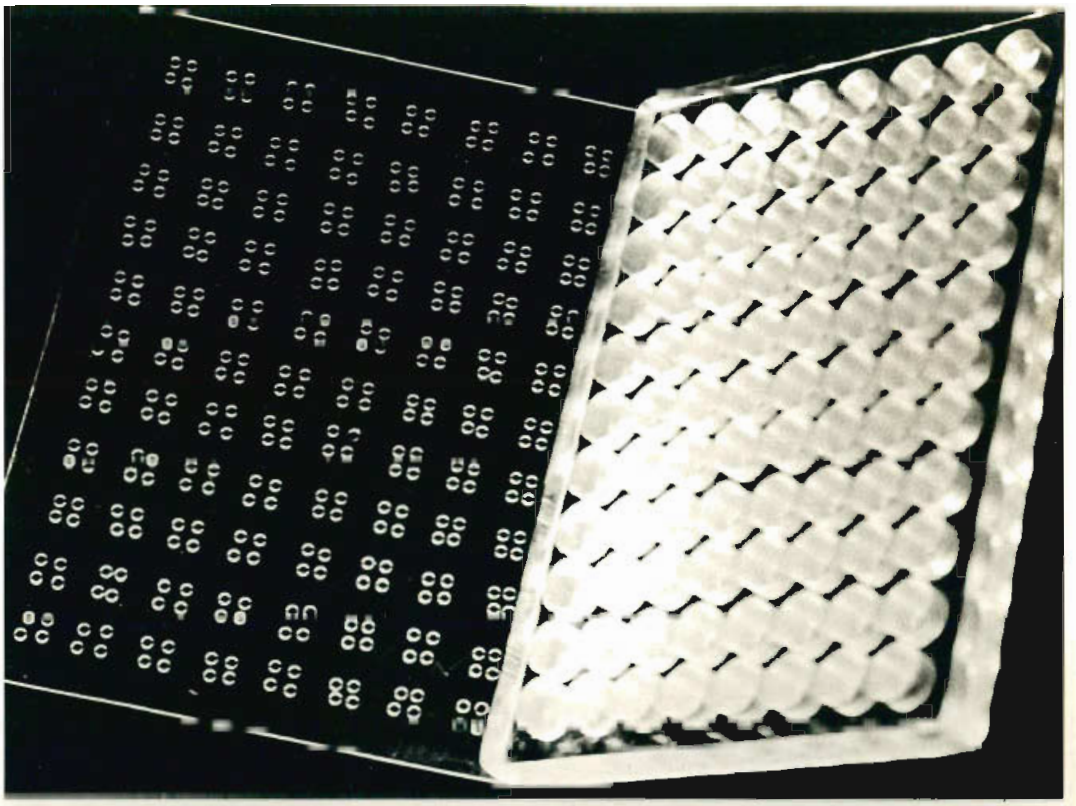

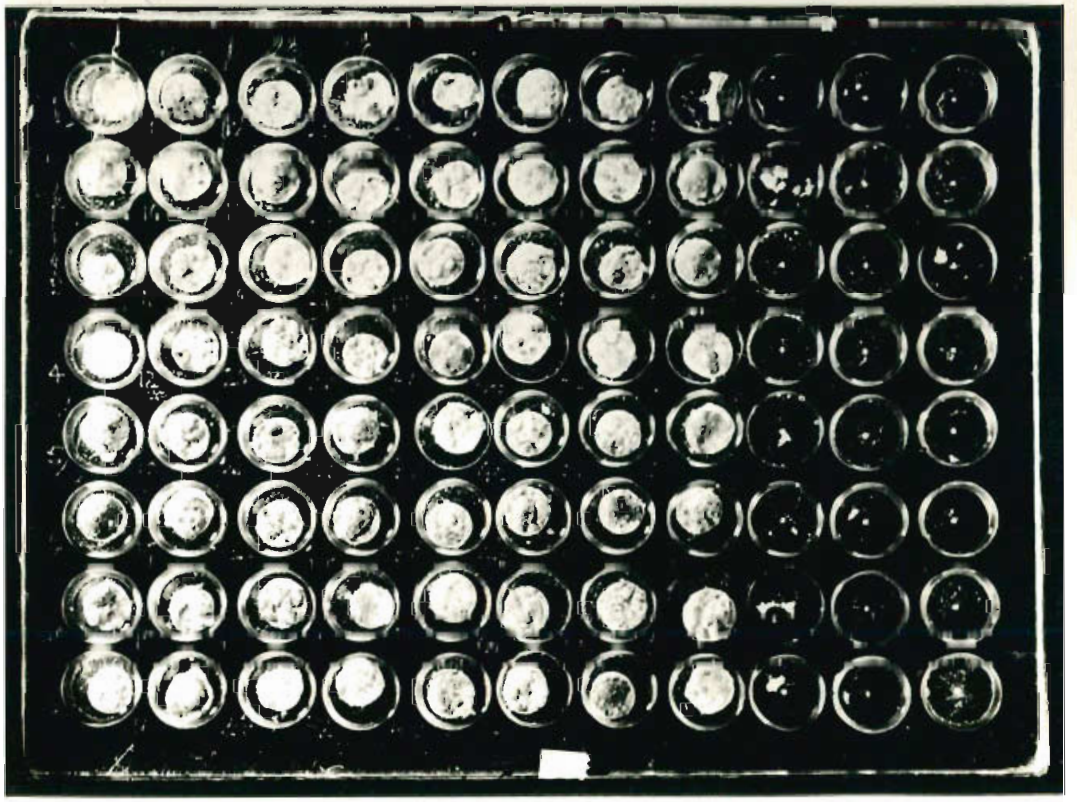

The modified electrode cell described in following sections was designed to overcome the constraints imposed by the Rank Brothers cell. The dimensions and gross features of the two cells are shown for comparison in Plate 2. A short description of the of the Rank Brothers cell and associated oxygen electrode follows to indicate which features were incorporated in the design and operation of the modified cell.

The Rank Brothers cell is a simple unit made of acrylic which consists of an internal, cylindrical, sample compartment and a surrounding jacket. The jacket permits water to be passed around the exterior of the sample compartment to control the temperature of the incubation water. An 'o'-ring seal and underlying teflon membrane separates the oxygen electrode from the water in the sample compartment. The electrode, embedded within an acrylic plate (Plate 3A), is united with the cell by a threaded compression ring (Plate 3A). An apical plug with air exclusion pore and circumferential 'o'-ring seal isolates the contents of the sample compartment from the atmosphere. The water in the sample compartment is circulated during incubation by a miniature stirrer bar magnetically coupled to a D.C. motor situated beneath the electrode baseplate. The motor is encased within a stainless steel sleeve and serves as a mount for the cell during operation.

The above-described features of the Rank Brothers unit were included in the modified cell. Two new features were introduced and some significant alterations were made to the dimensions of the cell. The internal diameter of the sample compartment was increased from 10 to 23 mm, whereas the length was reduced from 42 to 33 mm. This permitted accommodation of the 17 mm diam. specimen disks while maintaining a small tissue to water volume ratio which was desirable for the detection of small changes in oxygen concentration. Two threaded cylindrical ports traversing the external water jacket and opening into the sample compartment were introduced (Plate 3). One accommodated a threaded specimen holder with circumferential 'o'-ring seal (Plates 3, 4, 5). This allowed the coralline disk to be positioned parallel to the vertical walls of the cell and at right angles to a horizontal beam of light. The specimen holder was hollow at one end, and when used for experimental purposes was filled with Orthodontic tray wax (Sybron Kerr, Romulus, Michigan, U.S.A.)(Plate 3). The second port, accommodating a threaded supporting sleeve with 'o'-ring seal, provided access for a Micromech LCD temperature probe (Plates 3, 5). The temperature probe was introduced to determine the efficiency of the thermoregulatory jacket.

Plate 2. Oxygen electrode cells for the measurement of aquatic plant photosynthesis.

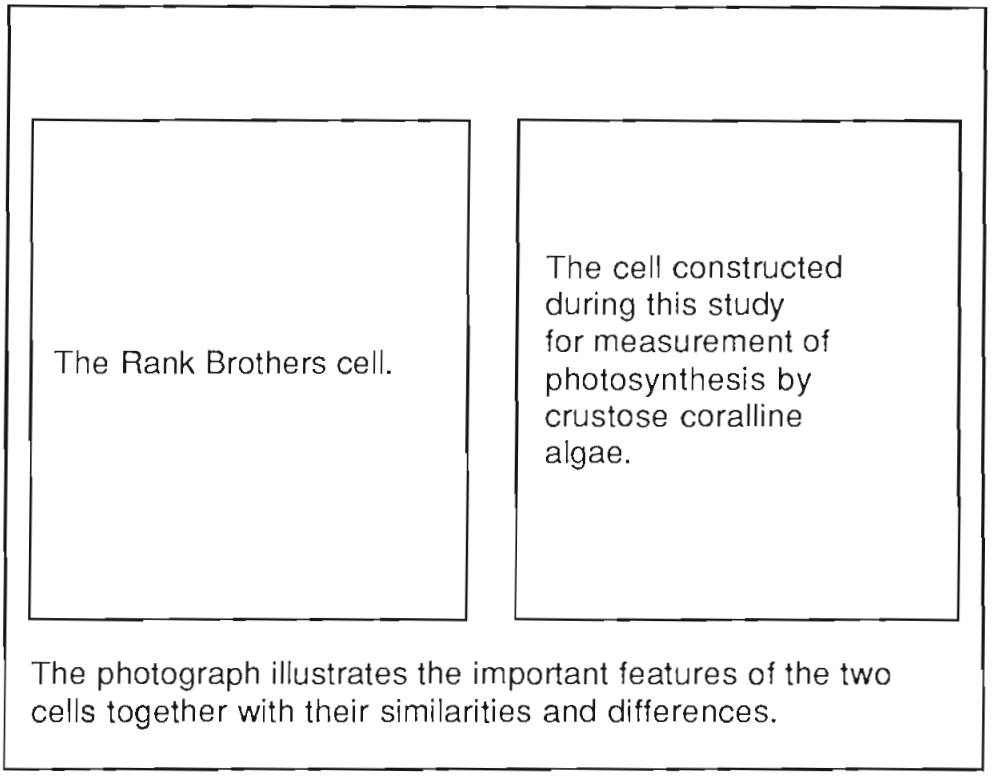

The Rank Brothers cell.

The cell constructed during this study for measurement of photosynthesis by crustose coralline algae.

The photograph illustrates the important features of the two cells together with their similarities and differences.

Plate 3. Exploded views of the specially constructed cell for measurements of photosynthesis in the laboratory.

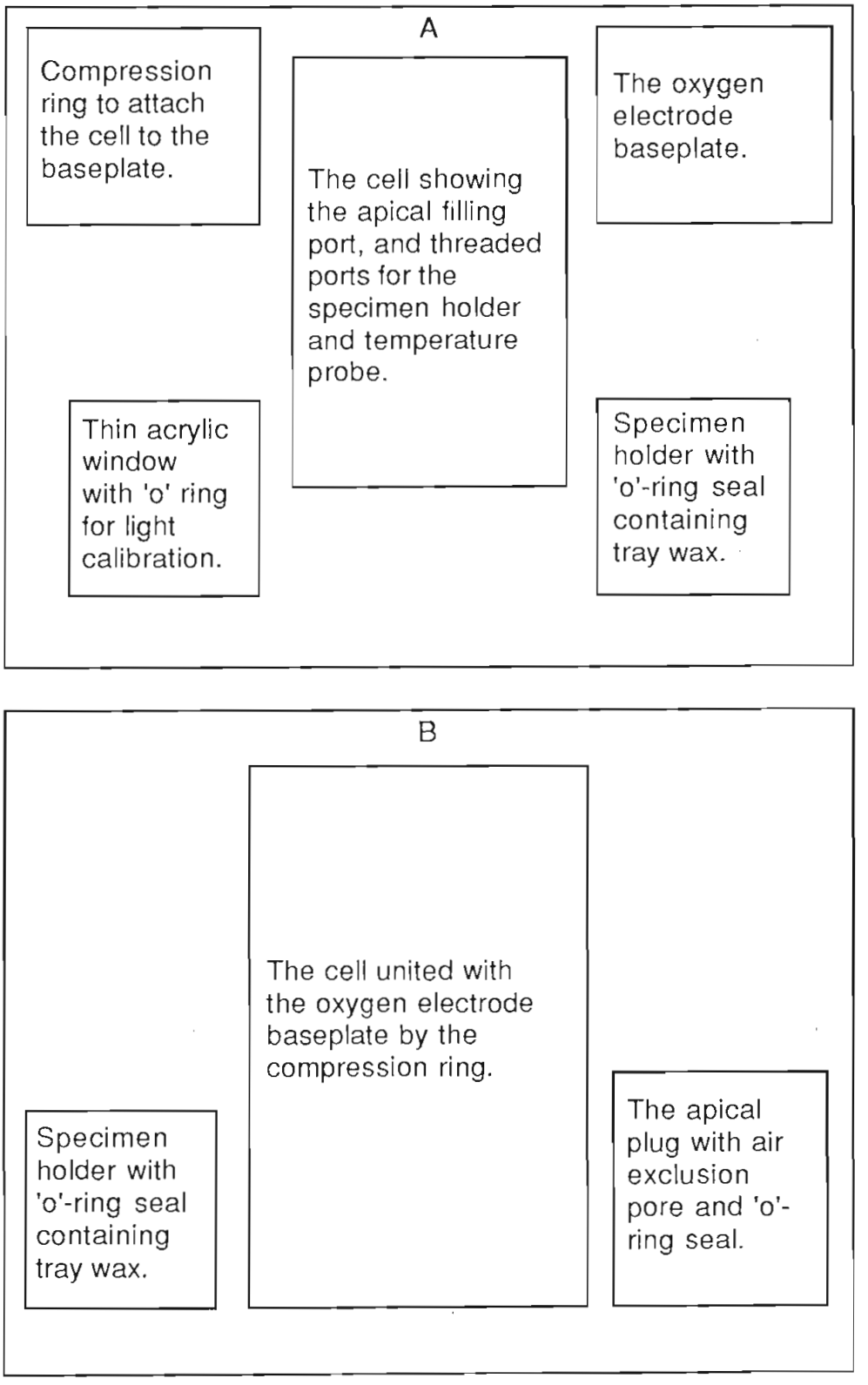

Plate 4. Different views of the oxygen electrode cell to show construction. The cell contains a crust of *Hydrolithon reinboldii.*

A

View front on to the direction of illumination.

B

Oblique view with temperature probe removed and baseplate locking screw in place.

C

Oblique view with the temperature probe and locking screw in place.

D

View normal to the direction of illumination.

Plate 5. Arrangement of the oxygen electrode cell and associated apparatus during operation.

A

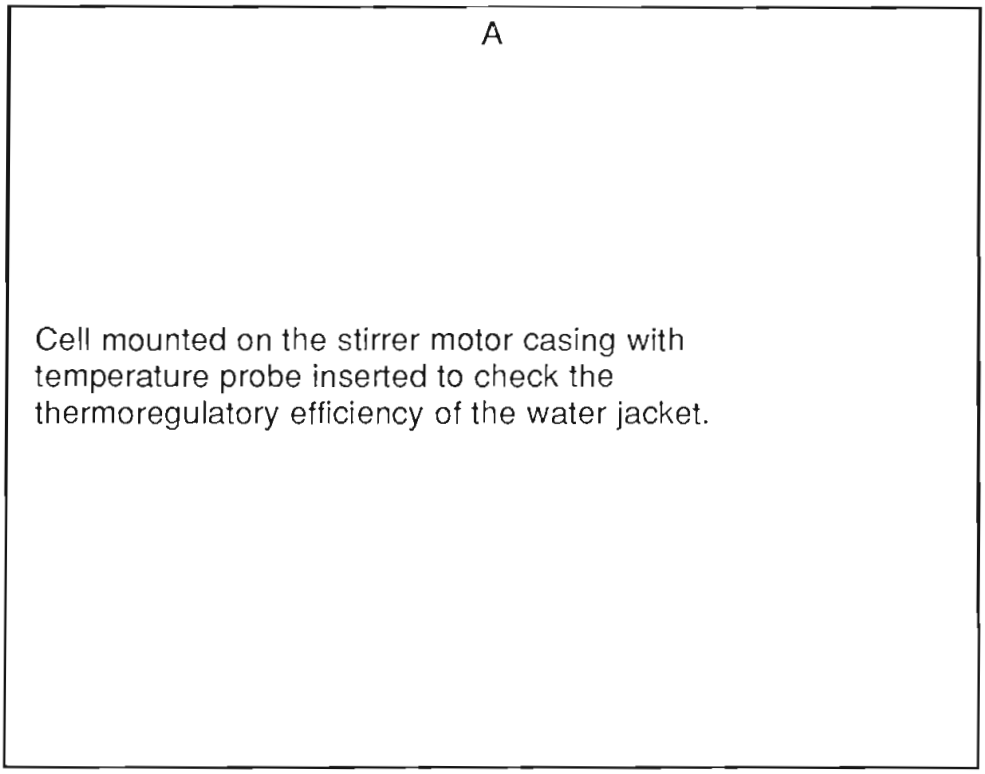

Cell mounted on the stirrer motor casing with temperature probe inserted to check the thermoregulatory efficiency of the water jacket.

B

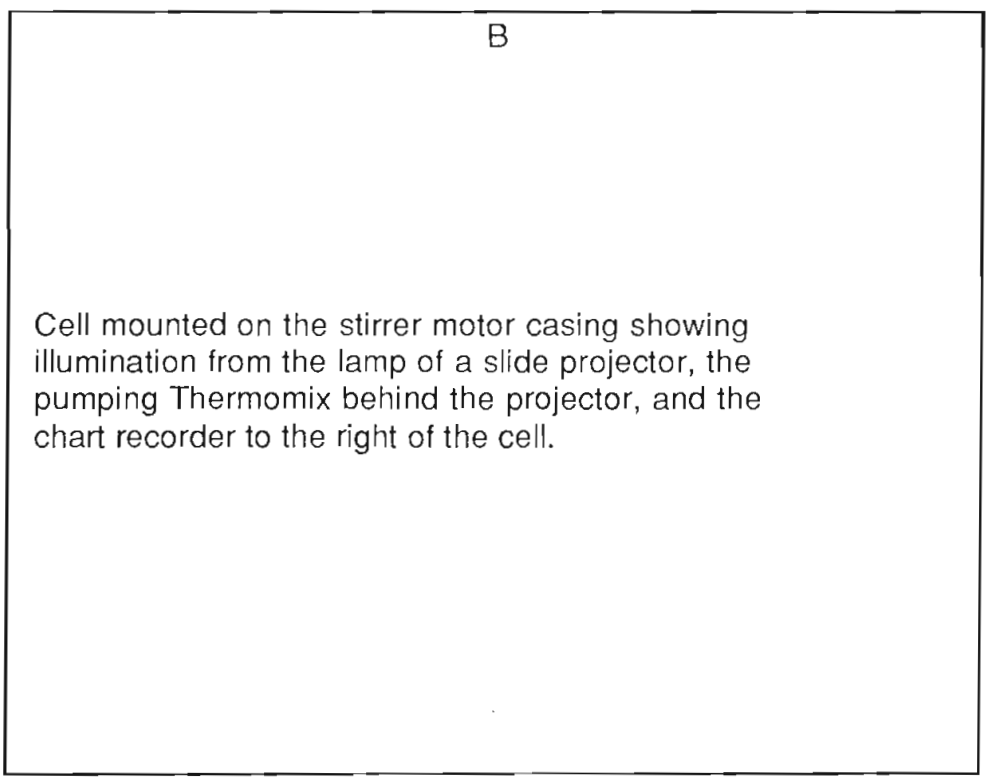

Cell mounted on the stirrer motor casing showing illumination from the lamp of a slide projector, the pumping Thermomix behind the projector, and the chart recorder to the right of the cell.

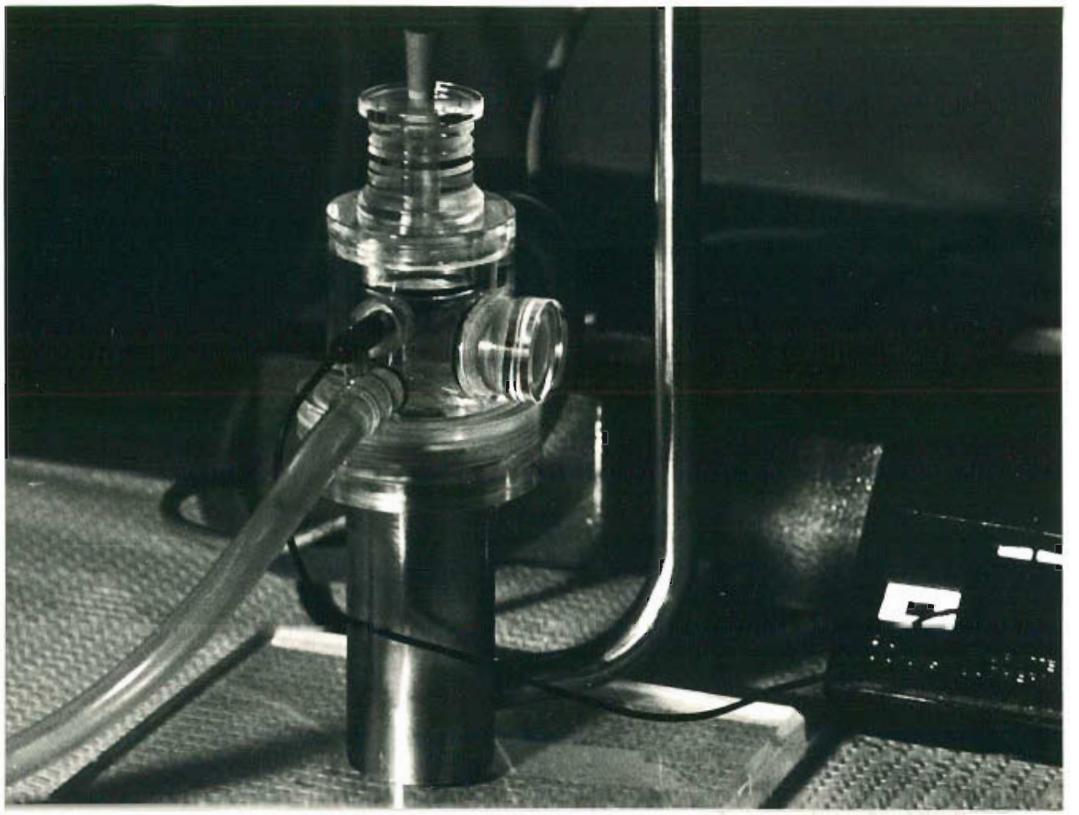

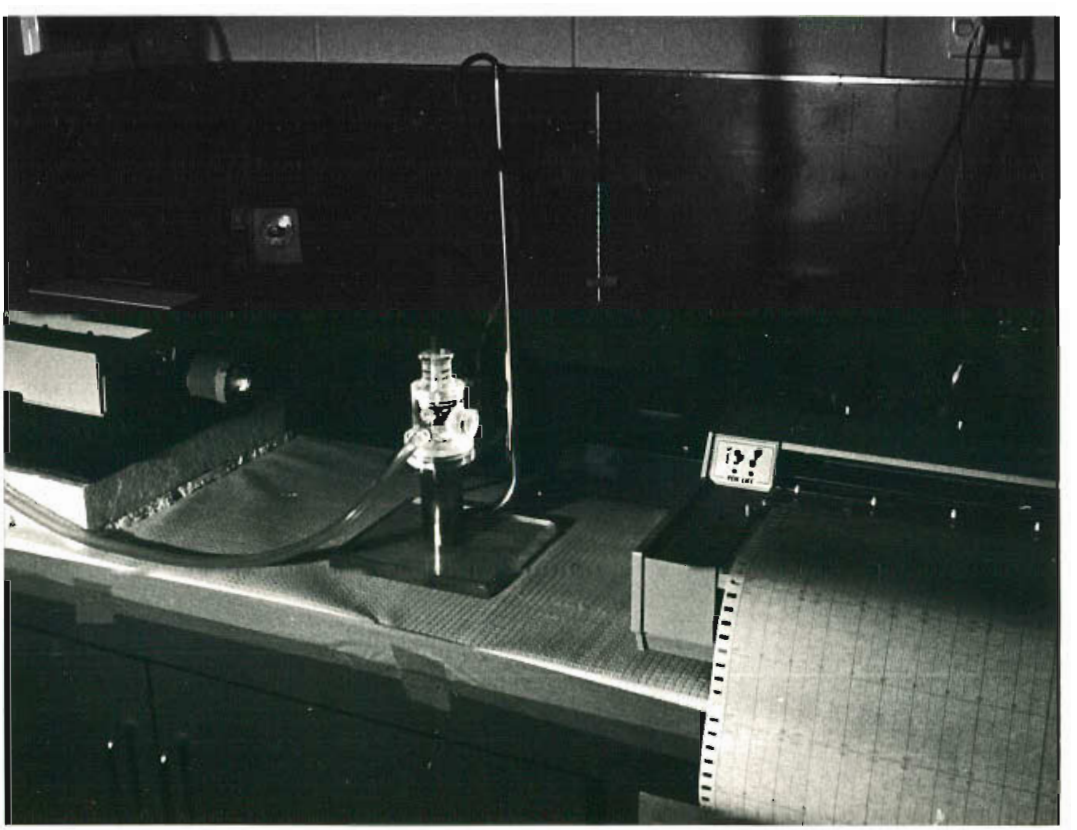

All components were manufactured on a lathe from clear, cast acrylic. The modified cell was designed to mate with the Rank Brothers oxygen electrode baseplate.

Illumination was provided by the 300 W quartz halogen bulb of a Hanimex slide projector positioned in front of the specimen chamber. A set of graded neutral density filters were produced by exposing Ilford Pan F (50 ASA, 18 DIN) black and white film to light passing through a set of Kodak Grey Card transparencies over a range of exposure times. The filters were used to vary the amount of irradiance projected onto the specimen during each experiment. The light from the projector bulb was passed through the infra-red glass filter of a fibre-optics lamp to reduce the heat of the light and to simulate the spectral distribution of submarine irradiance (see Fig. 3).

The water in the sample compartment was maintained at a constant temperature of 25 $\pm$ 0.1 °C by circulating water through the jacket of the electrode cell with a Braun Pumping Thermomix (Model 1441).

Changes in dissolved oxygen concentration were measured with the Rank Brothers galvanic oxygen electrode ('Clark'-type)(Plate 3A), coupled to a Rank Brothers signal amplifier and a Shimadzu chart recorder (Model R-112M)(Plate 5).

Calibration of equipment

Light calibration was carried out by inserting a thin (1 mm thick) acrylic window with circumferential 'o'-ring seal (Plate 3A) into the aperture of the specimen port (Plate 3B) and replacing the specimen holder with a Li-190 SB quantum sensor. The acrylic window was positioned 1 mm closer to the light source than the nominal position for the specimen, so that the surfaces of the light sensor and specimen would equate with one another. The incident light was measured as photosynthetic photon flux density (PPFD in µEinsteins m^{-2} s^{-1}, 400-700 nm). A correction was made for the amount of light energy absorbed or reflected by the acrylic window. The percentage of light transmitted through the acrylic window was measured in a DMS Varian 90 Spectrophotometer. The percentage transmission was essentially uniform at 86.4 $\pm$ 1.2% over the region of PAR (400-700 nm). The PPFD applied to the

Fig. 3. Transmission spectra across the PAR region (400-700 nm) for the infra-red heat filter and a 1% solution of $CuSO_4$.

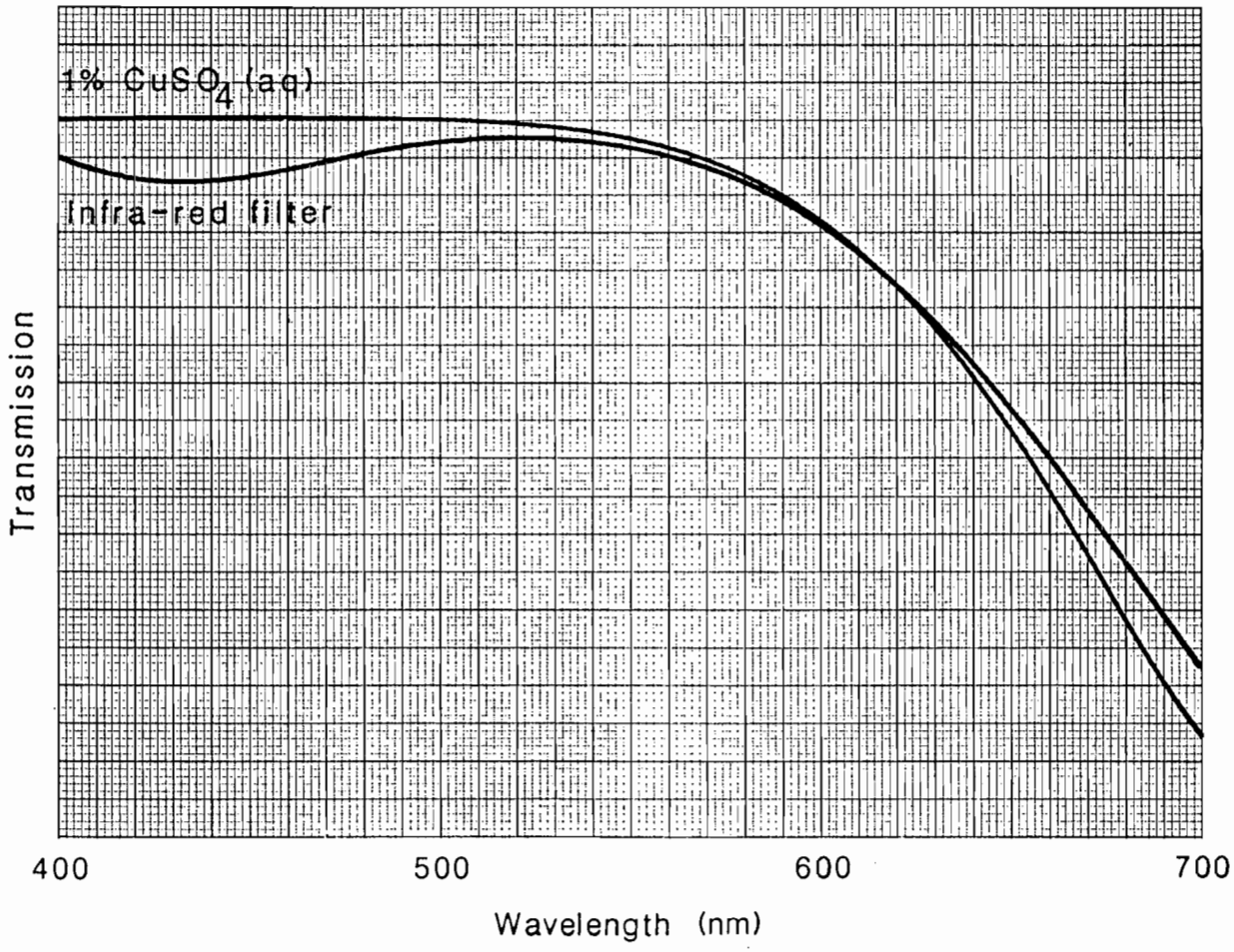
1% $CuSO_4$ (aq)
Infra-red filter
Transmission
400
500
600
700
Wavelength (nm)

specimens was consequently assumed to be 13.6% higher than the PPFD measured by the sensor.

Light was calibrated every three days over the duration of the experiments with an additional calibration performed each time a new set of neutral density filters was used.

Temperature calibration was initially performed using the Micromech temperature probe (Plates 4C, 5A), which had previously been calibrated against a mercury thermometer with 0.1 °C graduations. A temperature of 25 ± 0.1 °C (≡ sea temperature at the time of experimentation) was maintained during experiments over the entire illumination range of 0-3150 μEinsteins m^{-2} s^{-1}. Once the heat exchange capabilities of the water jacket were established to be adequate, the probe was removed and the port plugged with a flush acrylic insert. Removal of the probe improved the efficiency of stirring and hence the uniformity of the electrode response. The thermostat of the Thermomix supplying water to the heat exhange jacket was set at the appropriate temperature at the conclusion of the calibration. Frequent checks were made of the temperature of the water circulating through the thermomix during each experiment.

Oxygen electrode calibration and fine tuning of the associated recording apparatus was carried out on a daily basis. The pen of the chart recorder was set at zero when all of the dissolved oxygen in the incubation water had been removed by reaction with sodium sulphite. The chamber was then flushed with several volumes of filtered seawater (0.45 μm Millipore filter) to remove residual traces of sodium sulphite before calibrating the recording apparatus for the concentration of oxygen in air-saturated seawater. The voltage output on the chart recorder was set for optimum sensitivity once a stable reading for air-saturated seawater was obtained. The salinity of the calibration and incubation seawater was determined with a Hamon Autolab (Model 602) temperature/salinity bridge which had previously been calibrated against Copenhagen I.A.P.S.O. Standard Seawater P-61 (chlorinity of 19.3785 °/oo). The solubility of oxygen in air-saturated seawater under the experimental conditions (temperature of 25 °C, seawater salinity of 34.5 °/oo and chlorinity of 19.095 °/oo) was determined from tables of Carpenter (1966).

Experimental procedures

All experiments were conducted between 0730 and 1800 h as pilot experiments revealed that the photosynthetic mechanism in some species may be suppressed during the hours of darkness.

Crustose coralline disks were lightly pressed into the the wax which filled the cavity of the specimen holder in a bath of filtered (0.45 µm Millipore filter) antibiotic seawater. A film of lens tissue soaked in seawater was placed over the living surface of the specimen to prevent dehydration and the specimen holder was inserted into the port providing access to the sample compartment. The cell was immediately filled with filtered (0.45 µm Millipore filter) antibiotic (see "Collection of coralline algal samples" above) seawater. Initial tests revealed no increase in respiration rate if the specimens were rapidly transfered to the sample compartment and then pressed into wax of the specimen holder with the holder already in position. This procedure was adopted for convenience in all subsequent experiments. Orthodontic tray wax is both chemically inert and malleable at room temperature, and thus provides an ideal substrate for these purposes. Air was expelled from the sample compartment by downward pressure on the apical plug (Plate 3B).

Test incubations showed that the coralline disks had slow rates of respiration and relatively rapid rates of photosynthesis. Since it was intended that no measurements would be made above the air-saturated value of oxygen in seawater this meant that long incubations would have to be performed with a disproportionate amount of the time spent monitoring dark respiration. In order to circumvent this problem and to reduce the duration of each incubation, after an initial period of dark incubation (15-20 min) the seawater was purged with nitrogen to reduce the concentration of dissolved oxygen to approximately 50% of its air-saturated value. To check that this procedure did not significantly affect the sample measurements, one replicate of each sample group was maintained in darkness until 50% of the dissolved oxygen had been consumed naturally by respiration. These full-term dark incubations were commenced during the night so that illumination could be provided at the same time of the day as for the shortened incubations. The dark respiration rate for all specimens was measured over a 10-15 min period following a brief (5-10 min) period of acclimatisation in the cell at low irradiance.

After the dissolved oxygen in the incubation water had been reduced to approximately 50% of its air-saturated value, either by purging with N_2 or by respiration of the specimen, illumination was provided. The irradiance applied to the specimen was sequentially increased from the lowest to the highest level by changing the neutral density filters in the slide projector. If the air-saturated oxygen value was reached before all irradiance levels had been applied the specimens were returned to darkness and the procedures repeated until all irradiance levels had been tested. The dark respiration rate and the rate of oxygen production under one or more irradiance levels were checked once again towards the end of each incubation to ensure that conditions had remained constant throughout the experiment.

At the conclusion of each experiment the coralline disks were snap-frozen in dry ice (CO_2 at -32°C) and stored in total darkness at -20°C.

Real surface areas were subsequently estimated using the method of Marsh (1970). Aluminium foil of known weight to surface area ratio, was carefully moulded over the contours and projections of the coralline disks. Overlapping portions were removed with scissors and the edges trimmed to fit the boundaries of the previously living layers. The foil 'skins' were then weighed and converted into estimates of real surface area.

Projected surface area was constant in all cases since the internal diameter of the core-drill determined the outer diameter of the disks.

Chlorophyll *a* (chl. *a*) and accessory pigments were extracted at 4°C using three volumes (5 ml) of 20% tetrahydrofuran (THF) in methanol (MeOH)(v:v) (Chalker & Dunlap 1982). The disks were crushed in a percussion press (Plate 6) and ground to a fine powder in a pestle and mortar before extraction of the pigments. A fine stream of 20% THF in MeOH (THF/MeOH) was used to wash out the residue in the mortar. The solvent extracts were ultrasonicated at 4°C for five minutes to assist release of membrane-bound pigment fractions and subsequently centrifuged at 5000 rpm for 5 min at 4°C in a Damon/IEC (B-20A)) refrigerated centrifuge to sediment particulate matter. Aliquots of each serial extract were scanned immediately in a Hitachi (U-3200) spectrophotometer to determine the absorbance by chl. *a* at 665 and 436 nm in a 1 cm path length quartz glass cuvette. Using an extinction coefficient for chl. *a* at 665 nm (ξ_{665a}), in 20%

Plate 6. Two percussion presses. One larger and dismantled on the left, the other smaller and fitted together on the right.

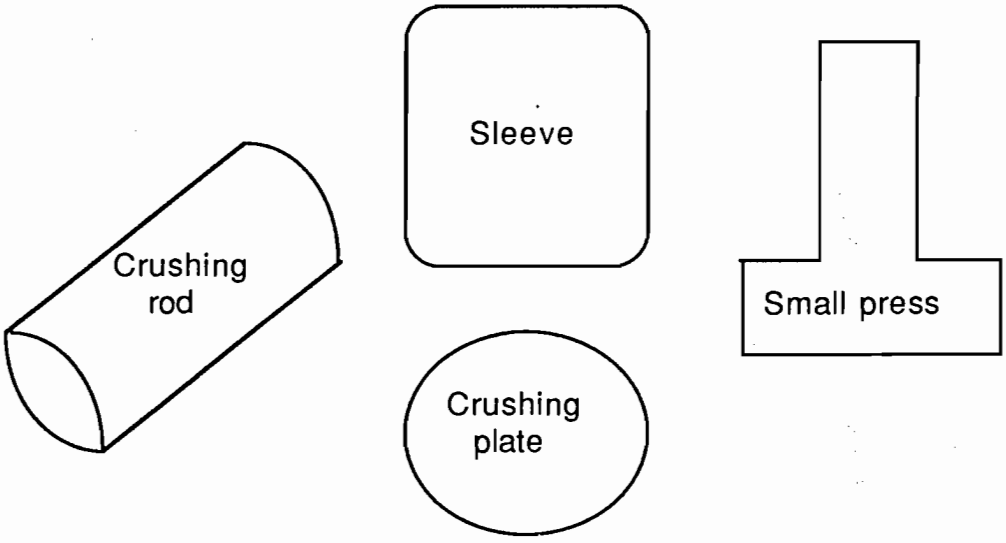

THF/MeOH, of 77.015 l g^{-1} cm^{-1} (Dr. Bruce E. Chalker - personal communication) the quantity of chl. *a* in each extract was determined from the equation:

$$\text{chl. } a = \frac{\text{volume of extract x absorbance at 665 nm}}{\varepsilon_{665a} \text{ x 1 cm (cuvette pathlength)}}.$$

The value of ε_{665a} was checked as follows. Chlorophyll *a* was extracted from three specimens of *N. fosliei* using 20% THF/MeOH, and the quantity in each extract was calculated from the absorbance at 665 nm using the ε_{665a} of Chalker. The same extracts were dried to constant weight in a Dynavac freeze drier at -50°C and redissolved in identical volumes of 90% acetone/distilled water ($D.H_2O$)(v:v). The chl. *a* contents were re-calculated using the $\varepsilon_{664.3}$ for chl. *a* in 90% acetone/$D.H_2O$ of Jeffrey & Humphrey (1975). The maximum difference in the amounts calculated for the two solvent systems was only 1% of the total chl. *a* in the 20% THF/MeOH extracts thus confirming the values of the extinction coefficients provided by Chalker and by Jeffrey & Humphrey.

Estimates of the proportion of chl. *a* attributable to any endolithic algae in the specimens were obtained by high performance liquid chromatography (HPLC) using a Waters (Model ALC/GPC 204) Liquid Chromatograph and Waters Data Module (Model 730). The solvent gradient was developed by Dr. Walter C. Dunlap (A.I.M.S.) for analysis of blue-green algal pigments. The gradient profile is given in Table 1. Detection was by visible wavelength absorption at 436 nm (0.01 absorbance units full scale [AUFS]). Pigment extracts were made from samples of endolithic algae taken from the non-living basal portions of additional coralline disks using the above-described extraction procedures. Aliquots (100 µl) of these extracts were separated on an RP-18 (Spheri-5, 25cm) column using a flow rate of 0.8 ml min^{-1}.

Extracts were also made of pure crustose coralline material by scraping the surfaces of coralline specimens with a scalpel blade without removing any endolithic algae from the underlying layers. Aliquots (100 µl) of these extracts were similarly analysed by HPLC. Comparisons between the HPLC traces of endolithic algal extracts and crustose coralline extracts revealed the presence of additional accessory pigments in the endolithic extracts. The endolithic accessory pigments are identified in the shaded regions of the representative traces shown in Plate 7. The cumulative peak areas of the accessory pigments in four endolithic algal extracts were calculated by

Table 1. Gradient profile for HPLC analysis of pigments extracted from crustose coralline algae and endolithic algae.
Solvent A, distilled water:methanol (50:50, v:v).
Solvent B, tetrahydrofuran (THF):methanol (10:90, v:v).

Time min	Flow ml min^{-1}	%A	%B
initial	0.80	25	75
20.0	0.80	25	75
45.0	0.80	0	100
65.0	0.80	0	100
70.0	1.50	0	100
80.0	1.50	0	100
85.0	1.50	25	75
100.0	0.80	25	75

Plate 7. HPLC separations of pigments extracted from *Hydrolithon reinboldii* and endolithic algae

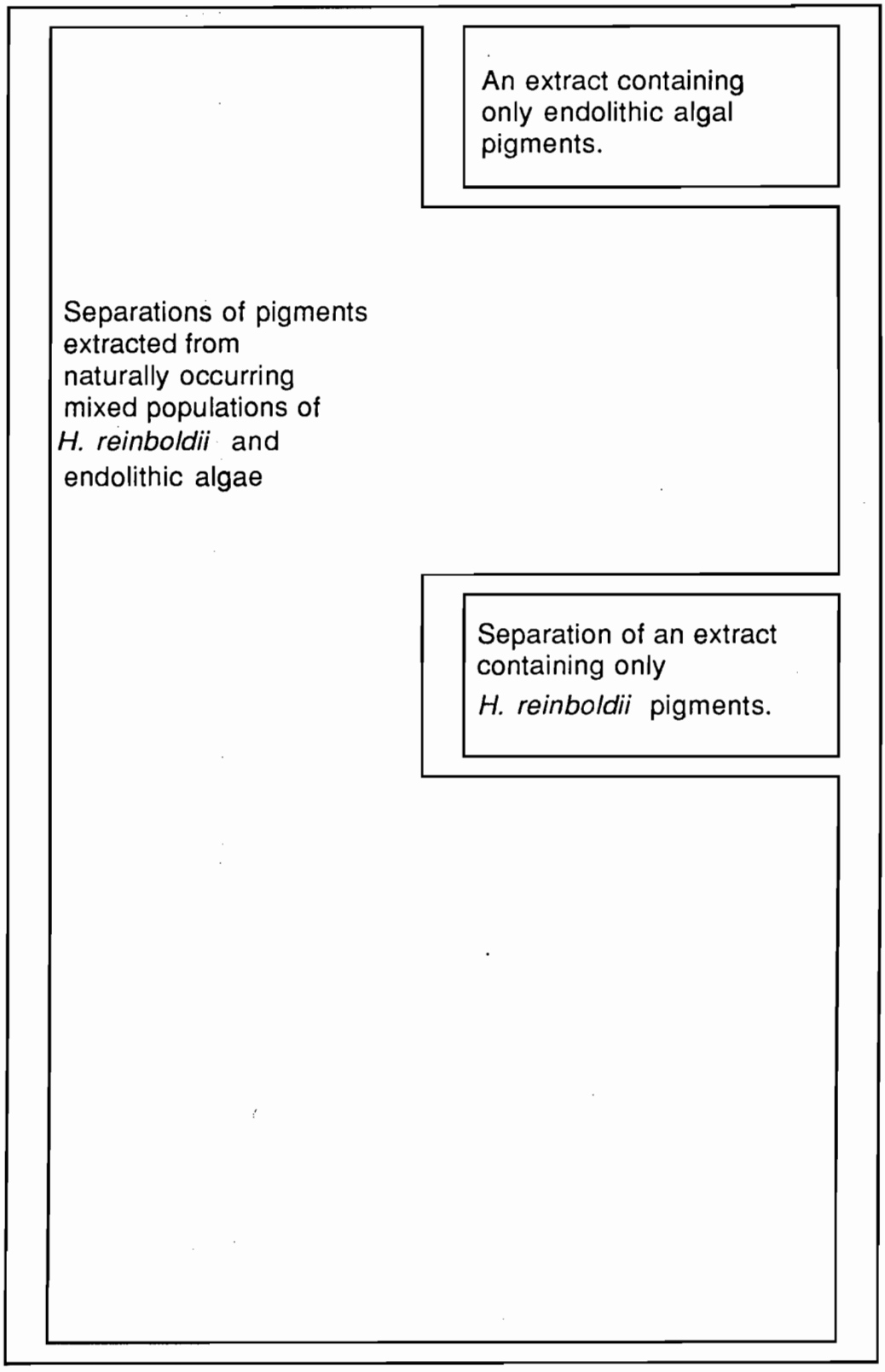

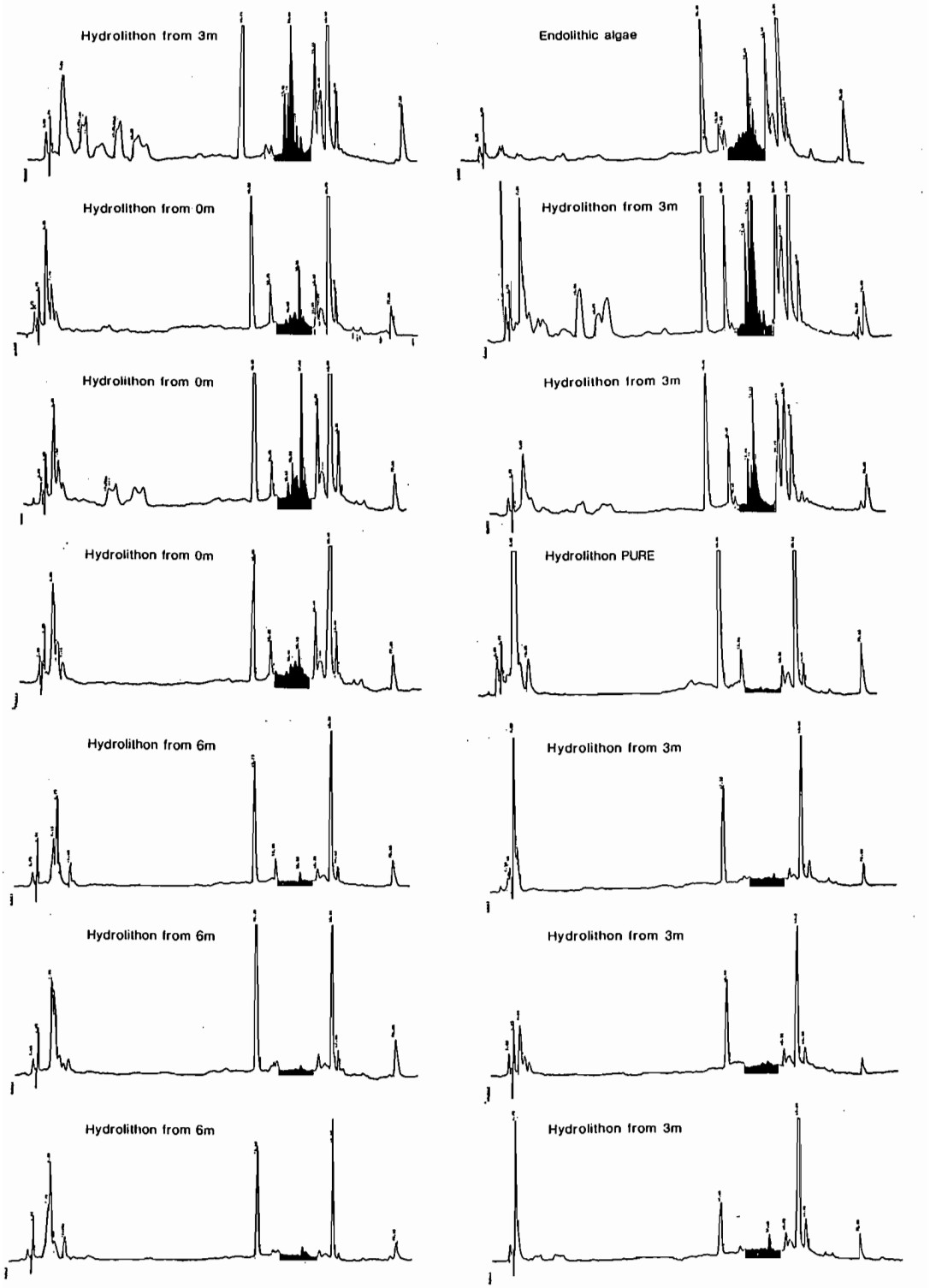
Hydrolithon from 3m
Endolithic algae
Hydrolithon from 0m
Hydrolithon from 3m
Hydrolithon from 0m
Hydrolithon from 3m
Hydrolithon from 0m
Hydrolithon PURE
Hydrolithon from 6m
Hydrolithon from 3m
Hydrolithon from 6m
Hydrolithon from 3m
Hydrolithon from 6m
Hydrolithon from 3m

digitizing the areas between the peak traces and the baselines. These areas were then compared with those for chl. *a* on the same traces (see Plate 7). The mean ratio between the quantity of chl. *a* and the total quantity of the specified accessory pigments was determined for the endolithic algal extracts. It was hoped that this ratio could be used to correct for the amount of chl. *a* contributed by endolithic algae to the extracts of the coralline disks.

2. 2. 2. ANALYSIS OF DATA

Light-saturation curves

Until this time light-saturation curves for photosynthesis have generally been described on the basis on four photokinetic parameters: the dark respiration rate (R), the initial slope of the curve (α), the light intensity at which the initial slope intercepts the horizontal asymptote (I_k), and the maximal rate of gross photosynthesis (P^g_m).

Among the functions which have been used to simulate light-saturation data for photosynthesis are:

the right rectangular hyperbola

$$P = P^g_m I(I+I_k)+R \qquad \text{(Wethey \& Porter 1976a,b),} \qquad (1)$$

a simple exponential function

$$P = P^g_m(1-e^{-I/I_k})+R \qquad \text{(Graus \& Macintyre 1976; Graus 1977),} \qquad (2)$$

and the hyperbolic tangent function

$$P = P^g_m \tanh(I/I_k)+R \qquad \text{(Chalker \& Taylor 1978; Chalker 1980).} \qquad (3)$$

These curves estimate different rates of transition from light-limited to light-saturated photosynthesis (see Fig. 4). In terms of photosynthesis, the rate of transition increases from Eq. (1) to Eq. (3).

Chalker (1981) has evaluated the accuracy with which each of these functions simulate light-saturation data for the endosymbiotic algae within hermatypic corals (zooxanthellae). He concluded that Eqs (2) and (3), a simple exponential and

Fig. 4. The shapes of light-saturation curves when data are modelled by (1) the hyperbolic tangent function (Eq. 3), (2) a simple exponential function (Eq. 2), and (3) the right rectangular hyperbola (Eq. 1).

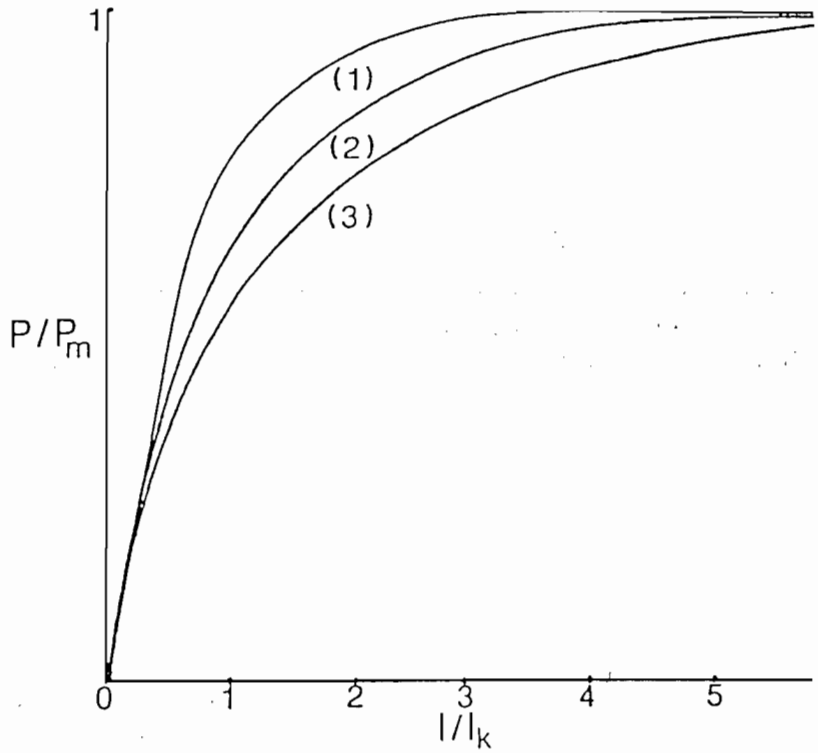
1
(1)
(2)
(3)
P/Pm
0
1
2
3
4
5
I/Ik

the hyperbolic tangent function, produce the most accurate simulations of the data, but that the hyperbolic tangent function generates the narrowest confidence intervals around the parameter estimates and is therefore to be preferred. This conclusion is supported by light-saturation data for marine phytoplankton provided by Jassby & Platt (1976).

Chalker (1980) also pointed out that each of the above-listed functions can be described in derivative terms using:

$$\frac{dP}{dI} = \alpha(P_m - P)\left(1 + \frac{\varepsilon P}{P_m}\right) + R \quad \text{(Chalker 1980).} \tag{3a}$$

Eq. (3a) introduces a fifth parameter, denoted as epsilon (ε). The magnitude of epsilon determines the extent of the portion of the light saturation curve which appears to be linear where the relationship between photosynthesis and irradiance is nearly directly proportional (Chalker 1980). Therefore the value of epsilon reflects the rate of transition from light-limited to light-saturated photosynthesis. Thus if $\varepsilon = -1$, Eq. (3a) integrates to the right rectangular hyperbola (Eq. 1). If $\varepsilon = 0$, Eq. (3a) integrates to the simple exponential (Eq. 2). If $\varepsilon = 1$, Eq. (3a) integrates to the hyperbolic tangent function (Eq. 3). For $-1 < \varepsilon < 1$, Eq. (3a) integrates to:

$$P = \frac{e^{(\varepsilon+1)(I/I_k)} - 1}{e^{(\varepsilon+1)(I/I_k)} + \varepsilon} + R \quad \text{(Chalker 1980)} \tag{4}$$

a general exponential function. Therefore, if ε is permitted to hold any value between -1 and 1, Eq. (3a) is capable of defining any curve which lies between the right rectangular hyperbola and the hyperbolic tangent.

However, because Eq. (3a) introduces a fifth descriptive parameter the confidence intervals around the parameter estimates tend to be wider. This reduces the statistical ability to resolve small differences between the parameters describing similar light-saturation curves. Nevertheless, the value of epsilon may well have physiological significance and its computation here is regarded as necessary for an accurate description of the relationship between photosynthesis and irradiance in crustose coralline algae. This argument will be extended in Section 2. 4. 3.

Light-saturation data were analysed by non-linear, least squares regression using subroutine (BMDP3R) of the BMDP statistical package (Health Sciences Computing Facility, University of California, Los Angeles). Each of the functions listed above were used by subroutine BMDP3R to estimate values for the mathematically descriptive parameters (R, α, I_k, P^g_m, ε |Eq. 4 only|). BMDP3R determined the asymptotic standard deviations of the parameter estimates, predicted values for each curve based on the modelling function supplied, and performed least squares analysis on the deviations between the predicted and observed values.

The first model tested was always the general exponential function (Eq. 4, with limits $-1 < \varepsilon < 1$) which could simulate any curve lying between the right rectangular hyperbola and the hyperbolic tangent. BMDP3R estimated values for the descriptive parameters by iteratively halving the residual sums of squares for each of the user-supplied parameter estimates. By this method the parameter estimates yielding the smallest residual sums of squares could be established. If ε approached any of the fixed values belonging to one of the other three functions (i.e., -1, 0, or 1) BMDP3R was run again using the most appropriate model to reduce the number of descriptive parameters and hence the confidence intervals of the estimates.

Three secondary parameters were calculated from the primary parameter estimates generated by BMDP3R. These included the ratio between the maximal rate of gross photosynthesis and the absolute dark respiration rate ($P^g_m/-R$), the irradiance at which photosynthetic oxygen production equalled respiratory consumption (I_c), and the irradiance at which photosynthesis was 95% light-saturated ($I_{0.95}$).

I_c was solved by rearrangement of the equations for each model as follows:

$$I_c = -RI_k/(P^g_m) \quad \text{(right rectangular hyperbola),} \tag{5}$$

$$I_c = I_k ln(P^g_m/P^g_m + R) \quad \text{(simple exponential),} \tag{6}$$

$$I_c = I_k \tanh^{-1}(-R/P^g_m) \quad \text{(hyperbolic tangent), and} \tag{7}$$

$$I_c = (I_k/(\varepsilon + 1)) ln((P^g_m - R\varepsilon)/(P^g_m + R)) \quad \text{(general exponential).} \tag{8}$$

$I_{0.95}$ was solved by rearrangement of each equation as follows:

$$I_{0.95} = 19I_k \quad \text{(right rectangular hyperbola),} \tag{9}$$

$$I_{0.95} = I_k ln(20) \quad \text{(simple exponential),} \quad (10)$$

$$I_{0.95} = \tanh^{-1}(0.95) I_k \quad \text{(hyperbolic tangent), and} \quad (11)$$

$$I_{0.95} = I_k((20-19\varepsilon)/(\varepsilon+1)) \quad \text{(general exponential).} \quad (12)$$

Statistical analysis

Analysis of variance (ANOVA) was performed on all modelled data sets to determine the significance of the proposed regression between photosynthesis and irradiance. Coefficients of determination (r^2 = sum of squares for the regression/corrected total sum of squares) were calculated for each of the regressions. The r^2 value is a measure of the proportion of the total variation which is explained by the proposed regression (Sokal & Rohlf 1981) and thus provides a measure of the accuracy with which a proposed model describes a given set of data.

Two-way ANOVAs were performed on the photokinetic parameters which were not affected by data normalisation. These parameters were I_c, I_k, ε, and the $P^g_m/-R$ ratio. Statistical comparisons were made between the parameter estimates for three of the four species of crustose coralline algae over three depths. The groups which were compared and their sample sizes (n) are shown in Fig. 5 One species, *Paragoniolithon conicum*, was omitted since its inclusion would have created an unbalanced design leading to a reduction in the power of the test. The parameter estimates for *Porolithon onkodes* at 6 m actually pertain to *P-I* curves for specimens obtained from shaded habitats at 1.5 m. It was considered acceptable to use these estimates in the tests because the measured PPFD at the 1.5 m shaded sites was equivalent to the PPFD at 6 m and the objective of the tests was to examine photoadaptation and not bathymetric adaptation *per se*. For these reasons the actual depth of 1.5 m will not be referred to again except in Fig. 9D, presented in Section 2. 4. Instead the 'depth' of sampling will be referred to as '6'm to indicate the relative PPFD.

The two-way ANOVAs were used to determine:
(i) if there were significant differences in the estimated values of I_c, I_k, ε, and P/R ratio, for different species of crustose coralline algae obtained from photically similar habitats, and

Fig. 5. Laboratory specimen groups tested by two-way ANOVA for significant differences in the values of parameters I_c, I_k, α, and $P^g_m/-R$. n = sample size. *Porolithon onkodes* specimens were not living at 6 m but experienced a PPFD equivalent to that depth.

DEPTH	SPECIES		
m	*Porolithon onkodes*	*Neogoniolithon fosliei*	*Hydrolithon reinboldii*
0	n = 6	n = 4	n = 5
3	n = 4	n = 4	n = 4
6	n = 4	n = 4	n = 4

(ii) if there were significant differences in the parameter estimates for individual species obtained from photically dissimilar habitats.

Residual analysis was performed on all data sets to satisfy assumptions made by the analysis of variance that the data was normally distributed and that the sample groups were equally variable (homoscedastic).

Student-Newman-Keuls (SNK) *a posteriori* range tests were used when ANOVAs revealed significant differences in the parameter estimates attributable to either a species or depth (≡ irradiance) effect to identify the major sources of variation within particular treatments. If, for example, I_c varied significantly with depth the SNK test identified the degree to which each depth affected the mean value of I_c. Depths causing similar effects were grouped together while depths causing different effects were grouped apart.

Significant differences in the value of epsilon with decreasing irradiance (i.e., increasing depth) were determined for each species using the Kruskal-Wallis (1952) non-parametric test. Non-parametric methods were employed because sample variances were not equal (heteroscedastic). If irradiance significantly affected the value of epsilon, multiple comparisons were made between paired treatments using STP (Sokal & Rohlf 1981) to establish the major sources of variation.

Rates of gross photosynthesis per day

Rates of gross photosynthesis per day were estimated by integrating the equation describing each *P-I* curve with the total amount of irradiance received by the specimen over the course of the day. Chalker *et al.* (1984) provide an equation which estimates the instantaneous rate of gross photosynthesis, at any time of day, by assuming that the change in irradiance through the day follows a sine curve which extends from civil dawn to civil twilight and peaks at the local solar noon. The length of day can be obtained from the Nautical Almanac (Her Majesty's Nautical Almanac Office 1985), peak noon irradiance must be measured at the collection site. The rate of gross photosynthesis per day can be estimated by numerically integrating the rate of gross photosynthesis over each minute of the day using a Simpson's rule approximation with the expected light intensities throughout the day, assuming zero cloud cover.

2. 3. *IN SITU* STUDIES

2. 3. 1. MATERIALS AND METHODS

Selection and preparation of crustose coralline algal samples

The underwater work was carried out on SCUBA. Specimens of the four selected species of crustose coralline algae were identified and marked for study along the transects described in Section 1. 2, during the period from March to July in 1986.

A minimum of four replicates of each species were selected at each of two or three depths as follows: *Porolithon onkodes* - 0, 2.5 (shaded) m; *Neogoniolithon fosliei* - 0, 3, 6 m; *Hydrolithon reinboldii* - 3, 6 m; *Paragoniolithon conicum* - 0, 6, 18 m.

Circular specimens (36 mm diam) were obtained by drilling through *in situ* coralline crusts with a diamond-tipped core drill. The core drill was driven at approximately 600 rpm by a Stenair heavy duty drill powered by compressed air from the diver's SCUBA tank. The core barrel was fabricated from mild steel on a lathe at the Lizard Island Research Station. The diamond tip was applied using electroplating techniques by Seismic Supplies International (Darra, Brisbane, Queensland, Australia).

A groove was cut through the coralline crust and into the substrate beneath to a depth of 10-15 mm. The substrate around the specimen was chipped away with a cold chisel to create a shallow trench approximately 50 mm wide and 10-15 mm deep. A fine skin of Orthodontic tray wax was smeared around the side of the projecting stub. A stainless steel band (10 mm wide) with an internal diameter exactly equivalent to the diameter of the coralline disk was tapped gently over the specimen with a hollow teflon drift. The teflon drift prevented dislodgement of the specimen by absorbing the shock and facilitated fitting of the stainless steel sleeve. The film of wax provided lubrication to assist the passage of the metal sleeve and ensured a water-tight seal. The steel band was fitted so that its upper margin exactly coincided with lowermost portion of the living layer of the coralline specimen (Fig. 6C). Specimens which were found to have weak attachment to the underlying substrate or showed obvious signs of boring by polychaete worms were not used for study.

Fig. 6. Details of the *in situ* incubation chamber and its application.
A. Plan drawing of the chamber showing probe fittings and ball-valves in exploded view.
B. Section drawing of the chamber showing oxygen probe, stirrer motor, and pH probe fittings in side view , and 'o'-ring seal surrounding the specimen aperture.
C. Section drawing showing the mating of the stainless steel mounting sleeve to a prepared core-drilled *in situ* specimen. Hatching denotes coralline crust substratum,

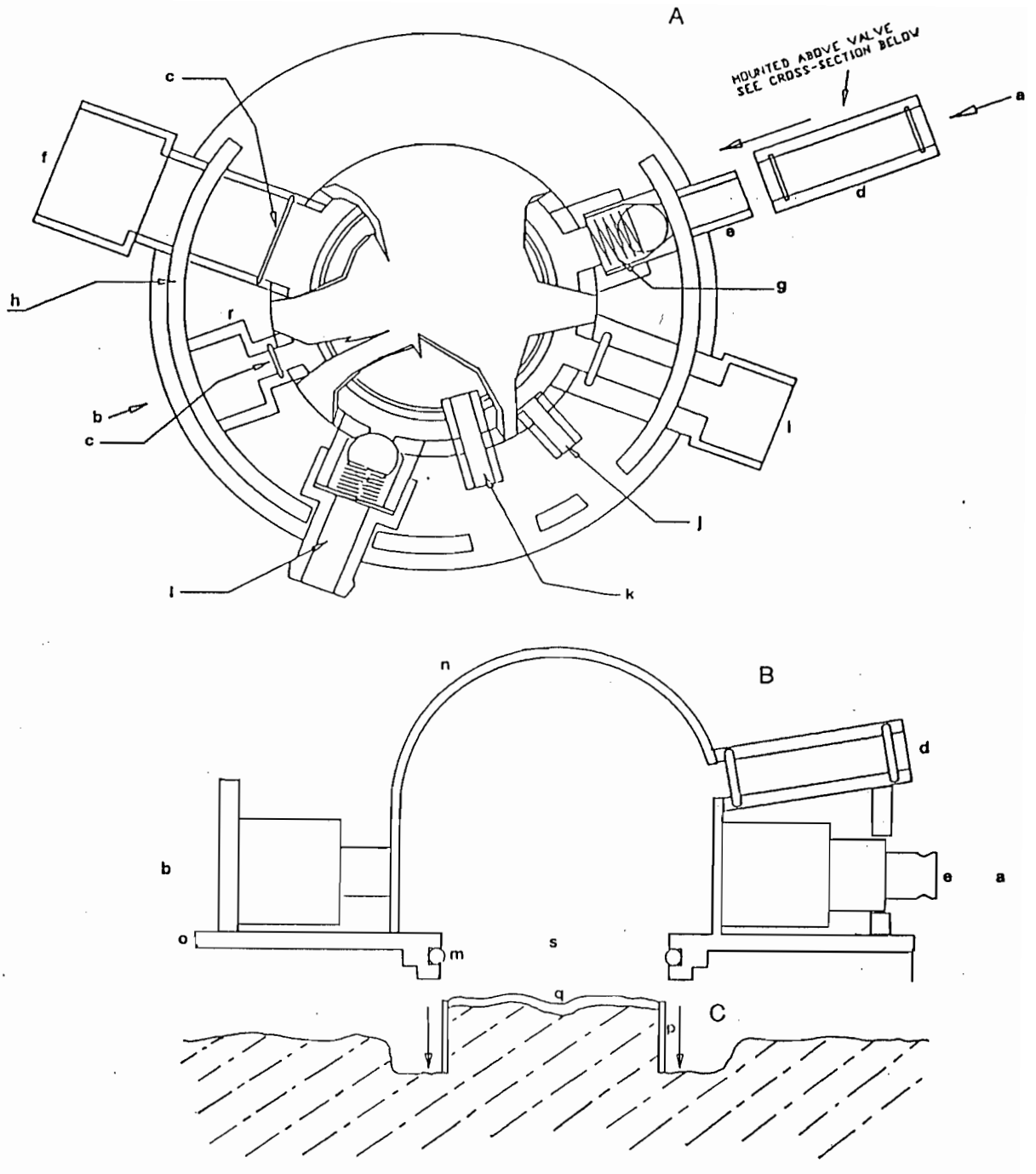

A	Plan
B	Section
C	Section
a-b	section cut
c	'o'-ring
d	pH electrode mount
e	inlet ball-valve
f	stirrer motor mount
g	spring
h	support ring
i	oxygen electrode mount
j	inlet
k	water outlet
l	outlet ball-valve
m	'o'-ring
n	specimen compartment
o	basal plate
p	sleeve
q	specimen
r	temperature probe mount
s	specimen port

The banded crustose coralline disks were marked with small sub-surface buoys and left for 7-10 days to allow regrowth of the cut margins. Growth taking place during this period was clearly visible with the naked eye.

Experimental apparatus

The experimental apparatus used during this investigation of crustose coralline *in situ* primary production was also used for the *in situ* studies of calcification. Many of the materials and methods described in this section are therefore also relevant to the following chapter.

A significant number of the items of equipment used in this study were constructed with the help of technical staff at the Lizard Island Research Station and the Australian Institute of Marine Science. Only items such as the monitoring electrodes and associated electrical components were available commercially. All of the acrylic used in the construction of the equipment was kindly donated by Cadillac Plastics Pty. Ltd., Townsville. Several of the methods were developed initially by scientists (notably Dr. D.J. Barnes and latterly Dr. B.E. Chalker) and technical staff (notably Mr. K. Carr, Mr. E. Gill, Mr. J-C Collingwood, and Mr. M.J. Devereux) at the A.I.M.S. These methods were modified and combined with several new procedures and pieces of apparatus developed specifically to meet the objectives of the *in situ* studies.

Since the equipment used in this study was of considerable complexity a brief overview is given as follows, so that when the component items are described their functional role will be more easily understood.

A small volume electrode chamber was built to slide over and seal against the stainless steel sleeve encircling the *in situ* coralline disk prepared for study. Oxygen, pH and temperature probes were inserted into the chamber once it had been fitted over the specimen. A replica of the electrode chamber (the simulation chamber), fitted with dummy probes but containing an underwater light sensor at an equivalent position to the coralline disk, was placed next to the electrode chamber in the same orientation. The probes and light sensor were linked by underwater cable to a datalogging device contained in a submersible housing. A small battery-powered pump, connected to the electrode chamber via a flexible hose, was used to flush the chamber at regular intervals. The probes were calibrated in a specially designed

constant temperature bath. The data stored by the logging device was accessed and retrieved onto floppy disk by an Epson computer.

The electrode chamber and simulation chamber

The electrode and simulation chambers were fabricated entirely out of acrylic. Circular sheets (85 mm diam, 3 mm thick) of ultra-violet transparent acrylic were clamped within an aluminium form (Plate 8), heated to 300°C in an oven, and blown using compressed air into short cylinders with hemispherical domes at one end. Brief immersion in cold water facilitated immediate solidification of the acrylic. Two of these domed cylinders of equal dimension were selected for construction of the electrode chamber (for the specimen) and the simulation chamber (for the light sensor). Each domed cylinder had an internal volume of 120 ml.

The features of the chambers are illustrated in Figs 6A,B, 7A, and Plates 9, 10, 11, which should be studied together with the following descriptions.

Basal plates (135 mm diam) with marginal rims (35 mm high, 3 mm thick), and 'o'-ring-grooved circular cavities (38.2 mm diam for the specimen chamber, 31.5 mm for the simulation chamber) in their centres, were glued to the open-ended bases of the acrylic domes. The basal plates and centrally located acrylic domes were then locked in the rotating head of a milling machine. Holes were bored through the marginal rims and into the cylindrical portions of the acrylic domes to take the electrodes. The location of each hole was precisely gauged for balance and to minimise shading of the specimen (Fig. 6A). All holes were bored within an arc of 240° such that one third of the marginal rim (acting to support the electrodes) could be cut away leaving a 120° open face with no occluding probe fittings for orientation towards the direction of maximum irradiance (Fig 6A, 7A, & Plates 9, 10, 11). Hollow mounts for each of the probes were fabricated from clear cast acrylic on a lathe. These mounting fittings were bored to accomodate specific probes and grooved to accomodate 'o'-ring seals, and were turned to fit precisely through the supporting rims and butt smoothly against the perimeter walls of the domed central cylinders (Plate 9). Four other fittings were turned to specification and glued to the exterior of the electrode chamber. These comprised an inlet and an outlet teflon ball valve to permit flushing of the chamber, and two nozzles to allow for the extraction of water

Plate 8. Aluminium form used to fashion the *in situ* specimen and light sensor chambers.

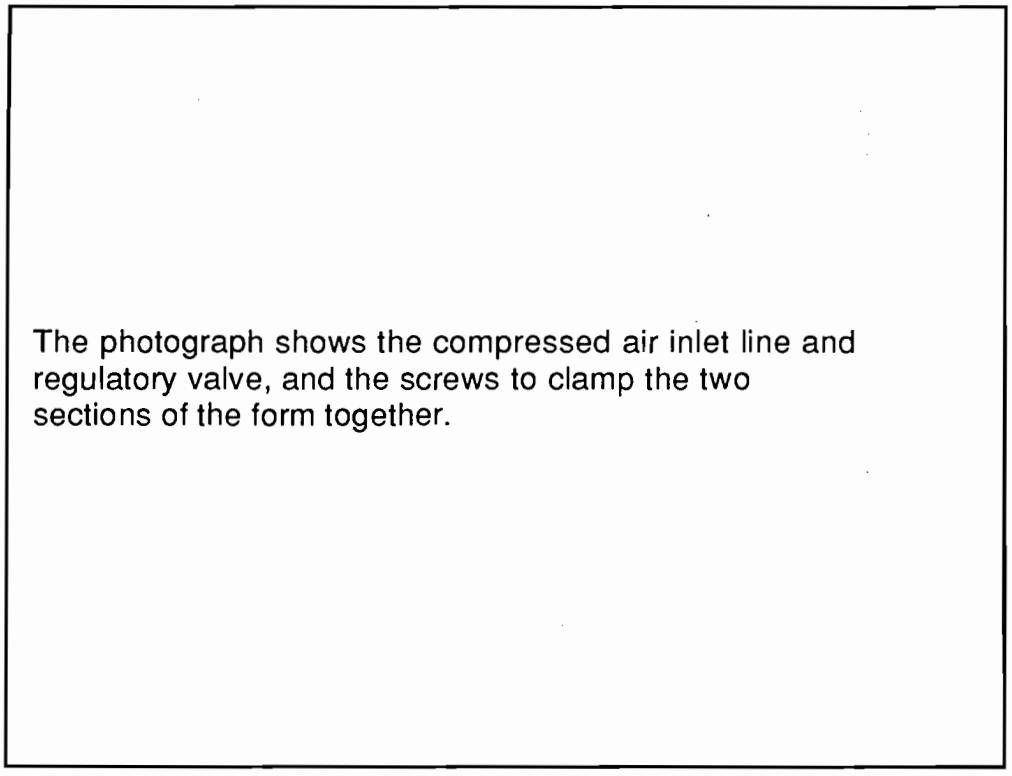

The photograph shows the compressed air inlet line and regulatory valve, and the screws to clamp the two sections of the form together.

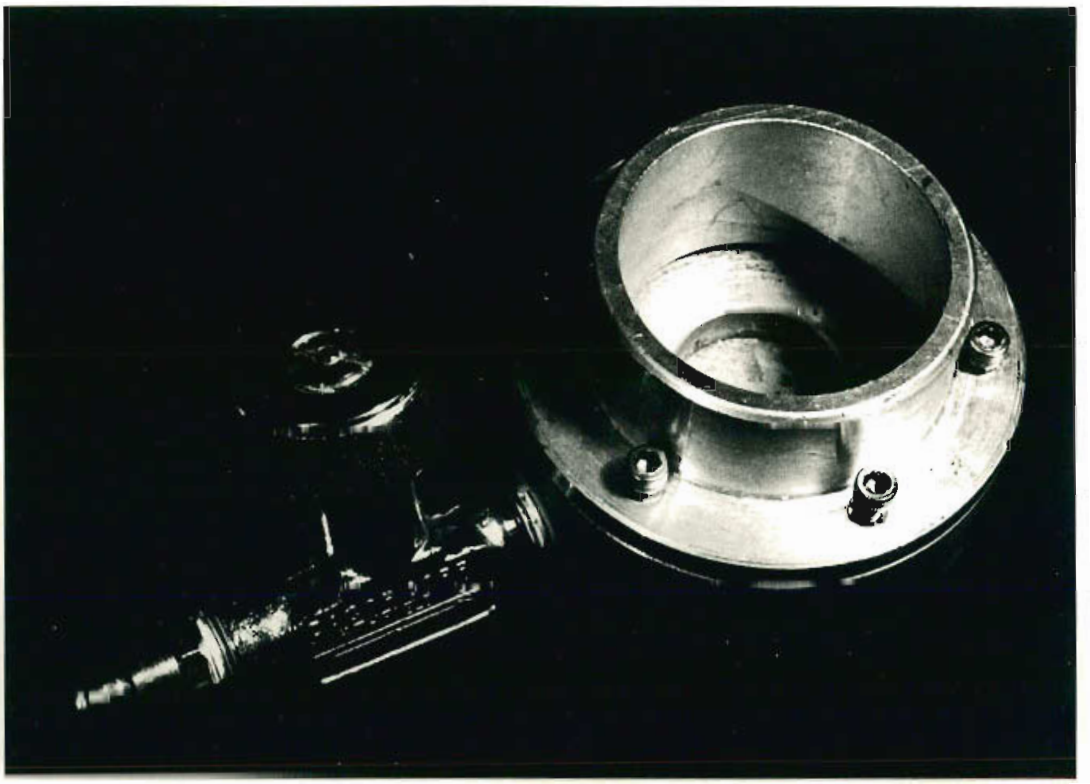

Fig. 7. Gross features of the *in situ* incubation chamber and internal details of the water sampling bottle.
A. Oblique view of the chamber showing gross construction.
B. Section drawing of the sampling bottle used to obtain incubation water samples. Chamber and bottle unite through hoses (u) and nozzles (j and k).

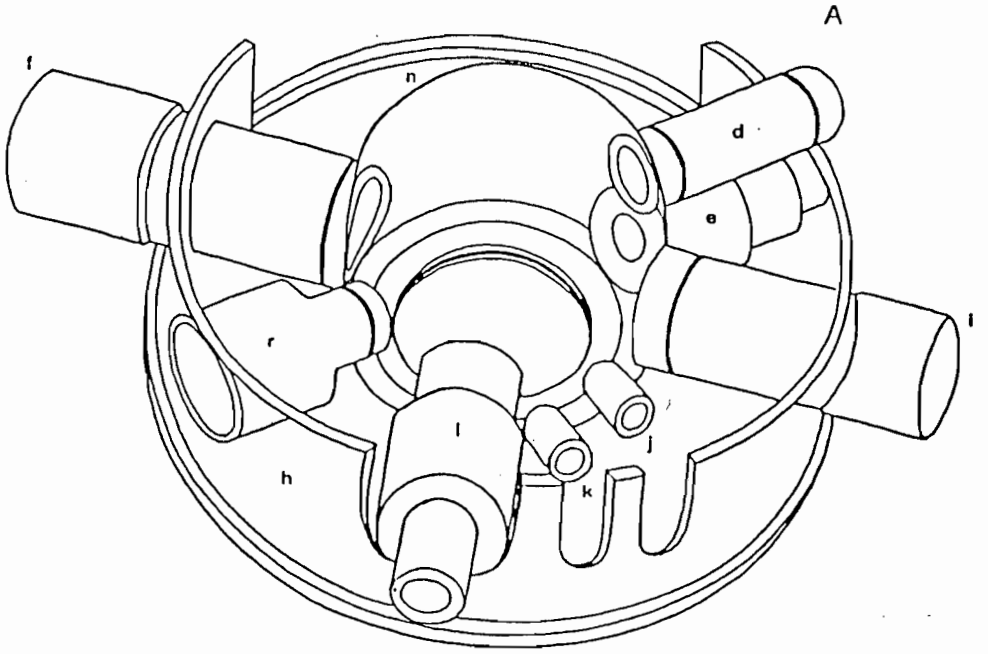

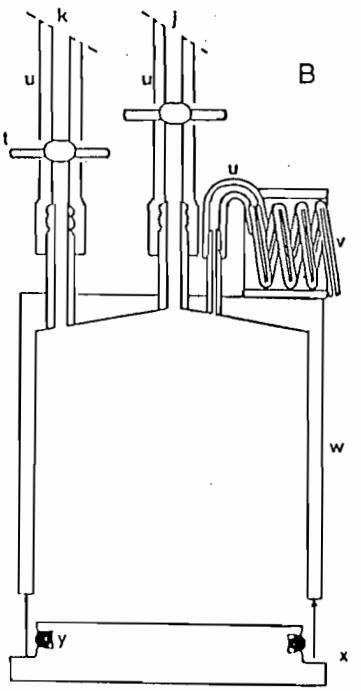

A Oblique
B Section

d pH electrode mount
e inlet ball-valve
f stirrer motor mount
h support ring
i oxygen electrode mount
j inlet
k water outlet
l outlet ball-valve
n specimen compartment
r temperature probe mount
t clamp
u hose
v expansion tube
x base
y 'o'-ring

Plate 9. The *in situ* incubation chamber

A

View from above showing probes inserted and core-drilled crust located in the specimen aperture. Views clockwise from top centre show the pH electrode (with pressure compensation fitting) above the water inlet ball-valve (with hose attached), the oxygen electrode with stirrer bar attached, the air inlet and water outlet nozzles for the collection of water samples, the water outlet ball-valve, the temperature probe, and the stirrer motor.

B

Oblique view with probes removed showing probe fittings with 'o'-ring seals, and the domed roof of the specimen chamber.

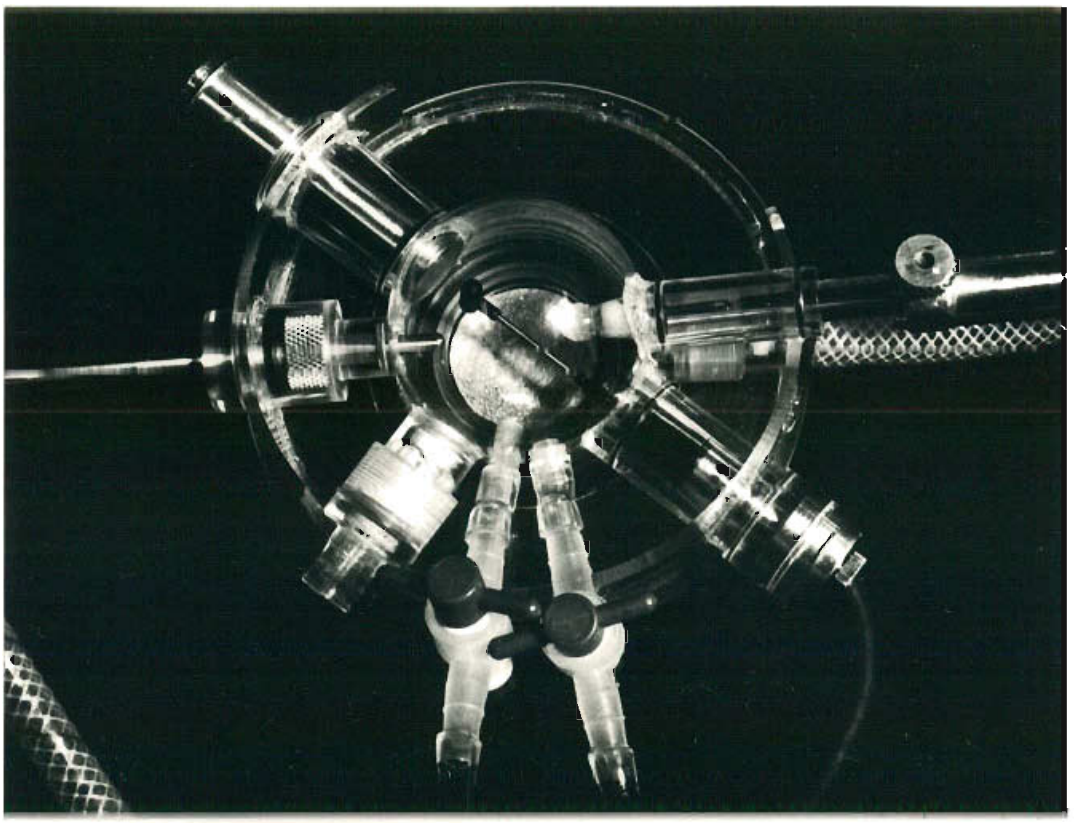

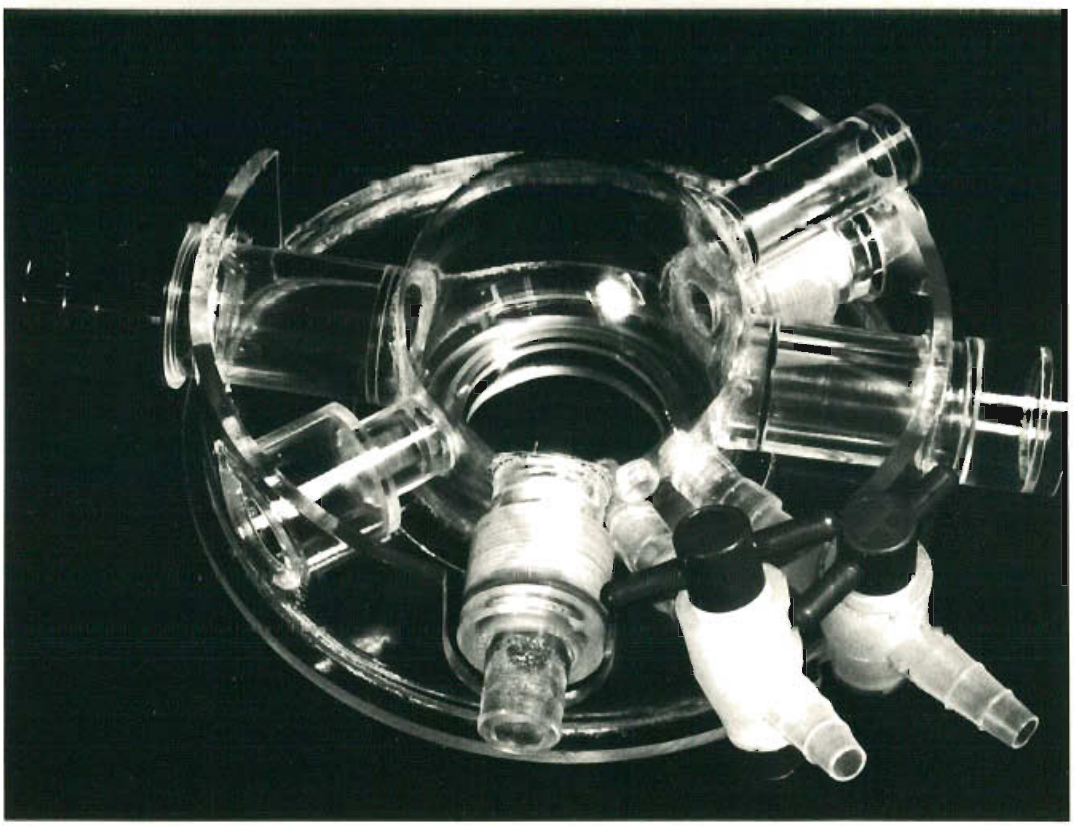

Plate 10. Various views of the *in situ* incubation chamber, two views of the simulated *in situ* incubation chamber, and three views of the water sampling bottle.

A

Incubation chamber with water sampling bottle attached, but base removed. Sampling bottle with three projecting nozzles, two connected by hoses to inlet and outlet nozzles on the specimen chamber, one smaller nozzle connected to a finely bored coil of stainless steel tubing housed within an acrylic cylinder. The hollow coil permits air to expand and leak out during underwater ascent. The base of the bottle press-fits with 'o'-ring seal.

B

Incubation chamber with sampling bottle attached.

C

Incubation chamber below with light sensor chamber above.

D

View of both chambers from above with water sampling bottle attached to the specimen chamber.

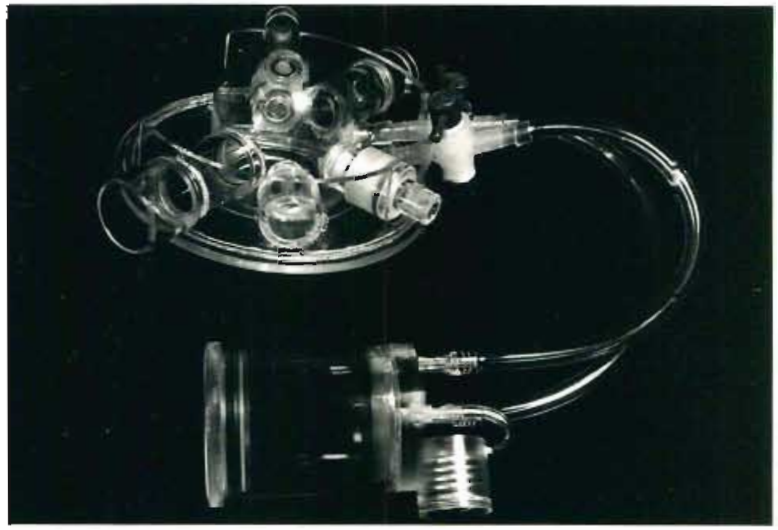

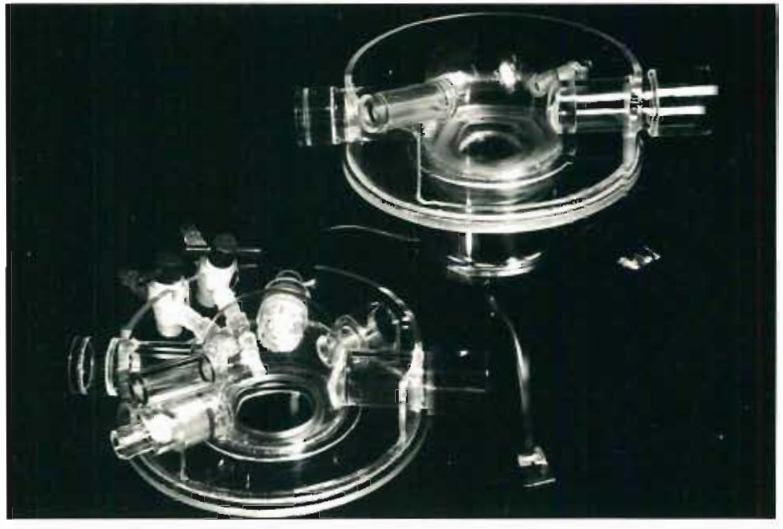

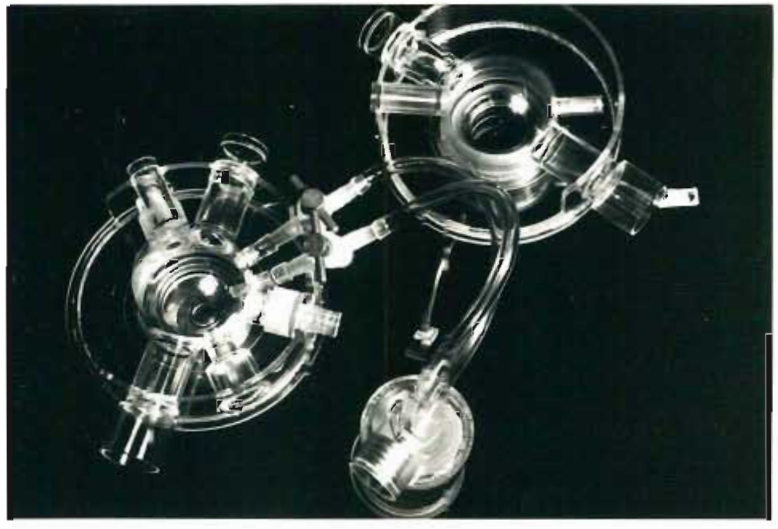

Plate 11. Combined *in situ* apparatus for the measurement of crustose coralline photosynthesis and calcification.

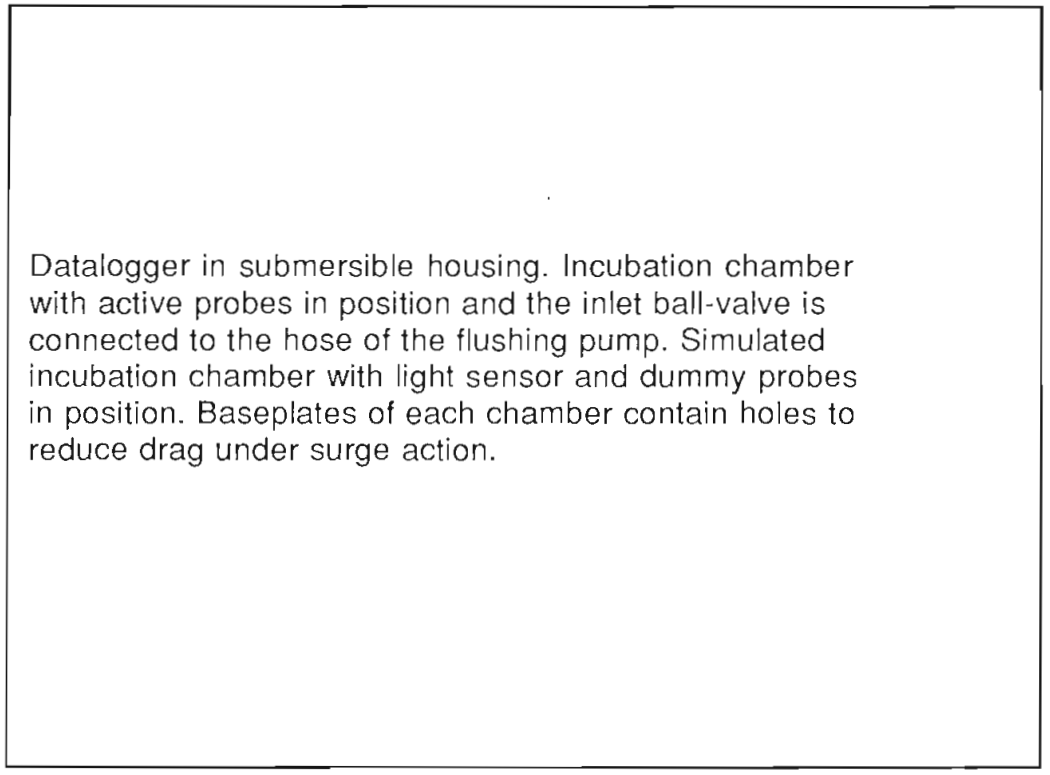

Datalogger in submersible housing. Incubation chamber with active probes in position and the inlet ball-valve is connected to the hose of the flushing pump. Simulated incubation chamber with light sensor and dummy probes in position. Baseplates of each chamber contain holes to reduce drag under surge action.

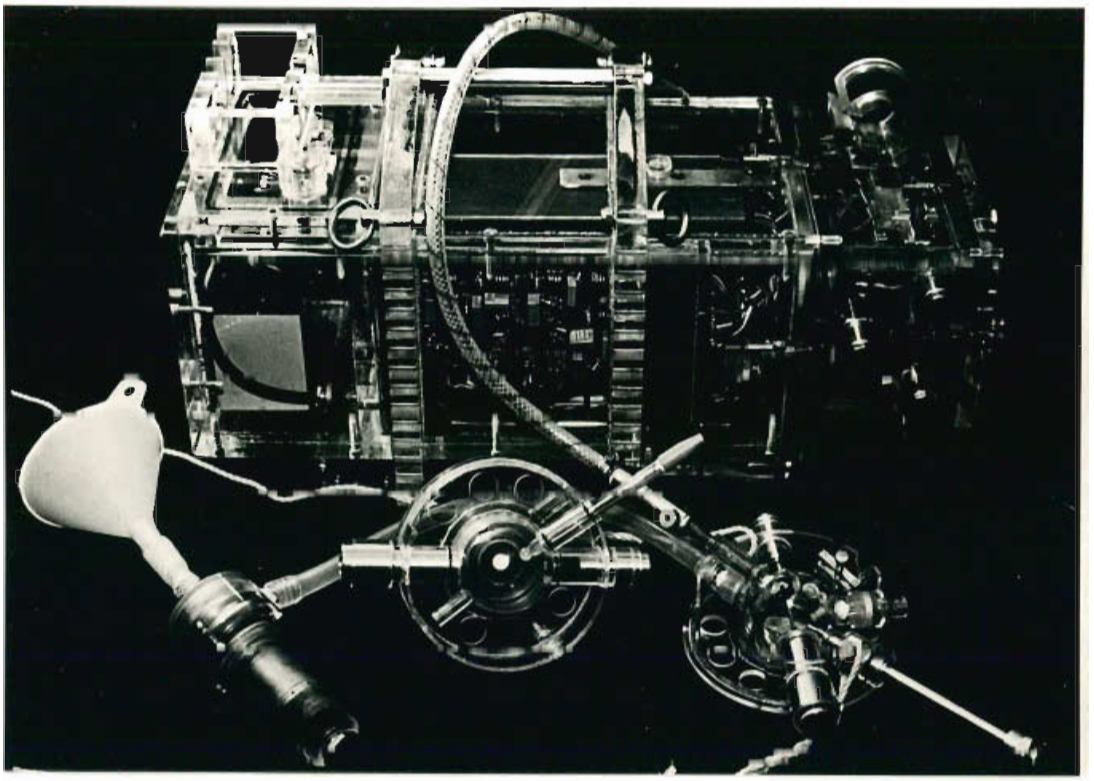

samples (Figs 6A, 7A, & Plates 9, 10). During incubation, short lengths of flexible hose were attached to the nozzles and the hoses were sealed with a clamp (Plate 11). The extraction of water samples was a component of the calcification studies and will be discussed later. Finally holes (17.5 mm diam) were bored through the baseplate of each chamber between the probe fittings to reduce drag under surge action (Plate 11).

The completed electrode chamber was thus fitted with acrylic mountings to accommodate pH, oxygen, and temperature probes, an encased D.C. motor with apical magnet to drive a stirrer bar attached to the oxygen electrode located opposite, and two spring loaded ball valves (Fig. 6A & Plate 9A). The simulation chamber included fittings to house dummy probes but was not fitted with ball valves or extraction nozzles (Plates 10C,D, 11).

The probes and light sensor

The probes used in the primary productivity studies were an EIL galvanic oxygen electrode and an Analog Devices thermister (Model AC 2626 K4 - Nortek Pty. Ltd., Townsville, Queensland) sensitive to 0.1°C. The oxygen electrode was used in conjunction with a 50 mm long EIL stirrer bar attachment so that the tip of the stirrer would magnetically couple with the apical magnet (Escap Model M16) on the shaft of the D.C. motor installed on the opposite side. The motor and apical magnet were sealed within a stainless steel case. The position of the oxygen electrode and stirrer bar attachment is shown in relation to the stirrer motor in Plate 9A.

The light sensor was an Li-192SB underwater quantum sensor. This was held firmly in position within the simulation chamber by twin 'o'-ring seals.

The pump

A small D.C. motor (Escap Model M1616 CH-207), magnetically coupled to a plastic impeller and housed within a pressure resistant acrylic case was used to drive water from the open sea through the chamber at a rate of approximately 500 ml min^{-1}. Water was taken into the pump through a gauze covered, wide-mouthed, filter funnel (See Plates 11, 12). A 12V gel cell battery (Yuasa NP6-12 12V, 6.0Ah) provided power for the pump.

Plate 12. Views of datalogger contained within the submersible pressure resistant acrylic housing, with probes and water pump attached via underwater cables, and one umbilicus to the recording apparatus. Probes and water pump (for flushing) are stored for transport in press-fit mountings. Underwater cables are stored against the sides of the housing in press-fit grooves.

A

Oblique view for front showing bulkhead compartment with operating switches, and 'o'-ring seals between detachable sections.

B

Oblique side view showing analog-digital printed circuit board (designed by the Electronics Workshop, A.I.M.S.) behind rows of stored underwater cable, and the battery compartment at the rear.

C

Oblique side view showing 'D' cell batteries held in racks against the side of the datalogger (behind rows of stored underwater cable), water pump with intake funnel covered with a fine mesh filter, and pressure-resistant hose acting as an umbilical conveying the wire from the pH electrode to the electrical connections in the bulkhead compartment.

D

Oblique view from above showing battery compartment at rear with probes stored in acrylic rack above, central compartment containing the datalogger with carrying handle and water pump held in press-fit mount above, and foremost bulkhead compartment with spring clip fittings.

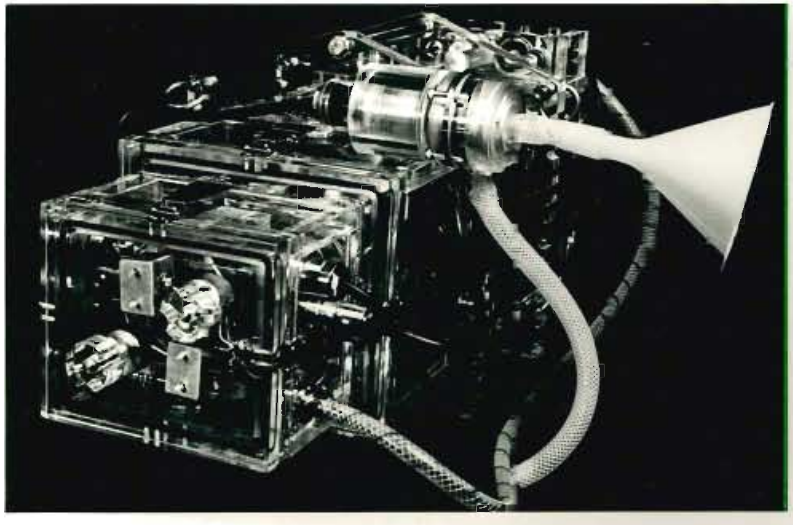

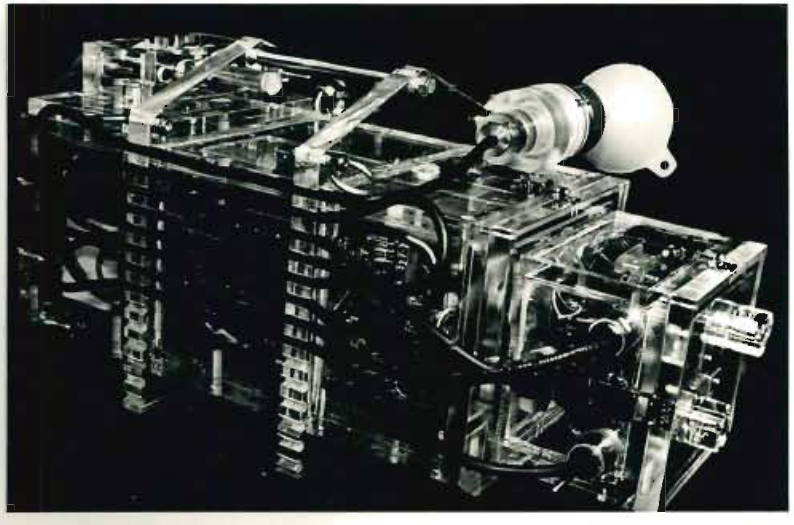

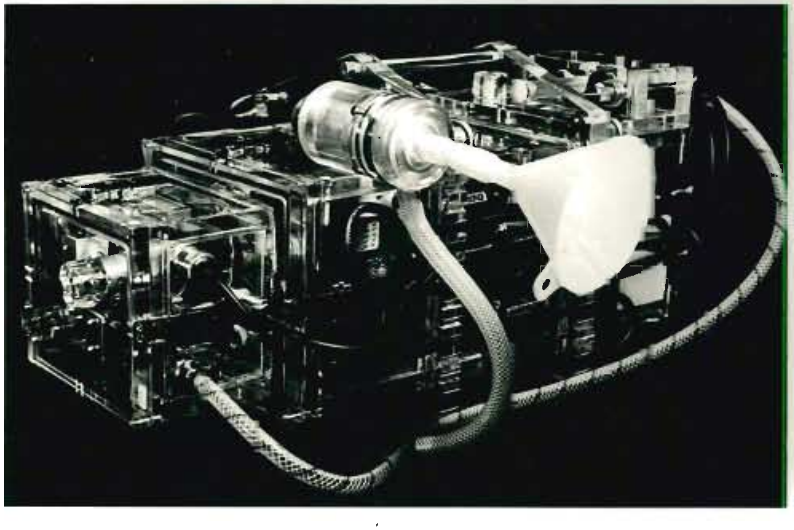

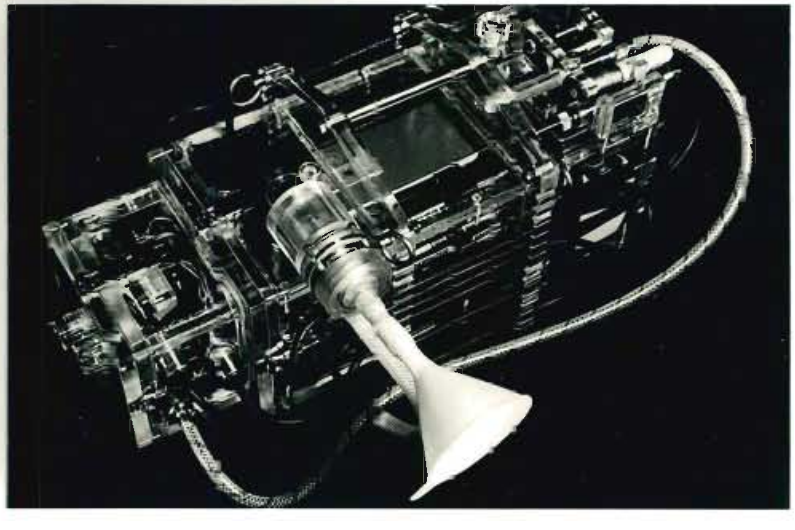

Electrical unions

Heavy duty rubber compression rings were used to seal the entry points of the underwater cables to the probe casings and datalogger housing.

The datalogging device

The datalogging device was designed and built at material cost by the A.I.M.S. Electronics Workshop. An RCA microboard computer (Model CDP18S607) including an RCA microprocessor and memory module (32 kilobytes RAM), were interfaced with an A.I.M.S. analog interface and control board, and an A.I.M.S. analog to digital module, to provide the datalogging package. Six 'D' cell alkaline batteries in series provided power for the logging operation.

The datalogger was sealed within a rectangular, submersible, pressure resistant housing constructed from sheets (15 mm thick) of acrylic (Plates 11, 12). The housing contained three independently sealed compartments. At the rear of the housing was a compartment for the 12V pump battery with a vertical access port to enable changing or re-charging of the battery between deployments. In the centre was a compartment for the datalogger with foam rubber cushioning to prevent shock damage. At the front was a detachable bulkhead compartment to provide access for the wires leading from the probes. Separation of the bulkhead compartment from the datalogger compartment provided an added safety precaution against flooding, assuming that the most likely place for leaks to occur was at the entry points for the connections from the probes and the pump. Electrical connections between the bulkhead compartment and the datalogger were provided by brass pins passing through teflon compression fittings. All separable sections of the housing, except for the 12V battery access port, were sealed using 'o'-rings and stainless steel spring clips. The 12V battery port was sealed by an 'o'-ring and screw fittings.

The front face of the bulkhead compartment was detachable permitting access to the RS 232 port to interface the datalogger with the Epson computer. The switches to control the operation of the datalogger underwater were mounted on the detachable face (Plate 12).

During transport to the experimental sites the probes were stored in a rack attached to the lid of the 12V battery compartment (Plates 11, 12). The underwater cables were held in twin sets of grooves on either side of the housing (Plates 11, 12). The pump was secured in a press-fit mounting above the bulkhead compartment (Plates 11, 12). Five acrylic pockets (one shown in Plate 11) containing a total of 5 kg of lead were attached to the sides and underside of the housing to make the datalogger just negatively buoyant. A carrying handle was fitted together with 4 stainless steel rings at the upper corners of the central compartment (Plates 11, 12B,D). The rings were fitted so that guy ropes bearing snap-hooks could be attached to the housing for anchorage.

The calibration bath

The bath for calibration of the electrodes was constructed from sheets of acrylic (12.5 mm thick)(Plate 14). It consisted of a rectangular tank with detachable lid, which was sealed during use with an 'o'-ring and 6 stainless steel spring clips. Suspended from the underside of the lid were several fittings, with access provided through holes drilled in the lid. These fittings were used to store the calibration solutions at the desired temperature prior to and during calibration of the electrodes. An inlet, carrying water at a constant temperature from a Braun (Model 1441) Pumping Thermomix, was directed onto a rotating wheel beneath a 1.5 l glass beaker suspended from the lid of the bath. At the centre of the wheel was a magnet. When the thermomix was activated the wheel and central magnet revolved driving a large stirrer bar in the 1.5 l beaker. In addition to the probe fittings was a submerged cylinder containing distilled water through which a fine stream of air was fed by an aquarium pump. A build up of air pressure in the cylinder caused a moist stream of air to flow through a fine (1 mm bore) coil of stainless steel tube submerged in the bath. The terminal end of the coil was attached to a hypodermic syringe via a short length of flexible hose and led into the 1.5 l beaker mentioned above. The needle of the hypodermic syringe released a gentle stream of moist air into the beaker containing freshly filtered seawater (0.45 µm Millipore filter). After a 12 hour period of continous aeration and stirring (see above) the solution was used to calibrate the oxygen electrode for the concentration of dissolved oxygen in air-saturated seawater. One additional beaker (1 l) was suspended from the lid of the bath so that the probes could be brought to the correct temperature prior to calibration. Water circulating through the bath was returned to the Thermomix via an outlet port.

Plate 13. Acrylic cell for the determination of zero oxygen.

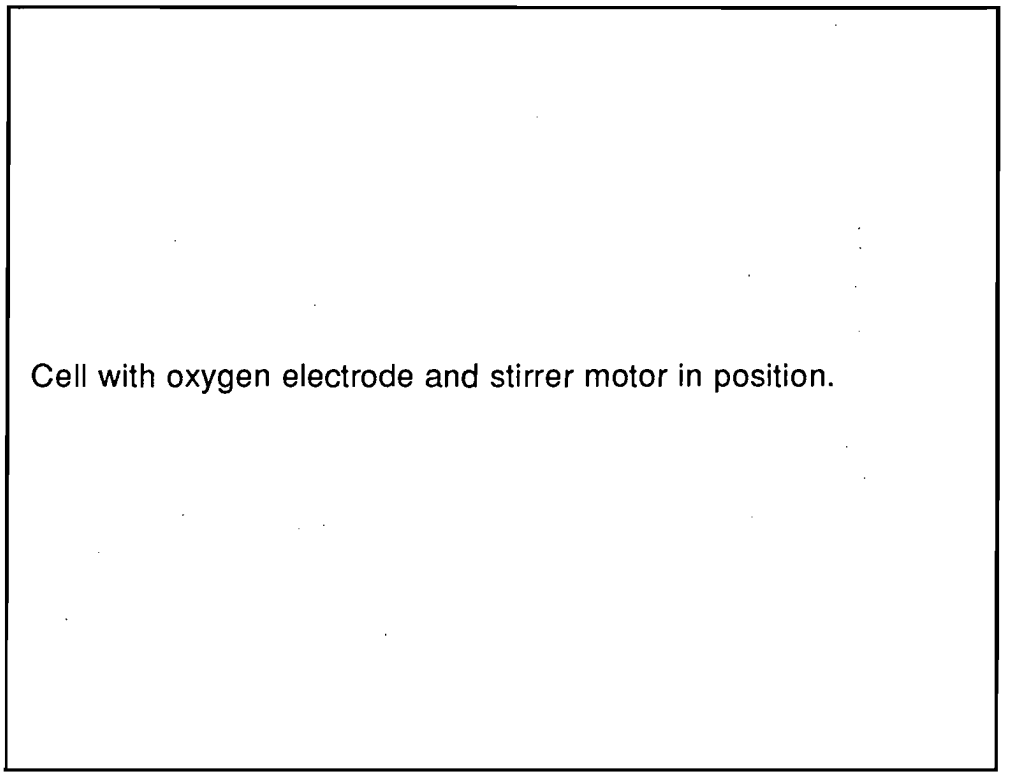

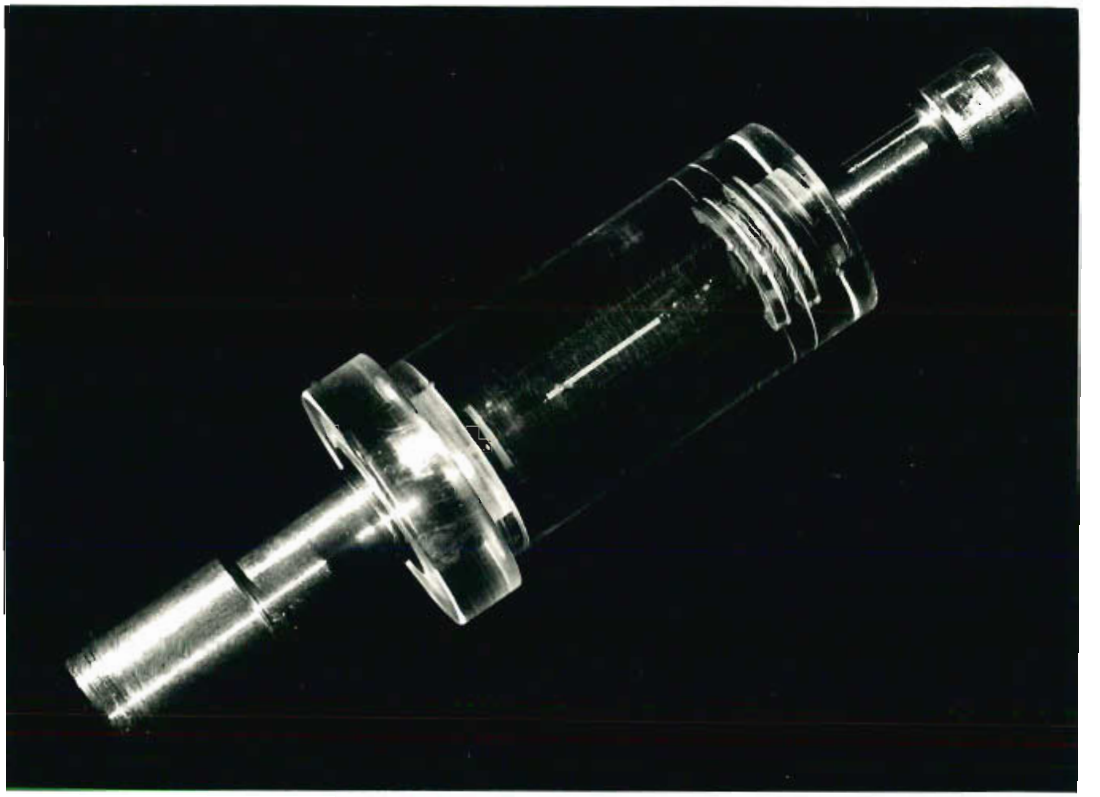

Calibration of sensors

Calibration values for the sensors were channelled directly to the Epson screen monitor via the RS 232 serial ports of the datalogger and the computer.

The Li-192SB underwater quantum sensor was calibrated over a range of PPFD from 0-2250 μEinsteins m^{-2} s^{-1}. Two Li-192SB sensors were used for the calibration. One was wired to the datalogger, the other to a Li-188B Integrating Quantum Radiometer/Photometer. The sensors were taped together and immersed in a bath of seawater beneath a variable illumination source. The voltage output of the datalogger for a given level of irradiance was converted into μEinsteins m^{-1} s^{-1} by comparison with the reading on the Radiometer/Photometer. The plot of voltage vs irradiance was linear over the measured range of PPFD. Irradiance values could thus be determined for any voltage level from the equation of the regression line. The readings on the Radiometer/Photometer were checked by directing the sensor towards the sun at noon on a clear day in March 1986. The recorded value of *ca* 2100 μEinsteins m^{-2} s^{-1} was close to the value reported by Barnes & Devereux (1984) at Rib Reef, near Townsville, in mid-March.

The quantum sensor was calibrated at the start, the middle, and at the end of the *in situ* incubations. Daily checks were made on the stability of the sensor by examining the values recorded at night during the previous incubation. The values recorded for the first calibration were very similar to the values recorded for all subsequent calibrations, and the percentage change over the entire period of field use did not exceed the calibration error quoted by Li-Cor inc./Li-Cor Ltd. for their sensor (± 5%).

The specimen and light sensor chambers were tested for equivalence in light transmission. An Li-192SB quantum sensor attached to a Li-188B Radiometer/Photometer was interchanged between the two chambers and the chambers were rotated under seawater through a number of angles in the path of a fixed illumination source. The maximum percentage difference between the readings for the two chambers was 3%.

The temperature probe was calibrated by immersion in a beaker of ice/water slurry to obtain a zero reading. A single reading was obtained at 23.55°C by

comparison with a Hewlett Packard quartz thermometer which was accurate to 0.05°C (American National Bureau of Standards). Multiple readings were taken at 0.1°C intervals between 23 and 29°C (the broadest range of seawater temperature likely to be encountered at Lizard Island) by immersion in a cooling beaker of warm water with a 0.1 °C graduated mercury thermometer. The response of the probe was linear and a calibration equation was calculated from the regression line. The stability of the probe was confirmed over a period of 6 weeks.

The oxygen electrode was calibrated in the laboratory before each *in situ* incubation. The electrode was held horizontally in mounting brackets projecting from the underside of the lid of the calibration beaker and placed beneath the surface of the air-saturated seawater. The seawater was earthed to an external connection on the datalogger by a fine stainless steel wire to complete the same electrical circuit as existed when the datalogger was deployed underwater. The stirrer motor was placed in a hollow fitting projecting through the side wall of the calibration bath and touching the outside of the beaker immediately in front of the stirrer bar on the electrode. The motor and hence the stirrer bar were activated during calibration. The calibration value was recorded once a stable reading had been obtained for a period of at least 3 minutes. The temperature of the calibration bath was periodically adjusted over the course of the *in situ* incubations to the temperature of the seawater at the experimental sites.

A calibration value for zero dissolved oxygen was obtained by sealing the electrode within a small-volume (5 ml) acrylic cylinder containing a solution of sodium sulphite in seawater (Plate 13). The stirrer motor was located in a socket in the lid of the cylinder.

Experimental procedures

Experiments of 24 hour duration were carried out between March and July in 1986. The seawater temperature ranged from 26.8 °C to 24.2°C over this period. The salinity of the seawater at the experimental sites was measured with a portable temperature-compensated salinity refractometer (American Optical Corporation Model 10419). The salinity remained more or less constant at 35 $\pm$ 0.3°/oo between March and July.

Plate 14. Constant temperature calibration bath.

A

View from above showing two beakers (top of frame), one containing a stirrer bar above a water-driven wheel, the other empty but with lid containing an aperture to admit the oxygen electrode for storage prior to calibration. The small nozzle adjacent to the large beaker feeds moist air through a hypodermic needle into the seawater in the beaker during oxygen calibration. The three small apertures with vials suspended beneath (bottom of frame) hold precision buffer solutions during pH calibration; the small aperture (below centre of frame) accomodates the temperature probe; the aperture with glass boiling tube suspended beneath (bottom left corner) holds pipettes; the medium sized beaker covered with lid(bottom & left of centre) stores ampoules containing precision buffer solutions; the acrylic cylinder with solid base and 'o'-ring sealed cover with projecting fine diameter nozzle (left side of frame) admits the air stream from an aquarium pump.

B

Side view showing suspended beakers with water jet directed onto the rotating wheel beneath the oxygen calibration beaker (left side), and the acrylic mountings suspended beneath the lid of the calibration beaker to hold the oxygen electrode opposite the stirrer motor when inserted into the acrylic fitting projecting through the side of the bath (left side wall)

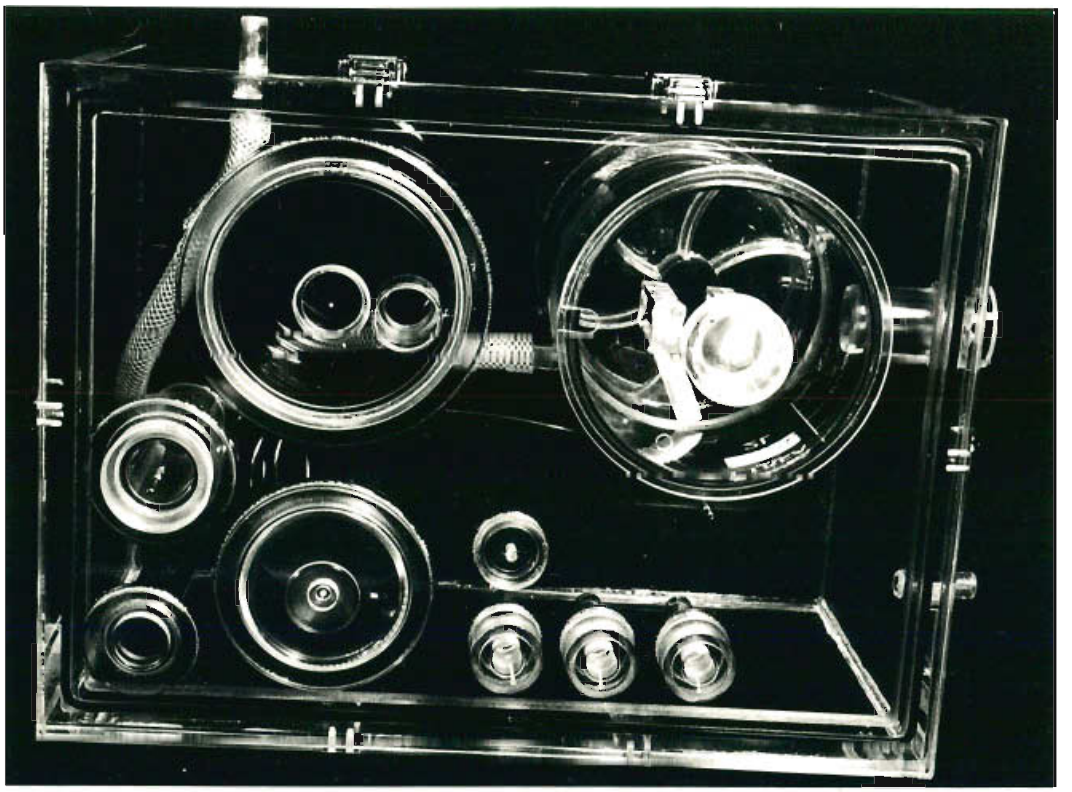

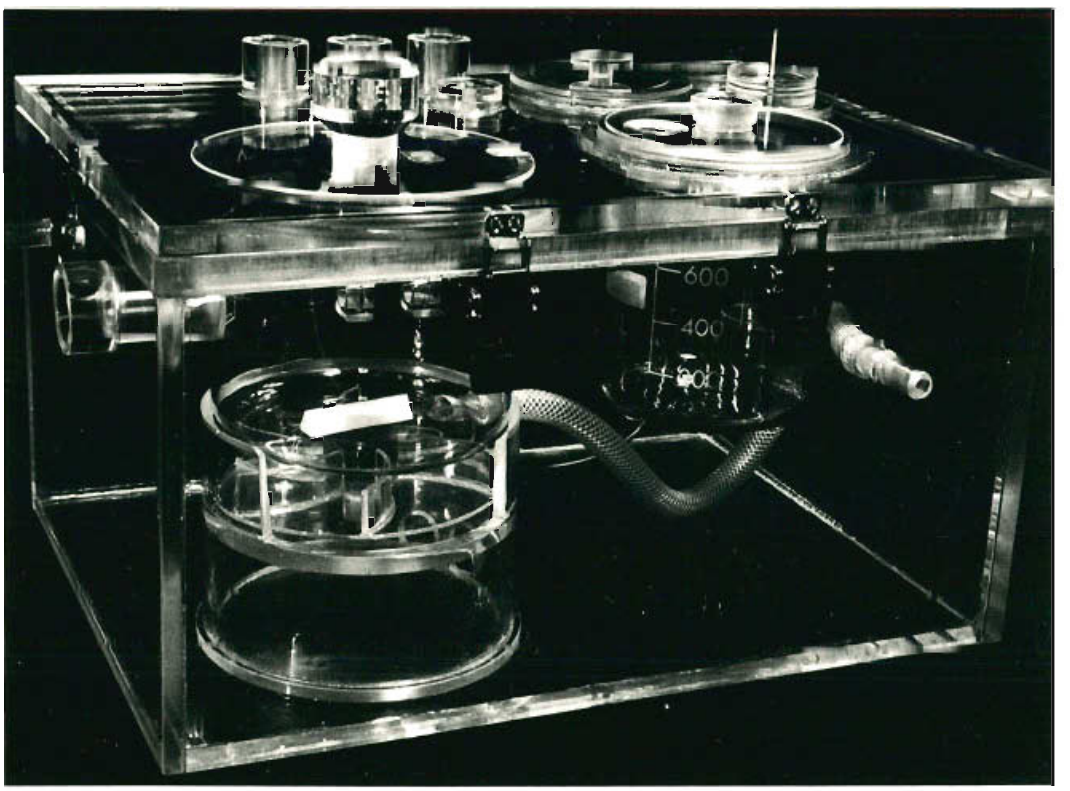
600
400

The probes were calibrated in the laboratory (see above) before each *in situ* incubation.The datalogger was programmed to read the probes and quantum sensor every 6 seconds and to store integrated values for every minute. The pump was activated for 3 min to flush the chamber at intervals ranging from 18-30 min depending on the circumstances. This was to ensure that the oxygen tension within the chamber did not rise to a level which would inhibit photosynthesis.

The chambers were transported to the experimental sites in a protective carrying box (Plate 15). The datalogger was transported within a foam lined container. At the mooring, the datalogger was attached to the snap-hook of a short line connected to a float. The float was attached by a longer line to the stern of the boat. The datalogger was lowered into the water and floated away from the boat pending collection on SCUBA. The carrying box containing the chambers accompanied the diver into the water and the two pieces of apparatus were swum to the experimental site. The datalogger was anchored to the reef by guy ropes at a convenient location close to the specimen. Dump weights were suspended from the handle of the datalogger for added stability. The electrode chamber was eased over the metal sleeve surrounding the specimen and positioned with the upper surface of the baseplate in line with the top of the sleeve. The electrode chamber was stabilised by two nylon guy ropes attached to 3 lb lead weights. The guy ropes possessed rubber tensioners and were spliced to the supporting rim of the electrode chamber. The probes were removed from the carrying rack and inserted through the mounting fittings into the specimen chamber. Finally, the simulated chamber containing the light sensor and dummy probes was secured next to the electrode chamber in the same orientation. The time was recorded and the logging operation was commenced.

The equipment was collected 24 hours later and the specimen with encircling band was chipped free from the substrate using a cold chisel. The specimen was transported to the laboratory in a container of seawater. The RAM-held data was accessed by user-written software and stored on floppy disk. The specimen was returned to the electrode chamber in a large container of seawater and the probes were re-installed. The chamber was then removed from the seawater and positioned above a pre-weighed beaker. The pH electrode was gently removed so that the water contained in the chamber could flow into the beaker without spillage. The beaker was re-weighed and the volume of water gravimetrically determined. The specimen was removed from the chamber, immediately snap-frozen (at -30°C) in dry ice, tightly

Plate 15. Protective box with carrying handle for the *in situ* chambers.

A

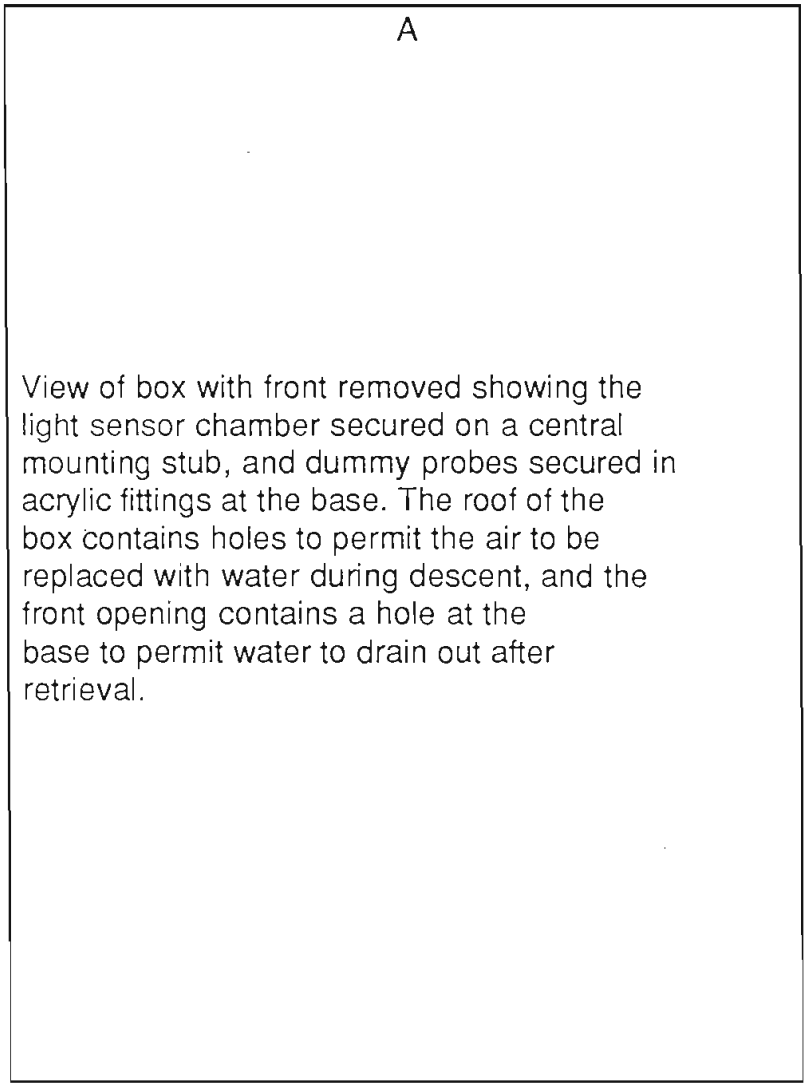

View of box with front removed showing the light sensor chamber secured on a central mounting stub, and dummy probes secured in acrylic fittings at the base. The roof of the box contains holes to permit the air to be replaced with water during descent, and the front opening contains a hole at the base to permit water to drain out after retrieval.

B

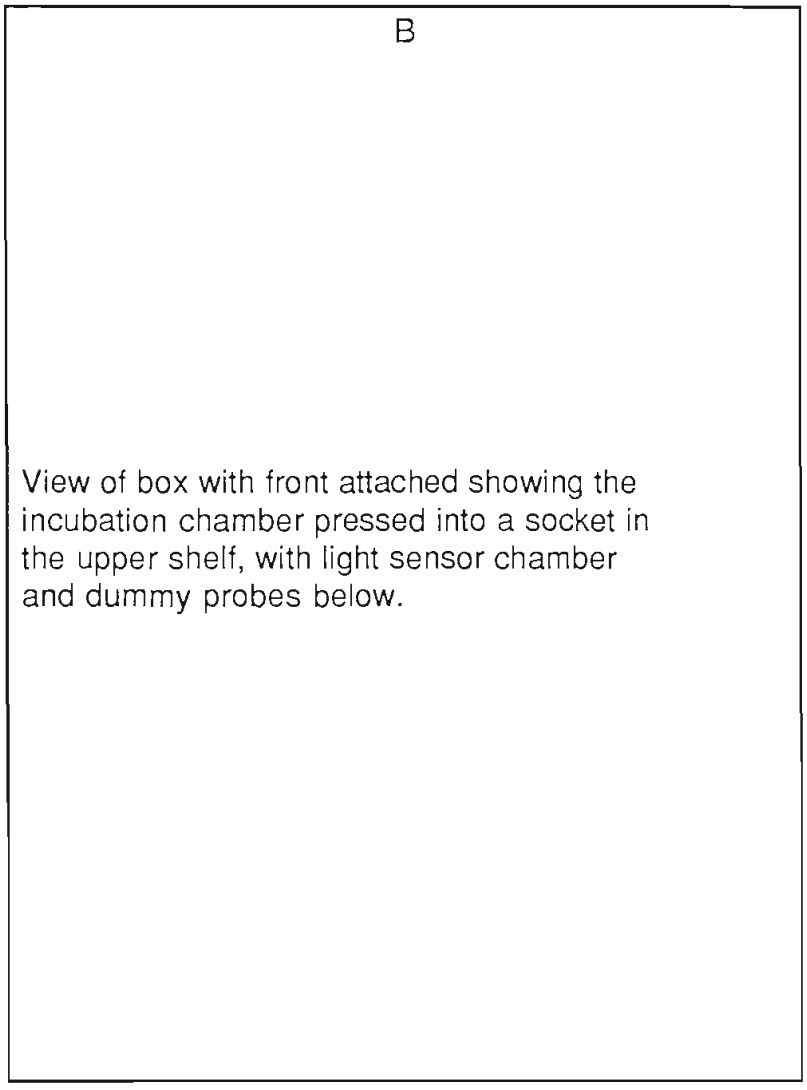

View of box with front attached showing the incubation chamber pressed into a socket in the upper shelf, with light sensor chamber and dummy probes below.

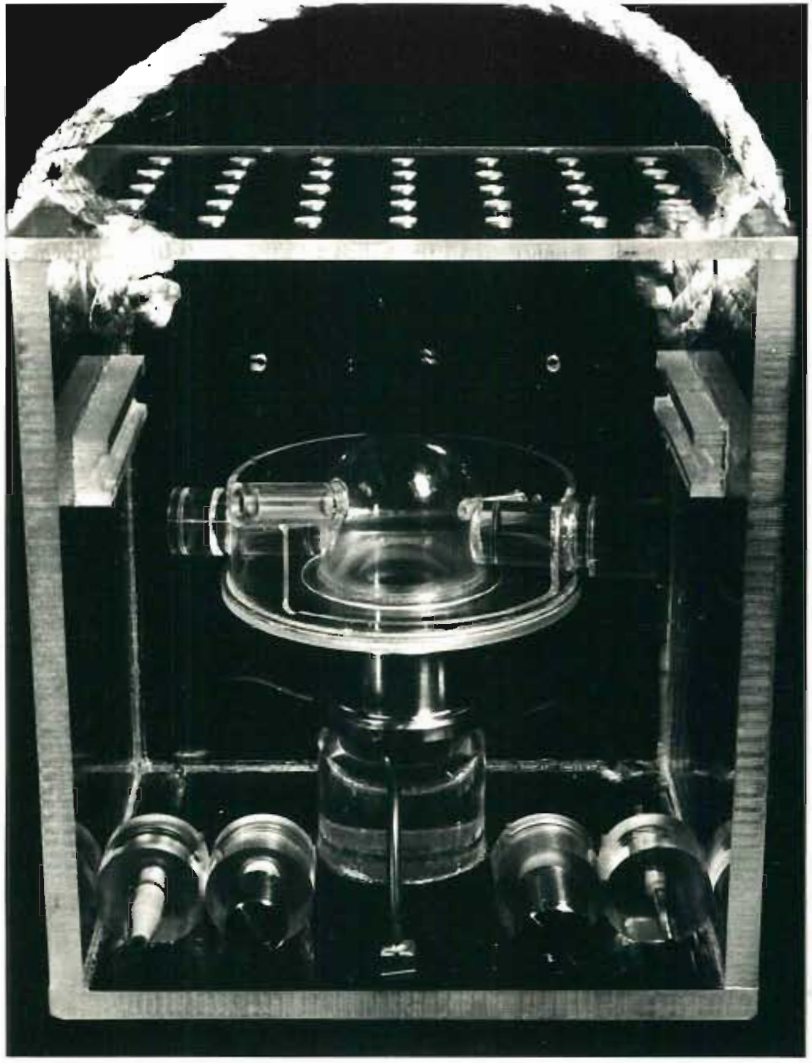

wrapped in heavy duty aluminium foil and stored in darkness at -20°C pending extraction of pigments and protein.

Real surface area, projected surface area, and **chlorophyll *a* content** were determined for each specimen by the methods described in Section 2. 2. 1.

2. 3. 2. ANALYSIS OF DATA

The *in situ* data were corrected for calibrations, temperature and salinity, and converted into micromolar changes in oxygen concentration per hour (μmol O_2 l^{-1} h^{-1}) on a computer using software originally written by Dr. D.J. Barnes (A.I.M.S.) and modified to suit the particular requirements. Changes in dissolved O_2 were converted into equivalent changes in carbon dioxide (μmol CO_2 l^{-1} h^{-1}) using the metabolic quotients derived from the calcification studies. The changes in O_2 and CO_2 concentration per hour were calculated for each interval between flushings of the chamber and these were regressed against the mean PPFD over the same periods.

Light-saturation curves

Light-saturation curves for *in situ* photosynthesis were analysed by non-linear, least squares regression using subroutine BMDP3R of the BMDP statistical package. The curves were modelled by the hyperbolic tangent function. The hyperbolic tangent function (Eq. 3) was used because the more variable nature of the *in situ* data when compared with the laboratory data gave no indication that alternative models needed to be sought and the hyperbolic tangent function has been the preferred function in the literature until now (Chalker 1981). Further analyses will confirm if the hyperbolic tangent function is the most appropriate model to use for *in situ* light-saturation data. Preliminary investigations suggest that models developed latterly to analyse laboratory *P-I* data may also be applicable to *in situ* data. However, applying the suite of functions described in Section 2. 2. 2 to a small number of test data sets did not significantly reduce the confidence intervals of the parameter estimates nor improve the coefficients of determination.

Further analyses of the light saturation curves followed the procedures described in Section 2. 2. 2.

Statistical analysis

ANOVAs were carried out to determine the significance of the proposed regressions between photosynthesis and irradiance using the hyperbolic tangent function.

Two-way ANOVAs were performed on the photokinetic parameters I_c, I_k, α, and $P^g_m/-R$ ratio. Statistical comparisons were made between the parameter estimates for *Porolithon onkodes*, *Neogoniolithon fosliei* and *Paragoniolithon conicum* at depths of 0 and 6 m. The sample sizes of the groups compared are given in Fig. 8. *Hydrolithon reinboldii* was not included in the tests because no measurements were made at 0 m. Similarly no comparisons were made between parameter estimates at 3 m beacause *P. onkodes* was not measured at this depth. The estimates for *P. onkodes* at 6 m actually resulted from experiments conducted in shaded habitats at a depth of 2.5 m. However, as with the laboratory studies, the PPFD available to these specimens was equivalent to a depth of 6 m and for this reason all further discussion will refer to the depth as '6' to equate with the PPFD.

Residual analysis was carried out on all data sets. Student-Newman-Keuls (SNK) tests were carried out where significant differences were found between the parameter estimates for different species. SNK tests were not performed on depth (≡ irradiance) effects since only two depths were compared.

2. 4. RESULTS AND DISCUSSION

The following sections present the results of the laboratory and *in situ* investigations of photosynthesis, which include studies of photoadaptation and estimates of primary production and consumption by crustose coralline algae. The results are combined with associated discussion to facilitate cross-referencing between text and figures. Laboratory and *in situ* investigations of photoadaptation and primary production are considered together for the purposes of comparison. An appraisal of data normalisation precedes description of the light saturation curves (*P-I* curves) and discussion of the modelling methods. The results of regression analyses between the photokinetic parameters describing the *P-I* responses of each species, and the percentages of surface irradiance (%SI) transmitted to the depths at which the algae

Fig. 8. *In situ* specimen groups tested by two-way ANOVA for significant differences in the values of parameters I_c, I_k, α, and $P^g_m/\text{-}R$. n = sample size. *Porolithon onkodes* specimens were not living at 6 m but experienced a PPFD equivalent to that depth.

DEPTH	SPECIES		
m	*Porolithon onkodes*	*Neogoniolithon fosliei*	*Paragoniolithon conicum*
0	n = 5	n = 4	n = 4
6	n = 4	n = 3	n = 4

were growing, are then discussed in the context of possible photoadaptation. Significant differences in the physiological attributes of the species are examined using ANOVAs. Compensation points and light saturation levels for the crustose corallines are then discussed and compared with other algae. Finally, rates of primary production and consumption are provided for each species at the depths sampled, and the rates are regressed against irradiance to permit estimation of carbon fixation throughout the measured range of PPFD.

2. 4. 1. DATA NORMALISATION

Individual rates of photosynthesis and respiration were normalised on the bases of projected surface area, real surface area, and chlorophyll *a* content. Real surface area produced marginally smaller coefficients of variation (*CV* = standard deviation expressed as a percentage of the mean) than projected surface area, and considerably smaller coefficients of variation than chlorophyll *a* content (Tables 2, 3). Attempts to correct chlorophyll *a* contents for the variable contributions by endolithic algae were unsuccessful. Plate 7 demonstrates that it is possible to distinguish accessory pigments originating from endolithic algae within the coralline skeletons, but the ratio between the quantities of these and the associated chlorophyll *a* is not consistent. Moreover, the amount of chlorophyll *a* originating from endolithic deposits is often large with respect to that extracted from the coralline tissue (Appendix 1; see also Wanders 1977). The net result is that the relative error involved in subtracting a large and variable value from an only slightly larger one is too great to permit meaningful standardisation on the basis of chlorophyll *a* content. Assimilation numbers have been calculated (see Tables 11, 12 presented in Section 2. 4. 7) but these are considered unreliable because they probably significantly underestimate the true values for the coralline algae for the reasons given above.

This study found real surface area to produce a greater reduction in the variability of the data than projected area (Tables 2, 3), which contrasts with an earlier study by Littler (1973a) where the reverse was found (cf Littler 1973c and Littler & Doty 1975). Littler's (1973a) result seems a little surprising since the high productivity of coral reef communities has been frequently attributed to enlargement of the photosynthetic surface (e.g., Dahl 1973, 1976; Wanders 1976; Smith 1981). Real surface area should thus provide a better gauge of production rate than projected area.

Table 2. Coefficients of variation (%*CV*) for laboratory estimates of P^{g}_{m}, P^{n}_{m}, and -*R* for different species, when data are normalised on the basis of projected surface area, real surface area, and chlorophyll *a* content respectively.

Species	Projected Area			Real Surface Area			Chlorophyll *a*		
	P^{g}_{m} %	P^{n}_{m} %	-*R* %	P^{g}_{m} %	P^{n}_{m} %	-*R* %	P^{g}_{m} %	P^{n}_{m} %	-*R* %
Porolithon onkodes	15.2	17.4	14.7	11.0	14.4	11.2	29.6	29.1	34.8
Neogoniolithon fosliei	14.9	16.6	14.5	9.5	11.7	9.2	16.6	17.5	16.8
Hydrolithon reinboldii	11.1	15.2	18.8	9.0	13.2	18.2	28.3	30.6	28.4
Paragoniolithon conicum	20.7	26.3	12.1	16.9	22.7	11.5	26.5	31.3	21.2
Mean *CV*	15.5	18.9	15.0	11.6	15.5	12.5	25.2	27.1	25.3
Grand Mean *CV*		**16.5**			**13.2**			**25.9**	

Table 3. Coefficients of variation (%*CV*) for *in situ* estimates of P^{g}_{m}, P^{n}_{m}, and -*R* for different species, when data are normalised on the basis of projected surface area, real surface area, and chlorophyll *a* content respectively.

Species	Projected Area			Real Surface area			Chlorophyll *a*		
	$P^g{}_m$ %	$P^n{}_m$ %	-*R* %	$P^g{}_m$ %	$P^n{}_m$ %	-*R* %	$P^g{}_m$ %	$P^n{}_m$ %	-*R* %
Porolithon onkodes	16.8	19.2	8.5	12.3	14.7	8.5	25.0	26.0	24.7
Neogoniolithon fosliei	13.7	18.3	4.8	9.0	13.8	11.3	13.3	16.2	14.8
Hydrolithon reinboldii	11.1	15.7	16.3	9.7	14.7	14.9	21.7	35.9	21.3
Paragoniolithon conicum	11.7	15.8	15.2	7.7	11.5	18.1	41.5	43.8	35.3
Mean *CV*	13.3	17.2	13.0	9.8	13.7	13.2	25.4	30.5	24.0
Grand Mean *CV*		14.5			12.2			26.6	

In fact, the ratio between real and projected surface area was often close to unity for the crustose corallines examined in this study. In consequence, the results did not differ greatly using either basis for normalisation. The small differences between projected and real surface area measurements, together with the relatively large variation in apparent rates of crustose coralline photosynthesis, and the errors involved in measuring each area parameter, may possibly explain the divergence between the results of Littler's (1973a) and the present study.

2. 4. 2. LIGHT SATURATION CURVES

Representative light-saturation curves (*P-I* curves) for each species, at the depth intervals studied, are presented in Figs 9, 10, 11, and 12. Tables 4 (laboratory) and 5 (*in situ*) present the parameter estimates which describe the significant features of each *P-I* curve. *In situ* data were modelled by the hyperbolic tangent function (Eq. 3). Laboratory data were modelled by one of four equations: the right rectangular hyperbola (Eq. 1), a simple exponential function (Eq. 2), the hyperbolic tangent function, and a general exponential function (Eq. 4). In each case the function selected was the one which produced the narrowest confidence intervals around the parameter estimates and the highest coefficient of determination (r^2) for the modelled data. The 95% confidence intervals for the parameter estimates and r^2 values are also included in Tables 4 and 5.

The *P-I* curves in Figs 9, 10, 11, and 12B-F are similar in shape to those obtained for phytoplankton when photoinhibition is not observed (e.g., Jassby & Platt 1976; MacCaull & Platt 1977; Scott & Jitts 1977; Harris 1978), intact hermatypic corals (eg., Barnes & Taylor 1973; Wethey & Porter 1976a, b; Scott & Jitts 1977; Porter 1980; Zvalinskii *et al.* 1980; Chalker 1981; Falkowski & Dubinsky 1981; Chalker *et al.* 1983; Porter *et al.* 1984; Jokiel & Morrissey 1986), as well as their isolated endosymbiotic algae (eg., Halldal 1968; Chalker & Taylor 1978; Crossland & Barnes 1978) and various macroalgae (eg., King & Schramm 1976; Vooren 1981; Carpenter 1985). Initially, photosynthesis is nearly directly proportional to irradiance. Thereafter the relationship becomes increasingly non-linear and with variable rate the curve approaches a horizontal asymptote. Photoinhibition was not observed in the present study except for the species *Paragoniolithon conicum* in the laboratory at

Fig. 9. Representative light-saturation curves for gross photosynthesis in *Porolithon onkodes*.

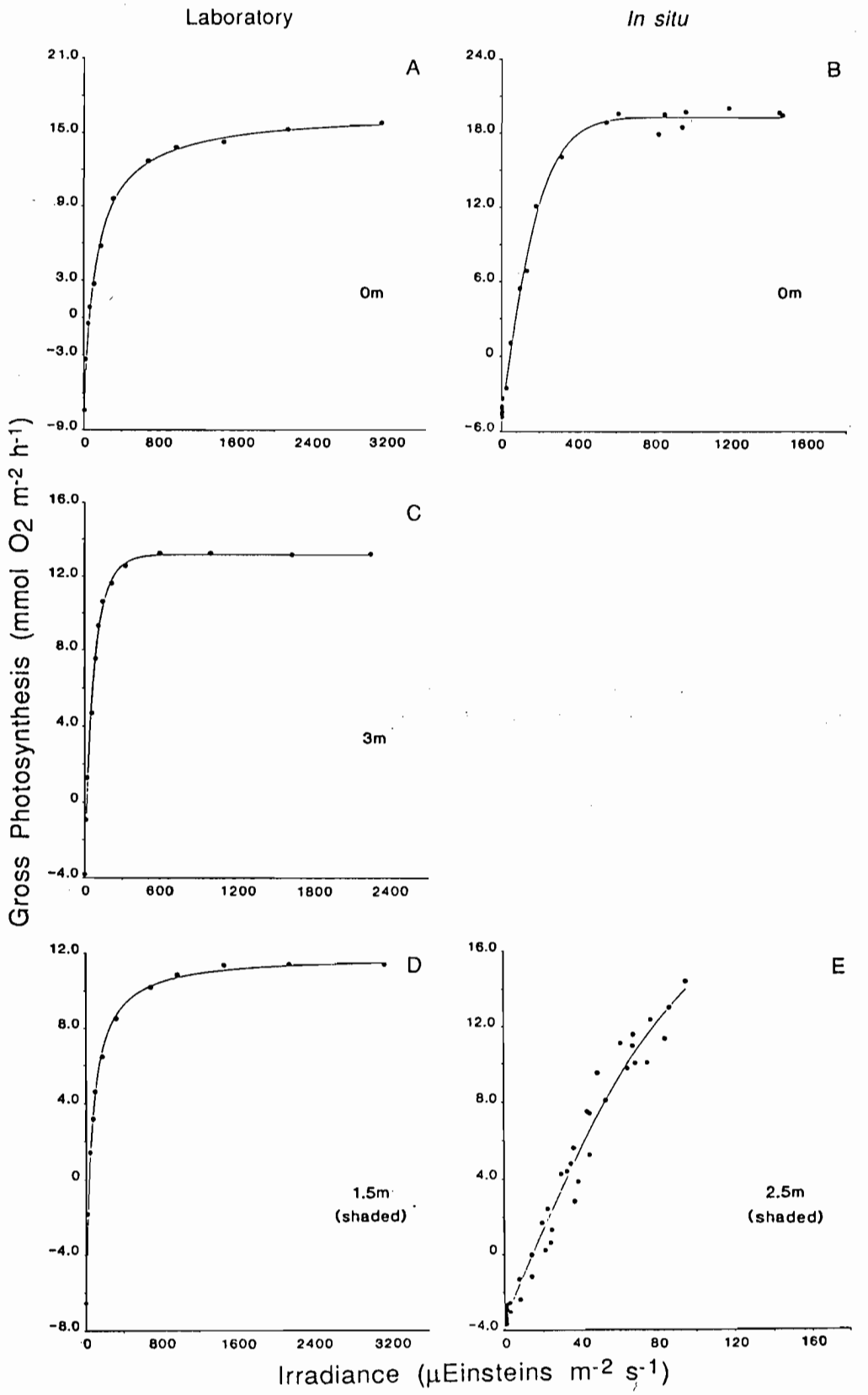
Porolithon onkodes
Laboratory
In situ
A
B
C
D
E
0m
0m
3m
1.5m
(shaded)
2.5m
(shaded)
Gross Photosynthesis (mmol O2 m-2 h-1)
Irradiance (µEinsteins m-2 s-1)

Fig. 10. Representative light-saturation curves for gross photosynthesis in *Neogoniolithon fosliei*.

Neogoniolithon fosliei

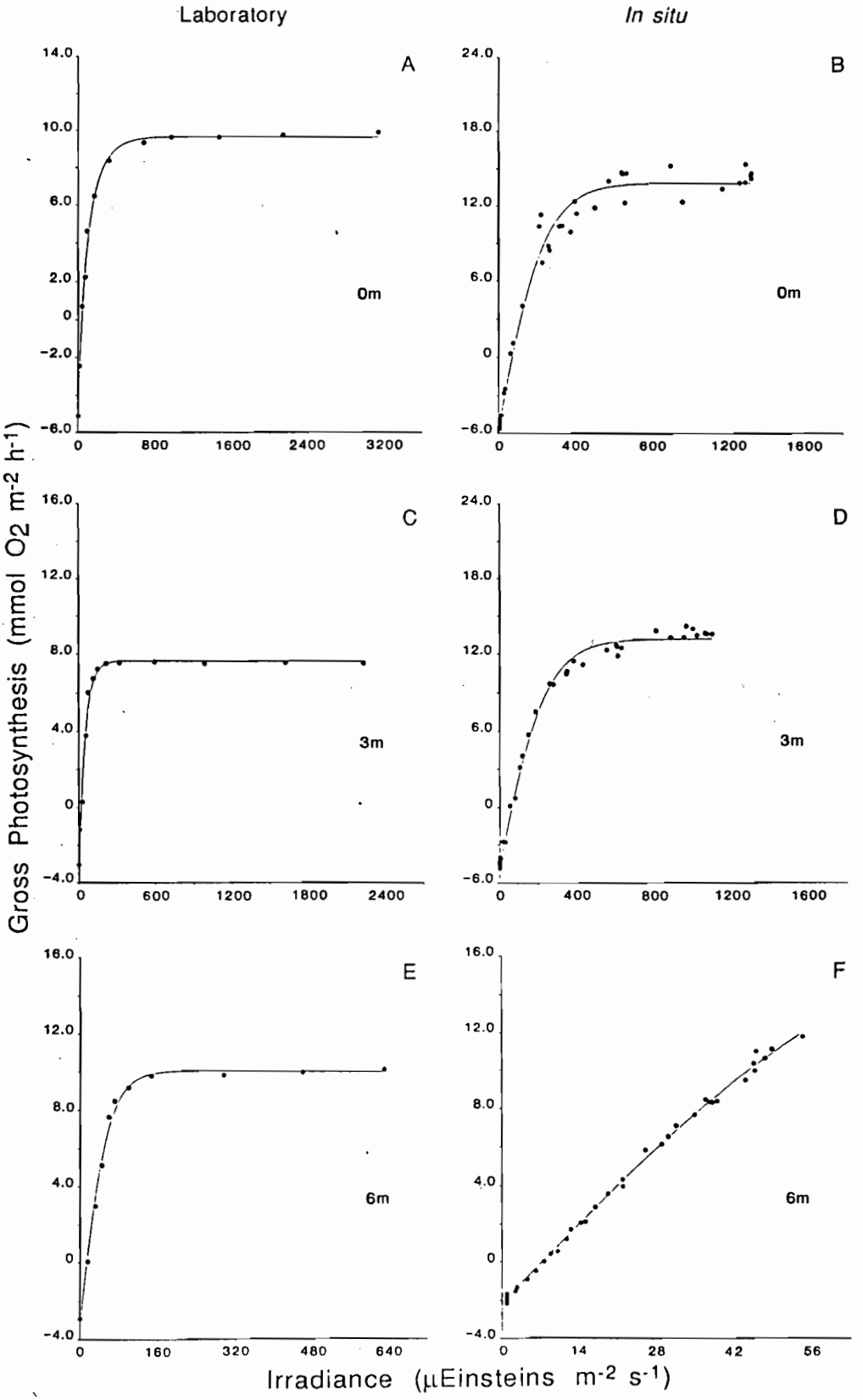

Fig. 11. Representative light-saturation curves for gross photosynthesis in *Hydrolithon reinboldii*.

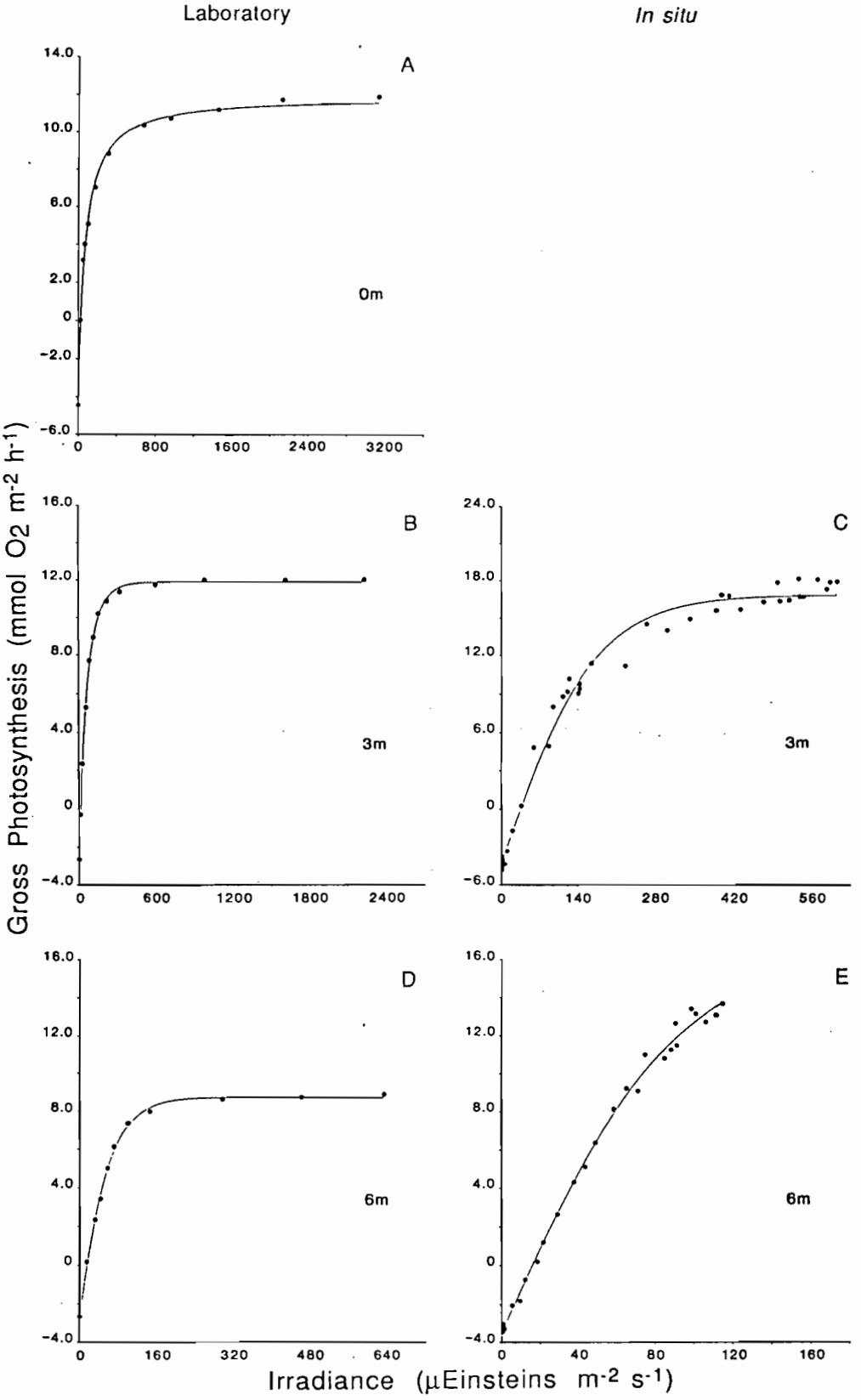
Hydrolithon reinboldii
Laboratory
In situ
A
0m
B
3m
C
3m
D
6m
E
6m
Gross Photosynthesis (mmol O2 m-2 h-1)
Irradiance (µEinsteins m-2 s-1)

Fig. 12. Representative light-saturation curves for gross photosynthesis in *Paragoniolithon conicum*.

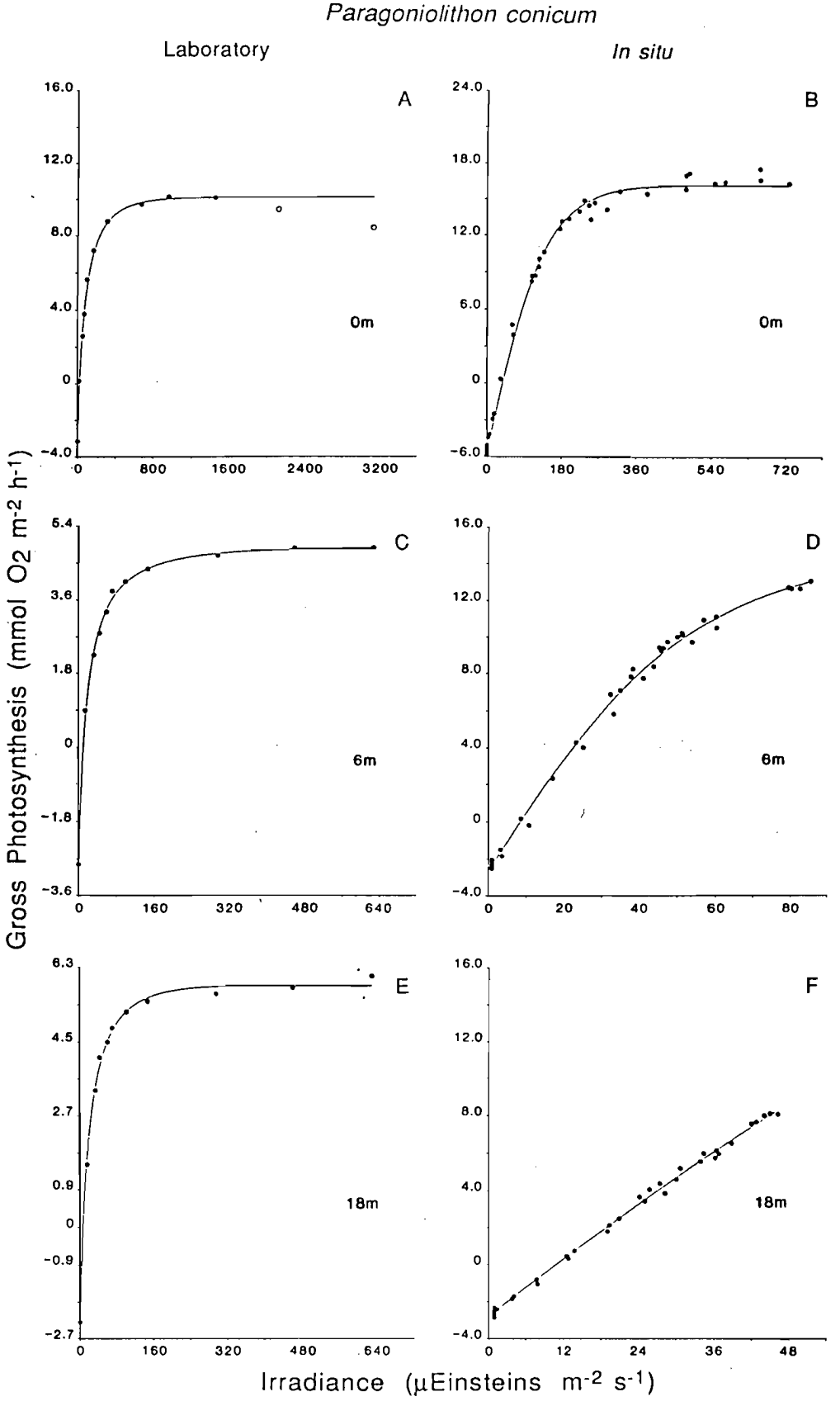
Paragoniolithon conicum
Laboratory
In situ
A
B
C
D
E
F
0m
0m
6m
6m
18m
18m
Gross Photosynthesis (mmol O2 m-2 h-1)
Irradiance (µEinsteins m-2 s-1)

Table 4. Parameter estimates, 95% confidence intervals (CI), and r^2 values for laboratory light-saturation curves for photosynthesis in different species of coralline algae from different depths (see text for parameter definitions). Mean values are given for each set of *n* (*n* = sample size) parameter estimates. The modelling function applied to each data set is indicated by the value for epsilon (ε). When ε=1, the modelling function was the hyperbolic tangent (Eq. 3); when ε=0, the modelling function was a simple exponential (Eq. 2); when ε=-1, the modelling function was the right rectangular hyperbola (Eq. 1); and when $-1<\varepsilon<1$ but $\varepsilon\neq0$, the modelling function was a general exponential (Eq. 4).

Species	Depth	n	P^g_m	P^n_m	R	P^g_m/-R	α	I_c	I_k	$I_{0.95}$	e	r^2
	m		mmol O_2 m^{-2}(proj.area) h^{-1}									
			20.3 ±0.69	16.1	-4.14 ±0.59	4.89 ±0.71	0.18 ±0.03	26.4	110 ± 15.5	492 ± 70	-0.46 ±0.25	0.999
			23.6 ±0.75	16.6	-6.95 ±0.68	3.39 ±0.35	0.16 ±0.02	49.4	144 ± 18.3	2736 ± 347	-1.00	0.998
P. onkodes	0	6	25.9 ±1.76	20.9	-5.02 ±1.45	5.16 ±1.53	0.22 ±0.07	27.3	120 ± 31.4	604 ± 159	-0.56 ±0.43	0.996
			30.2 ±2.41	23.2	-7.06 ±1.81	4.29 ±1.15	0.21 ±0.07	41.0	142 ± 38.4	843 ± 229	-0.66 ±0.40	0.995
			12.9 ±0.30	9.3	-3.64 ±0.28	3.55 ±0.28	0.12 ±0.01	34.9	111 ± 9.7	2109 ± 183	-1.00	0.999
			21.2 ±0.68	16.2	-4.98 ±0.47	4.26 ±0.43	0.18 ±0.02	35.1	118 ± 10.8	936 ± 86	-0.81 ±0.12	0.999
		x	22.4	17.1	-5.30	4.26	0.18	35.7	124	1286	-0.75	0.998
			15.2 ±1.28	10.3	-4.97 ±0.86	3.06 ±0.59	0.21 ±0.06	33.8	71.2± 14.7	783 ± 161	-0.91 ±0.24	0.995
			14.9 ±0.54	9.7	-5.21 ±0.47	2.86 ±0.28	0.17 ±0.03	41.9	89.5± 13.8	386 ± 60	-0.42 ±0.27	0.999
N. fosliei	0	4	16.8 ±0.78	11.9	-4.90 ±0.67	3.44 ±0.50	0.17 ±0.04	37.0	100 ± 19.5	443 ± 86	-0.45 ±0.34	0.998
			13.6 ±0.57	9.7	-3.89 ±0.49	3.50 ±0.46	0.17 ±0.03	29.4	78.7± 12.6	452 ± 73	-0.64 ±0.23	0.998
		x	15.1	10.4	-4.74	3.22	0.18	35.5	84.9	516	-0.61	0.998
			15.7 ±0.74	10.3	-5.34 ±0.69	2.94 ±0.41	0.29 ±0.05	24.0	54.9± 8.5	1043 ± 161	-1.00	0.996
			13.9 ±0.65	8.7	-5.24 ±0.62	2.65 ±0.34	0.22 ±0.04	28.9	62.7± 9.9	1192 ± 188	-1.00	0.996
H. reinboldii	0	5	16.4 ±0.40	12.4	-4.01 ±0.38	4.08 ±0.40	0.29 ±0.03	18.0	57.3± 4.7	1089 ± 89	-1.00	0.999
			16.1 ±0.87	11.9	-4.11 ±0.82	3.91 ±0.81	0.23 ±0.05	22.2	70.8± 13.1	1344 ± 248	-1.00	0.995
			14.4 ±0.75	8.75	-5.65 ±0.71	2.55 ±0.35	0.28 ±0.05	25.7	60.0± 8.7	969 ± 165	-1.00	0.996
		x	15.3	10.4	-4.87	3.23	0.26	23.8	59.4	1128	-1.00	0.998
			15.1 ±1.35	11.5	-3.59 ±0.61	4.20 ±0.80	0.15 ±0.03	30.5	99.3± 15.1	986 ± 150	-0.88 ±0.28	0.998
			9.9 ±0.30	7.0	-2.91 ±0.27	3.41 ±0.33	0.18 ±0.02	18.9	54.5± 5.6	1035 ± 55	-1.00	0.999
P. conicum	0	5	13.3 ±0.49	10.1	-3.13 ±0.35	4.24 ±0.50	0.19 ±0.03	21.2	71.3± 8.1	488 ± 55	-0.74 ±0.16	0.999
			15.9 ±0.83	11.9	-4.02 ±0.72	3.96 ±0.74	0.16 ±0.04	29.9	96.7± 21.3	421 ± 93	-0.43 ±0.39	0.997
			19.8 ±0.61	16.0	-3.70 ±0.53	5.33 ±0.78	0.20 ±0.02	21.8	96.7± 11.1	1838 ± 212	-1.00	0.999
		x	14.8	11.3	-3.47	4.23	0.18	24.5	83.7	954	-0.81	0.999
			17.4 ±1.12	12.9	-4.49 ±0.93	3.88 ±0.84	0.18 ±0.07	26.5	94.6± 32.2	216 ± 73	0.48 ±1.02	0.996
			16.9 ±0.53	13.2	-3.67 ±0.45	4.60 ±0.58	0.25 ±0.04	17.4	68.1 ± 9.7	271 ± 38	-0.35 ±0.24	0.999
P. onkodes	3	4	16.2 ±0.90	12.7	-3.46 ±0.75	4.67 ±1.05	0.15 ±0.05	25.1	108 ± 31.6	263 ± 77	0.35 ±0.83	0.997
			18.6 ±0.99	14.1	-4.54 ±0.50	4.10 ±0.50	0.27 ±0.04	22.3	70.1± 7.5	773 ± 83	-0.91 ±0.16	0.999
		x	17.3	13.3	-4.04	4.31	0.21	22.8	85.2	381	-0.11	0.999
			11.3 ±0.76	7.6	-3.66 ±0.67	3.07 ±0.60	0.30 ±0.10	16.2	37.2± 10.8	183 ± 53	-0.54 ±0.39	0.995
			11.0 ±0.64	7.6	-3.32 ±0.60	3.30 ±0.63	0.21 ±0.04	18.6	51.5± 7.3	154 ± 22	0.00	0.993
N. fosliei	3	4	14.6 ±0.96	10.9	-3.68 ±0.87	3.95 ±0.97	0.17 ±0.03	25.0	85.6± 13.7	256 ± 41	0.00	0.992
			18.0 ±1.45	12.8	-5.13 ±1.11	3.50 ±0.81	0.33 ±0.11	20.5	53.9± 15.2	364 ± 103	-0.73 ±0.34	0.994
		x	13.7	9.8	-3.95	3.46	0.25	20.0	57.1	240	-0.32	0.997
			16.1 ±0.89	12.3	-3.76 ±0.70	4.28 ±0.83	0.23 ±0.06	20.5	70.5± 14.6	436 ± 90	-0.69 ±0.26	0.997
			9.9 ±0.45	8.0	-1.95 ±0.38	5.10 ±1.02	0.21 ±0.04	11.2	47.9± 8.8	270 ± 49	-0.63 ±0.23	0.998
H. reinboldii	3	4	16.3 ±0.51	12.6	-3.66 ±0.43	4.45 ±0.54	0.27 ±0.04	16.5	60.2± 7.8	312 ± 40	-0.57 ±0.18	0.999
			14.6 ±0.35	11.9	-2.68 ±0.30	5.44 ±0.62	0.25 ±0.03	12.2	57.8± 6.2	240 ± 26	-0.39 ±0.17	0.999
		x	14.2	11.2	-3.01	4.82	0.24	15.1	59.1	315	-0.57	0.999
			17.3 ±0.54	11.0	-6.27 ±0.51	2.76 ±0.24	0.31 ±0.04	26.6	56.0± 5.8	1064 ± 109	-1.00	0.998
			18.2 ±0.98	11.6	-6.63 ±0.92	2.75 ±0.41	0.25 ±0.05	32.8	72.1± 13.2	1369 ± 251	-1.00	0.995
P. onkodes	'6'	4	13.6 ±0.21	7.5	-6.11 ±0.20	2.22 ±0.08	0.29 ±0.02	27.3	47.1± 2.3	894 ± 44	-1.00	0.999
			18.3 ±0.48	11.9	-6.37 ±0.45	2.87 ±0.22	0.26 ±0.03	30.5	69.2± 6.1	1315 ± 116	-1.00	0.999
		x	16.9	10.6	-6.34	2.65	0.28	29.3	61.1	1161	-1.00	0.998
			10.6 ±0.36	8.1	-2.51 ±0.32	4.23 ±0.56	0.14 ±0.01	18.4	76.5± 4.7	140 ± 9	1.00	0.998
			14.3 ±0.49	11.5	-2.84 ±0.44	5.04 ±0.80	0.19 ±0.01	14.8	73.7± 4.6	135 ± 8	1.00	0.998
N. fosliei	6	5	13.3 ±0.85	10.1	-3.20 ±0.78	4.14 ±1.04	0.23 ±0.03	14.4	58.6± 6.7	107 ± 12	1.00	0.994
			13.9 ±0.45	10.7	-3.14 ±0.37	4.42 ±0.55	0.16 ±0.03	19.4	84.1± 13.3	155 ± 24	0.98 ±0.61	0.999
			11.8 ±0.31	9.2	-2.61 ±0.28	4.52 ±0.50	0.19 ±0.10	13.9	61.8± 2.9	113 ± 5	1.00	0.999
		x	12.8	9.9	-2.86	4.47	0.18	16.2	70.9	130	1.00	0.998
			12.9 ±0.56	11.0	-1.86 ±0.45	6.90 ±1.71	0.21 ±0.04	9.8	62.0± 10.9	202 ± 36	-0.12 ±0.40	0.998
			12.1 ±0.40	9.8	-2.29 ±0.30	5.28 ±0.72	0.20 ±0.03	13.4	61.7± 7.3	245 ± 29	-0.35 ±0.24	0.999
H. reinboldii	6	4	12.5 ±0.59	10.0	-2.49 ±0.50	5.02 ±1.03	0.19 ±0.05	14.0	66.4± 14.7	146 ± 32	0.55 ±0.71	0.998
			11.4 ±0.52	8.8	-2.62 ±0.44	4.34 ±0.76	0.18 ±0.04	15.6	63.0± 13.4	145 ± 31	0.46 ±0.65	0.998
		x	12.2	10.0	-2.24	5.39	0.19	13.2	63.3	185	0.14	0.999
			7.7 ±0.31	4.9	-2.82 ±0.22	2.74 ±0.24	0.42 ±0.06	10.2	18.4± 2.1	186 ± 22	-0.89 ±0.13	0.999
			12.6 ±0.60	10.4	-2.21 ±0.50	5.68 ±1.31	0.26 ±0.06	9.5	48.7± 9.8	152 ± 31	-0.06 ±0.46	0.998
P. conicum	6	5	13.2 ±0.77	10.3	-2.83 ±0.60	4.64 ±1.03	0.32 ±0.08	10.7	41.4± 8.5	211 ± 43	-0.56 ±0.33	0.997
			10.6 ±0.96	7.8	-2.74 ±0.39	3.86 ±0.65	0.34 ±0.06	10.6	30.7± 4.0	325 ± 42	-0.90 ±0.27	0.998
			8.8 ±0.25	6.7	-2.15 ±0.22	4.10 ±0.44	0.25 ±0.03	10.6	34.7± 3.3	660 ± 62	-1.00	0.999
		x	10.6	8.1	-2.55	4.20	0.32	10.3	34.8	307	-0.68	0.999
			9.8 ±0.77	8.0	-1.84 ±0.66	5.32 ±1.95	0.27 ±0.11	7.7	36.6± 12.9	116 ± 41	-0.08 ±0.75	0.994
			8.2 ±0.52	6.1	-2.11 ±0.40	3.88 ±0.77	0.24 ±0.06	11.1	33.6± 6.9	213 ± 44	-0.70 ±0.29	0.997
P. conicum	18	5	7.2 ±0.17	5.1	-2.16 ±0.14	3.35 ±0.23	0.44 ±0.05	6.7	16.6± 1.6	110 ± 10	-0.72 ±0.11	1.000
			8.2 ±0.39	5.9	-2.32 ±0.33	3.55 ±0.53	0.44 ±0.09	7.1	18.8± 3.5	131 ± 24	-0.75 ±0.19	0.998
			10.7 ±0.43	8.2	-2.41 ±0.33	4.41 ±0.64	0.21 ±0.04	13.9	51.1± 7.4	220 ± 32	-0.42 ±0.27	0.999
		x	8.8	6.6	-2.17	4.10	0.32	9.3	31.3	158	-0.54	0.999

Table 5. Parameter estimates, 95% confidence intervals (CI), and r^2 values for *in situ* light-saturation curves for photosynthesis in different species of coralline algae from different depths (see text for parameter definitions). Mean values are given for each set of *n* (*n*=sample size) parameter estimates. The modelling function applied to each data set was the hyperbolic tangent (Eq.3). Values with confidence intervals greater than 25% of the mean values for photosynthesis and respiration, or greater than 50% of the mean values for the remaining parameters are shown in parentheses and were not included in calculations of the means. Wider confidence intervals were allowed for estimates of I_k and $I_{0.95}$ because of the smaller number of data points upon which estimates of I_k and hence $I_{0.95}$ were based.

Species	Depth	n	P^g_m	P^n_m	R	$P^g_m/-R$	α	I_c	I_k	$I_{0.95}$	r^2
	m		$mmolO_2m^{-2}$(projected area)h^{-1}								
			21.4 ±0.30	17.1	-4.25 ±0.14	5.02 ±0.18	0.10 ±0.00	41.5	206 ± 9.9	377 ± 18	0.999
			24.0 ±0.41	19.4	-4.57 ±0.21	5.25 ±0.26	0.10 ±0.01	44.9	233 ± 13.9	427 ± 26	0.998
P. onkodes	0	5	23.2 ±0.43	17.7	-5.51 ±0.24	4.21 ±0.20	0.12 ±0.01	48.5	200 ± 12.8	367 ± 23	0.997
			26.8 ±0.93	21.7	-5.11 ±0.54	5.25 ±0.58	0.09 ±0.01	59.2	307 ± 39.1	562 ± 72	0.989
			21.6 ±0.86	16.9	-4.66 ±0.51	4.63 ±0.54	0.08 ±0.01	59.8	273 ± 42.5	500 ± 78	0.984
		x	**23.4**	**18.6**	**-4.82**	**4.87**	**0.10**	**50.8**	**244**	**446**	**0.993**
			8.2 ±0.43	13.7	-4.47 ±0.25	4.07 ±0.25	0.09 ±0.01	53.1	212 ± 20.7	388 ± 38	0.992
			19.7 ±0.59	16.1	-3.61 ±0.34	5.46 ±0.54	0.09 ±0.01	41.9	226 ± 25.7	414 ± 47	0.987
N. fosliei	0	4	19.3 ±0.50	13.9	-5.40 ±0.26	3.57 ±0.20	0.08 ±0.01	71.1	247 ± 21.0	452 ± 38	0.991
			25.5 ±0.47	20.9	-4.66 ±0.22	5.48 ±0.28	0.13 ±0.01	37.6	203 ± 10.7	372 ± 20	0.996
		x	**20.7**	**16.1**	**-4.54**	**3.72**	**0.09**	**50.9**	**222**	**407**	**0.992**
			22.7 ±0.34	17.5	-5.19 ±0.22	4.38 ±0.19	0.19 ±0.01	28.1	121 ± 8.8	221 ± 16	0.996
			21.9 ±0.33	16.3	-5.59 ±0.16	3.91 ±0.13	0.15 ±0.01	37.8	145 ± 6.2	265 ± 11	0.997
P. conicum	0	4	20.3 ±0.59	15.9	-4.34 ±0.36	4.68 ±0.42	0.13 ±0.01	34.0	156 ± 18.6	287 ± 34	0.987
			18.5 ±0.40	14.2	-4.25 ±0.24	4.35 ±0.26	0.11 ±0.01	37.8	162 ± 13.1	296 ± 24	0.993
		x	**20.8**	**16.0**	**-4.84**	**4.33**	**0.15**	**34.4**	**146**	**267**	**0.993**
			28.6 ±0.59	23.3	-5.26 ±0.34	5.43 ±0.36	0.14 ±0.01	38.3	206 ± 14.5	377 ± 27	0.995
			17.8 ±0.28	13.2	-4.59 ±0.15	3.89 ±0.14	0.07 ±0.00	63.9	242 ± 12.5	443 ± 23	0.997
N. fosliei	3	4	23.6 ±1.03	18.1	-5.50 ±0.54	4.30 ±0.46	0.15 ±0.02	38.2	161 ± 19.4	296 ± 36	0.973
			21.9 ±0.51	15.8	-6.19 ±0.26	3.55 ±0.17	0.12 ±0.00	54.2	187 ± 14.1	342 ± 26	0.993
		x	**23.0**	**17.6**	**-5.38**	**4.29**	**0.12**	**48.7**	**199**	**365**	**0.990**
			21.1 ±0.46	16.9	-4.19 ±0.24	5.05 ±0.31	0.12 ±0.01	35.2	175 ± 10.9	321 ± 20	0.993
			17.6 ±0.50	11.9	-5.77 ±0.27	3.06 ±0.17	0.12 ±0.01	51.9	153 ± 13.1	280 ± 24	0.988
H. reinboldii	3	4	19.4 ±0.50	15.4	-4.02 ±0.28	4.82 ±0.36	0.13 ±0.01	32.5	155 ± 13.5	283 ± 25	0.990
			18.5 ±0.43	14.8	-3.70 ±0.23	5.00 ±0.33	0.08 ±0.01	44.4	219 ± 16.8	401 ± 31	0.993
		x	**19.2**	**14.7**	**-4.42**	**4.48**	**0.11**	**41.0**	**175**	**321**	**0.991**
			23.2 ±4.00	19.7	-3.48 ±0.25	6.68 ±1.25	0.24 ±0.02	14.8	97.9± 23.0	179 ± 42	0.981
			(27.0 ±7.35)	(23.3)	-3.63 ±0.10	(7.44 ±4.07)	0.21 ±0.01	17.8	131 ± 39.1	241 ± 143	0.972
P. onkodes	6'	4	16.4 ±1.66	13.2	-3.17 ±0.16	5.17 ±0.58	0.31 ±0.02	10.4	53.3± 7.9	98 ± 14	0.990
			(35.2 ±63.1)	(31.0)	-4.20 ±0.24	8.34 ±15.0	0.30 ±0.03	14.0	(117 ±222)	(214 ±406)	0.973
		x	**19.8**	**16.5**	**-3.62**	**6.73**	**0.27**	**14.3**	**94**	**173**	**0.979**
			13.2 ±1.51	9.7	-3.52 ±0.78	3.74 ±0.93	0.24 ±0.07	15.0	54.9± 18.4	101 ± 34	0.924
			24.3 ±2.84	22.1	-2.19 ±0.06	11.1 ±1.34	0.30 ±0.01	7.3	81.2± 11.4	149 ± 21	0.998
N. fosliei	6	4	14.3 ±1.02	10.8	-3.48 ±0.13	4.11 ±0.33	0.17 ±0.01	20.3	82.0± 10.0	150 ± 18	0.992
			31.0 ±4.73	27.7	-3.26 ±0.08	9.49 ±1.47	0.22 ±0.01	15.2	144 ± 25.6	263 ± 47	0.999
		x	**20.7**	**17.6**	**-3.11**	**7.12**	**0.23**	**14.5**	**90**	**166**	**0.978**
			19.0 ±0.81	14.8	-4.22 ±0.34	4.50 ±0.41	0.15 ±0.01	29.4	130 ± 15.4	238 ± 28	0.991
			26.0 ±0.98	21.9	-4.09 ±0.33	6.36 ±0.57	0.15 ±0.01	26.9	170 ± 15.2	311 ± 28	0.995
H.reinboldii	6	4	20.6 ±1.08	17.1	-3.46 ±0.13	5.96 ±0.38	0.22 ±0.01	16.1	95.1± 8.5	174 ± 16	0.998
			20.3 ±0.73	16.9	-3.34 ±0.30	6.07 ±0.59	0.21 ±0.01	16.7	100 ± 9.4	184 ± 17	0.990
		x	**21.5**	**17.7**	**-3.78**	**5.72**	**0.18**	**22.3**	**124**	**227**	**0.993**
			13.4 ±0.40	9.8	-3.67 ±0.19	3.66 ±0.22	0.13 ±0.01	28.1	100 ± 8.5	184 ± 16	0.996
			13.5 ±0.80	10.2	-3.35 ±0.37	4.03 ±0.51	0.15 ±0.02	22.9	90.4± 14.5	166 ± 27	0.983
P. conicum	6	4	19.1 ±1.89	16.4	-2.75 ±0.09	6.96 ±0.73	0.34 ±0.01	8.1	55.9± 7.4	102 ± 14	0.996
			17.1 ±0.57	14.5	-2.61 ±0.11	6.57 ±0.35	0.31 ±0.01	8.5	55.4± 3.3	102 ± 6	0.997
		x	**15.8**	**12.7**	**-3.10**	**5.30**	**0.23**	**16.9**	**76**	**138**	**0.993**
			(26.4 ±8.02)	(23.7)	-2.77 ±0.07	9.56 ±2.91	0.26 ±0.01	10.9	104 ± 34.5	190 ± 63	0.998
			(21.6 ±18.0)	(18.9)	-2.69 ±0.10	(8.01 ±6.69)	0.30 ±0.02	9.2	(72.9± 65.3)	(134 ±120)	0.989
P. conicum	18	4	14.7 ±2.10	11.8	-2.85 ±0.12	5.16 ±0.77	0.24 ±0.01	12.1	61.9 ± 12.2	113 ± 22	0.992
			11.2 ±0.69	7.9	-3.33 ±0.14	3.37 ±0.25	0.26 ±0.02	13.0	42.4 ± 5.3	78 ± 10	0.990
		x	**13.0**	**9.9**	**-2.91**	**6.03**	**0.26**	**11.3**	**69**	**127**	**0.992**

extreme irradiance levels (Fig. 12A) well above those normally encountered in the field.

Two striking features are observed among the curves presented in Figs 9, 10, 11, and 12. First, *in situ* specimens living under much reduced irradiance near the lower depth limits of their species distributions rarely attain photosynthetic saturation (Figs 9E, 10F, 11E, 12F). Second, rates of photosynthesis are noticeably higher for a given irradiance under *in situ* conditions (Figs 9B,E, 10B,D,F, 11C,E, 12B,D,F) than in the laboratory (Figs 9A,D, 10A,C,E, 11B,D, 12A,C,E). This is especially pronounced among specimens obtained from deeper water. Possible explanations for the latter phenomenon will be given in Section 2. 4. 4.

Photoadaptation, by definition, implies that the efficiency of light utilization increases with decreasing irradiance in order to maximise photosynthetic carbon assimilation. Optimally, the size and organisation of the photosynthetic apparatus should be finely adjusted to the quantity of available submarine light. Optimally light-adapted plants should therefore show daily light response profiles which mirror the curve of irradiance through the day. Theoretically, photosynthesis should approach saturation at the time of peak irradiance. The representative *in situ P-I* curves for coralline algae existing at 6 m provide an interesting comparison. *Paragoniolithon conicum*, which also shows the greatest ability to grow in low light and deep water, exhibits a *P-I* curve (Fig. 12D) which comes very close to this theoretical optimum. *Hydrolithon reinboldii* which similarly appears to be a shade-tolerant species, though not to the same degree as *P. conicum*, shows a lesser tendency towards saturation under peak irradiance (Fig. 11E). *Porolithon onkodes*, which typically occurs in high irradiance environments shows little evidence of saturation under similar peak irradiance (Fig. 9E). The curve for *N. fosliei* (Fig. 10F) is virtually a straight line but the lower ambient irradiance levels prevent direct comparison with the other three species.

When there is no evidence of saturation the quantity of light-reaction components must exceed the amount which can be used in photosynthesis. This indicates an overproduction of photochemical apparatus which may reflect a greater metabolic demand for photosynthetic products which cannot be provided in full under the ambient conditions of irradiance. Alternatively, if the metabolic cost of producing and maintaining superfluous apparatus is low this may be a simple form of insurance

for maximum photon capture under conditions of changing irradiance (see Larkum & Barret 1983 for discussion of adaptation to varying illumination). Conceivably there are situations where corallines would benefit from readily available additional photochemical apparatus such as following the instantaneous removal of shading structures, but this seems an unlikely explanation for the following reasons. First, the sudden removal of solid shading structures from the windward reef slope at Lizard Island is a rare event which only tends to occur during storms. Wave induced movement of flexible canopies can lead to light 'flecking' upon understory species, but this is likely to be of great significance only in shallow areas where water movement is pronounced and where the dominant light component is downwelling irradiance. Second, it is hard to envisage why corallines would maintain larger amounts of photochemical apparatus than is necessary for much of the time when the amounts can be adjusted to suit new conditions of irradiance over relatively short periods, i.e., hours or days (e.g., Miller & Holt 1976; see reviews by Kirk 1983 and Larkum & Barret 1983, and references given therein). Third, the failure to reach saturated levels of photosynthesis appears to be correlated with a decline in abundance of the species in the field. Fourth, coralline algae sampled at the low limits of their species distributions show little net carbon gain over the course of a 24 hour day (see Tables 14 & 15 presented in Section 2. 4. 7). It therefore seems likely that the near-linear *P-I* responses observed in the *in situ* data (Figs 9E, 10F, 11E, 12F) reflect real limits in the photoadaptive capabilities of the coralline algae and not simply an incidental overproduction of photochemical apparatus. What this may mean in physiological and biochemical terms is not within the scope of this study. A detailed review of the physiology and biochemistry of light-harvesting processes in algae has been provided by Larkum & Barret (1983).

2. 4. 3. MODELLING THE LIGHT-SATURATION CURVES OF CRUSTOSE CORALLINE ALGAE

There are still no mathematical models which describe all possible features of the relationship between photosynthesis and irradiance (Larkum & Barret 1983). Larkum & Barret argue for an approach which optimally considers all facets of the relationship including the light reactions, the supply of CO_2, respiration, photorespiration, the supply of photochemical intermediates, the rate of electron transport, and the enzyme kinetics of the system. This approach is undoubtably

necessary for a detailed understanding of the reactions which limit photosynthesis. However, such an approach is often impractical and unnecessary when the objective is simply to describe major features of the relationship and to statistically estimate important parameters such as the rate of photosynthesis or respiration, or the efficiency of light utilisation (α and I_k). In these circumstances, accurate simulations of the response curve of photosynthesis versus irradiance (*P-I* curve) can be obtained on the basis of simple empirical formulae (e.g., Jassby & Platt 1976; Platt *et al.* 1980; Chalker 1981).

Until now the hyperbolic tangent function has been widely adopted as the preferred model for simulating the *P-I* curves of several algal groups including phytoplankton, fleshy macroalgae, and coral zooxanthellae (e.g., Jassby & Platt 1976; Porter 1980; Chalker 1981; Chalker *et al.* 1983; Porter *et al.* 1984; Carpenter 1985). When *P-I* curves were constructed for crustose coralline algae from *in situ* data using the hyperbolic tangent function (Figs 9B,E, 10B,D,F, 11C,E, 12B,D,F) the fitted regressions were visually accurate. However, when less variable *P-I* datasets were obtained under controlled conditions in the laboratory the hyperbolic tangent function did not always provide the most accurate description of the data. Fig. 13 demonstrates the value of testing a range of mathematical functions when simulating the *P-I* curve of a crustose coralline alga. For the experimental dataset shown in Fig. 13, the right rectangular hyperbola clearly overestimates P^g_m and underestimates the curve in the region of inflexion. The simple exponential function has the reverse effect, as indeed would the hyperbolic tangent function were it fitted. The general exponential function (Eq. 3a or 4), which most accurately simulates this dataset, has been proposed on theoretical grounds (Chalker, 1980); but it has not been previously used.

As discussed in Section 2. 2. 2., all of the commonly used models for describing *P-I* curves, excluding the general exponential function, are described by four variables: P^g_m, R, α, and I_k. The general exponential function requires a fifth variable, denoted here by epsilon (ε). Essentially, ε holds a fixed value in each of the other modelling functions and is therefore not a variable. The great advantage of the general exponential function is that the additional variable ε (with limits: $-1<\varepsilon<1$) allows the model to simulate any dataset with characteristics lying somewhere between the hyperbolic tangent function and the right rectangular hyperbola. Moreover, it provides greater flexibility for modelling the region between the onset of saturation (I_k) and P^g_m. Larkum & Barret (1983) have discussed the importance of this region

Fig. 13 An experimental light-saturation data set simulated by three different functions: (1) a general exponential function (Eq. 4), (2) a simple exponential function (Eq. 2), and (3) the right rectangular hyperbola (Eq. 1).

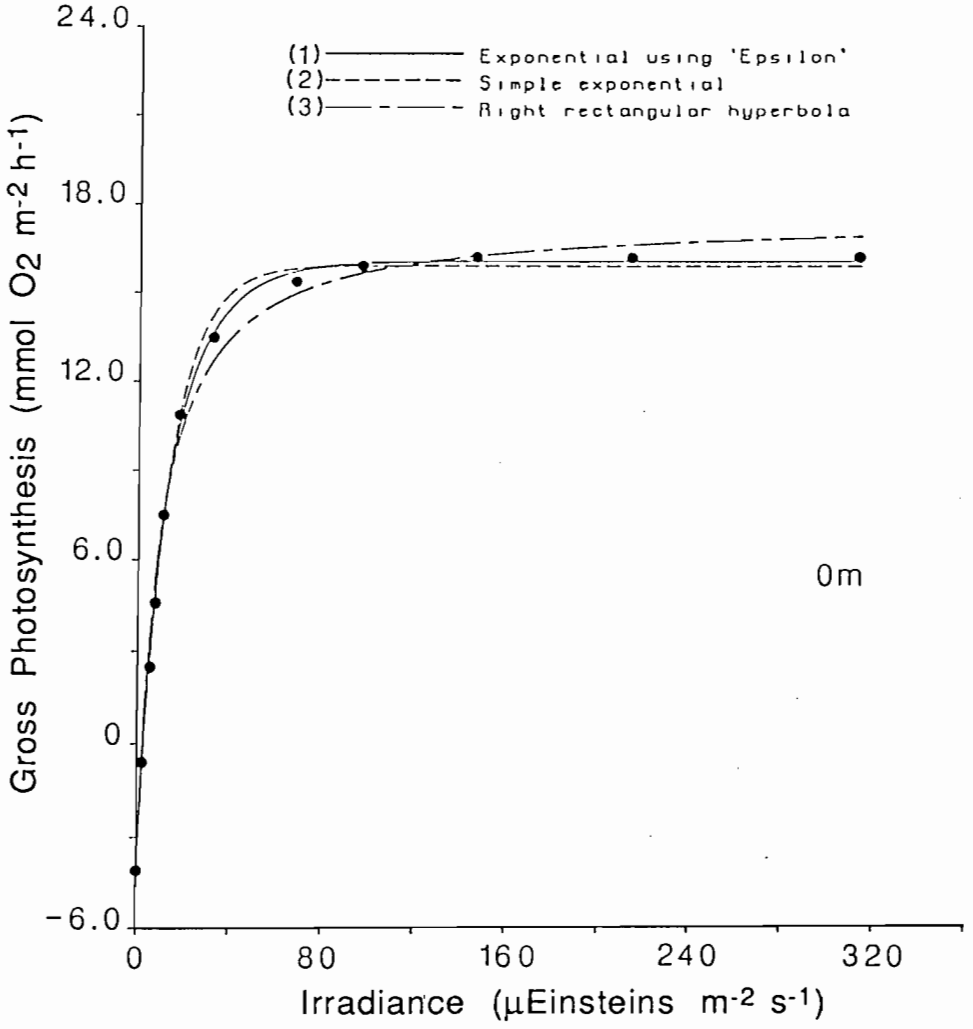
(1) Exponential using 'Epsilon'
(2) Simple exponential
(3) Right rectangular hyperbola
Gross Photosynthesis (mmol O2 m-2 h-1)
24.0
18.0
12.0
6.0
0
-6.0
0m
0
80
160
240
320
Irradiance (µEinsteins m-2 s-1)

since it represents the transition between the different reactions which limit photosynthesis. The initial slope of the curve is limited by incident light and largely determined by the light-harvesting capacity of the plant. Near light saturation the supply of ATP or NADPH, or the activation of RuBP carboxylase (Perchorowicz *et al.* 1981) is possibly the limiting process. At light saturation, enzyme turnover controls the rate of photosynthesis. Photoinhibition may or may not occur at still higher light intensities. In physiological terms, the magnitude of ε may provide a useful measure of the rate of transition between the various reactions which limit photosynthesis. In physical terms, the value of ε may provide a measure of light-related anatomical structuring (see later discussion).

If datasets are first fitted by non-linear, least squares regression analysis using the general exponential function (Eq. 4), then curves with characteristics different to those of the hyperbolic tangent function, simple exponential, or right rectangular hyperbola, can be described by five variables including a non-integer value for ε. If, during incremental halving of the residual sums of squares, ε was found to approach the integer value for any of the other curves then the appropriate four-parameter model was selected. The variable ε then assumed the integer value (1, 0, or -1) characteristic of the model used.

In theory, the *P-I* curve of an infinitely thin photosynthetic layer will approximate to the hyperbolic tangent function which may deviate from a curve composed of two straight lines because of the removal of the product (Dr. B.E. Chalker - personal communication). All cells will receive the same quanta of light, there will be equal barriers to diffusion, and all cells will saturate at the same rate. Conversely a thick layer of photosynthetic tissue should either show the effects of cellular shading, or increased resistance to gaseous diffusion, or both. This would reduce the rate at which the curve approaches a horizontal asymptote, so extending the region of inflexion. Equivalent effects should be evident in the *P-I* curves for multi-layered photosynthetic communities. The resultant curve is thus a combination of a number of different *P-I* curves, each with slightly different saturation rates.

In mature crustose coralline algae, the photosynthetic layer is composed of rows of vertical filaments juxtapositioned parallel to one another. New cells are cut off from a sub-apical meristem during upward growth of the crust. As growth continues $CaCO_3$ builds up in the cell walls resulting in a gradient in wall density from younger

to older cells in the thallus. Cytoplasmic continuity is maintained via primary pit connections and sometimes secondary pit connections or fusions between cells in the filaments. Presumably cells deeper in the crust cease photosynthetic activity when they become so heavily impregnated with $CaCO_3$ that cellular functions, such as the harvesting of light energy, are inhibited (see also Borowitzka & Vesk 1978). Before this occurs, the deeper cell layers will receive considerably less light than those at the surface. A gradient in resistance to gaseous diffusion may also exist. It follows that a heavily calcified cellular framework should give rise to a *P-I* response curve with the characteristics of a thick or multi-layered photosynthetic structure, even though the crust itself may be relatively thin.

In a similar fashion to 'sun' plant leaves, the actively photosynthesizing layer of crusts growing under high irradiance should be thicker. This is supported by the generally (cf *P. onkodes* and *N. fosliei*) greater biomass (i.e., protein content per unit area) of shallow water crustose coralline specimens (Table 6). At the same time, and presumably as a consequence of the thicker photosynthetic layer, the amount of $CaCO_3$ through which light must pass to reach the deeper cell layers will be greater. This will result in the establishment of a pronounced gradient in light levels reaching different layers in the crust. In consequence, specimens living in high light environments should generally show *P-I* curves with characteristics typical of multi-layered photosynthetic communities (e.g., Figs 9A and 11A). In effect the lower layers become shade-adapted with respect to the upper layers (see Larkum & Barret 1983) and the transition from light-limited to light-saturated photosynthesis becomes more gradual. It seems likely that a calcified cell layer will exaggerate the effects observed in optically dense algal thalli wherein photosynthesis shows a lesser tendency towards saturation (Rabinowitch 1951). Hence, in order to accurately simulate the *P-I* response curve of a compact, multi-layered, or calcium carbonate impregnated algal thallus, the chosen model should incorporate a variable for determining the rate of transition from light-limited to light-saturated photosynthesis. Such a model is the general exponential function which includes the variable ε.

The curves presented in Figs 9A and 11A (and to a lesser degree 10A) show that photosynthesis is not entirely light-saturated at irradiance levels beyond those which occur at the sea surface in the study area when the sun is directly overhead (*ca* 2250 μEinsteins m^{-2} s^{-1} max). Similar observations have been made on well-developed arborescent reef communities where saturated levels of photosynthesis are

Table 6. Mean (x) protein content per unit of real surface area of different species at the designated depths. Numbers in parentheses indicate the number of samples (*n*). Confidence intervals (CI) are given at the 95% probability level. The asterisk (*) denotes that the specimens came from shaded locations where the PPFD was equivalent to a depth of 6 m.

Depth	*P. onkodes*			*N. fosliei*			*H. reinboldii*			*P. conicum*		
	g protein m^{-2} real surface area											
m	x	CI	*n*	x	CI	*n*	x	CI	*n*	x	CI	*n*
0	6.11	±2.55	(5)	7.06	±0.75	(4)				2.81	±1.02	(4)
3				3.99	±2.00	(4)	4.04	±1.33	(4)			
6	*5.34	±2.54	(4)	2.15	±1.36	(4)	2.82	±1.21	(4)	1.55	±0.67	(4)

not approached even at the highest levels of PAR encountered (e.g., Kohn & Helfrich 1957; Marsh & Smith 1978; Kinsey 1979; Jokiel & Morrissey 1986). Jokiel & Morrissey (1986) further suggest that corals and macroalgae become more sun-adapted by increasing the amount of shaded tissue. The crustose coralline algae which frequently dominate the exposed edges of coral reefs may achieve the same end by accumulation of $CaCO_3$ within their tissues. Indeed, it was suggested over a century ago that the accumulation of $CaCO_3$ may be a protective mechanism against high irradiance (Berthold 1882).

With specific regard to this laboratory study, specimens obtained from high light environments typically gave rise to *P-I* curves with ε values close or equal to -1 (Table 4). Their light response curves were thus best simulated by the right rectangular hyperbola, or general exponential function with negative values for ε. As the quantity of available irradiance diminished, and presumably the actively photosynthetic layer was effectively 'thinner', the value of ε rose on occasions to 1 (Fig. 11E, & Table 4 - specimens of *N. fosliei* obtained from a depth of 6 m). Low light specimens therefore showed *P-I* curves which were better simulated by the hyperbolic tangent, simple exponential, or general exponential function with more positive values for ε.

After all curves were fitted, an interesting pattern emerged in the value of ε for different specimen groupings. Fig. 14 shows trends in the value of ε for specimens of each species sampled over a gradient of PPFD. Statistically significant regressions ($P \leq 0.05$) were found for the species *Neogoniolithon fosliei* and *Hydrolithon reinboldii*. A similar but statistically non-significant trend was observed for *Paragoniolithon conicum*. Only *Porolithon onkodes* showed no such pattern. Specimens of *P. onkodes* obtained from 0 m possessed more negative ε values than those obtained from 3 m. However, specimens obtained from 1.5 m, where shading reduced the available PPFD to a level similar to that measured at 6 m, showed a complete departure from the general rule. In the absence of further information it can only be concluded that different factors are operating in shade-dwelling specimens of this species in shallow water.

Fig. 14. Double logarithmic plots of epsilon (ε) against the percentage of surface irradiance transmitted to the depth of collection (%SI), for laboratory specimens of the different species. r^2 values and significance levels (P) are shown in parentheses for each regression.

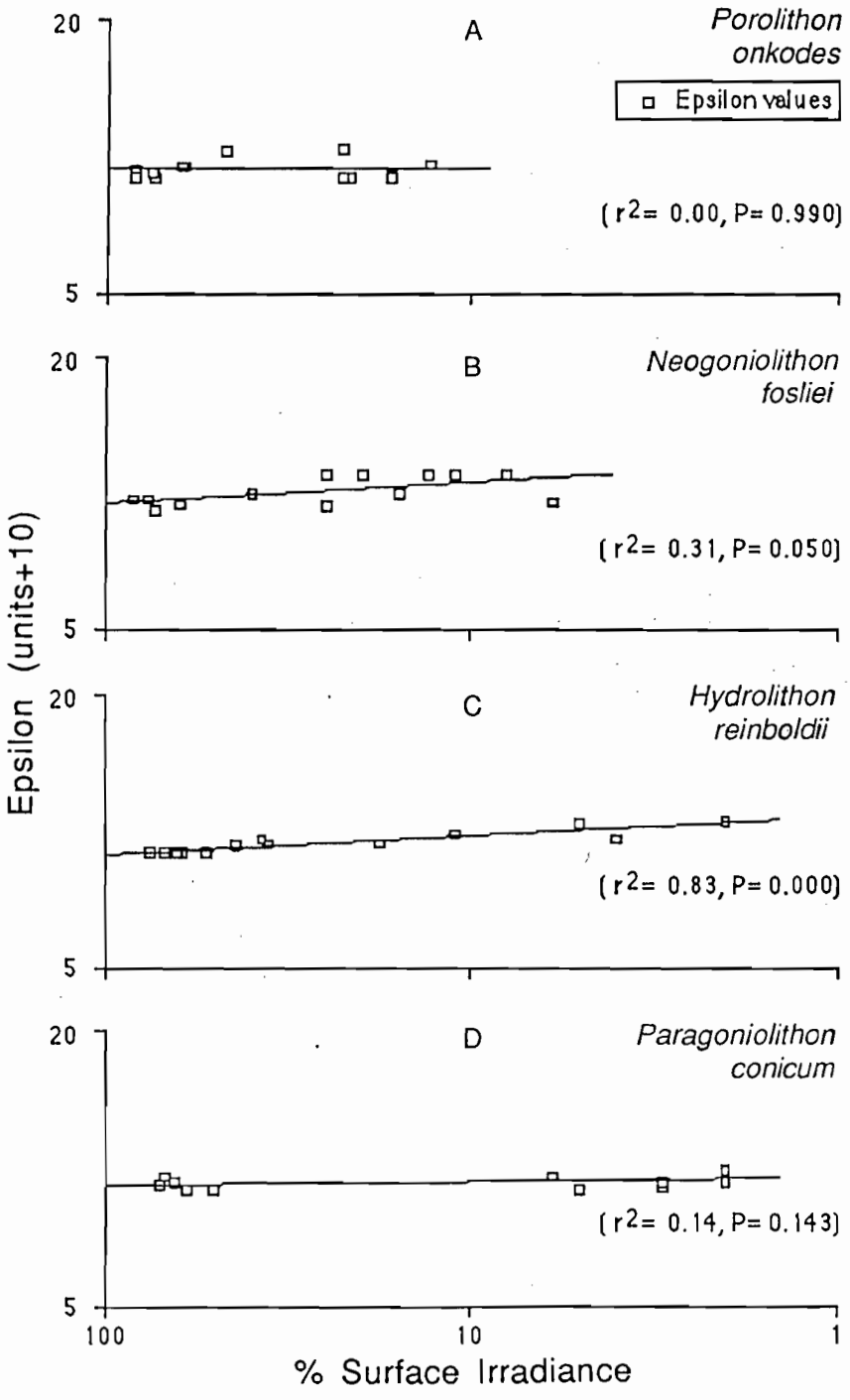
A
Porolithon onkodes
Epsilon values
(r2= 0.00, P= 0.990)
B
Neogoniolithon fosliei
(r2= 0.31, P= 0.050)
C
Hydrolithon reinboldii
(r2= 0.83, P= 0.000)
D
Paragoniolithon conicum
(r2= 0.14, P= 0.143)
20
5
Epsilon (units+10)
100
10
1
% Surface Irradiance

2. 4. 4. PHOTOADAPTIVE TRENDS AMONG DESCRIPTIVE PARAMETERS

It is generally accepted that adaptation of the photosynthetic apparatus to decreasing irradiance is evidenced by significant changes in the photokinetic parameters which describe the essential features of *P-I* curves (i.e. R, α, I_c, I_k, and $I_{0.95}$). These changes may be summarised as follows. The rate of respiration (R) decreases with decreasing irradiance (Wethey & Porter 1976b; Davies 1977, 1980; Zvalinski *et al.* 1980; Falkowski & Dubinski 1981; Chalker *et al.* 1983; McCloskey & Muscatine 1984; Porter *et al.* 1984). The initial slope of the *P-I* curve (α) increases with decreasing irradiance (King & Schramm 1976; Ramus *et al.* 1976; Wethey & Porter 1976a; Li & Titlyanov 1978; Falkowski & Owens 1978, 1980; Zvalinski *et al.* 1980; Falkowski & Dubinsky 1981; Leletkin & Zvalinski 1981; Titlyanov 1981; Chalker *et al.* 1983; Porter *et al.* 1984). The compensation light intensity (I_c) decreases with decreasing irradiance (Kawaguti 1937; Parsons & Takahashi 1973; Davies 1977; Harris 1978; Falkowski & Dubinsky 1981; Chalker *et al.* 1983; Kirk 1983; Porter *et al.* 1984; Carpenter 1985). The light intensity at which the initial slope intercepts the horizontal asymptote (I_k), and hence also the light intensity at which photosynthesis is 95% saturated ($I_{0.95}$), decreases with decreasing irradiance (Parsons & Takahashi 1973; Wethey & Porter 1976a,b; Davies 1977; Harris 1978; Chalker *et al.* 1983; Kirk 1983; Porter *et al.* 1984).

Chalker *et al.* (1983) have provided further information about the photoadaptive responses of reef corals by demonstrating a double logarithmic proportionality between many of the photokinetic parameters which describe *P-I* curves and the percentages of surface irradiance (%SI) which are transmitted to the depths at which the corals are growing. The natural logarithms of I_k, $I_{0.95}$, I_c, and R are all directly proportional to the logarithm of the %SI. The logarithms of α and $P^g_m/\text{-}R$ are inversely proportional to the logarithm of %SI. Accepting these relationships are evidence of coral photoadaptation, do crustose coralline algae respond in a similar fashion, and do certain coralline species show greater capacities for photoadaptation?

With one or two exceptions, Figs 15, 16, 17, 18, 19, and 20 demonstrate that the relationships described above for corals are also true of crustose coralline algae. Apart from the double logarithmic plot of $P^g_m/\text{-}R$ versus %SI for *in situ* specimens of *N. fosliei* (Fig. 17B), the only exceptions to the trends described above

Fig. 15. Double logarithmic plots of I_c, I_k, $I_{0.95}$ against the percentage of surface irradiance transmitted to the depth of collection (%SI), for laboratory specimens of the different species. r^2 values and significance levels (P) are shown in parentheses for each regression.

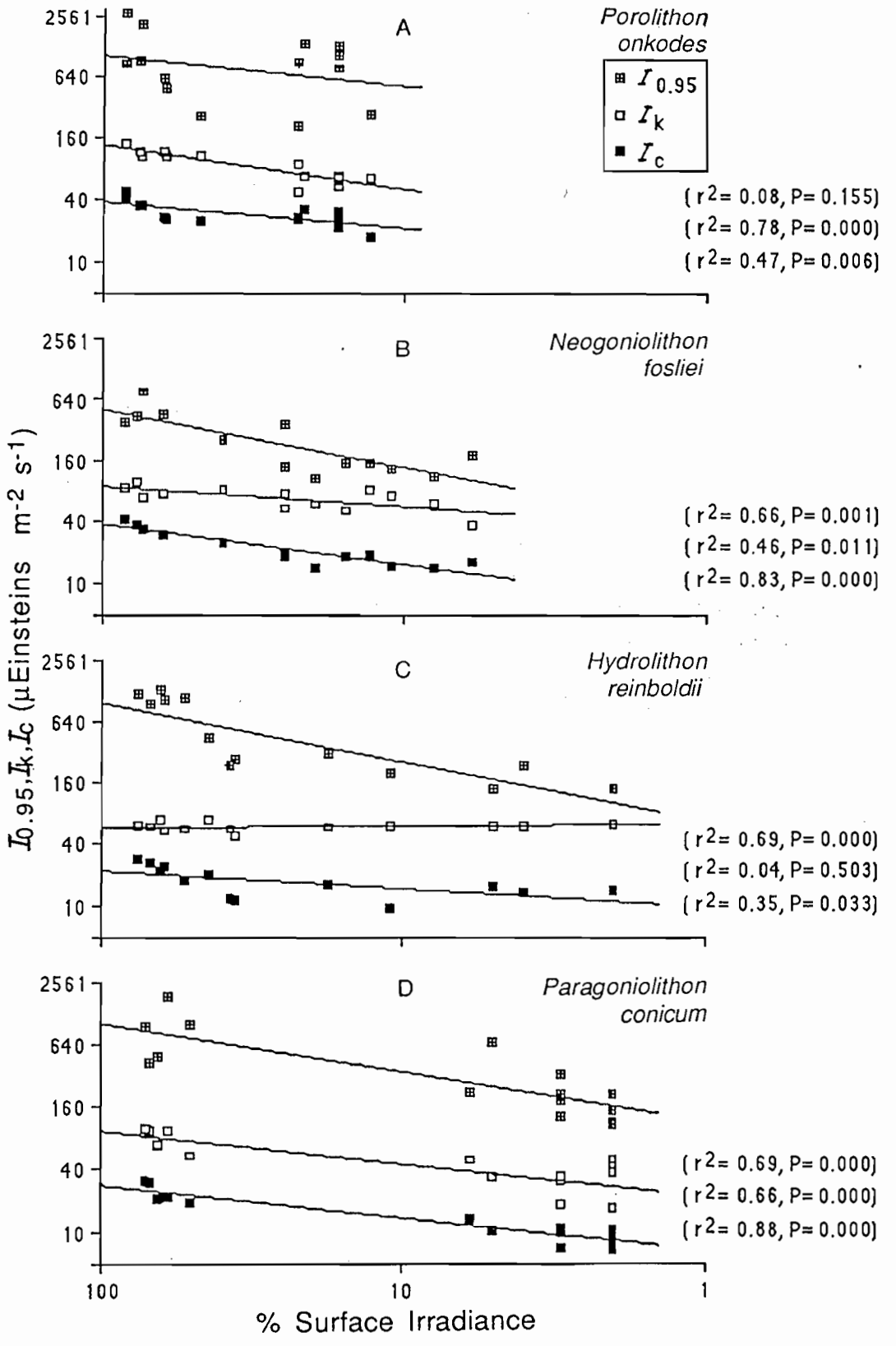
A
Porolithon onkodes
$I_{0.95}$
I_k
I_c
(r2= 0.08, P= 0.155)
(r2= 0.78, P= 0.000)
(r2= 0.47, P= 0.006)
B
Neogoniolithon fosliei
(r2= 0.66, P= 0.001)
(r2= 0.46, P= 0.011)
(r2= 0.83, P= 0.000)
C
Hydrolithon reinboldii
(r2= 0.69, P= 0.000)
(r2= 0.04, P= 0.503)
(r2= 0.35, P= 0.033)
D
Paragoniolithon conicum
(r2= 0.69, P= 0.000)
(r2= 0.66, P= 0.000)
(r2= 0.88, P= 0.000)
2561
640
160
40
10
100
10
1
$I_{0.95}, I_k, I_c$ (µEinsteins m^{-2} s^{-1})
% Surface Irradiance

Fig. 16. Double logarithmic plots of I_c, I_k, $I_{0.95}$ against the percentage of surface irradiance transmitted to the depth of measurement (%SI), for *in situ* specimens of the different species. r^2 values and significance levels (P) are shown in parentheses for each regression.

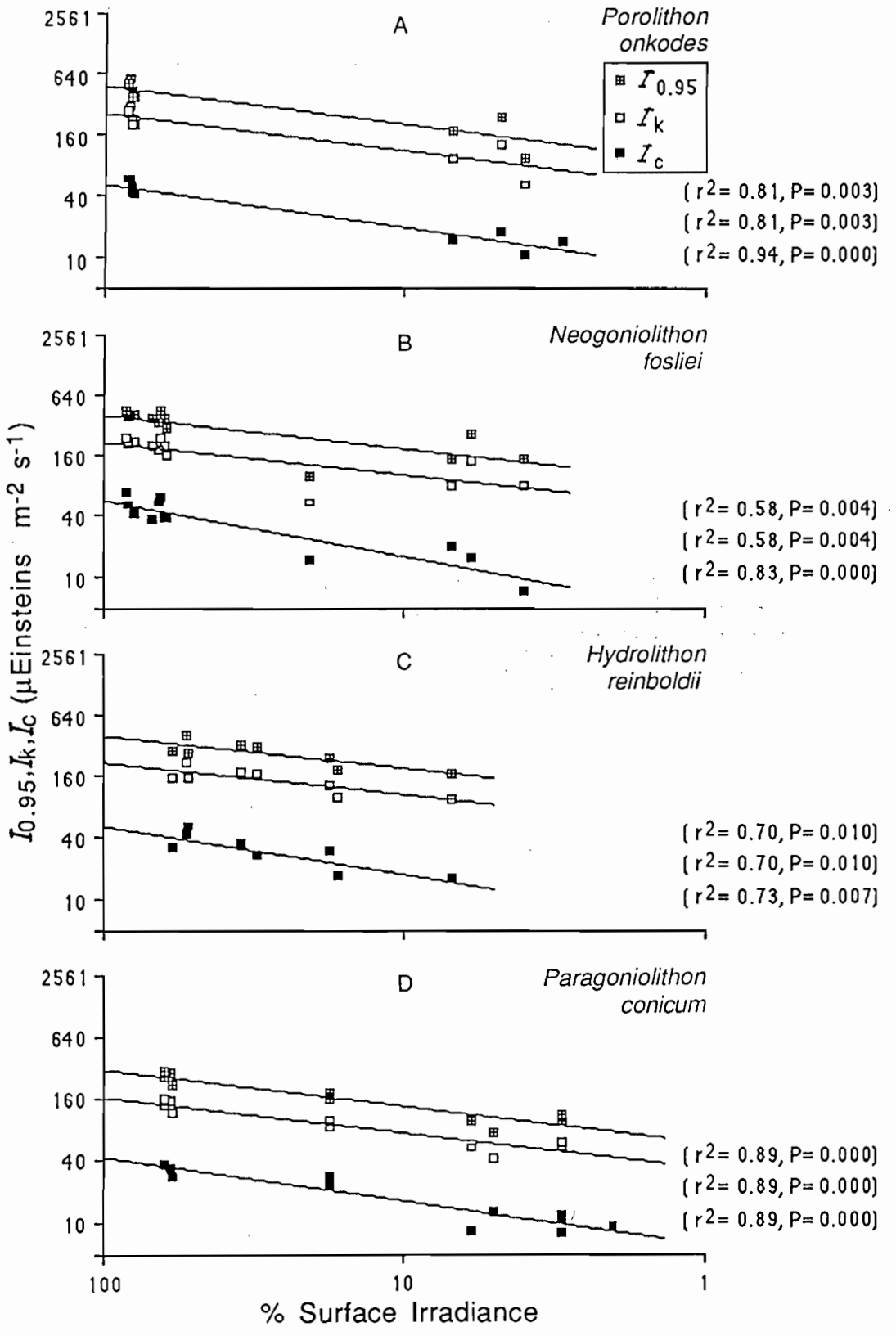
A
Porolithon onkodes
$I_{0.95}$
I_k
I_c
(r^2= 0.81, P= 0.003)
(r^2= 0.81, P= 0.003)
(r^2= 0.94, P= 0.000)
B
Neogoniolithon fosliei
(r^2= 0.58, P= 0.004)
(r^2= 0.58, P= 0.004)
(r^2= 0.83, P= 0.000)
C
Hydrolithon reinboldii
(r^2= 0.70, P= 0.010)
(r^2= 0.70, P= 0.010)
(r^2= 0.73, P= 0.007)
D
Paragoniolithon conicum
(r^2= 0.89, P= 0.000)
(r^2= 0.89, P= 0.000)
(r^2= 0.89, P= 0.000)
2561
640
160
40
10
100
10
1
$I_{0.95}, I_k, I_c$ (µEinsteins m^{-2} s^{-1})
% Surface Irradiance

Fig. 17. Double logarithmic plots of $P^{g}_{m}/-R$, R, P^{g}_{m} against the percentage of surface irradiance transmitted to the depth of measurement (%SI), for laboratory specimens of the different species. r^2 values and significance levels (P) are shown in parentheses for each regression.

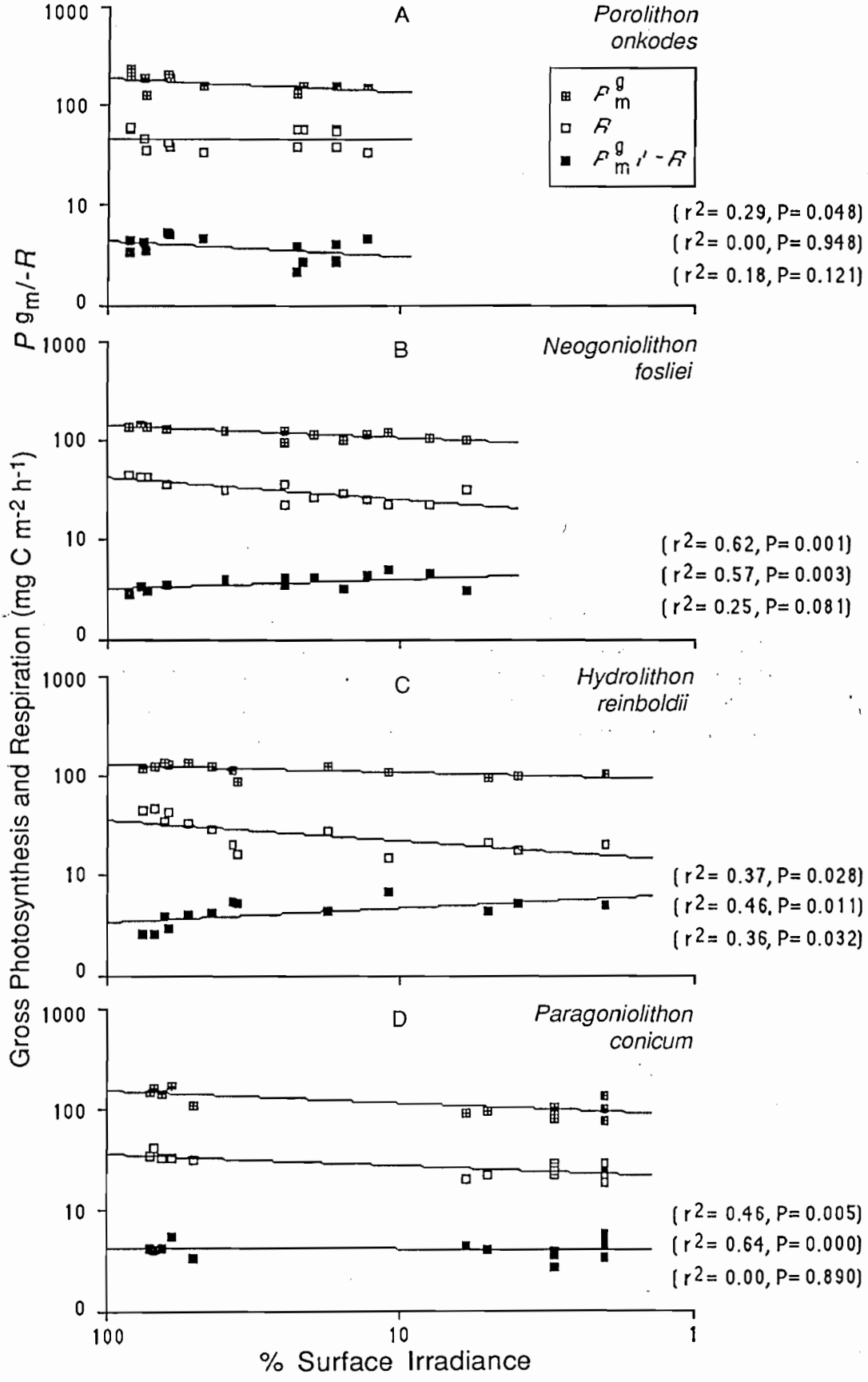
A
Porolithon onkodes
B
Neogoniolithon fosliei
C
Hydrolithon reinboldii
D
Paragoniolithon conicum
P^g_m
R
$P^g_{m'} - R$
(r^2= 0.29, P= 0.048)
(r^2= 0.00, P= 0.948)
(r^2= 0.18, P= 0.121)
(r^2= 0.62, P= 0.001)
(r^2= 0.57, P= 0.003)
(r^2= 0.25, P= 0.081)
(r^2= 0.37, P= 0.028)
(r^2= 0.46, P= 0.011)
(r^2= 0.36, P= 0.032)
(r^2= 0.46, P= 0.005)
(r^2= 0.64, P= 0.000)
(r^2= 0.00, P= 0.890)
$P g_m/-R$
Gross Photosynthesis and Respiration (mg C m^{-2} h^{-1})
1000
100
10
0
100
10
1
% Surface Irradiance

Fig. 18. Double logarithmic plots of $P^{g}m/-R$, R, $P^{g}m$ against the percentage of surface irradiance transmitted to the depth of measurement (%SI), for *in situ* specimens of the different species. r^2 values and significance levels (P) are shown in parentheses for each regression.

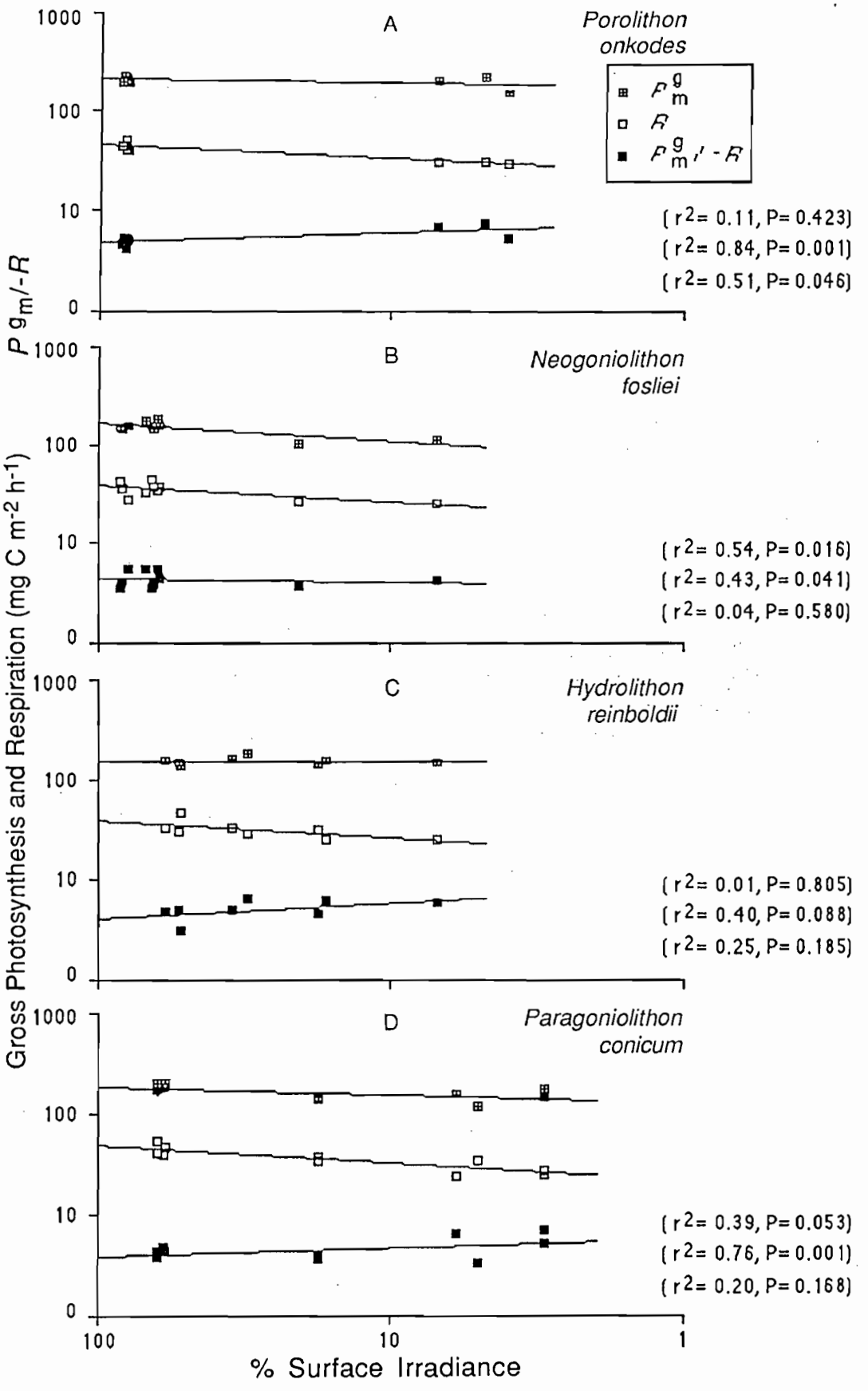
A
Porolithon onkodes
P^g_m
R
$P^g_{m'} - R$
(r^2= 0.11, P= 0.423)
(r^2= 0.84, P= 0.001)
(r^2= 0.51, P= 0.046)
B
Neogoniolithon fosliei
(r^2= 0.54, P= 0.016)
(r^2= 0.43, P= 0.041)
(r^2= 0.04, P= 0.580)
C
Hydrolithon reinboldii
(r^2= 0.01, P= 0.805)
(r^2= 0.40, P= 0.088)
(r^2= 0.25, P= 0.185)
D
Paragoniolithon conicum
(r^2= 0.39, P= 0.053)
(r^2= 0.76, P= 0.001)
(r^2= 0.20, P= 0.168)
1000
100
10
0
100
10
1
$P g_m/-R$
Gross Photosynthesis and Respiration (mg C m^{-2} h^{-1})
% Surface Irradiance

Fig. 19. Double logarithmic plots of alpha (α) against the percentage of surface irradiance transmitted to the depth of measurement (%SI), for laboratory specimens of the different species. r^2 values and significance levels (P) are shown in parentheses for each regression.

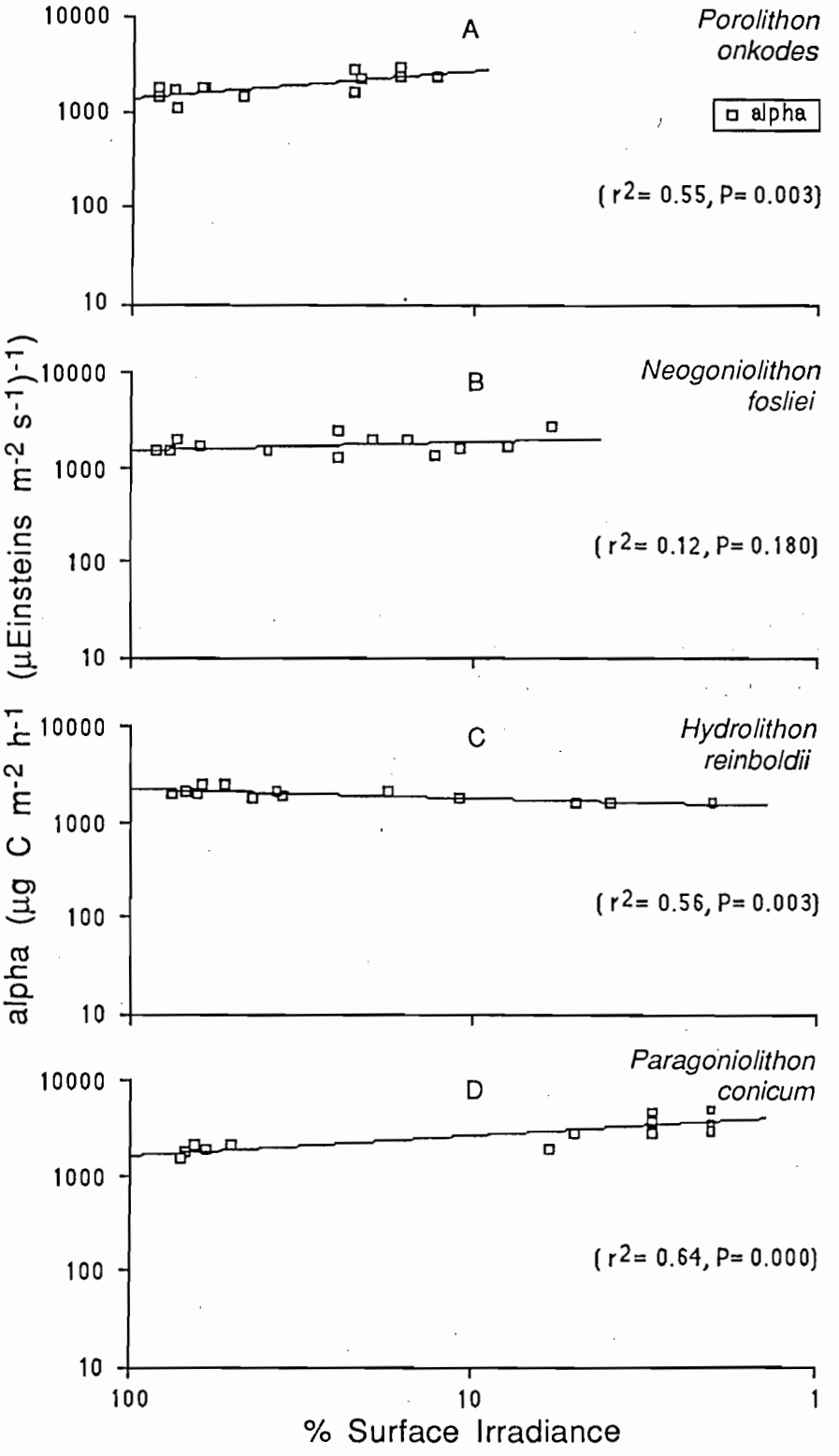
A
Porolithon onkodes
alpha
(r2= 0.55, P= 0.003)
B
Neogoniolithon fosliei
(r2= 0.12, P= 0.180)
C
Hydrolithon reinboldii
(r2= 0.56, P= 0.003)
D
Paragoniolithon conicum
(r2= 0.64, P= 0.000)
10000
1000
100
10
alpha (µg C m-2 h-1 (µEinsteins m-2 s-1)-1)
100
10
1
% Surface Irradiance

Fig. 20. Double logarithmic plots of alpha (α) against the percentage of surface irradiance transmitted to the depth of measurement (%SI), for *in situ* specimens of the different species. r^2 values and significance levels (P) are shown in parentheses for each regression.

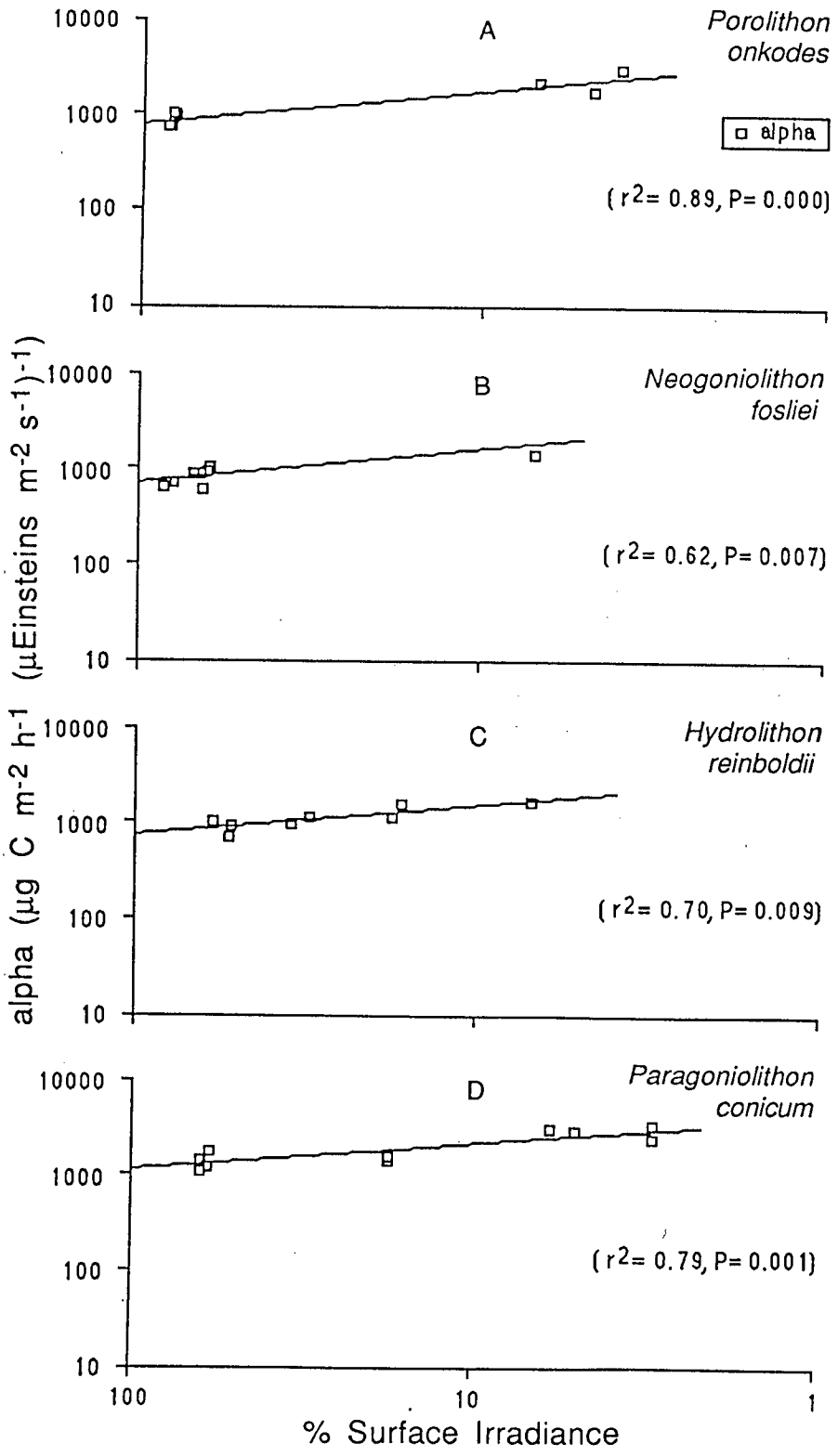
A
Porolithon onkodes
alpha
(r2= 0.89, P= 0.000)
B
Neogoniolithon fosliei
(r2= 0.62, P= 0.007)
C
Hydrolithon reinboldii
(r2= 0.70, P= 0.009)
D
Paragoniolithon conicum
(r2= 0.79, P= 0.001)
10000
1000
100
10
alpha (µg C m-2 h-1)
(µEinsteins m-2 s-1)-1)
100
10
1
% Surface Irradiance

were found among laboratory data. It should be noted though that only two of the regressions between $P^g_m/-R$ and %SI were found to be significant at the 95% probability level for laboratory or *in situ* data (Figs 17C, 18A). Even so, as a general rule it appears that P^g_m and R both fall with decreasing irradiance, while $P^g_m/-R$ has a tendency to rise (Figs 17B,C, 20A,C,D).

Trends observed among *in situ* data for R, ε, I_c, I_k, and $I_{0.95}$, are all consistent with those published in the literature for phytoplankton (Falkowski & Owens 1978, 1980; Falkowski 1980), benthic macroalgae (Talling 1961; Steemann Nielsen 1975; King & Schramm 1976; Ramus *et al.* 1976; Li & Titlyanov 1978; Carpenter 1985) and the zooxanthellae within reef corals (Falkowski & Dubinsky 1981; Chalker *et al.* 1983; Porter *et al.* 1984). Regressions between the logarithms of each of the above-listed photokinetic parameters and the logarithms of the percentages of surface irradiance transmitted to the depths at which the crustose coralline specimens were growing were all highly significant at the 95% probability level (Figs 16, 18, 20).

In most instances, the same relationships could be demonstrated for laboratory data (Figs 15A,B,D, 17, 19A,D). However, as stated previously, there were a few notable exceptions. For *H. reinboldii*, neither α increased (Fig. 19C) nor I_k decreased (Fig. 15C) in response to decreasing irradiance. Similarly, for *N. fosliei* the value of α did not significantly increase with decreasing irradiance (Fig. 19B, $P=0.18$) or increasing water depth (Table 4). These anomalies, and the noted reduction in photosynthetic rate when specimens were measured in the laboratory (see Section 2. 4. 2, Figs. 9, 10, 11, 12, and a comparison of the data in Tables 4 & 5), suggest that inappropriate methods may have been used in the laboratory experiments.

The methods employed in the laboratory and *in situ* studies differed in a number of respects. These are listed below with arguments as to why all but the last can be discounted, on logical or experimental grounds, as possible explanations for the observed differences in result.

(i) The specimens used in the laboratory experiments were removed from their natural substratum, ground free of non-living basal substrate, transported under seawater to the laboratory, and subsequently transfered to the oxygen electrode cell. These procedures may have caused a degree of trauma. However, specimens were not removed from the reef surface until they had completely regenerated their damaged

margins and when measured in the laboratory had similar respiration rates to the *in situ* crusts. This suggests that the specimens used for laboratory experiments were not unduly affected by the collecting or handling procedures.

(ii) Penicillin and Streptomycin were used to suppress bacterial respiration during incubations in the laboratory. These antibiotics might also have suppressed coralline photosynthesis. Published evidence does indicate that streptomycin in high concentrations leads to a degradation of chlorophyll *a* (Provasoli *et al.* 1948; Wolken 1956). However, the concentrations used were at the level recommended for routine cell culture (Commonwealth Serum Laboratories) and were at least 10-fold less than those used by other workers to demonstrate chlorophyll degradation. More directly, pilot experiments were conducted during 1984 to examine the effects of antibiotics on coralline photosynthesis. Under constant illumination no change in photosynthetic rate was observed in specimens incubated over an 8-hour period after the antibiotics penicillin and streptomycin had been added (unpublished data). The concentrations used in the pilot study were the same as those which were used in the final experiments.

(iii) The crusts used in the laboratory experiments had a diameter less than half that of the *in situ* specimens. No significant differences were noted in the thickness of the photosynthetic layer because the laboratory and *in situ* specimens were sub-sampled from crusts of similar dimension. It is difficult to conceive that smaller specimens with a larger circumference to surface area ratio would for this reason alone exhibit lower rates of photosynthesis since the margin is considered to be the principal region of active growth (Adey & Vassar 1975; Steneck & Adey 1976).

(iv) Laboratory incubations were performed using a smaller (*ca* 15 ml) volume of seawater without replacement of the seawater at regular intervals. Nutrients may thus have become limiting or waste products might have accumulated in the incubation water. However, the ratio of crust surface area to water volume was consistent between laboratory and *in situ* experiments. Oxygen tensions were never allowed to exceed those of the initial incubation water and thus the demand for nutrients should not have exceeded the amount available at the start of each experiment. Moreover, since nutrient flux is principally governed by the rate of metabolism, specimens from shallow water with higher metabolic rates should have shown greater departures from *in situ* values than specimens from deeper water with lower metabolic rates but this was not supported by the data (compare metabolic rates shown in Tables 4 & 5). Similarly, a build up of toxic substances was not indicated by the data because there was no change in respiration rate in the dark, nor photosynthetic rate in the light,

from the beginning to the end of the experiment, which also indicated that nutrients were not limiting.

(v) There may have been very small differences in the rates of water motion produced by the stirring units in each of the incubation chambers. However, all efforts were made to ensure that these were equal, and the data of other workers suggests that rates of coralline photosynthesis are not significantly affected by rates of water movement so long as some agitation is provided (Marsh 1970; Littler 1973a; Littler & Doty 1975).

(vi) At times there were small differences in the temperature of the incubation water used in each of the studies. However, the temperature of the incubation water used in the laboratory experiments was constant at 25°C which was always close to the temperature recorded during the *in situ* incubations (24.2- 26.8°C).

(vii) Laboratory experiments were conducted during the spring, whereas most of the *in situ* experiments were carried out in autumn. However, seasonal differences in the rates of algal primary production are largely due to changes in irradiance (e.g., Carpenter 1985). Since changes in irradiance throughout the year essentially follow a sine curve with a summer maximum and winter minimum, the amount of irradiance in spring should be more or less equivalent to the amount of irradiance in autumn. Moreover, when differences were measured in the amount of irradiance available to the specimens over the two periods of the year, the peak noon values were invariably higher at the time of the laboratory investigations (see Tables 14 & 15 presented in Section 2. 4. 7).

(viii) Much of the non-living, basal substrate of the crusts used in the laboratory experiments was removed by grinding before measurements were taken. This reduced the amount of endolithic algae contained in each crust without appearing to affect the living crust itself. Although only a few measurements have been made on the productivity of endolithic communities existing beneath the living surface of actively growing organisms, most evidence from corals suggests that their rates are likely to be very low as a function of the extremely reduced irradiance (Kanwisher & Wainwright 1967; Franzisket 1968; Halldal 1968).

Pilot experiments demonstrated that crusts from which the living coralline surface had been mechanically removed, and which thus contained only the endolithic communities, showed little capacity for oxygen production (unpublished data). In fact, three out of the four pilot experiments showed low variable rates of net oxygen consumption. The fourth showed slight rates of net oxygen production but only at

irradiance levels far above those which could be reasonably expected to pass through the living coralline layer. However, sufficient damage may have occurred to the endolithic algae during removal of the coralline layer to have led to a reduction in net oxygen production. Experiments involving intact crusts and ^{14}C assimilation would be preferable for the resolution of this problem. Such incubations have been carried out but the results are yet to be analysed.

Specimens stained with acridine orange showed strong chlorophyll fluorescence throughout the living coralline tissue, but little among the underlying endolithic populations. Microscopic examination of sectioned coralline crusts revealed that the vast majority of endolithic species were blue-green algae (i.e., cyanobacteria). Dr. Y. Sorokin (personal communication) suggests that much of the blue-green flora is likely to be photosynthetically inactive. This is supported by the observed lack of viable chlorophyll fluorescence.

Further indirect evidence for discounting the possibility that photosynthetic rates were reduced by the removal of endolithic algae comes from an analysis of the bathymetric distribution of such endolithic communities. Visual observation and pigment analyses (Plate 7) indicate that endolithic populations are more abundant in shallow water. If endolithic algae do measurably contribute to the overall photosynthetic rates of coralline crusts then their removal should have had a more significant affect on the rates of the shallow water specimens. In fact, greater differences were observed in the rates of the deep-water specimens (compare data shown in Tables 4 & 5).

(ix) The laboratory incubations were carried out under artifical light using neutral density filtration to simulate light at depth. This is the most plausible explanation for the observed differences between the laboratory and *in situ* results. The light used for the laboratory incubations was probably inappropriate for all but the most highly illuminated specimens which were collected from the shallowest locations where the spectral distribution of the light was modified least by attenuation. These specimens belonged to the species *P. onkodes* and were collected from exposed locations at 0 m. Mean rates of photosynthesis for *P. onkodes* at 0 m under laboratory and *in situ* conditions were in close aggreement (Tables 4 & 5). However, photosynthetic rates for specimens of *P. onkodes* and the other three species obtained from deeper or more shaded locations were inconsistent. The laboratory rates were typically lower and the difference increased with depth or increasing shade.

Fig. 3 demonstrates that the infra-red heat filter covering the lens of the illumination source during laboratory experiments provided a good simulation of the light environment in seawater as compared with a 1% aqueous solution of $CuSO_4$ (w:w). However, it is well known that the spectral distribution of light in seawater changes with depth (Jerlov 1976). Therefore, while the spectrum of light applied to the specimens of *P. onkodes* from 0 m was probably comparable to *in situ* conditions, the spectrum applied to deeper or shaded specimens was probably not. Jitts (1963) has cautioned against the use of neutral density filters in bathymetric studies of marine plant primary production, but many laboratory investigations continue to take this approach (e.g., Marsh 1970; Littler 1973c; Littler & Doty 1975; Vooren 1981; Hawkins & Lewis 1982; Littler *et al.* 1986). This is undoubtably a product of the difficulties involved in firstly determining *in situ* spectral distribution, and secondly in correctly simulating it. It has been argued by certain workers that light quality does not affect algal photosynthesis (Dring 1971; Drew 1983; Ramus & Van der Meer 1983), even though Doty (1962 - cited from Jitts 1963) compared rates of algal photosynthesis under neutrally filtered and simulated *in situ* light (using wavelength-selective glass filters) and concluded that neutral density filtration could lead to a serious underestimation of *in situ* primary production. His conclusion (resulting from work with Jitts and Saijo) is supported by the results of this study. Moreover, Vooren (1981), who estimated productivity using artificial light and neutral density filtration, even went as far as to provide corrections for his data to account for known variation in the spectral composition of submarine light. He suggested that production rates measured using neutral density filtered light must be increased by up to 15% for red algae (*ca* 5% for crustose corallines) and by up to 50% for brown algae. Tables 4 & 5 suggest that in the worst cases production for the crustose corallines studied here may be underestimated by 30-40%. However, Vooren did not determine his corrections experimentally, and absolute comparisons between laboratory and *in situ* production rates cannot be made for the data reported in the present study. This is because biochemical standards (i.e., pigment content) upon which to normalise productivity data could not be accurately determined, and because specimens were not always obtained from environments of equal PPFD for the laboratory and *in situ* experiments. Larkum & Barret (1983) have called for more studies to elucidate the effects of light quality on algal photosynthesis. The need for such studies is supported by the data presented here. Moreover, this study emphasises the importance of *in situ* investigations for determining natural rates of primary production.

2. 4. 5. SOURCES OF VARIATION AMONG PHOTOADAPTIVE PARAMETERS

Analyses of variance

Two-way analyses of variance were performed on the parameters I_c, I_k, α, and $P^g_m/-R$ to determine major sources of variation. The factors examined were species and depth. Depth was an approximate index of irradiance, and on this basis analyses included data for *P. onkodes* collected from shaded locations in shallow water where the measured PPFD was similar to that at a depth of 6 m. Range tests were not performed if significant interactions occurred. Similarly, if depth effects were significant among *in situ* data, range tests were not needed since only two depths were included in the analyses. The results are presented in Table 7A-D.

I_c: Depth was a highly significant factor in determining the value of I_c. Variation in I_c was not significant between 3 and 6 m among laboratory specimens. Principal changes in I_c therefore occurred between 0 and 3 m. This is consistent with a change in reef profile at a depth of 2-3 m from essentially horizontal to a steeply inclined slope. Below 2-3 m inclination of the forereef slope away from the direction of incident sunlight severely reduces the available PPFD and explains the more marked changes in I_c between 0 and 3 m than between 3 and 6 m. I_c was proportional to PPFD (see Figs 15 & 16) but not to depth.

Laboratory data also revealed significant species effects. *In situ* measurements did not. This is most reasonably explained by differences in the two sampling strategies. Selection of specimens for laboratory measurements was not biassed by the need to accommodate an *in situ* incubation chamber. Even though the incubation chamber was of small dimension and spatially separated from the datalogger, deployment within confined spaces was sometimes impossible without disrupting the immediate environment. In consequence, more cryptic species tended to be sampled from higher irradiance environments than would have been typical for the population mean at a given depth interval. This is not regarded as a serious bias since Figs 15 and 16 demonstrate that the logarithm (*ln*) of I_c is directly proportional to *ln* %SI. I_c can therefore be calculated for any %SI over the range of measured values.

I_k: Species and depth both significantly affected the value of I_k. The SNK range test partitioned the *in situ* species effects into two groups. The first included

Table 7. Results of two-way ANOVAs and *a posteriori* range tests performed on parameter estimates of I_c (A), I_k (B), alpha (α) (C), and P^g_m (D), describing features of the laboratory and *in situ* light-saturation curves for photosynthesis. The factors tested were species and depth. Values show the significance of each factor and of the interaction between the factors in explaining the observed variation. Range tests indicate significantly different sample means within tested groups when species or depth factors are significant at the 95% probability level. Po denotes *Porolithon onkodes*, N denotes *Neogoniolithon fosliei*, H denotes *Hydrolithon reinboldii*, and Pa denotes *Paragoniolithon conicum*. Depth in metres is indicated by 0, 3, or 6. XXXX denotes that a range test was not appropriate (see text).

I_c	Species	Depth	Species * Depth
Laboratory	**0.000**	**0.000**	0.089
Range test	**(Po)(N)(H)**	**(0)(3,6)**	XXXX
In situ	0.234	**0.000**	0.075
Range test	XXXX	**(0)(6)**	XXXX

I_k	Species	Depth	Species * Depth
Laboratory	**0.000**	**0.000**	**0.000**
Range test	XXXX	XXXX	XXXX
In situ	**0.003**	**0.000**	0.093
Range test	**(Po,N)(Pa)**	**(0)(6)**	XXXX

α	Species	Depth	Species * Depth
Laboratory	0.277	0.196	**0.001**
Range test	XXXX	XXXX	XXXX
In situ	0.449	**0.000**	0.086
Rangetest	XXXX	XXXX	XXXX

$P^g_m/-R$	Species	Depth	Species * Depth
Laboratory	**0.009**	**0.014**	**0.000**
Range test	XXXX	XXXX	XXXX
In situ	HETEROSCEDASTIC		
Range test	XXXX	XXXX	XXXX

Table 8. Results of Kruskal-Wallis tests performed on parameter estimates of epsilon (ε) for laboratory light-saturation curves for photosynthesis of different species at different depths. P denotes significance level. '6' m denotes that values were obtained for specimens living in shaded environments in shallow water (1.5-2.5 m) where PPFD was equivalent to a real depth of 6 m.

P. onkodes and *N. fosliei*, which are both abundant in high irradiance environments, and the second comprised *P. conicum*, which is more abundant in low irradiance environments.

α: appeared independent of species in both treatments. Depth, however, significantly affected α under *in situ* but not laboratory conditions. The apparent lack of significant depth-related effects on the results of laboratory experiments probably exemplifies the problems previously discussed regarding the influence of inappropriate spectral distribution (see Section 2. 4. 4.).

P^g_m/-R: varied both with species and depth under laboratory conditions. However, when *ln* $P^g_m/-R$ was regressed against *ln* %SI for individual species the slope of the line was rarely significantly different from zero (Fig. 17). The lack of significant relationship between *ln* $P^g_m/-R$ and *ln* %SI is also suggestive of problems relating to spectral composition. Even so, regressions between *ln* $P^g_m/-R$ and *ln* %SI for *in situ* data were similarly inconclusive (Fig. 18), probably because of the large errors associated with estimating P^g_m under sub-saturating irradiance and the relative inappropriateness of using a surface area measure to normalise physiological data.

ANOVA was not performed on *in situ* $P^g_m/-R$ data because all cells were not equally variable (heteroscedastic). Samples from deeper water were considerably more variable than samples from shallow water. Attempts to achieve homoscedasticity by transformation were unsuccessful.

All ANOVAs revealed some level of interaction between depth and species ($P<0.1$). However, interactions at the 95% level ($P<0.05$) were only evident among laboratory data (for I_k, α, and $P^g_m/-R$). The interaction term was probably reduced among *in situ* data because specimens were sampled from more uniform photic environments within each depth category. Nonetheless, both sets of data indicate that different species of crustose coralline algae occupy rather different photic environments within the depth range examined. This is consistent with the observed patterns of distribution. In shallow water *P. conicum* tends to be more abundant in shaded locations, whereas *P. onkodes* and *N. fosliei* are more abundant on substrata exposed to direct light. *H. reinboldii* is more evenly distributed across both exposed and shaded sites.

Kruskal-Wallis tests

Kruskal-Wallis non-parametric tests were used to determine if, for each species, there were significant differences ($P<0.05$) in the value of ε for specimens growing at different depth intervals (and hence under different irradiance conditions). The results are presented in Table 8. Significant differences were found in the value of ε for *P. onkodes*, *N. fosliei* and *H. reinboldii*, but not for *P. conicum*. *A. posteriori* range tests using multiple comparisons by STP were applied to the ε data for *N. fosliei* and *H. reinboldii*. *P. onkodes* was not included in the range tests because the prerequisite of the STP test for equal sample sizes could not be satisfied without risk of bias. For *N. fosliei* significant differences were found between 6 m and the other two shallower depths (i.e., 0 and 3 m). For *H. reinboldii* significant differences were found in the value of ε for each of the three depth intervals (i.e., 0, 3, and 6 m).

These results are interesting because they comply with above stated observations that *N. fosliei* and *H. reinboldii* are broadly distributed across high and low light environments whereas *P. conicum* is generally distributed throughout more evenly shaded environments.

2. 4. 6. IRRADIANCE REQUIRED FOR COMPENSATION (I_c), THE ONSET OF SATURATION (I_k), AND SATURATION ($I_{0.95}$) OF PHOTOSYNTHESIS

From *in situ* data (see Table 5), mean I_c values for *P. onkodes* ranged from 14.3 μEinsteins m^{-2} s^{-1} at '6' m to 50.8 μEinsteins m^{-2} s^{-1} at 0 m. For *N. fosliei*, I_c ranged from 14.5 μEinsteins m^{-2} s^{-1} at 6 m to 50.9 μEinsteins m^{-2} s^{-1} at 0 m. For *H. reinboldii*, I_c ranged from 22.3 μEinsteins m^{-2} s^{-1} at 6 m to 41.0 μEinsteins m^{-2} s^{-1} at 3 m. Finally, for *P. conicum*, I_c ranged from 11.3 μEinsteins m^{-2} s^{-1} at 18 m to 34.4 μEinsteins m^{-2} s^{-1} at 0 m. For the reasons previously discussed concerning the difficulties in accommodating highly cryptic specimens in the *in situ* sampling programme, the lower I_c values for each species do not necessarily represent their limits to light compensation. Indeed, laboratory-based estimates of I_c were typically lower (Table 4), particularly for *H. reinboldii*. In fact, since it has been argued that most laboratory specimens were probably subjected to light of less than natural spectral distribution (see Section 2. 4. 4), if the correct illumination had been applied

Species	Kruskal-Wallis Test ε vs depth	STP (range test) depth groupings
P. onkodes	P < 0.050	(0,'6')(3)
N. fosliei	P < 0.009	(0, 3) (6)
H. reinboldii	P < 0.009	(0) (3) (6)
P. conicum	P > 0.102	(0, 3, 6)

the differences between laboratory and *in situ* estimates of I_c would probably have been even greater. Because the laboratory estimates are considered to be in error the actual values will not be considered further. However, relative differences in the values of I_c are still important because the reduced bias in the selection of laboratory specimens, when compared with the selection of *in situ* specimens (see Section 2. 4. 5), resulted in samples which were more representative of the individual species distributions. Thus, variation in the laboratory estimates of I_c for each species probably provides a better relative measure of differences between the species. For example, at 6 m *H. reinboldii* had a lower mean I_c value than *N. fosliei* or *P. onkodes*, but a higher mean I_c value than *P. conicum*. By and large, *P. onkodes* had the highest values for I_c, followed in descending order by *N. fosliei*, *H. reinboldii*, and finally *P. conicum* (Table 4). This series is consistent with the observed photic distributions of the species (Fig. 2).

From *in situ* data (Table 5), the mean I_k values for *P. onkodes* ranged from 94 μEinsteins m^{-2} s^{-1} at '6' m to 244 μEinsteins m^{-2} s^{-1} at 0 m. For *N. fosliei*, the value of I_k ranged from 90 μEinsteins m^{-2} s^{-1} at 6 m to 222 μEinsteins m^{-2} s^{-1} at 0 m. For *H. reinboldii*, the value of I_k ranged from 124 μEinsteins m^{-2} s^{-1} at 6 m to 175 μEinsteins m^{-2} s^{-1} at 3 m. Finally, for *P. conicum*, the value of I_k ranged from 69 μEinsteins m^{-2} s^{-1} at 18 m to 146 μEinsteins m^{-2} s^{-1} at 0 m. Previous discussion has identified problems with the estimation of I_k from laboratory experiments. However, it is important to note that in relative terms the I_k values for *P. conicum* in the laboratory were half as large as those for *N. fosliei* and *H. reinboldii* at a depth of 6 m (Table 4), which infers a greater efficiency of light utilisation (Steemann Nielsen 1975) and hence a greater capacity for adaptation to shade. Among *in situ* data the distinctions between the I_k values for each species are less obvious but generally speaking *P. onkodes* has the highest values, *P. conicum* the lowest values, and *N. fosliei* and *H. reinboldii* have intermediate values (Tables 4, 5).

Lastly, visual estimates of the irradiance at which saturation occurs are generally considered to be approximately twice as large as I_k (see Table 5) if the hyperbolic tangent function is used to model *P-I* data (Chalker *et al.* 1983). Strictly speaking the term 'saturating irradiance', often quoted as I_{sat}, has no real meaning because P^g_m is approached asymptotically and I_{sat} is therefore an undefinable quantity. It is much better therefore to choose a value which is very close to the hypothetical maximum but which can be properly defined in mathematical terms (Dr. B.E. Chalker

- personal communication). For this reason the value of $I_{0.95}$ has been chosen here and the term is used synonymously with the I_{sat} values quoted by other workers throughout the following text. It should be noted that in practical terms the value of P^g_m at $I_{0.95}$ is probably as accurate a measure of the photosynthetic capacity as is necessary if the intention is to determine values at the 95% confidence level.

The mean $I_{0.95}$ values for *in situ* specimens of *P. onkodes* ranged from 173 μEinsteins m^{-2} s^{-1} at '6' m to 446 μEinsteins m^{-2} s^{-1} at 0 m. For *N. fosliei*, the value of $I_{0.95}$ ranged from 166 μEinsteins m^{-2} s^{-1} at 6 m to 407 μEinsteins m^{-2} s^{-1} at 0 m. For *H. reinboldii*, the mean value of $I_{0.95}$ ranged from 227 μEinsteins m^{-2} s^{-1} at 6 m to 321 μEinsteins m^{-2} s^{-1} at 3 m. Finally, for *P. conicum*, the mean value of $I_{0.95}$ ranged from 127 μEinsteins m^{-2} s^{-1} at 18 m to 267 μEinsteins m^{-2} s^{-1} at 0 m. Once again, absolute values for $I_{0.95}$ from laboratory experiments cannot be considered because of the doubts previously raised regarding their relevancy to *in situ* data. However, when crustose coralline *P-I* data were modelled by the four functions described in Section 2. 2. 2., the irradiance needed to drive photosynthesis to 95% of its saturated value ($I_{0.95}$) was highly variable (Table 4). On a conjectural basis, if theories are invoked concerning the effects of differential amounts of $CaCO_3$ in the tissues of calcareous algae on the shape of their *P-I* curves, then the similarly variable nature of $CaCO_3$ data (see Table 20, presented in Section 3. 4. 8) may in part explain the observed variation in $I_{0.95}$ (Table 4) in the data for photosynthesis.

Kirk (1983) has reviewed existing literature on estimates of I_c, I_k, and $I_{0.95}$ for aquatic plants. For fleshy macroalgae, in temperate seas, the value of I_c generally ranges from 6 to 24 μEinsteins m^{-2} s^{-1}, I_k ranges from 56 to 160 μEinsteins m^{-2} s^{-1} (although only a few estimates are available), and $I_{0.95}$ ranges from 25 to 700 μEinsteins m^{-2} s^{-1}. No crustose coralline algae or other tropical marine algae were included in the survey. The crustose coralline algae studied *in situ* here have I_c and I_k values which fall within the ranges reported by Kirk at low irradiances, but values which are considerably greater than those reported by him at high irradiances (Table 5). Values for I_c from the laboratory experiments were similarly above the values reported by Kirk under high irradiance although the values for I_k were consistent with the range given by him. The $I_{0.95}$ values of the *in situ* data presented in this study (which were modelled using the hyperbolic tangent function) fall within the range given by Kirk, while the laboratory estimates (modelled using the functions given in Section 2. 2. 2.) were considerably greater under high irradiance.

Marsh (1970) reported mean values of *ca* 11 μEinsteins $m^{-2}s^{-1}$ for I_c, and 200 μEinsteins m^{-2} s^{-1} for $I_{0.95}$, for shallow water specimens of what he assumed to be *P. onkodes* (after Lee 1967) on reefs in the Marshall Islands and near Hawaii. Littler (1973a) reported a mean value of *ca* 10 μEinsteins m^{-2} s^{-1} for I_c and a mean value of *ca* 194 μEinsteins m^{-2} s^{-1} for $I_{0.95}$ for specimens of the coralline alga *Sporolithon erythraeum* in shallow water on a Hawaiian fringing reef. Littler (1973c) and Littler & Doty (1975) reported that equivalent values for the species *P. onkodes* were considerably higher, with I_c occurring at around 19 μEinsteins m^{-2} s^{-1} and $I_{0.95}$ occurring between 194 and 387 μEinsteins m^{-2} s^{-1}. Wanders (1976) and Vooren (1981) both reported I_c values of *ca* 30 μEinsteins m^{-2} s^{-1}, and $I_{0.95}$ values of 130-150 μEinsteins m^{-2} s^{-1} and 70-140 μEinsteins m^{-2} s^{-1} respectively for crustose coralline algae obtained from shallow and deep sites on the reef of Curacao, Netherlands Antilles. The data presented here for I_c are a little higher than those of Wanders (1976) for shallow water crustose Corallinaceae, and somewhat lower than those of Vooren (1981) for deep water crustose Corallinaceae, but nonetheless are reasonably close. The I_c values presented by Littler (1973a) for *S. erythraeum*, and by Marsh (1970), Littler (1973c), and Littler & Doty (1975) for *P. onkodes* are significantly lower.

Since Vooren (1981) used artificial illumination, and did not attempt to simulate submarine irradiance, his values are probably greater than might have been obtained with natural light. Wanders (1976), in contrast, did use submarine light but made his measurements on coralline crusts which had been cut from the reef. In consequence, the endolithic algae which typically occupy the undersurfaces of these specimens would probably have been exposed to far greater irradiance than normal. As a result, their contribution to oxygen production might have reduced the irradiance needed for compensation of the entire crust. Similar biasses may have contributed to the values reported by Littler (1973c) and Littler & Doty (1975), but it is equally possible that the differences in the reported values may simply be a product of natural variation. The results of Marsh (1970) are a little harder to explain since no specimens of *P. onkodes* (obtained from the reef crest or reef flat) in this study were ever found to have an I_c value anywhere near as low as 11 μEinsteins m^{-2} s^{-1} (see Tables 4 & 5). Indeed, only one specimen at '6' m was recorded with an I_c as low as 11 μEinsteins m^{-2} s^{-1} (Tables 5). Marsh's estimate of I_c for *P. onkodes* seems abnormally low given the similarity between the estimates of Wanders (1976), Vooren (1981), and this study. Possibly the species was *S. erythraeum*, or one exhibiting

similar light responses, in which case agreement would be found with the results of Littler (1973a).

With regard to $I_{0.95}$, the ranges reported in this study are considerably higher than those reported by the authors mentioned above (see Table 9 for comparison). However, all other authors based their estimates on hand-fitted *P-I* curves, or other visual estimates, and did not attempt to mathematically simulate the relationship between crustose coralline photosynthesis and irradiance. For this reason, their estimates of $I_{0.95}$ are probably reduced because P^g_m is approached asymptotically with small changes in photosynthetic rate occurring over large changes in irradiance. In the absence of rigorous mathematical procedures which allow the shapes of *P-I* curves to be statistically examined, there are considerable difficulties in estimating $I_{0.95}$ (see also Kirk 1983).

In classical terms, 'sun' algae become saturated at irradiance levels between approximately 500 and 1000 μEinsteins m^{-2} s^{-1}, whereas 'shade' algae become saturated at irradiance levels of between 50 and 200 μEinsteins m^{-2} s^{-1} (Raven & Glidewell 1975; Raven & Smith 1977). By these definitions, most of the crustose coralline algae examined in this study are intermediate between 'sun' and 'shade' algae. Deep specimens possess the saturation characteristics of 'shade' algae, and shallow specimens approach the saturation characteristics of 'sun' algae (Table 9). However, preliminary re-analysis of *in situ P-I* data using the modelling methods applied to the laboratory data indicated that the shapes of these *P-I* curves may also change in a similar though less significant fashion to the laboratory curves with increasing depth and decreasing irradiance. That is to say the value of ε may be different for shallow as opposed to deep-water specimens. The magnitude of ε profoundly affects the relationship between I_k and $I_{0.95}$. For example, if $\varepsilon = 1$ (i.e., the hyperbolic tangent function, Eq. 3) then $I_{0.95} = 1.83 \times I_k$, but if $\varepsilon = -1$ (i.e., the right rectangular hyperbola, Eq. 1) then $I_{0.95} = 19 \times I_k$. This may be seen by comparing the values for I_k and $I_{0.95}$ in Table 4. If the value of ε also increases with depth among *in situ* data then individuals living at 0 m may be found to exhibit $I_{0.95}$ values typical of 'sun' algae.

Table 9. Available data on mean saturation light intensities (I_{sat}) for various species of crustose coralline algae compared with typical values for 'sun' and 'shade' algae. Data include estimates from this and other studies. Data for this study are for estimates of 95% saturating irradiance ($I_{0.95}$). * denotes that the species was not positively identified. ~ denotes that the actual depth was not quoted but could be deduced from site descriptions provided in the reference. '6' denotes that specimens were not living at 6 m but experienced a PPFD equivalent to that depth.

Study	Species	Depth m	I_{sat} μEinsteins m^{-2} s^{-1}
Marsh 1970	*Porolithon onkodes**	~0	200
Littler 1973a	*Sporolithon erythraeum*	~0	194
	Porolithon onkodes	~0	387
Littler & Doty 1975	*Porolithon onkodes*	~0	194-387
Wanders 1976	*Lithophyllum* sp.		
	Neogoniolithon solubile	0.5-3	130-150
	Porolithon pachydermum		
Vooren 1981	*Archaeolithothamnion dimotum*	25	
	Hydrolithon boergesenii	11	70-140
	Hydrolithon boergesenii	25	
***In situ* study**	***Porolithon onkodes***	**0**	**446**
	Porolithon onkodes	**'6'**	**173**
	Neogoniolithon fosliei	**0**	**407**
	Neogoniolithon fosliei	**3**	**365**
	Neogoniolithon fosliei	**6**	**166**
	Hydrolithon reinboldii	**3**	**321**
	Hydrolithon reinboldii	**6**	**227**
	Paragoniolithon conicum	**0**	**267**
	Paragoniolithon conicum	**6**	**138**
	Paragoniolithon conicum	**18**	**127**
Raven & Glidewell 1975 Raven & Smith 1977	'shade' algae		50-200
Raven & Smith 1977	'sun' algae		500-1000

2. 4. 7. RATES OF PRIMARY PRODUCTION

Metabolic Quotients

Rates of carbon fixation were calculated for each species by multiplying values for oxygen production by the reciprocal of the appropriate net photosynthetic quotient (i.e., 1/net *PQ*) given in Table 10. Mean net *PQ*s were determined using the methods described in Section 3. 3. Respiratory quotients (*RQ*) could not be determined because the pH changes which occurred during dark incubations in the middle of the day were not equivalent to those which occurred at night. Presumably a lag exists in the exchange of carbon dioxide following periods of rapid photosynthesis and calcification. *RQ* was therefore assumed to be the reciprocal of net *PQ*. Kinsey (1979) has shown this is a valid assumption for most reef communities. This is particularly likely if the organisms are autotrophic because the products which are consumed during the night must be the those which are produced during the day. Moreover, if RQ = net PQ^{-1} then net PQ = true PQ. Net *PQ* will be referred to simply as *PQ* in the following discussion since it is assumed that net PQ = true PQ.

The mean *PQ*s for *P. onkodes*, *N. fosliei*, and *H. reinboldii* lay between 1.21 and 1.33. The *PQ* for *P. conicum* was 1.07. These results are well within the range of published estimates for other marine macrophytes. Buesa (1980) determined a mean *PQ* of 1.21 for 16 species of marine plants, with individual estimates ranging from 1.00 to 1.46. Brandt & Raben (1912-22) and Ketchum & Redfield (1949) found a similar range from 0.86 to 1.47. Ryther (1956) advocated that a general mean value of 1.25 should be used for productivity estimates. Strickland (1960) and Littler & Murray (1974) recommended a slightly lower value of 1.20.

Although the published estimates of *PQ* from several independent investigations are similar it is unfortunate that specific determinations of *PQ* are not undertaken more often in productivity studies. Estimates of primary production and calcification are highly sensitive with respect to the value assigned to *PQ* (see Barnes 1983). Table 10 demonstrates a clear difference between the *PQ* of *P. conicum* and the *PQ*s of the other three species. If productivity estimates had been based on a general mean value for *PQ* of say 1.20, then estimates for *P. conicum* would have been reduced by just over 10%, whereas estimates for *N. fosliei* and *H. reinboldii* would have been increased by 5.5% and 9.8% respectively. Therefore, without

Table 10. Net photosynthetic quotients (net *PQ*) of individual specimens, and mean net *PQ* values for each species.

Specimen	Species	Depth m	net *PQ*	mean net *PQ*
1	*Porolithon onkodes*	0	1.26	
2	*Porolithon onkodes*	0	1.19	
3	*Porolithon onkodes*	0	1.14	1.21
4	*Porolithon onkodes*	0	1.13	
5	*Porolithon onkodes*	0	1.34	
3	*Neogoniolithon fosliei*	3	1.48	
1	*Neogoniolithon fosliei*	6	1.15	1.27
4	*Neogoniolithon fosliei*	6	1.18	
2	*Hydrolithon reinboldii*	3	1.45	
3	*Hydrolithon reinboldii*	3	1.24	1.33
1	*Hydrolithon reinboldii*	6	1.30	
2	*Paragoniolithon conicum*	6	1.09	
3	*Paragoniolithon conicum*	6	1.05	1.07
4	*Paragoniolithon conicum*	6	1.06	

specific knowledge of the value of *PQ*, estimates of primary production could be in error by 20% or more if an inappropriate value is chosen from the range of published values.

Since *PQ* is the ratio between O_2 produced and CO_2 consumed (i.e., $\Delta O_2/\Delta CO_2$), a value of 1.0 infers that the primary product of photosynthesis is carbohydrate (Buesa 1980). Values greater than 1.0 suggest that the primary products of photosynthesis are storage compounds such as fats which are more highly reduced than carbohydrate (i.e., a smaller ratio of O to C atoms). Fat is the primary storage product, but the synthesis of other compounds such as protein can also elevate the value of *PQ*. The question therefore arises as to why *P. conicum* should produce largely carbohydrate, while the other three species synthesize significant amounts of fat or other compounds at a similar reduction level (see Table 10). Presumably storage products are synthesised when rates of photosynthesis exceed the demands of respiration and growth. A preponderance of carbohydrate production might thus infer that the rate of carbon fixation is only sufficient to support the day to day requirements of the plant, possibly as a result of lower external energy supplies. This may occur when individuals exist in light-limiting situations. Indeed, there appears to be some correlation between a reduction in irradiance and a fall in the value of *PQ*. For example, *P. conicum* generally occupies low to intermediate light environments and typically has low values for *PQ* (Table 10). Although samples were not sufficiently large to examine this relationship statistically, the variation found in the value of *PQ* both within and between different species (Table 10) is worthy of further discussion.

There is considerable difference between the mean value of *PQ* for *P. conicum* and the mean *PQ* values for the other three species. There is also a considerable difference between the *PQ* of specimens of *N. fosliei* at 6 m and the *PQ* of the specimen measured at 3 m (Table 10). Calculation of the integrated rates of primary production per day revealed a notable decline in net production between the depths of 3 and 6 m for *N. fosliei* and between 0 and 6 m for *P. conicum* (see Table 15 presented later in this section). In contrast, *H. reinboldii* showed no reduction in net primary production between the depths of 3 and 6 m (see Table 15), and likewise showed no significant change in the value of *PQ*. These data suggest a link between carbon gain per day and the value of *PQ* (Table 10).

Myers & Cramer (1948) maintained that where investigators found a *PQ* of unity, the value was an experimental artifact arising from procedures which invariably involved growing organisms under sub-saturating irradiance and then measuring the fluxes of O_2 and CO_2 under saturating irradiance to satisfy the requirements of the manometric techniques employed. On the strength of this claim and on the basis of other data, Ryther (1956) concluded that a *PQ* of between 1.1 and 1.3 was probably more reasonable. However, the specimens of *P. conicum* treated in this study were grown and measured under the same conditions of natural irradiance. The *PQ* values of close to 1.0 for *P. conicum* (Table 10) therefore do not represent experimental artifacts resulting from incorrect illumination.

It has been reported that the value of *PQ* can vary with such factors as temperature (Forward 1960), irradiance, the dominant product (Strickland 1960), and with the phase of life cycle of the species (Fogg 1968). However, Buesa (1980) concluded that neither temperature nor irradiance affected the value of *PQ* in marine plants off the coast of Cuba. This is in contrast with the results of this study which suggest that some link, either direct or indirect, exists between irradiance and the value of *PQ*.

For the purposes of discussion, the first basic premise must be that significant quantities of storage materials are not produced until the rate of photosynthetic carbon production exceeds the rate of respiratory consumption. This implies that at some stage a transition occurs between the production of carbohydrate and the synthesis of fat (or other more highly reduced compounds). This premise is supported by the knowledge that a reciprocal process takes place during darkness (French *et al.* 1934). French *et al.* (1934) grew the green alga *Chlorella* in light and then starved the alga in darkness for a prolonged period. After 10-20 hours the value of *RQ* dropped by over 40%. French *et al.* concluded that there were two respiratory substrates, one of which was exhausted preferentially. Presumably during photosynthesis, the reciprocal transition from carbohydrate to fat or protein production takes place gradually to satisfy the various growth demands of the plant. However, if the organism is existing under limiting conditions of irradiance it may never attain sufficiently saturated rates of photosynthesis to produce significant amounts of storage materials. There seems to be some agreement between this hypothesis and the *P-I* curves which were constructed for the *in situ* data. In this study the *P-I* curves of four of the specimens which were used to determine the the *PQ* values for specimens

existing at 6 m are shown in Fig. 21. One curve is for the species *N. fosliei* (Fig. 21A), one is for *H. reinboldii* (Fig. 21B), and two are for *P. conicum* (Fig. 21C,D). The specimen of *N. fosliei* was clearly operating well below saturation at maximum irradiance (Fig. 21A) and had a *PQ* of 1.18. The specimen of *H. reinboldii*, in contrast, approached full saturation at peak irradiance (Fig. 21B) and had a *PQ* of 1.30. The lower *PQ* value (1.18) for specimen number 4 of *N. fosliei* at 6 m when compared with the value (1.48) obtained for specimen number 3 at 3 m (Table 10) might thus be explained on the grounds that photosynthesis was light- (or otherwise - see Larkum & Barret 1983) limited. The absence of a noticeable difference between the *PQ* value (1.30) of the *H. reinboldii* specimen (number 1) from 6 m and the values for the two specimens (numbers 2 and 3) from 3 m (1.45 and 1.24 respectively, see Table 10) might be explained on the grounds that photosynthesis was not light-limited.

However, these considerations are not sufficient to explain the low *PQ* values for *P. conicum* at 6 m. Specimen number 4 was operating at sub-saturated levels of photosynthesis under maximum irradiance (Fig. 21D) and had a *PQ* of 1.06. Specimen number 2 was very nearly light-saturated with respect to photosynthesis (Fig. 21C) and yet still possessed a *PQ* of only 1.09. In fact, all three *PQ* estimates for *P. conicum* at 6 m were very similar (Table 10) even though the specimens received quite different amounts of irradiance (see Table 15 presented later in this section). This suggests that additional controls may be operative in *P. conicum*. Furthermore, both of the *P-I* curves shown for *P. conicum* (Fig. 21C,D) demonstrate greater saturation of photosynthesis in these specimens than was the case for specimen number 4 of *N. fosliei* (Fig. 24A), and yet both still had significantly lower *PQ* values.

These inconsistencies possibly indicate that specimens respond to the absolute rate of production rather than to the state of the reaction equilibria which define the various regions of *P-I* curves (see Section 2. 4. 3). However, if production rate is the critical determinant of *PQ*, then the specimens of *P. onkodes* which were measured at 0 m should have possessed the highest *PQ* values. This is clearly not the case (compare Table 10 with Tables 12 & 15). In addition, *P. conicum* did not exhibit lower production rates than *N. fosliei* at 6 m (see Tables 12 & 15 presented later in this section), but still had significantly lower values for *PQ* (Table 10).

Fig. 21. Light-saturation curves for gross photosynthesis by four *in situ* specimens of three species which were used to determine values for PQ at 6 m.

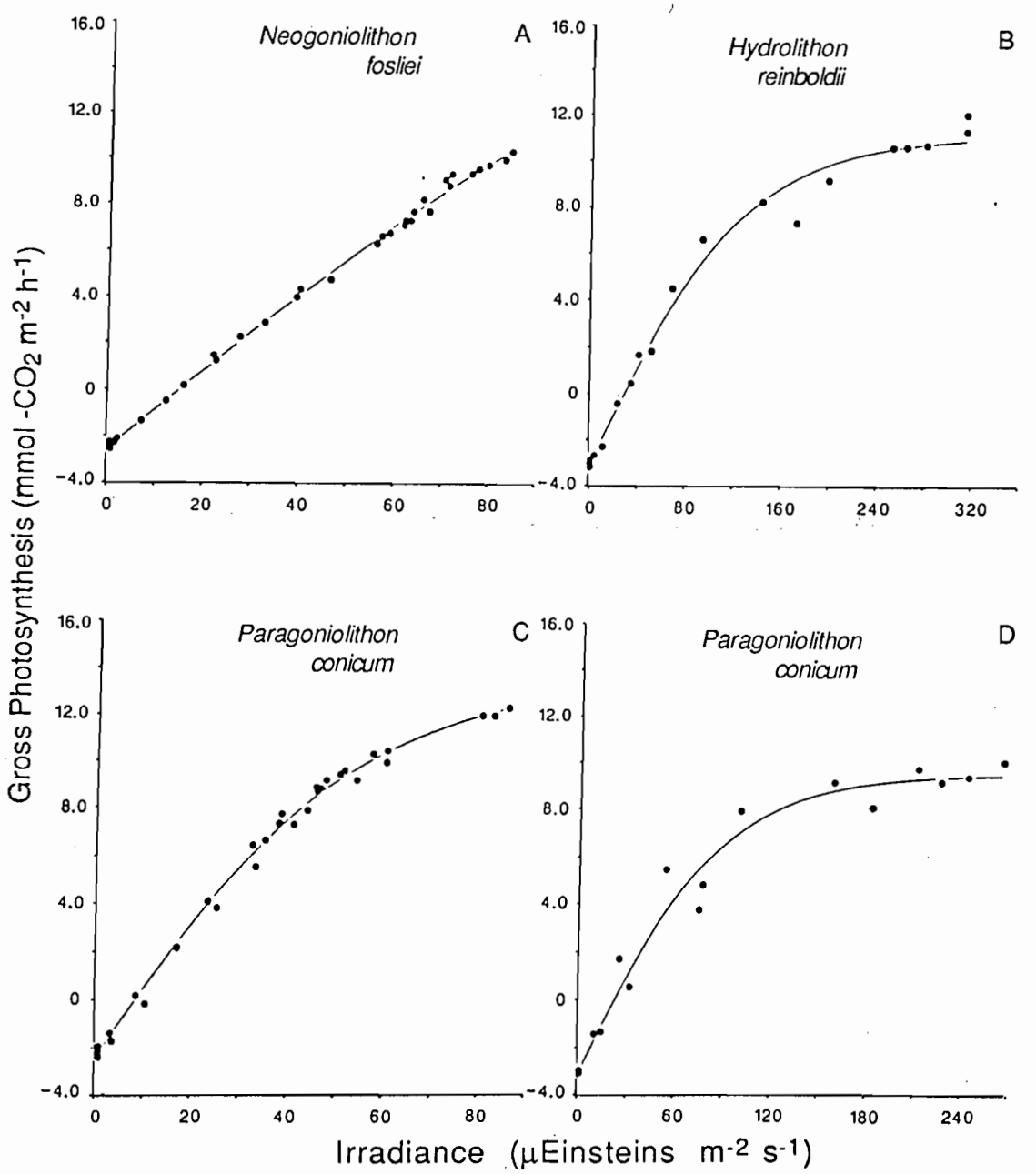
Neogoniolithon fosliei
A
Hydrolithon reinboldii
B
Paragoniolithon conicum
C
Paragoniolithon conicum
D
Gross Photosynthesis (mmol -CO2 m-2 h-1)
Irradiance (µEinsteins m-2 s-1)
16.0
12.0
8.0
4.0
0
-4.0
0
20
40
60
80
160
240
320
120
180

One of the most obvious morphological differences between *P. conicum* and the other three species is that it tends to produce relatively thin but extensive crusts. The other species all produce thicker, more heavily calcified crusts which tend to be more limited in lateral extent. If analogies can be made with terrestrial plants, 'shade' leaves are generally large and thin and are arranged upon the stem in a fashion which reduces overshading. 'Sun' leaves are typically smaller and thicker, since ample light is available to saturate many layers of cells, and their arrangement upon the stem is less critical in preventing overshading. It has been noted that algal growth forms show parallel adaptations (e.g., Littler 1980; Littler *et al.* 1983). For example, Littler (1980) interpreted the thin construction of the thalli of algae such as *Ulva californica* and *Enteromorpha* spp. as an adaptation for minimising self-shading, and Arnold & Murray (1980) found a positive correlation among benthic green algae between 'thinness' of thallus and photosynthetic efficiency. In the context of the crustose coralline species studied here, *P. conicum* generally has a significantly lower protein content to surface area ratio than any of the other three species (Table 6) at a given depth, which is indicative of a thinner photosynthetic layer. Given the broad similarity in rates of carbon fixation and $P^{g}_{m}/-R$ ratios for the four species (see Tables 12 & 15), it is possible that relatively more energy goes toward lateral extension than upward growth of the crust in *P. conicum*. This would produce a thinner photosynthetic layer more suited to effective light capture in low light environments.

Similar variation in growth form has been recorded in reef corals such as *Montastrea annularis* which exhibits changes in its form and pattern of growth with decreasing irradiance (Barnes & Taylor 1973; Grauss & MacIntyre 1976). In shallow water, colonies are dome-shaped and rates of calcification are uniform throughout the polyp layer. In deep water, colonies become plate-like and enhanced growth occurs at the margin, which is in consequence less heavily calcified. The enhanced growth at the margin is attributed to active transport and translocation of photosynthate from older parts to the sites of growth. Similar mechanisms for species of the branching coral *Acropora* were proposed by Pearse & Muscatine (1971) and later confirmed using radioisotope procedures by Taylor (1973).

Since crusts extend more rapidly outward than upward (Adey & Vassar 1975), it is likely that a significant amount of the photosynthate produced near the centre of the crust is translocated to the perimeter. Presumably carbohydrate is transported and metabolised more easily than fat. The notable difference in the mean

value of *PQ* for *P. conicum*, compared with other species, might thus reflect a greater relative production of easily transportable and consumable products to expedite growth at the margin. If translocation does occur in crustose coralline algae it would be interesting to determine the proportion and nature of carbon compounds transported under different circumstances, and by different species. If the hypothesis outlined above has any credence, carbohydrates such as glucose should be produced and transported preferentially in species exhibiting shade-adapted growth forms. Low molecular weight carbohydrates appear to be translocated preferentially from zooxanthellae to their coral or tridacnid hosts (Muscatine 1967).

Rates of primary production per hour

Discussion will be confined largely to data for crustose coralline primary production since data for other algal groups have been reviewed elsewhere (e.g., Lewis 1977; Larkum 1983). Moreover, since this is the only study of crustose coralline productivity where photosynthetic quotients were specifically determined, comparisons with the estimates of other workers will be largely restricted to oxygen data.

Maximal rates of gross primary production, net primary production, and dark respiration for laboratory and *in situ* experiments are given in Tables 11 and 12. Rates are provided in both units of carbon and oxygen, and are expressed per hour per square metre of projected surface area, per square metre of real surface area, and per gram of chlorophyll *a*. Rates of primary production per square metre of crust surface (i.e., real surface area) will be emphasized since these data are both the least variable and the most meaningful in ecological terms (Lewis 1977). The results are column-graphed in Fig. 22 to facilitate comparison between the species. Data for *in situ* rates of primary production will be given greater emphasis since doubts have been raised concerning the reliability of laboratory estimates. In fact, further cause for doubt arises from comparison of Figs. 22A and B (see below).

Relative rates of primary production

The laboratory data typically showed declining rates of net primary production for each species with increasing depth (Fig. 22A). In contrast, the maximal rate of net primary production for *P. onkodes*, *N. fosliei*, and *H. reinboldii* under

Table 11. Mean maximal rates of gross primary production, net primary production, and consumption (in the dark) per hour for different species from different depths under laboratory conditions. Mean values (x) are presented with 95% confidence intervals (CI) for oxygen and carbon metabolism on the bases of projected surface area (PA), real surface area (RA), and chlorophyll *a* content (Chl. *a*) respectively.

Species	Depth m	n	Basis	Gross Production								Net Production								Consumption							
				mmol Oxygen per hour				mg Carbon per hour				mmol Oxygen per hour				mg Carbon per hour				mmol Oxygen per hour				mg Carbon per hour			
				(min)	x	CI	(max)	(min)	x	CI	(max)	(min)	x	CI	(max)	(min)	x	CI	(max)	(min)	x	CI	(max)	(min)	x	CI	(max)
P. arkodes	0	6	sq. m. PA	(12.9)	22.4 ± 7.2		(30.2)	(128.0)	221.5 ± 71.1		(299.7)	(9.3)	17.1 ± 5.9		(23.2)	(91.9)	169.0 ± 58.1		(229.7)	(3.6)	5.3 ± 1.7		(7.1)	(36.1)	52.5 ± 17.3		(69.9)
			sq. m. RA	(12.4)	19.5 ± 4.9		(24.3)	(122.6)	193.4 ± 48.3		(241.2)	(8.9)	14.9 ± 4.1		(18.7)	(88.1)	147.5 ± 40.8		(184.9)	(3.5)	4.6 ± 1.2		(6.0)	(34.5)	45.9 ± 12.2		(59.7)
			g Chl. *a*	(61.2)	121.9 ±49.4		(171.4)	(606.2)	1208.5 ±489.4		(1699.3)	(43.9)	92.9 ±38.4		(131.4)	(435.5)	920.5 ±381.0		(1302.7)	(17.2)	29.1 ±12.6		(40.0)	(170.8)	288.0 ±124.5		(396.6)
N. fosliei	0	4	sq. m. PA	(13.6)	15.1 ± 2.0		(16.8)	(128.8)	143.2 ± 18.8		(159.2)	(9.7)	10.4 ± 1.6		(11.9)	(91.5)	98.3 ± 15.1		(113.0)	(3.9)	4.7 ± 0.9		(5.2)	(36.8)	44.8 ± 8.3		(49.2)
			sq. m. RA	(13.4)	14.4 ± 1.4		(15.6)	(127.1)	136.1 ± 12.9		(147.5)	(9.2)	10.1 ± 1.2		(11.1)	(86.5)	95.4 ± 11.8		(104.7)	(3.8)	4.5 ± 0.7		(4.9)	(36.3)	42.6 ± 6.7		(46.5)
			g Chl. *a*	(27.6)	35.4 ± 9.3		(40.6)	(261.0)	335.1 ± 88.3		(383.5)	(19.7)	24.3 ± 6.0		(28.8)	(186.4)	229.6 ± 56.9		(272.0)	(7.9)	11.2 ± 3.9		(14.1)	(74.5)	105.6 ± 36.5		(133.4)
H. reinboldii	0	5	sq. m. PA	(13.9)	15.3 ± 1.4		(16.4)	(125.6)	138.1 ± 13.1		(148.0)	(8.7)	10.4 ± 2.3		(12.4)	(78.2)	94.1 ± 21.0		(111.8)	(4.0)	4.9 ± 1.0		(5.7)	(36.2)	44.0 ± 9.2		(51.1)
			sq. m. RA	(13.4)	14.2 ± 1.1		(15.1)	(120.8)	128.8 ± 9.7		(136.7)	(8.2)	9.7 ± 2.0		(11.3)	(74.5)	87.7 ± 18.4		(102.3)	(3.7)	4.5 ± 1.0		(5.3)	(33.2)	41.1 ± 8.9		(48.1)
			g Chl. *a*	(64.4)	97.7 ±33.4		(124.4)	(581.9)	883.2 ±302.3		(1125.1)	(40.1)	67.4 ±31.3		(92.6)	(362.5)	609.7 ±283.0		(837.1)	(24.3)	30.3 ± 5.3		(35.2)	(219.4)	273.5 ± 48.4		(318.4)
P. coniaum	0	5	sq. m. PA	(9.9)	14.8 ± 4.8		(19.8)	(111.8)	166.3 ± 54.3		(222.2)	(7.0)	11.3 ± 4.4		(16.0)	(79.1)	127.3 ± 49.2		(180.5)	(2.9)	3.5 ± 0.6		(4.0)	(32.7)	39.0 ± 6.8		(45.2)
			sq. m. RA	(9.6)	13.2 ± 3.2		(16.0)	(108.5)	148.5 ± 36.1		(179.5)	(6.8)	10.1 ± 3.0		(13.0)	(76.7)	113.3 ± 33.7		(145.8)	(2.8)	3.1 ± 0.5		(3.7)	(31.8)	35.1 ± 5.2		(41.7)
			g Chl. *a*	(23.8)	46.5 ±21.7		(67.7)	(267.6)	523.0 ±243.9		(762.0)	(16.8)	35.7 ±18.7		(55.0)	(189.2)	402.1 ±210.6		(619.1)	(7.0)	10.8 ± 3.2		(12.7)	(78.4)	120.9 ± 36.1		(143.1)
P. arkodes	3	4	sq. m. PA	(16.2)	17.3 ± 1.6		(18.6)	(160.2)	171.2 ± 15.5		(184.6)	(12.7)	13.2 ± 0.9		(14.1)	(125.9)	131.2 ± 9.0		(139.6)	(3.5)	4.0 ± 0.8		(4.5)	(34.3)	40.1 ± 8.2		(45.0)
			sq. m. RA	(15.1)	15.6 ± 0.6		(16.1)	(149.7)	154.4 ± 5.9		(159.3)	(11.2)	11.9 ± 0.7		(12.3)	(111.1)	118.4 ± 7.3		(121.6)	(3.3)	3.6 ± 0.5		(3.9)	(33.2)	36.0 ± 4.7		(38.9)
			g Chl. *a*	(68.2)	87.9 ±42.0		(128.5)	(675.7)	871.0 ±416.0		(1273.8)	(53.3)	67.1 ±29.7		(95.4)	(528.7)	664.8 ±294.6		(945.7)	(14.8)	20.8 ±12.5		(33.1)	(147.0)	206.2 ±123.6		(328.1)
N. foslici	3	4	sq. m. PA	(11.0)	13.7 ± 4.9		(18.0)	(103.7)	129.3 ± 46.6		(169.7)	(7.6)	9.7 ± 3.9		(12.8)	(71.7)	92.0 ± 36.5		(121.3)	(3.3)	3.9 ± 1.2		(5.1)	(31.4)	37.3 ± 11.4		(48.5)
			sq. m. RA	(10.5)	11.9 ± 2.4		(13.4)	(99.3)	112.8 ± 22.7		(126.7)	(7.1)	8.5 ± 2.2		(9.9)	(67.6)	80.2 ± 20.5		(93.4)	(3.2)	3.4 ± 0.4		(3.8)	(30.1)	32.6 ± 3.9		(36.2)
			g Chl. *a*	(52.2)	65.1 ±14.2		(72.4)	(493.1)	615.6 ±134.0		(684.4)	(35.2)	46.3 ±12.6		(54.1)	(322.7)	435.4 ±125.9		(511.4)	(17.0)	18.8 ± 2.3		(20.5)	(160.4)	177.7 ± 21.6		(194.0)
H. reinboldii	3	4	sq. m. PA	(9.9)	14.2 ± 4.5		(16.3)	(89.7)	128.6 ± 40.3		(147.3)	(8.0)	11.2 ± 3.3		(12.6)	(72.1)	101.4 ± 29.6		(114.1)	(1.9)	2.8 ± 1.1		(3.7)	(17.6)	27.2 ± 11.7		(34.0)
			sq. m. RA	(9.6)	12.5 ± 3.0		(13.9)	(86.6)	112.9 ± 27.0		(125.7)	(7.7)	9.9 ± 2.2		(10.7)	(69.6)	89.1 ± 19.5		(96.4)	(1.9)	2.6 ± 1.0		(3.2)	(17.0)	23.9 ± 8.6		(29.4)
			g Chl. *a*	(74.0)	142.4 ±75.0		(193.9)	(668.7)	1287.1 ±677.7		(1752.9)	(56.7)	112.2 ±59.5		(150.3)	(512.6)	1014.9 ±538.3		(1358.7)	(17.3)	30.1 ±16.2		(43.6)	(156.2)	272.2 ±146.9		(394.3)
P. arkodes	'6'	4	sq. m. PA	(13.6)	16.9 ± 3.4		(18.3)	(134.5)	167.1 ± 33.2		(181.3)	(7.5)	10.5 ± 3.1		(11.9)	(74.0)	104.2 ± 30.7		(118.2)	(6.1)	6.3 ± 0.3		(6.6)	(60.5)	62.9 ± 3.2		(65.7)
			sq. m. RA	(12.8)	15.1 ± 2.3		(16.0)	(127.2)	149.5 ± 22.5		(158.4)	(7.1)	9.4 ± 2.3		(10.2)	(70.0)	93.1 ± 23.1		(101.0)	(5.4)	5.7 ± 0.3		(5.8)	(53.8)	56.5 ± 2.6		(57.4)
			g Chl. *a*	(76.0)	114.0 ±40.9		(139.5)	(753.1)	1129.6 ±405.7		(1383.0)	(48.5)	70.3 ±25.1		(88.8)	(480.2)	696.7 ±249.0		(880.4)	(27.5)	43.7 ±19.2		(56.6)	(272.9)	432.9 ±190.2		(560.7)
N. fosliei	6	5	sq. m. PA	(10.6)	12.8 ± 2.0		(14.3)	(100.6)	120.8 ± 19.3		(135.3)	(8.1)	9.9 ± 1.8		(11.5)	(76.8)	93.7 ± 16.6		(108.5)	(2.5)	2.9 ± 0.4		(3.2)	(23.8)	27.0 ± 3.9		(30.3)
			sq. m. RA	(10.0)	11.4 ± 1.3		(12.3)	(94.7)	108.2 ± 12.6		(116.3)	(7.7)	8.9 ± 1.2		(9.9)	(72.3)	83.9 ± 11.0		(93.3)	(2.4)	2.6 ± 0.3		(2.9)	(22.4)	24.3 ± 3.0		(27.3)
			g Chl. *a*	(39.6)	56.1 ±13.3		(65.1)	(374.6)	530.0 ±125.6		(615.6)	(30.3)	43.5 ±10.4		(50.4)	(286.1)	411.1 ± 98.2		(476.2)	(9.4)	12.6 ± 3.2		(15.1)	(88.5)	119.0 ± 30.6		(142.3)
H. reinboldii	6	4	sq. m. PA	(11.4)	12.2 ± 1.0		(12.9)	(102.9)	110.4 ± 8.6		(116.2)	(8.8)	10.0 ± 1.4		(11.0)	(79.2)	90.1 ± 12.8		(99.4)	(1.9)	2.2 ± 0.5		(2.6)	(16.8)	20.3 ± 4.2		(23.7)
			sq. m. RA	(10.6)	11.3 ± 0.9		(11.8)	(96.1)	102.0 ± 8.2		(106.8)	(8.2)	9.2 ± 1.3		(10.1)	(74.0)	83.3 ± 11.7		(91.4)	(1.7)	2.1 ± 0.5		(2.4)	(15.5)	18.7 ± 4.1		(22.1)
			g Chl. *a*	(75.7)	106.9 ±38.7		(137.9)	(684.7)	966.1 ±350.2		(1246.4)	(64.8)	86.0 ±28.2		(110.4)	(585.5)	777.3 ±255.4		(998.1)	(11.0)	20.9 ±11.3		(27.5)	(99.2)	188.8 ±102.3		(248.3)
P. coniaum	6	5	sq. m. PA	(7.7)	10.6 ± 3.1		(13.2)	(87.0)	118.9 ± 35.3		(148.0)	(4.9)	8.0 ± 3.2		(10.4)	(52.2)	90.2 ± 35.7		(116.6)	(2.2)	2.6 ± 0.5		(2.8)	(24.2)	28.7 ± 5.1		(31.9)
			sq. m. RA	(7.1)	9.8 ± 3.0		(12.1)	(80.2)	110.2 ± 33.5		(136.1)	(4.5)	7.4 ± 3.0		(10.0)	(51.0)	83.6 ± 34.1		(112.1)	(2.0)	2.4 ± 0.4		(2.6)	(22.9)	26.5 ± 4.0		(29.3)
			g Chl. *a*	(48.6)	69.3 ±32.5		(100.9)	(546.9)	779.0 ±365.8		(1135.3)	(32.8)	52.7 ±29.5		(79.2)	(368.6)	593.2 ±332.2		(890.8)	(11.9)	16.5 ± 5.2		(21.7)	(133.5)	185.8 ± 58.1		(244.5)
P. coniaum	18	5	sq. m. PA	(7.2)	8.8 ± 1.8		(10.7)	(81.3)	99.3 ± 20.8		(119.8)	(5.1)	6.7 ± 1.9		(8.2)	(57.1)	74.9 ± 20.8		(92.6)	(1.8)	2.2 ± 0.3		(2.4)	(20.7)	24.4 ± 3.3		(27.2)
			sq. m. RA	(6.8)	7.9 ± 1.1		(8.9)	(76.6)	89.1 ± 11.9		(100.6)	(4.8)	6.0 ± 1.3		(7.3)	(53.8)	68.0 ± 14.2		(81.7)	(1.6)	1.9 ± 0.3		(2.2)	(18.1)	21.1 ± 3.5		(24.3)
			g Chl. *a*	(94.8)	108.8 ±14.1		(122.7)	(1066.1)	1224.2 ±158.3		(1380.0)	(73.3)	81.7 ±14.3		(99.6)	(824.4)	918.6 ±160.7		(1120.7)	(21.5)	27.2 ± 6.6		(32.3)	(241.7)	305.5 ± 74.1		(363.8)

Table 12. Mean maximal rates of gross primary production, net primary production, and consumption (in the dark) per hour for different species from different depths under *in situ* conditions. Mean values (x) are presented with 95% confidence intervals (CI) for oxygen and carbon metabolism on the bases of projected surface area (PA), real surface area (RA), and chlorophyll *a* content (Chl. *a*) respectively.

Species	Depth m	n	Basis	Gross Production								Net Production								Consumption							
				mmol Oxygen per hour				mg Carbon per hour				mmol Oxygen per hour				mg Carbon per hour				mmol Oxygen per hour				mg Carbon per hour			
				(min)	x	CI	(max)	(min)	x	CI	(max)	(min)	x	CI	(max)	(min)	x	CI	(max)	(min)	x	CI	(max)	(min)	x	CI	(max)
P. onkodes	0	5	sq. m. PA	(21.0)	23.0 ± 2.9		(26.4)	(207.9)	227.8 ± 29.0		(261.3)	(16.6)	18.3 ± 2.7		(21.3)	(164.7)	181.3 ± 26.7		(211.5)	(4.2)	4.7 ± 0.7		(5.4)	(41.4)	46.9 ± 6.5		(53.7)
			sq. m. RA	(20.3)	21.3 ± 1.4		(22.9)	(201.6)	211.2 ± 13.9		(227.3)	(16.1)	16.9 ± 1.5		(18.6)	(159.3)	167.6 ± 14.6		(184.0)	(4.0)	4.4 ± 0.5		(5.0)	(40.1)	43.6 ± 5.1		(49.8)
			g Chl. *a*	(55.0)	83.7 ±31.5		(106.0)	(545.0)	829.6 ±312.1		(1051.1)	(44.0)	66.2 ±24.3		(83.1)	(436.5)	656.5 ±240.7		(824.1)	(10.9)	17.5 ± 7.7		(22.9)	(108.5)	173.1 ± 75.9		(227.0)
M. fosliei	0	4	sq. m. PA	(17.9)	20.3 ± 4.8		(25.1)	(169.2)	192.0 ± 45.7		(236.9)	(13.5)	15.9 ± 4.9		(20.5)	(127.6)	149.9 ± 46.2		(193.6)	(3.5)	4.5 ± 1.1		(5.3)	(33.5)	42.1 ± 10.3		(50.2)
			sq. m. RA	(15.9)	17.0 ± 2.2		(19.2)	(150.1)	160.8 ± 20.9		(181.2)	(11.7)	13.3 ± 2.7		(15.7)	(110.9)	125.3 ± 25.8		(148.1)	(3.1)	3.8 ± 1.0		(4.6)	(28.9)	35.5 ± 9.1		(43.1)
			g Chl. *a*	(34.4)	36.4 ± 3.4		(39.3)	(341.0)	360.4 ± 33.8		(389.7)	(24.8)	28.3 ± 4.5		(32.1)	(234.1)	267.4 ± 42.9		(303.8)	(6.4)	8.1 ± 2.3		(9.6)	(63.1)	79.9 ± 22.9		(95.5)
P. conicum	0	4	sq. m. PA	(18.2)	20.5 ± 2.7		(22.3)	(204.3)	230.3 ± 30.9		(251.2)	(14.0)	15.7 ± 2.0		(17.2)	(157.4)	176.8 ± 22.5		(193.8)	(4.2)	4.8 ± 1.0		(5.5)	(46.9)	53.5 ± 10.9		(61.8)
			sq. m. RA	(15.9)	17.5 ± 2.1		(18.8)	(178.5)	196.7 ± 24.0		(211.5)	(12.2)	13.4 ± 1.5		(14.5)	(137.5)	151.0 ± 16.4		(163.2)	(3.6)	4.1 ± 0.8		(4.7)	(40.2)	45.7 ± 9.4		(53.4)
			g Chl. *a*	(106.6)	140.6 ±69.6		(209.1)	(1199.3)	1581.3 ±782.6		(2352.6)	(83.8)	107.4 ±48.9		(155.7)	(942.9)	1208.0 ±550.2		(1750.9)	(22.8)	33.2 ±20.7		(53.5)	(256.3)	373.3 ±232.4		(601.7)
M. fosliei	3	4	sq. m. PA	(17.5)	22.6 ± 6.6		(28.1)	(165.2)	213.5 ± 62.4		(265.7)	(13.0)	17.3 ± 6.4		(22.9)	(122.5)	163.5 ± 60.2		(216.8)	(4.5)	5.3 ± 1.0		(6.1)	(42.6)	50.0 ± 9.2		(57.5)
			sq. m. RA	(15.7)	17.6 ± 2.9		(20.3)	(148.0)	166.8 ± 27.4		(191.8)	(11.6)	13.5 ± 3.3		(16.6)	(109.8)	127.4 ± 30.8		(156.6)	(3.7)	4.2 ± 0.7		(4.9)	(35.3)	39.4 ± 7.0		(46.1)
			g Chl. *a*	(38.6)	63.2 ±25.7		(76.0)	(374.2)	599.8 ±236.1		(718.1)	(29.4)	48.5 ±21.2		(60.1)	(277.6)	458.8 ±200.8		(568.3)	(10.2)	14.9 ± 5.6		(18.2)	(96.5)	141.0 ± 53.3		(172.2)
H. reinboldii	3	4	sq. m. PA	(17.3)	18.8 ± 2.2		(20.8)	(156.6)	170.2 ± 19.9		(187.7)	(11.7)	14.5 ± 3.1		(16.6)	(105.4)	131.0 ± 28.3		(150.5)	(3.6)	4.3 ± 1.4		(5.7)	(32.9)	39.2 ± 12.3		(51.2)
			sq. m. RA	(15.8)	17.5 ± 1.9		(18.8)	(143.1)	158.1 ± 17.0		(170.1)	(10.6)	13.5 ± 2.9		(15.1)	(96.3)	121.7 ± 26.3		(136.4)	(3.5)	4.0 ± 1.2		(5.2)	(31.4)	36.4 ± 10.6		(46.8)
			g Chl. *a*	(54.4)	96.5 ±49.7		(132.3)	(492.0)	872.9 ±449.5		(1195.8)	(36.6)	75.3 ±43.8		(104.8)	(331.1)	680.9 ±395.6		(947.9)	(17.7)	21.2 ± 6.9		(27.4)	(159.7)	192.0 ± 62.4		(247.9)
P. onkodes	'6'	2	sq. m. PA	(16.1)	21.8 ± 9.1		(26.5)	(159.8)	216.2 ± 90.3		(262.7)	(13.0)	18.4 ± 8.7		(22.9)	(128.9)	182.8 ± 86.4		(227.4)	(3.1)	3.4 ± 0.4		(3.6)	(30.9)	33.4 ± 3.9		(35.3)
			sq. m. RA	(15.7)	20.0 ± 6.8		(23.2)	(155.2)	198.7 ± 67.4		(230.3)	(12.6)	16.9 ± 6.7		(20.1)	(125.2)	167.8 ± 66.4		(199.3)	(3.0)	3.1 ± 0.1		(3.2)	(30.0)	30.8 ± 1.3		(31.5)
			g Chl. *a*	(75.0)	88.7 ±33.9		(111.1)	(743.7)	879.6 ±335.7		(1101.5)	(63.8)	74.9 ±32.0		(96.2)	(632.3)	742.0 ±317.3		(953.5)	(11.2)	13.9 ± 4.0		(15.5)	(111.4)	137.7 ± 39.7		(153.5)
M. fosliei	6	2	sq. m. PA	(13.0)	13.5 ± 1.6		(14.0)	(122.5)	127.6 ± 15.4		(132.8)	(9.5)	10.2 ± 2.1		(10.9)	(89.8)	96.4 ± 19.9		(103.1)	(3.1)	3.3 ± 0.5		(3.5)	(32.3)	32.5 ± 0.6		(32.7)
			sq. m. RA	(11.0)	11.6 ± 1.8		(12.2)	(103.6)	109.4 ± 17.4		(115.1)	(8.0)	8.7 ± 2.1		(9.5)	(75.9)	82.6 ± 20.2		(89.3)	(2.7)	2.8 ± 0.3		(2.9)	(25.8)	26.7 ± 2.8		(27.7)
			g Chl. *a*	(67.6)	70.8 ± 9.8		(74.1)	(638.8)	669.7 ± 92.5		(700.5)	(49.5)	52.8 ± 9.8		(56.1)	(468.2)	499.2 ± 93.0		(530.2)	(18.0)	18.0 ± 0.1		(18.1)	(170.4)	170.5 ± 0.5		(170.7)
H. reinboldii	6	4	sq. m. PA	(18.7)	21.1 ± 4.6		(25.6)	(168.6)	198.8 ± 41.5		(231.2)	(14.5)	17.4 ± 4.5		(21.5)	(131.2)	157.2 ± 40.3		(194.8)	(3.3)	3.7 ± 0.7		(4.1)	(29.7)	33.6 ± 5.9		(37.5)
			sq. m. RA	(16.0)	17.9 ± 3.3		(21.1)	(144.6)	162.2 ± 29.7		(190.5)	(12.4)	14.8 ± 3.3		(17.8)	(112.5)	133.7 ± 29.9		(160.6)	(2.9)	3.2 ± 0.5		(3.6)	(26.1)	28.6 ± 4.5		(32.1)
			g Chl. *a*	(101.2)	144.0 ±66.2		(190.1)	(915.4)	1302.0 ±598.3		(1718.5)	(78.7)	119.1 ±59.0		(160.2)	(712.0)	1076.8 ±533.8		(1448.3)	(18.7)	24.9 ± 7.8		(29.9)	(169.4)	225.2 ± 70.8		(270.3)
P. conicum	6	3	sq. m. PA	(13.2)	14.4 ± 3.6		(16.8)	(148.5)	162.4 ± 40.6		(189.5)	(9.6)	11.3 ± 4.5		(14.3)	(108.0)	126.9 ± 50.7		(160.6)	(2.6)	3.2 ± 0.9		(3.6)	(28.8)	35.5 ± 10.4		(40.5)
			sq. m. RA	(12.7)	13.4 ± 1.7		(14.5)	(143.0)	150.2 ± 19.0		(162.8)	(9.2)	10.4 ± 2.8		(12.3)	(104.0)	117.0 ± 31.9		(138.0)	(2.2)	3.0 ± 1.2		(3.5)	(24.8)	33.3 ± 13.0		(39.0)
			g Chl. *a*	(60.4)	120.7 ±104		(181.0)	(679.9)	1358.2 ±1174		(2035.7)	(43.9)	96.1 ±95.1		(153.4)	(494.3)	1080.6 ±1070		(1725.8)	(16.5)	24.7 ±12.4		(30.0)	(185.6)	277.6 ±140.0		(337.2)
P. conicum	18	2	sq. m. PA	(11.0)	12.7 ± 5.1		(14.4)	(124.1)	143.2 ± 57.4		(162.3)	(7.8)	9.7 ± 5.8		(11.6)	(87.3)	109.1 ± 65.5		(130.9)	(2.8)	3.0 ± 0.7		(3.3)	(31.5)	34.1 ± 8.0		(36.8)
			sq. m. RA	(10.4)	11.8 ± 4.3		(13.2)	(116.7)	132.7 ± 48.1		(148.8)	(7.3)	8.9 ± 5.0		(10.7)	(82.1)	101.0 ± 56.7		(119.9)	(2.6)	2.8 ± 0.8		(3.1)	(28.8)	31.7 ± 8.7		(34.6)
			g Chl. *a*	(88.5)	132.6 ±132		(176.7)	(995.6)	1491.9 ±1489		(1988.1)	(62.3)	102.4 ±120		(142.5)	(700.4)	1151.7 ±1353		(1603.0)	(26.2)	30.2 ±12.0		(34.2)	(295.2)	340.1 ±134.9		(385.1)

Fig. 22. Column-graphs of the mean maximal rate of gross primary production, net primary production, and dark respiration, for different species at the depth of collection or measurement indicated. Lines are 95% confidence intervals.
A. Laboratory data.
B. *In situ* data.

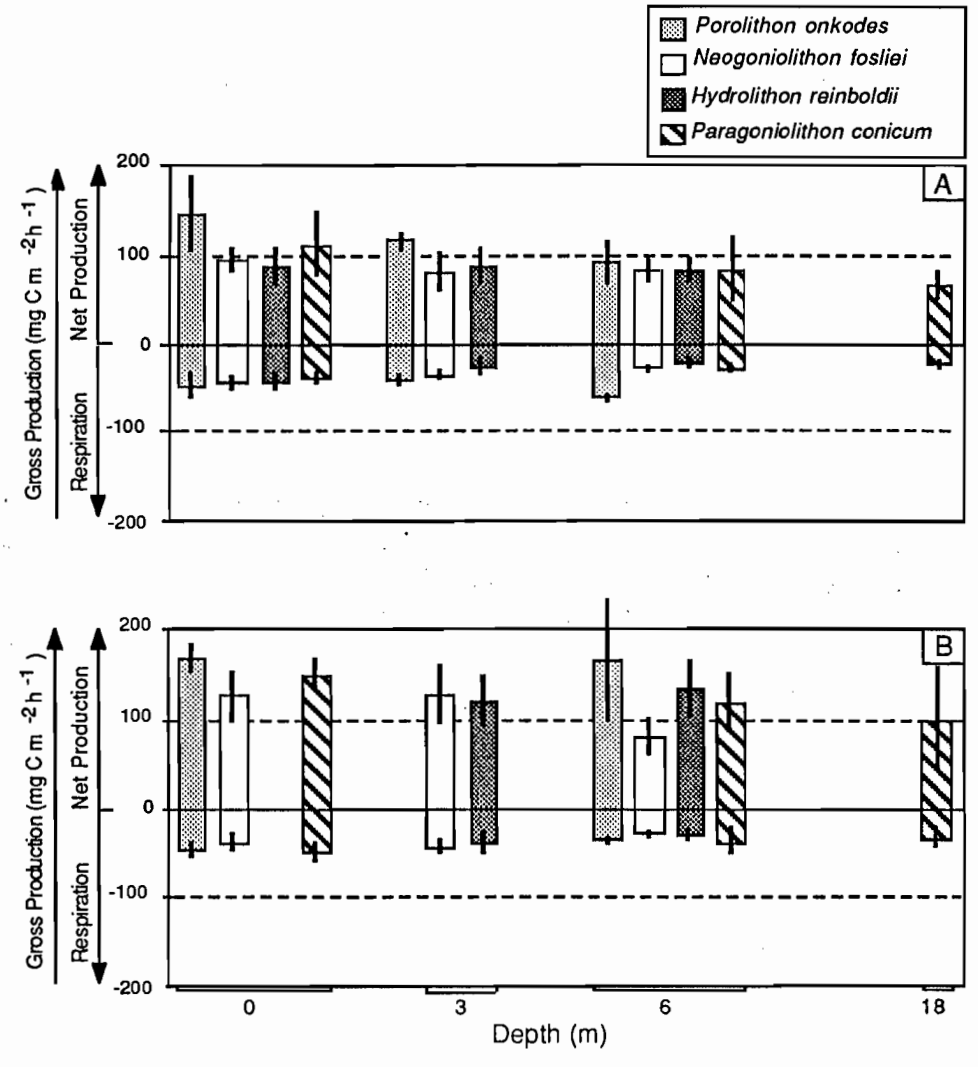
Porolithon onkodes
Neogoniolithon fosliei
Hydrolithon reinboldii
Paragoniolithon conicum
A
B
Gross Production (mg C m -2 h -1)
Net Production
Respiration
200
100
0
-100
-200
0
3
6
18
Depth (m)

in situ (Fig. 22B) conditions appeared to be closely correlated with the depth at which a given species reaches peak abundance (Fig. 2). For example, between 0 and 3 m *N. fosliei* achieves maximum abundance and its rate of production was above that of *H. reinboldii*, but between 3 and 6 m *H. reinboldii* achieves maximum abundance and its rate of production was above that of *N. fosliei*.

Rates of net primary production are somewhat misleading for *P. onkodes* at a PPFD-equivalent depth of 6 m. This species is very rarely found at 6 m on the windward reef slope at Lizard Island, but is common in shaded locations at depths of 1 to 3 m where light levels are similar to those at 6 m. It appears that *P. onkodes* does not compete well with turf algae or grow in situations where significant sediment deposition takes place, i.e., under conditions of reduced grazing pressure and/or wave action. On the reef slope at Lizard Island it does not appear to grow much below 3 m, presumably both as a function of the reduced grazing pressure and because it does not appear capable of regularly sloughing its outer epithallial layer at regular intervals. Epithallial sloughing is a process exhibited by many coralline algae, apparently in response to stress (Borowitzka & Vesk 1978; Masaki *et al.* 1981; Fujita & Masaki 1982; Masaki *et al.* 1984; Johnson & Mann 1986). The uppermost cell layer(s) (epithallial layer) becomes detached from the crust and is shed to the surrounding seawater. The process appears to act as an antifouling mechanism benefiting the corallines in areas supporting large populations of fleshy algae and where sediment deposition is significant.

P. conicum does not appear to show regular epithallial sloughing either and this may explain why it is generally found on steeply inclined surfaces, such as occur on the reef slope, where light levels are insufficient to support high cover of turf algae. Its greater occurrence on inclined surfaces might also indicate a degree of intolerance to sediment burial. Even so, *P. conicum* is problematic in that it shows relatively high levels of net primary productivity at 0 m, where wave-action and grazing reduce turf cover and sediment deposition, and yet it is not a dominant component on the reef crest. Laboratory *P-I* curves indicate some level of photoinhibition at very high light intensities (Fig. 12A), and it is possible that strong natural irradiance has a more damaging effect in the long term than is evidenced by short-term metabolic measurements. Indeed, *P. conicum* is rarely found in exposed locations in very shallow water, but may occur on the basal parts of coral heads and in crevices. Possibly competition from *P. onkodes* contributes to its reduced abundance.

Alternatively the rate of organic carbon production may be less critical in areas of high erosive potential than the rate of carbonate deposition (see Chapter 3). At intermediate depths *P. conicum* has similar rates of photosynthesis to *H. reinboldii*, and it is the only one of the four species which occurs in any abundance much below 8 or 9 m.

In contrast to *P. onkodes* and *P. conicum*, both *N. fosliei* and *H. reinboldii* show evidence of epithallial sloughing. This is not so pronounced in *H. reinboldii*, but is very obvious in *N. fosliei*. The entire upper cell layer of *N. fosliei* is shed as one continuous sheet with some regularity. It appears that regular epithallial sloughing enables these two species to develop on relatively flat surfaces, under conditions of reduced water motion and grazing pressure. *N. fosliei* and *H. reinboldii* were found to exhibit significantly greater long-term (1 y) growth rates than *P. conicum* and *P. onkodes* on flat concrete blocks in the Lizard Island reef environment (unpublished data). However, on the outer barrier reefs near Lizard Island, *P. onkodes* and *P. conicum* are the dominant crustose corallines. *P. onkodes* and *P. conicum* thus appear to predominate in areas of high grazing pressure and water motion, whereas *N. fosliei* and *H. reinboldii* are relatively more successful in areas supporting high turf cover or where sediment deposition is significant.

Actual rates of primary production

Mean rates of gross primary production, net primary production, and consumption, in terms of oxygen and carbon per hour, are presented for each species at the depths studied in Tables 11 and 12. *In situ* rates of net carbon production (Table 12) per square metre of crust surface were highest for *P. onkodes* at depths of 0 and '6' m and lowest for *P. conicum* at the greatest depth of 18 m. Rates of net carbon production at 0 m were *ca* 168 mg C m^{-2}(real surface area) h^{-1} for *P. onkodes*. This compares with rates which ranged from *ca* 83 mg C m^{-2} h^{-1} at 6 m to *ca* 125 mg C m^{-2} h^{-1} at 3 m for *N. fosliei*; from *ca* 122 mg C m^{-2} h^{-1} at 3 m to *ca* 134 mg C m^{-2} h^{-1} at 6 m for *H. reinboldii*; and from *ca* 101 mg C m^{-2} h^{-1} at 18 m to *ca* 151 mg C m^{-2} h^{-1} at 0 m for *P. conicum*.

Comparative rates of primary production

Several workers have estimated the primary productivity of various species of crustose coralline algae occurring on coral reefs. Invariably these estimates have been based on measurements carried out in the laboratory or, at best, under simulated *in situ* conditions. No studies other than the one described here have attempted to measure actual *in situ* rates of production and consumption. Furthermore, no other studies have documented *PQ* values for coralline algae, or indeed any other calcareous algae. In consequence, virtually all estimates of carbon fixation have been based on simulated *in situ* measurements of oxygen production using assumed values for *PQ* (usually 1.0, e.g., Littler 1973a,c; Littler & Doty 1975; Wanders 1976; Vooren 1981; Hawkins & Lewis 1982; Littler *et al.* 1986). The data produced in this study strongly suggest that knowledge of the appropriate values for *PQ* is essential for accurate estimates of carbon production. Indeed, it is also clear that a *PQ* of 1.0 is quite inappropriate for several important species of crustose coralline algae (see Table 10), but that it may be appropriate for others (e.g., *P. conicum*, Table 10). Given this variation it seems unwise to make comparisons with the productivity estimates of other studies on the basis of carbon metabolism. Consequently, the oxygen data presented in Tables 11 and 12 have been converted into units of mass and set out with the estimates of other workers in Table 13. The data is arranged with the highest measured rates at the top and the lowest at the bottom. When certain rate parameters are missing (e.g. net O_2 m^{-2}[real surface area] h^{-1} for *P. onkodes* from Littler & Doty's study [1975]) the data are ordered according to the priorities set out in the following scheme: net O_2/real area > net O_2/projected area > gross O_2/real area > gross O_2/projected area.

The following features should be noted in Table 13. First, *in situ* rates of oxygen production are typically higher than simulated *in situ* rates of oxygen production. Second, rates of production for *Porolithon* spp. are usually higher than for other taxa obtained from similar depths. Third, the laboratory-based measurements of this study bear greater similarity to the estimates from other laboratory or simulated *in situ* studies than to the present *in situ* results. It appears that almost all laboratory and simulated *in situ* investigations give rise to productivity estimates which are somewhat lower than equivalent estimates made under true *in situ* conditions. Problems with light quality are again likely to be important because, with only one or two exceptions, comparable production rates for laboratory and *in situ* specimens are only

Table 13. Available data on mean maximal rates of net and gross primary production per hour for crustose coralline algae on coral reefs, determined from this and other studies, expressed on the bases of both real surface area (real area) and projected area (proj. area). *In situ* data from this study are highlighted in bold face. ~ denotes that the actual depth was not quoted but could be inferred from site descriptions provided in the reference. '6' denotes that specimens were not living at 6 m but experienced a PPFD equivalent to that depth.

Study	Species	Depth	n	Net Oxygen Production mg O_2 m^{-2} h^{-1}		Gross Oxygen Production mg O_2 m^{-2} h^{-1}	
				real area	proj. area	real area	proj. area
In situ study	**Porolithon onkodes**	**0**	**4**	**541**	**586**	**682**	**736**
In situ study	**Porolithon onkodes**	**'6'**	**4**	**541**	**589**	**640**	**698**
Littler 1973a	**Porolithon onkodes**	~0		563			
Laboratory study	Porolithon onkodes	0	6	477	547	624	717
In situ study	**Hydrolithon reinboldii**	**6**	**4**	**474**	**557**	**573**	**675**
In situ study	**Neogoniolithon fosliei**	**3**	**4**	**432**	**554**	**563**	**723**
Littler & Doty 1975	Porolithon gardineri	~0			533		
In situ study	**Hydrolithon reinboldii**	**3**	**4**	**432**	**464**	**560**	**602**
In situ study	**Paragoniolithon conicum**	**0**	**4**	**429**	**502**	**560**	**656**
In situ study	**Neogoniolithon fosliei**	**0**	**4**	**426**	**509**	**544**	**650**
Littler 1973c	Porolithon gardineri	~0	2				600
Littler 1973c	Porolithon onkodes	~0	12				517
Littler & Doty 1975	Porolithon onkodes	~0			480		
Hawkins & Lewis 1982	Porolithon onkodes (mostly)	~0	10	380		600	
Laboratory study	Porolithon onkodes	3	4	381	422	499	554
Marsh 1970	Porolithon onkodes (probably)	~0	32	360		480	
Wanders 1976	Neogoniolithon solubile	0.5-3	17	340		430	
In situ study	**Paragoniolithon conicum**	**6**	**3**	**333**	**362**	**429**	**461**
Laboratory study	Paragoniolithon conicum	0	5	323	362	422	474
Laboratory study	Neogoniolithon fosliei	0	4	323	333	460	483
Laboratory study	Hydrolithon reinboldii	3	4	317	358	400	454
Laboratory study	Hydrolithon reinboldii	0	5	310	333	454	490
Laboratory study	Porolithon onkodes	'6'	4	301	336	483	541
Laboratory study	Hydrolithon reinboldii	6	4	294	320	362	390
Laboratory study	Neogoniolithon fosliei	6	5	285	317	365	410
In situ study	**Neogoniolithon fosliei**	**6**	**2**	**278**	**326**	**371**	**432**
Laboratory study	Neogoniolithon fosliei	3	4	272	310	381	438
Littler 1973c	Sporolithon erythraeum	~0	9				360
Litter et al. 1986	Unidentified sp.	81	4		267		
Laboratory study	Paragoniolithon conicum	6	5	237	256	314	339
In situ study	**Paragoniolithon conicum**	**18**	**1**	**234**	**250**	**333**	**352**
Wanders 1976	Porolithon pachydermum	0.5-3	21	220		320	
Wanders 1976	Lithophyllum sp. 3	0.5-3	25	200		280	
Laboratory study	Paragoniolithon conicum	18	5	192	214	253	282
Wanders 1976	Lithophyllum intermedium	0.5-3	18	190		280	
Wanders 1976	Lithophyllum sp. 4	0.5-3	19	150		230	
Vooren 1981	Hydrolithon boergesenii	11	2	120		220	
Vooren 1981	Hydrolithon boergesenii	25	3	120		220	
Vooren 1981	Archaeolithothamnion dimotum	25	7	110		210	

observed for shallow water populations of the genus *Porolithon* (see Section 2. 4. 4; and the results of Littler 1973a, Littler & Doty 1975, and the present laboratory study given in Table 13).

Rates of primary production per day

The rate of gross primary production per day was estimated by integrating the equation describing the *P-I* curve of a given individual with the predicted changes in irradiance over the course of a cloudless day (see Section 2. 2. 2). The rate of consumption per day was calculated by multiplying the rate of consumption per hour by 24. The rate of net primary production per day was calculated by subtracting amount of carbon consumed from the amount of carbon produced. The results of these calculations are presented in Tables 14 & 15.

From Table 15, *P. onkodes* showed the highest mean rates of net primary production per day at a depth of 0 m. However, at '6' m the rate of production by *P. onkodes* was reduced by over 70%. At a depth of 0 m *N. fosliei* accumulated only 70% of the carbon gained by *P. onkodes* at the same depth over the course of a day. *N. fosliei* had a similar level of productivity at 3 m, but the rate fell to a under 50% of this value at 6 m. *H. reinboldii*, in contrast, had a similar level of productivity to *N. fosliei* at 3 m and showed no decline in rate at 6 m. *P. conicum* showed rates of carbon accumulation which were intermediate to those of *P. onkodes* and *N. fosliei* at 0 m, but at 6 and 18 m its rate of production had decreased to 58% and 15% respectively of the rate measured at 0 m.

It is essential that these rates of production be examined in terms of the light energy received by the specimens. The data in Figs 23 and 24 demonstrate that the rate of organic carbon production per day is significantly ($P<0.05$) related to peak noon irradiance at the site of collection or measurement, for all estimates except those for net primary production by *H. reinboldii*. Figs 25 and 26 show the same data regressed as curvi-linear functions which were fitted using second order polynomial equations. Polynomial fits usually yielded higher coefficients of determination but were marginally less significant as a result of the greater number of mathematical terms describing the regression line. Even so, it is interesting that curvi-linear functions provide a more accurate description of the data, because this perhaps suggests that maximum productivity does not necessarily occur under the highest

Table 14. Integrated rates of gross primary production, net primary production, and consumption per day for different species from different depths under laboratory conditions. Data is for carbon metabolism. *P/R* ratios and peak noon irradiance levels at the sites of collection are included.

Species	Depth	n	Gross Production	Net Production	Consumption	P/R	Peak Noon Irradiance μEinsteins
			g Carbon m^{-2} d^{-1}				m^{-2} s^{-1}
			2.380	1.448	-0.931	2.56	1689
			2.228	0.795	-1.433	1.56	1689
P. onkodes	0	6	2.636	1.646	-0.990	2.66	1689
			2.910	1.559	-1.351	2.15	1689
			1.396	0.567	-0.829	1.68	1689
			2.298	1.219	-1.080	2.13	1689
		x	2.308	1.206	-1.102	2.12	1689
			1.652	0.581	-1.072	1.54	1683
			1.661	0.544	-1.117	1.49	1683
N. fosliei	0	4	1.830	0.801	-1.029	1.78	1683
			1.580	0.709	-0.871	1.81	1683
		x	1.681	0.659	-1.022	1.66	1683
			1.554	0.506	-1.048	1.48	1636
			1.450	0.357	-1.093	1.33	1636
H. reinboldii	0	5	1.637	0.841	-0.796	2.06	1636
			1.625	0.785	-0.840	1.93	1638
			1.489	0.325	-1.165	1.28	1638
		x	1.551	0.563	-0.988	1.62	1637
			1.737	0.894	-0.843	2.06	1629
			1.294	0.532	-0.762	1.70	1633
P. conicum	0	5	1.756	0.954	-0.802	2.19	1633
			2.052	1.051	-1.001	2.05	1633
			2.034	1.226	-0.808	2.52	1633
		x	1.775	0.931	-0.843	2.10	1632
			1.753	0.828	-0.925	1.89	498
			1.585	0.782	-0.803	1.97	281
P. onkodes	3	4	1.894	1.099	-0.796	2.38	1037
			1.518	0.585	-0.933	1.63	367
		x	1.688	0.824	-0.864	1.97	546
			0.948	0.166	-0.781	1.21	130
			1.163	0.442	-0.722	1.61	346
N. fosliei	3	4	1.519	0.760	-0.759	2.00	864
			1.446	0.577	-0.869	1.66	540
		x	1.269	0.486	-0.783	1.62	470
			1.505	0.801	-0.705	2.14	974
			1.054	0.646	-0.408	2.58	777
H. reinboldii	3	4	1.351	0.685	-0.666	2.03	389
			1.420	0.908	-0.512	2.77	821
		x	1.333	0.760	-0.573	2.38	740
			1.577	0.199	-1.378	1.14	371
			1.573	0.196	-1.377	1.14	480
P. onkodes	'6'	4	1.385	0.011	-1.374	1.01	515
			1.469	0.177	-1.292	1.14	371
		x	1.501	0.146	-1.355	1.11	434
			1.159	0.621	-0.537	2.16	535
			1.300	0.747	-0.553	2.35	235
N. fosliei	6	5	1.386	0.731	-0.655	2.17	427
			1.293	0.668	-0.624	2.07	278
			1.100	0.557	-0.543	2.03	170
		x	1.248	0.665	-0.582	2.16	329
			1.115	0.744	-0.371	3.00	234
			0.644	0.197	-0.447	1.44	85.2
H. reinboldii	6	4	0.484	0.037	-0.447	1.08	42.6
			0.820	0.289	-0.531	1.54	106
		x	0.766	0.317	-0.449	1.77	117
			0.708	0.005	-0.703	1.01	69.7
			0.716	0.141	-0.575	1.25	42.9
P. conicum	6	5	0.719	0.183	-0.701	1.03	42.8
			0.743	0.089	-0.654	1.14	64.2
			0.747	0.197	-0.550	1.36	107
		x	0.727	0.123	-0.637	1.16	65.3
			0.638	0.184	-0.454	1.41	43.0
			0.635	0.088	-0.547	1.16	64.4
P. conicum	18	5	0.575	0.026	-0.549	1.05	35.5
			0.769	0.185	-0.584	1.32	64.3
			0.812	0.303	-0.508	1.60	129
		x	0.686	0.157	-0.528	1.31	67.2

Table 15. Integrated rates of gross primary production, net primary production, and consumption per day for different species from different depths under *in situ* conditions. Data is for carbon metabolism. *P/R* ratios and peak noon irradiance levels at the sites of measurement are included.

Species	Depth	n	Gross Production	Net Production	Consumption	P/R	Peak Noon Irradiance	Date
			g Carbon m^{-2} d^{-1}				μEinsteins m^{-2} s^{-1}	
			2.330	1.366	-0.964	2.42	1516	30.4.86
			2.450	1.470	-0.975	2.51	1479	7.5.86
P. onkodes	0	5	2.422	1.228	-1.195	2.03	1474	8.5.86
			2.513	1.477	-1.038	2.42	1445	14.5.86
			2.275	1.221	-1.054	2.16	1441	15.5.86
		x	**2.408**	**1.352**	**-1.045**	**2.31**	**1471**	
			1.687	0.801	-0.885	1.91	1347	26.6.86
			1.765	1.071	-0.694	2.54	1350	1.7.86
N. fosliei	0	4	1.712	0.676	-1.036	1.65	1353	3.7.86
			2.052	1.258	-0.794	2.59	1359	13.7.86
		x	**1.804**	**0.952**	**-0.852**	**2.17**	**1352**	
			2.449	1.289	-1.160	2.11	1250	8.7.86
			2.399	1.119	-1.280	1.87	1252	9.7.86
P. conicum	0	4	2.151	1.187	-0.964	2.23	1255	11.7.86
			2.042	1.057	-0.985	2.07	1257	12.7.86
		x	**2.260**	**1.163**	**-1.097**	**2.07**	**1254**	
			2.144	1.297	-0.847	2.53	1100	20.5.86
			1.627	0.710	-0.917	1.77	1130	22.5.86
N. fosliei	3	4	1.770	0.855	-0.915	1.93	650	23.5.86
			1.748	0.643	-1.105	1.58	700	26.5.86
		x	**1.822**	**0.876**	**-0.946**	**1.95**	**895**	
			1.801	0.991	-0.810	2.22	615	24.5.86
			1.612	0.488	-1.125	1.43	920	27.5.86
H. reinboldii	3	4	1.824	1.017	-0.806	2.26	1000	10.6.86
			1.687	0.934	-0.754	2.24	900	11.6.86
		x	**1.731**	**0.858**	**-0.874**	**2.04**	**859**	
			1.534	0.777	-0.757	2.03	120	30.6.86
			0.906	0.150	-0.756	1.20	70	4.7.86
P. onkodes	'6'	4	1.177	0.458	-0.720	1.64	70	6.7.86
			1.003	0.096	-0.907	1.11	50	7.7.86
		x	**1.155**	**0.370**	**-0.785**	**1.50**	**76**	
			1.204	0.541	-0.663	1.82	390	27.4.86
			0.981	0.657	-0.368	2.66	70	9.6.86
N. fosliei	6	4	0.904	0.232	-0.672	1.34	115	13.6.86
			0.958	0.398	-0.560	1.71	87	17.6.86
		x	**1.012**	**0.457**	**-0.566**	**1.88**	**166**	
			1.488	0.716	-0.771	1.93	350	23.4.86
			2.001	1.281	-0.720	2.78	550	16.5.86
H. reinboldii	6	4	1.219	0.593	-0.627	1.95	130	18.5.86
			1.634	1.008	-0.626	2.61	300	19.5.86
		x	**1.586**	**0.900**	**-0.686**	**2.32**	**333**	
			1.561	0.625	-0.936	1.67	355	16.4.86
			1.586	0.724	-0.862	1.84	350	21.4.86
P. conicum	6	4	1.134	0.511	-0.623	1.82	54	28.5.86
			1.463	0.868	-0.595	2.46	105	16.6.86
		x	**1.436**	**0.682**	**-0.754**	**1.95**	**216**	
			1.073	0.308	-0.765	1.40	50	18.6.86
			0.733	0.012	-0.721	1.02	30	20.6.86
P. conicum	18	4	0.875	0.183	-0.692	1.26	55	21.6.86
			1.047	0.217	-0.830	1.26	80	24.6.86
		x	**0.932**	**0.180**	**-0.752**	**1.24**	**54**	

Fig. 23. Plots of mean integrated gross primary production, net primary production, and consumption per day, against peak noon irradiance at the sites of collection for laboratory specimens of the different species. Fitted lines show linear regressions. Equations of the regression lines are shown in boxes. r^2 values and significance levels (P) for each regression are shown in parentheses.

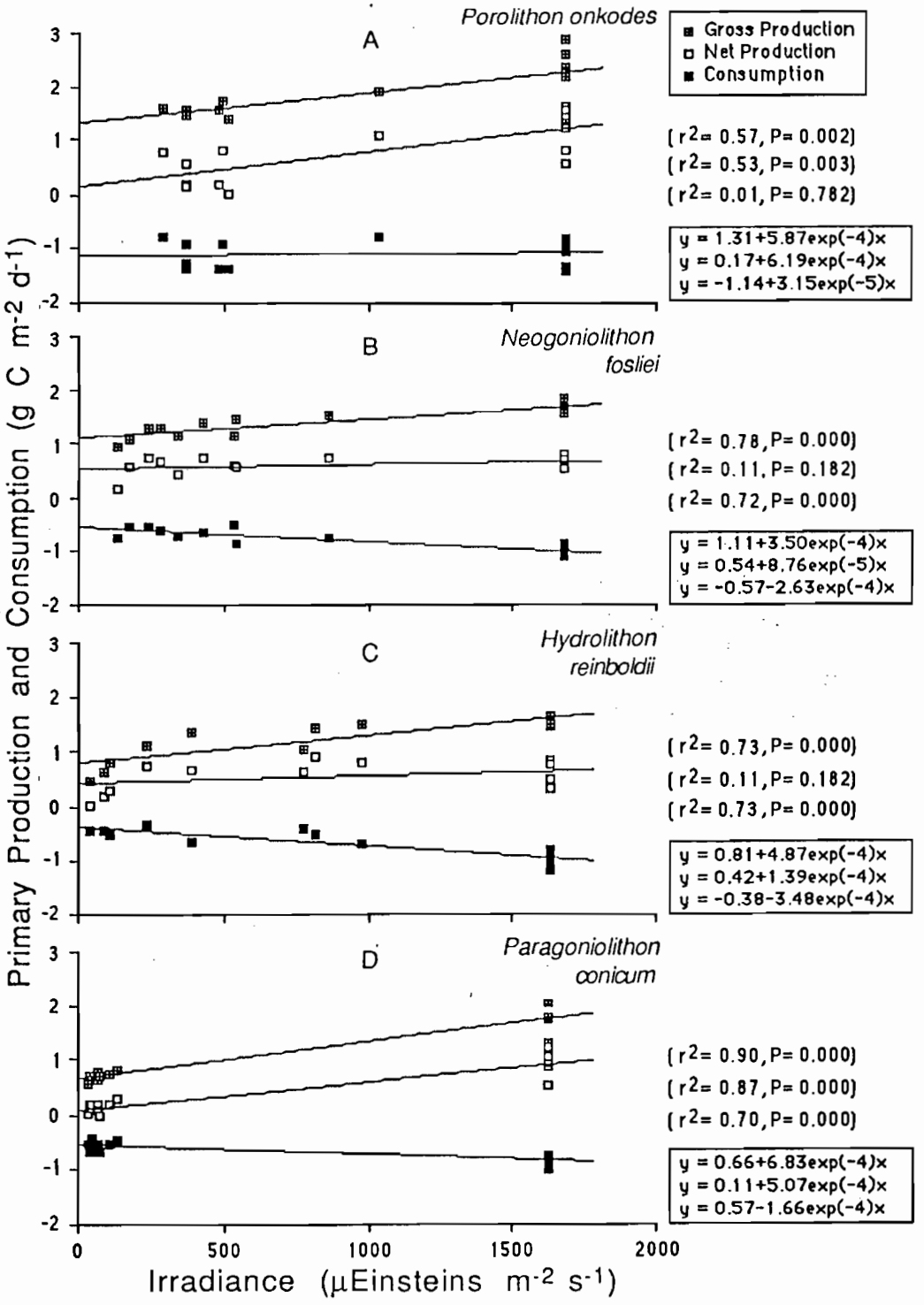
Porolithon onkodes
A
Gross Production
Net Production
Consumption
(r2= 0.57, P= 0.002)
(r2= 0.53, P= 0.003)
(r2= 0.01, P= 0.782)
y = 1.31+5.87exp(-4)x
y = 0.17+6.19exp(-4)x
y = -1.14+3.15exp(-5)x
B
Neogoniolithon fosliei
(r2= 0.78, P= 0.000)
(r2= 0.11, P= 0.182)
(r2= 0.72, P= 0.000)
y = 1.11+3.50exp(-4)x
y = 0.54+8.76exp(-5)x
y = -0.57-2.63exp(-4)x
C
Hydrolithon reinboldii
(r2= 0.73, P= 0.000)
(r2= 0.11, P= 0.182)
(r2= 0.73, P= 0.000)
y = 0.81+4.87exp(-4)x
y = 0.42+1.39exp(-4)x
y = -0.38-3.48exp(-4)x
D
Paragoniolithon conicum
(r2= 0.90, P= 0.000)
(r2= 0.87, P= 0.000)
(r2= 0.70, P= 0.000)
y = 0.66+6.83exp(-4)x
y = 0.11+5.07exp(-4)x
y = 0.57-1.66exp(-4)x
Primary Production and Consumption (g C m-2 d-1)
Irradiance (µEinsteins m-2 s-1)
0
500
1000
1500
2000

Fig. 24. Plots of mean integrated gross primary production, net primary production, and consumption per day, against peak noon irradiance at the sites of measurement for *in situ* specimens of the different species. Fitted lines show linear regressions. Equations of the regression lines are shown in boxes. r^2 values and significance levels (P) for each regression are shown in parentheses.

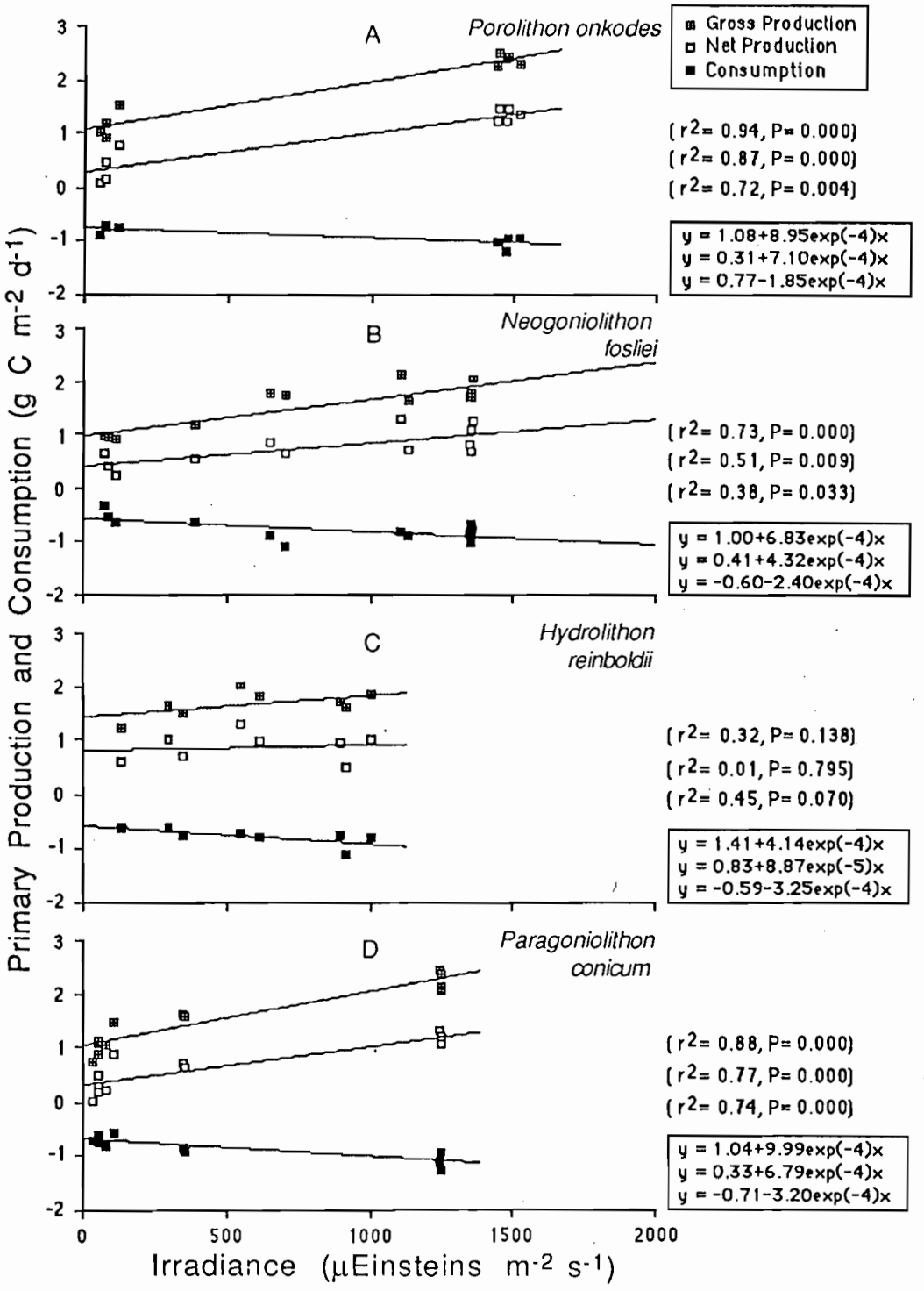
A
Porolithon onkodes
B
Neogoniolithon fosliei
C
Hydrolithon reinboldii
D
Paragoniolithon conicum
Gross Production
Net Production
Consumption
(r2= 0.94, P= 0.000)
(r2= 0.87, P= 0.000)
(r2= 0.72, P= 0.004)
y = 1.08+8.95exp(-4)x
y = 0.31+7.10exp(-4)x
y = 0.77-1.85exp(-4)x
(r2= 0.73, P= 0.000)
(r2= 0.51, P= 0.009)
(r2= 0.38, P= 0.033)
y = 1.00+6.83exp(-4)x
y = 0.41+4.32exp(-4)x
y = -0.60-2.40exp(-4)x
(r2= 0.32, P= 0.138)
(r2= 0.01, P= 0.795)
(r2= 0.45, P= 0.070)
y = 1.41+4.14exp(-4)x
y = 0.83+8.87exp(-5)x
y = -0.59-3.25exp(-4)x
(r2= 0.88, P= 0.000)
(r2= 0.77, P= 0.000)
(r2= 0.74, P= 0.000)
y = 1.04+9.99exp(-4)x
y = 0.33+6.79exp(-4)x
y = -0.71-3.20exp(-4)x
Primary Production and Consumption (g C m-2 d-1)
Irradiance (µEinsteins m-2 s-1)
3
2
1
0
-1
-2
0
500
1000
1500
2000

Fig. 25. Plots of mean integrated gross primary production, net primary production, and consumption per day, against peak noon irradiance at the sites of collection for laboratory specimens of the different species. Fitted lines show second order polynomial regressions. Equations of the regression lines are shown in boxes. r^2 values and significance levels (P) for each regression are shown in parentheses.

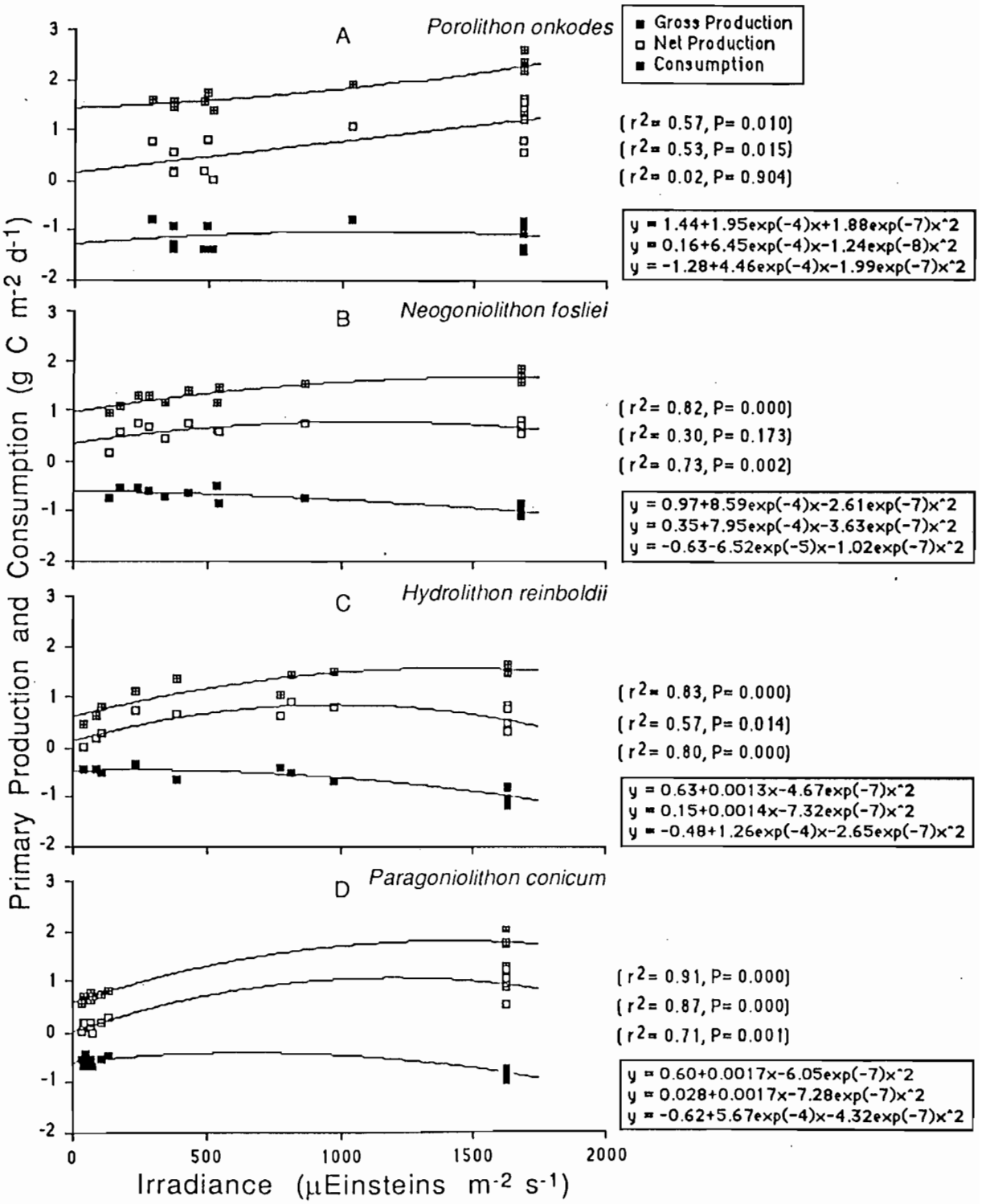
A
Porolithon onkodes
B
Neogoniolithon fosliei
C
Hydrolithon reinboldii
D
Paragoniolithon conicum
Gross Production
Net Production
Consumption
(r2= 0.57, P= 0.010)
(r2= 0.53, P= 0.015)
(r2= 0.02, P= 0.904)
y = 1.44+1.95exp(-4)x+1.88exp(-7)x^2
y = 0.16+6.45exp(-4)x-1.24exp(-8)x^2
y = -1.28+4.46exp(-4)x-1.99exp(-7)x^2
(r2= 0.82, P= 0.000)
(r2= 0.30, P= 0.173)
(r2= 0.73, P= 0.002)
y = 0.97+8.59exp(-4)x-2.61exp(-7)x^2
y = 0.35+7.95exp(-4)x-3.63exp(-7)x^2
y = -0.63-6.52exp(-5)x-1.02exp(-7)x^2
(r2= 0.83, P= 0.000)
(r2= 0.57, P= 0.014)
(r2= 0.80, P= 0.000)
y = 0.63+0.0013x-4.67exp(-7)x^2
y = 0.15+0.0014x-7.32exp(-7)x^2
y = -0.48+1.26exp(-4)x-2.65exp(-7)x^2
(r2= 0.91, P= 0.000)
(r2= 0.87, P= 0.000)
(r2= 0.71, P= 0.001)
y = 0.60+0.0017x-6.05exp(-7)x^2
y = 0.028+0.0017x-7.28exp(-7)x^2
y = -0.62+5.67exp(-4)x-4.32exp(-7)x^2
Primary Production and Consumption (g C m-2 d-1)
Irradiance (µEinsteins m-2 s-1)
0
500
1000
1500
2000

Fig. 26. Plots of mean integrated gross primary production, net primary production, and consumption per day, against peak noon irradiance at the sites of measurement for *in situ* specimens of the different species. Fitted lines show second order polynomial regressions. Equations of the regression lines are shown in boxes. r^2 values and significance levels (P) for each regression are shown in parentheses.

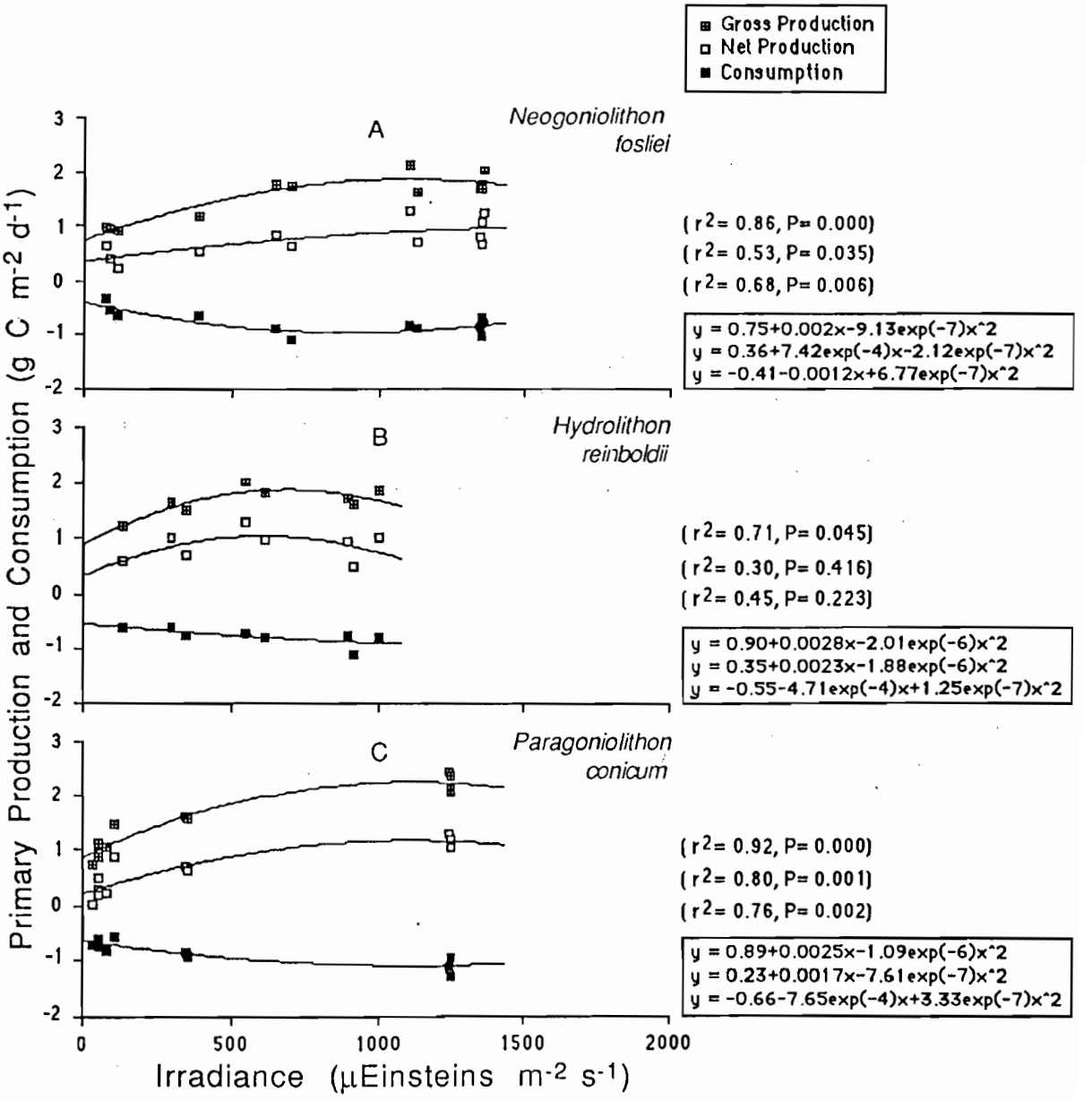
Gross Production
Net Production
Consumption
A
Neogoniolithon fosliei
B
Hydrolithon reinboldii
C
Paragoniolithon conicum
(r2= 0.86, P= 0.000)
(r2= 0.53, P= 0.035)
(r2= 0.68, P= 0.006)
y = 0.75+0.002x-9.13exp(-7)x^2
y = 0.36+7.42exp(-4)x-2.12exp(-7)x^2
y = -0.41-0.0012x+6.77exp(-7)x^2
(r2= 0.71, P= 0.045)
(r2= 0.30, P= 0.416)
(r2= 0.45, P= 0.223)
y = 0.90+0.0028x-2.01exp(-6)x^2
y = 0.35+0.0023x-1.88exp(-6)x^2
y = -0.55-4.71exp(-4)x+1.25exp(-7)x^2
(r2= 0.92, P= 0.000)
(r2= 0.80, P= 0.001)
(r2= 0.76, P= 0.002)
y = 0.89+0.0025x-1.09exp(-6)x^2
y = 0.23+0.0017x-7.61exp(-7)x^2
y = -0.66-7.65exp(-4)x+3.33exp(-7)x^2
Primary Production and Consumption (g C m-2 d-1)
Irradiance (µEinsteins m-2 s-1)
3
2
1
0
-1
-2
0
500
1000
1500
2000

irradiance. Regardless of the choice of regression either provides a valuable means of predicting the rates of primary production per day for these species of coralline algae under any given noon-time irradiance in the field.

The regressions presented in Figs 23, 24, 25, and 26 establish that the rates of production per day by the crustose coralline algae studied here are closely correlated with the amount of irradiance received during the course of a day. Carpenter (1985) arrived at the same conclusion for turf algae. Carpenter also reported that the net production rate of turf algae fell during field incubations when cloud cover temporarily reduced the level of irradiance. The same phenomenon was also observed during the *in situ* experiments with crustose corallines. Carpenter concluded that the productivity of shallow water algal communities was probably limited by a combination of irradiance and nutrient availability, rather than nutrient availability alone (Odum & Odum 1955; Lewis 1977). This seems particularly likely for dense algal stands and for algal types which show the saturation kinetics typical of multi-layered communities (see Figs 9A, 10A, 11A) since deeper layers do not saturate even at the highest levels of PAR encountered (e.g., Kohn & Helfrich 1957; Marsh & Smith 1978; Kinsey 1979).

At this stage it is appropriate to compare the rates of primary production per day for the crustose coralline algae studied *in situ* (Table 15) with the rates given for other marine plants. According to Larkum (1983), rates of carbon fixation per day for benthic algae range from 0.1-4 g C m^{-2}, for turf algae from 1-6 g C m^{-2}, for sand algae from 0.1-0.5 g C m^{-2}, for phytoplankton from 0.1-0.5 g C m^{-2}, for seagrasses from 1-7 g C m^{-2}, and for zooxanthellae are *ca* 0.6 g C m^{-2} d^{-1}. In this study, the rates of *in situ* primary production per day for crustose coralline algae ranged from 0.2-1.4 g C m^{-2}.

Dahl (1973) has calculated that the real surface area of a coral reef crest may be as much as 15 times the projected area. Relief factors of this magnitude are not usually observed for the crests of reefs in the vicinity of Lizard Island (personal observations). However, the surface topographies of the windward crests and slopes of reefs in the northern GBR are consistent with a relief factor of around 5:1 (personal observations). A ratio of this order was determined for the windward slope at Lizard Island, whereas for the reef crest the ratio was reduced to about 3:1 (unpublished data). Using the more conservative estimate of 3:1, the crustose coralline productivity

would be 0.5-4.1 g C m^{-2}(projected area) d^{-1}. Extrapolating these estimates into carbon fixed per annum per square metre of reef (i.e., multiplying by 365) would yield a range of *ca* 197-480 g C m^{-2} y^{-1} if the reef surface were entirely covered with crustose corallines. If the upper ratio of 5:1 is used, the range would be 329-2467 g C $m^{-2}y^{-1}$. Littler & Doty (1975) estimated the surface cover of *P. onkodes* on the seaward slope of a Hawaiian fringing reef to be 41%. Others have estimated the surface cover of crustose corallines in some reef areas (the reef crest and shallow seaward reef slope) to be as much as 90% (e.g., Sheveiko 1981; Atkinson & Grigg 1984). Surface cover of 90% is not uncommon on the shoulders and shallow seaward slopes of outer barrier reefs in the northern GBR (personal observations). Using the lower real:projected surface area ratio of 3:1, a lower crustose coralline surface cover of 41%, and an upper surface cover of 90%, and assuming the dominant crustose coralline species to be *P. onkodes*, the estimated range in annual net production rate for shallow windward reef environments would be *ca* 607-1332 g C m^{-2} y^{-1}. Using the higher ratio of 5:1 the range would increase to 1012-2221 g C m^{-2} y^{-1}.

Sournia (1976) has published gross production rates of 1387 g C m^{-2} y^{-1} for a community dominated by the coralline *Neogoniolithon frutescens* which was about half of the gross production for the reef community as a whole (2628 g C m^{-2} y^{-1}). Lewis (1977) concluded from this and other published information that crustose coralline algae were important contributors to reef production, but had rates of production which were lower than those of other primary producers on the reef. However, the calculated net productivity of a monospecific stand of *P. onkodes* with 90% cover on a reef crest with a relief factor of 5:1 is 2221 g C m^{-2} y^{-1} which approaches the estimate provided by Sournia (1976) for gross production. Sournia's (1976) measurements relate to *in situ* reef communities and not individual specimens. Until now the only estimates of the rates of primary production by individual crustose coralline algae have come from laboratory or simulated *in situ* studies involving less than optimal methods and certain invalid assumptions. It is perhaps fortunate that the effects of such erroreous procedures may partly cancel one and another out. For example, Wanders (1976) estimated the gross and net production rates of an entire reef community in shallow water from individual measurements of primary production by crustose coralline algae, fleshy, and filamentous algae, and from the estimates of Kanwisher & Wainwright (1967) for hermatypic corals. For his own measurements on macroalgae he used simulated *in situ* methods, which probably resulted in reduced rates of photosynthesis (see Table 13). At the same time, however, he assumed a *PQ*

of 1.0 for all algal species, which as pointed out both here (Table 10) and elsewhere (Ryther 1956; Strickland 1960; Littler & Murray 1974; Buesa 1980) is probably not true for most algae. If Wanders had used a mean *PQ* of 1.2 to estimate the carbon productivity of the macroalgal groups then their calculated rates of production would have been reduced by almost 17%. Recalculating Wanders data using a *PQ* of 1.2, and combining the estimates of Kanwisher & Wainwright (1967) for corals, yields a community gross production rate of 5529 g C m^{-2}(projected area) y^{-1} and a net production rate of 2237 g C m^{-2}(projected area) y^{-1} for reef surface with a relief factor of 5.5:1, as measured by Wanders (1976). This net production rate is almost identical with the rate calculated in this study for a monospecific stand of *P. onkodes* with 90% cover and a surface relief factor of 5:1 (i.e., 2221 g C m^{-2} y^{-1}). For a relief factor of 5.5:1 the gross productivity of *P. onkodes* would be 4351 g C m^{-2}(projected area) y^{-1} and the net productivity would be 2443 g C m^{-2}(projected area) y^{-1}.

Wanders (1976) has pointed out that his gross community productivity estimates agree with those for other reef ecosystems measured using the "flow-rate" technique (Sargent & Austen 1949, 1954; Odum & Odum 1955; Kohn & Helfrich 1957; Odum *et al.* 1960; Gordon & Kelly 1962; Qasim *et al.* 1972). However, as is the case for the estimates presented in this thesis, his estimates of net community primary production are about 10 times higher than all but one of the studies employing the "flow-rate" technique (Qasim *et al.* 1972). The results of this study and those of Wanders (1976) support the conclusion that measurements of net rates of primary productivity for whole reef communities are greatly reduced by the respiratory activities of non-producing organisms (Odum 1969).

In conclusion, the great abundance of crustose coralline algae on coral reefs, and the rates of *in situ* production determined during this study, suggest that the importance of crustose coralline algae as contributors of organic carbon may have been widely underestimated in the past. Neither *in situ* community measurements, nor laboratory or simulated *in situ* estimates of crustose coralline primary production are reliable indicators of the actual rates of carbon production by these algae on coral reefs.

CHAPTER 3

CALCIFICATION

3. 1. INTRODUCTION

There are two fundamental questions which need to be asked about calcification on coral reefs. How does calcification occur, and how fast does it occur? Coral reefs exist because a relatively small number of different organisms secrete relatively large amounts of calcium carbonate ($CaCO_3$) within or beneath their living tissues. Coral reefs can occur at sea level in the tropics because the biological rate of calcification is rapid enough to counteract the physical processes leading to limestone erosion. The major calcifiers on coral reefs are the hermatypic or 'stony' corals and the calcareous red algae, principally crustose members of the Corallinaceae.

It has been suggested that corals deposit the bulk of the $CaCO_3$ which becomes added to the reef (Bak 1976). This is arguable because some cores drilled through coral reefs indicate that corals comprise the greater proportion of the reef facies (e.g., Hubbard *et al.* 1986), others indicate coralline algae are the dominant elements (e.g., Gross *et al.* 1969), and yet more reveal variable and alternating proportions of the two (e.g., Adey 1978b; Davies 1983). The pattern which appears to be emerging is that the relative proportions of corals and coralline algae in reef cores largely depends upon the depths to which the cores are taken and the geographical and physical locations where they are drilled (e.g., Adey 1975; Davies 1983). This is not surprising since the relative cover of hard corals and coralline algae also changes with reef location, reef environment, and with water depth (e.g., Stearn *et al.* 1977; Done 1983). Adey (1978b) suggests that rates of upward reef growth are more rapid when corals predominate but that the degree of consolidation is greater when the reef rock is built by coralline algae. To date it has been difficult to compare the rates of carbonate deposition by corals and coralline algae because the available data have largely concerned rates of net accretion, which do not take into account losses due to physical and biological erosion. Relative rates of net accretion are likely to be biassed in favour of corals because coralline algae typically predominate on the wave-exposed margins of coral reefs (e.g., Foslie 1907; Tracey *et al.* 1948; Emery *et al.* 1954; Dawson 1961; Ladd 1961; Lee 1967; Marsh 1970; Littler & Doty 1975),

which are areas of great erosive potential and difficult environments to work in. True comparisons can only be made from estimates of gross calcification, and only this data can answer the question of how much material is lost in the process of reef maintenance and growth. Such information is critical for an understanding of what cost is involved in the maintenance of a wave-resistant reef front. The wave-resistant margin is perhaps the most significant part of a coral reef because the protection it affords permits the development of most other shallow water reef communities (Dawson 1961; Ladd 1961). Coralline algae are the principal cementing agents (Wray 1971) which create the structural integrity and resilience of the reef front and their importance in this regard cannot be overstressed.

Calcification has not been studied extensively in coralline algae as a whole, and only rarely in reef-building species. Most of the studies which have been undertaken have not provided data which can be used to estimate the likely contribution by coralline algae to reef growth. This has largely resulted from the continued use of radioisotopes to measure calcification. There are many problems with the use of radioisotopes in calcification studies (Barnes & Crossland 1977, 1982; Crossland & Barnes 1977), the most important being the passive rate of isotopic exchange (Bohm 1978; Borowitzka 1979). Isotopic exchange has nothing to do with biological processes. Even with improved procedures which attempt to control it (Bohm 1978; Borowitzka 1979) there are difficulties in determining how much of what is measured as incorporation is the result of biological precipitation.

Perhaps the most convenient alternative to radioisotopes is the alkalinity anomaly technique which was developed independently by Kinsey (1972) and Smith (1973). The alkalinity anomaly technique has two major advantages. First, it permits the measurement of total inorganic carbon flux. Second, with suitable manipulation and knowledge of the appropriate photosynthetic and respiratory quotients, it can be adapted for use with electrodes (pH, O_2, & temperature), thus avoiding the need for titrations (see Barnes 1983). However, the technique is not without constraints. These essentially arise from the need to make certain assumptions about the factors which affect the carbonate equilibrium in seawater (see Section 3. 2. 2 for details). Kinsey (1978b) has shown that most of these assumptions are valid under normal environmental conditions.

The alkalinity anomaly method has now been used for over a decade with some considerable success to measure calcification in flowing water systems, usually over reef flats (see references given in Smith 1983 and Kinsey 1985). It therefore seems surprising that attempts have not generally been made to adapt the technique for measurement of the calcification rates of specific reef organisms. Borowitzka (1977) suggests that one drawback with the technique is that large volumes of biological material are required in order to make reliable measurements. However, it will be demonstrated in this study that relatively small amounts of material can be used, particularly if the technique is adapted for use with pH, O_2, and temperature electrodes.

If calcification is measured by this method then simultaneous data for photosynthesis are also obtained. Photosynthesis is now known to play a major role in light-enhanced calcification (Kawaguti & Sakamuto 1948; Goreau 1963; Pearse 1972; Vandermuelen *et al.* 1972; Bohm & Goreau 1973; Digby 1977a,b), but despite the efforts of numerous workers the nature of the relationship is not yet understood. The term light-enhanced calcification implies that there is a basic calcification mechanism which is independent of light, but is stimulated or augmented by it. The truth of this assumption has been questioned on more than one occasion (Chalker 1976; Borowitzka & Larkum 1976a; Borowitzka 1979). The issue has not been resolved because radioisotope procedures generally rely upon dark calcification to provide an arbitrary baseline from which to measure light-enhanced calcification. However, it is intriguing that when Borowitzka & Larkum (1976a) compared the dark rate of ^{45}Ca incorporation by living and dead specimens of *Halimeda* they found a higher rate of incorporation in the dead material. Also, Borowitzka (1979) could not detect any dark calcification in *Amphiroa foliacea*. These studies indicate that algal calcification may not occur in the dark and may be entirely a light-driven process presumably associated with photosynthesis. It is therefore logical to measure calcification and photosynthesis in parallel and relate both to the available irradiance. By constructing light-saturation curves for calcification (*C-I* curves) it was hoped that comparisons with the curves for photosynthesis (*P-I* curves) would yield information about the degree of relation between the two processes. Moreover, the *C-I* curves would provide statistically supported estimates of the light-enhanced and dark calcification rates, an opportunity to determine if crustose coralline algae photoadapt with respect to calcification, and models with which to predict the calcification rate for any amount of irradiance over the measured range of PPFD.

The objectives of the calcification study were therefore:

(i) to measure the *in situ* calcification rates of four dominant reef-building crustose coralline algae,

(ii) to construct light-saturation curves for calcification,

(iii) to determine if the shapes of the *C-I* curves change with depth and irradiance,

(iv) to compare the *C-I* and *P-I* curves for similarities and differences in their shapes,

(v) to determine if such comparisons provide information about the calcification process,

(vi) to integrate rates of calcification per hour with the changes in irradiance known to occur over the course of a cloudless day, and

(vii) to determine if the rate of calcification per day could be related to the peak noon irradiance at the site of measurement.

3. 2. *IN SITU* CALCIFICATION

3. 2. 1. MATERIALS AND METHODS

Calcification was measured by a method which required direct information about the rate of photosynthesis. The materials and methods used for the *in situ* measurement of photosynthesis were therefore directly relevant to the measurement of calcification. These procedures have already been described in detail (Section 2. 3. 1). The following deals only with the materials and methods specific to the studies of calcification which were not covered in Section 2. 3. 1.

Experimental apparatus

The pH electrode used for the calcification studies was a Radiometer GK2401C glass electrode. The electrode was inserted into the submersible cell (Plates 9, 10, 11) through an acrylic mount affixed to the domed portion of the chamber (Figs 6A,B, 7, Plates 9A, 11) at an angle of 10° to the horizontal (Fig. 6B). The pH electrode had to be pointing slightly downward to ensure a continuous gravitational flow of electrolyte through the porous pin of the electrode so as to maintain the electrical bridge between the internal reference solution and the external medium. In most circumstances the slope of the reef dictated a downward angle for the electrode but on horizontal surfaces the angle of insertion was important.

A stainless steel sleeve was fabricated with two internal 'o'-rings to slide over the glass portion of the electrode and cover the electrolyte filling hole (Fig. 27, Plates 9A, 11). One internal 'o'-ring sealed against the electrode immediately above the filling hole while the other sealed immediately below it. The fitting was joined with a hose-clamp to a section of high pressure hose acting as an umbilicus to convey the wire from the electrode to the datalogger (Plates 11, 12). A small stainless steel funnel was externally threaded and silver-soldered to the side of the sleeve. When fitted, the funnel lay directly above the filling hole of the electrode. An internally threaded cap with pressure equilibration hole was lined with a fine rubber diaphragm and screwed onto the funnel, thus isolating the contents of the electrode from the atmosphere. Prior to deployment underwater, the fitted electrode was filled almost to the lip of the funnel with electrolyte (Radiometer S4004 KCl)(Fig. 27). The cap was screwed onto the funnel trapping a small volume of air between the rubber diaphragm and the surface of the electrolyte. The air bubble was compressed by the diaphragm as the electrode was taken underwater thus facilitating pressure equalisation and ensuring a continuous flow of electrolyte through the porous pin.

Calibration of the pH electrode

The pH electrode was calibrated before each *in situ* incubation using Radiometer precision buffer solutions S1510 (pH = 7.410 ± 0.005 at 25°C) and S1500 (pH = 6.865 ± 0.005 at 25°C). The buffer solutions, contained within sealed glass ampoules, were brought to the correct temperature in a water-filled beaker suspended from the lid of the constant temperature bath (see Section 2. 3. 1). The pH electrode was stabilised before calibration in the manufacturer's recommended storage buffer (Radiometer buffer solution S1316 pH = 4.01 ± 0.01 at 25°C). The electrode was calibrated separately for each buffer solution. The buffer solution was poured into a small glass vial suspended from the lid of the calibration bath (Plate 14A) and a fine stainless steel wire was placed in the solution to provide a ground connection to the datalogger. The tip of the electrode was immersed in the buffer and the calibration value was recorded after 3 min of stable readings. Since the pH of seawater (*ca* 8.3) does not fall within the range of precision buffer solutions manufactured by Radiometer (Copenhagen, Denmark) the linearity of the electrode response over the range of interest was checked with a phosphate buffer at pH 8.4 (3.86 ml 1M KH_2PO_4 + 6.14 ml 1M Na_2HPO_4). When calibrated, the electrode yielded realistic values for seawater pH.

Fig. 27. Section drawing showing stainless steel fitting for pressure compensation of the pH electrode employed in the *in situ* measurements of calcification.

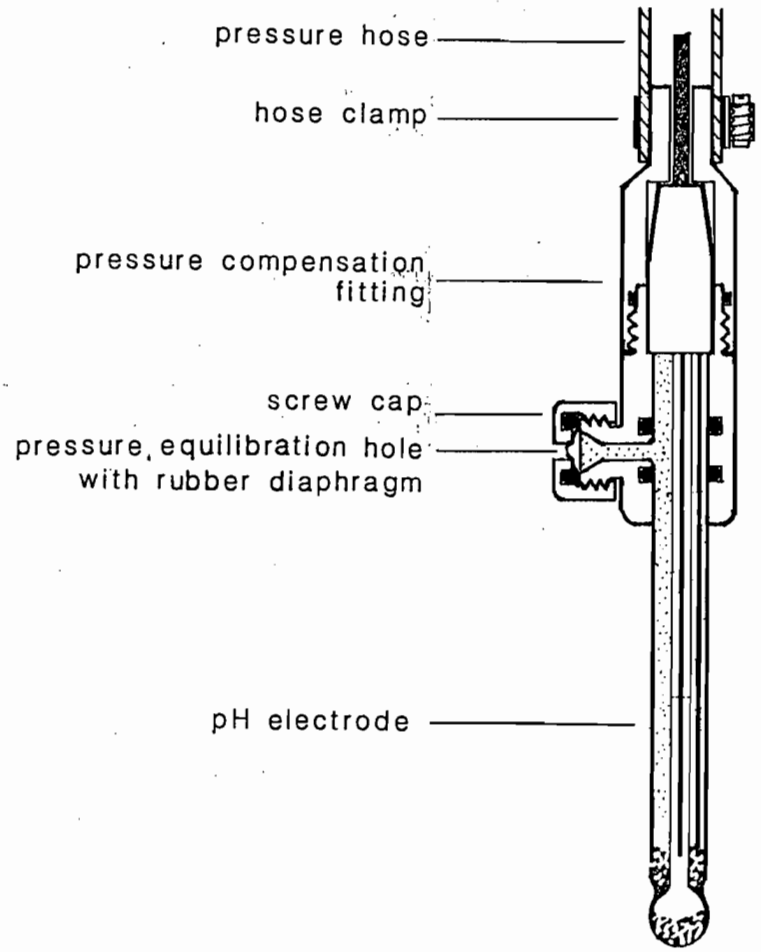
pressure hose
hose clamp
pressure compensation fitting
screw cap
pressure equilibration hole with rubber diaphragm
pH electrode

Great care was taken to prevent contamination of the pH electrode during handling. The tip of the electrode was wrapped in moistened parafilm during transport to the experimental sites.

Experimental procedures

The datalogger read the pH electrode every six seconds and recorded integrated values for every minute. These readings were used along with those for oxygen, light, and temperature to calculate the calcification rates of the coralline disks. The rate of calcification was essentially determined by subtracting the change in pH calculated to have resulted from photosynthesis and respiration from the total change in pH (see following sections).

The calcification data were normalised by **real surface area**, **projected surface area**, and **total protein content**. The protein contained within each specimen was extracted after the chl. *a* and fat soluble accessory pigments had been removed (see Section 2. 2. 1). The protein was removed by heating the finely ground coralline material for 30 min at 90°C in two serial volumes of 1 N sodium hydroxide. The amount in each extract was determined by the Bio-Rad protein assay (Bio-Rad Laboratories 1979), which is founded on the method of Bradford (1976). Bradford observed that the absorbance maximum for an acidic solution of the dye Coomassie Brilliant Blue G-250 changed from 465 nm to 595 nm when complexed with protein. The absorbance at 595 nm is proportional to the concentration of protein in the sample.

A standard curve was prepared by mixing a fixed volume (5 ml) of the dye reagent with a series of aqueous protein standards (200 µl each). Absorbances were read against a reagent blank at 595 nm after 15 min using a Hitachi (U-3200) spectrophotometer. Three replicates were used for each determination. The protein standard was bovine gamma globulin (BGG - Bio-Rad Laboratories). Chalker *et al.* (1983) have shown that protein assays based on the method of Bradford (1976) using the BGG standard give very similar results to assays based on the method of Lowry *et al.* (1951) using a protein standard of bovine serum albumen (BSA - Sigma Chemical Company). The standard curve was prepared by plotting protein concentration against absorbance at 595 nm. The data was not entirely linear as

claimed by Bio-Rad (1979) and a second order polynomial was found to produce a more accurate description of the data ($r^2>0.99$).

The protein extracts of the coralline specimens were first tested for natural absorbance at 595 nm to ensure that no substances would interfere with the protein determinations. 100 µl aliquots of the coralline extracts were neutralised with equal volumes of 1 N hydrochloric acid (HCl) and 5 ml of the dye reagent was added. The solutions were gently shaken on a vortex mixer without frothing and their absorbances were read 15 min later as described above. The quantity of protein in each extract was determined from the standard curve of protein concentration versus absorbance at 595 nm.

3. 2. 2. ANALYSIS OF DATA

Several investigators (Park 1969; Strickland & Parsons 1972; Smith 1973; Skirrow 1975; Smith & Key 1975; Smith & Kinsey 1978) have described in detail how measurements of pH and total alkalinity can be used to estimate biological calcification by the alkalinity anomaly technique. Barnes (1983) developed the methodology further to enable estimation of calcification rate based upon pH and oxygen measurements, in conjunction with predetermined values for the photosynthetic and respiratory quotients. The alkalinity anomaly technique is based on certain assumptions, all of which can be demonstrated to be valid under normal circumstances.

Alkalinity may be defined as the capacity of a solution to neutralise hydrogen ions. Seawater alkalinity or total alkalinity (*TA*) is governed by three systems: carbonate alkalinity (*CA*), borate alkalinity (*BA*), and hydroxide alkalinity (*HA*) where:

$$TA = CA + BA + HA. \tag{13}$$

Carbonate alkalinity arises from the hydration of carbon dioxide (CO_2) to carbonic acid (H_2CO_3), with subsequent dissociation into bicarbonate (HCO_3^-) and carbonate (CO_3^{2-}) ions:

$$H_2O + CO_2 \Leftrightarrow H_2CO_3 \Leftrightarrow H^+ + HCO_3^- \Leftrightarrow 2H^+ + CO_3^{2-}. \quad (14)$$

Carbonate alkalinity is thus determined by the concentration of bicarbonate and carbonate ions in solution:

$$CA = HCO_3^- + 2CO_3^{2-}. \quad (15)$$

From Eq. (14), the total amount of inorganic carbon in seawater is the combined concentrations of four species of carbon dioxide:

$$\Sigma CO_2 = CO_2 + H_2CO_3 + HCO_3^- + CO_3^{2-}. \quad (16)$$

Total inorganic carbon could thus be estimated by quantifying and summing each of the four species of carbon dioxide.

Alternatively, total inorganic carbon can be estimated by multiplying the carbonate alkalinity by the product of a number of terms which describe the partitioning of carbon dioxide species in seawater, for given conditions of temperature, salinity, and pressure:

$$\Sigma CO_2 = CA\left(\frac{a_H k_{1c} + k_{1c}k_{2c} + a_H^2}{a_H k_{1c} + 2k_{1c}k_{2c}}\right), \quad (17)$$

where a_H is the hydrogen activity (10^{-pH}) and k_{1c} and k_{2c} are the first and second dissociation constants for carbonic acid.

The amount of boron (ΣB) in seawater is not significantly affected by biological processes and is constant for a given salinity (S):

$$\Sigma B = 0.01.S. \quad (18)$$

Providing pH and temperature are known the borate alkalinity can be calculated from:

$$BA = \Sigma B\left(\frac{a_H k_{1b} + 2k_{1b}k_{2b}}{a_H^2 + a_H k_{1b} + k_{1b}k_{2b}}\right), \quad (19)$$

where k_{1b} and k_{2c} are the first and second dissociation constants for boric acid. The dissociation constants are functions of temperature and salinity.

Hydroxide alkalinity results from the dissociation of water:

$$H_2O \Leftrightarrow OH^- + H^+. \tag{20}$$

Since the concentration of hydroxide ions (OH^-) in solution is directly proportional to the concentration of hydrogen ions (H^+) the hydroxide alkalinity can be estimated from pH where:

$$HA = \frac{(10^{-14-aH})^2}{10^{-pH}}. \tag{21}$$

By rearranging Eq. (13) to solve for carbonate alkalinity:

$$CA = TA - BA - HA, \tag{22}$$

and by combining Eqs (17) and (22), total inorganic carbon can be estimated from:

$$\Sigma CO_2 = (TA - BA - HA)D, \tag{23}$$

where D is the function in parentheses in Eq. (17).

Under normal conditions, the only significant factors affecting the total amount of inorganic carbon in coral reef waters are photosynthesis (P), respiration (R), and calcification ($Calc$), so that:

$$\Delta\Sigma CO_2 = \Delta CO_{2P-R} + \Delta CO_{2Calc}. \tag{24}$$

Photosynthesis and calcification both lower the carbonate alkalinity, and hence total inorganic carbon, by removal of ionic carbon dioxide species (CO_3^{2-}, HCO_3^-). Respiration has the reverse effect due to the liberation of carbon dioxide species. However, the removal or liberation of carbonate species during photosynthesis and respiration has no effect on the total alkalinity of the seawater. For each mole of carbonate or bicarbonate ions removed or produced during photosynthesis and

respiration there is an equivalent change in the number of hydrogen ions present in solution. This may be understood by consideration of four equations which describe the conversion of carbon dioxide species into carbohydrate during photosynthesis:

$$CO_3^{2-} + 2H^+ \rightarrow CH_2O + O_2 \tag{25}$$

$$HCO_3^- + H^+ \rightarrow CH_2O + O_2 \tag{26}$$

$$H_2CO_3 \rightarrow \begin{matrix} H^+ + HCO_3^- \\ \text{or} \\ 2H^+ + CO_3^{2-} \end{matrix} \rightarrow CH_2O + O_2 \tag{27}$$

$$CO_2 + H_2O \rightarrow H_2CO_3 \rightarrow \begin{matrix} H^+ + HCO_3^- \\ \text{or} \\ 2H^+ + CO_3^{2-} \end{matrix} \rightarrow CH_2O + O_2 \tag{28}$$

Calcification, on the other hand, does alter the total alkalinity of the seawater because if bicarbonate ions are removed hydrogen ions are produced:

$$Ca^{2+} + HCO_3^- + H^+ \rightarrow CaCO_3 + 2H^+, \tag{29}$$

and if carbonate ions are removed:

$$Ca^{2+} + CO_3^{2-} + 2H^+ \rightarrow CaCO_3 + 2H^+. \tag{30}$$

The result of both equations (29) and (30) is that for each mole of CO_2 removed from the seawater 2 moles of H^+ are produced. Since alkalinity is the capacity to neutralise acid, the precipitation of 1 mole of $CaCO_3$ reduces the total alkalinity by two molar equivalents. The change in total inorganic carbon due to calcification is therefore half the change in total alkalinity:

$$\Delta CO_{2Calc} = \tfrac{1}{2}\Delta TA. \tag{31}$$

Combining Eq.s (24) and (31) gives:

$$\Delta \Sigma CO_2 = \Delta CO_{2P-R} + \tfrac{1}{2}\Delta TA. \tag{32}$$

Rearranging Eq. (32) to solve for the change in inorganic carbon due to photosynthesis and respiration, and substituting Eq. (23) for total inorganic carbon gives:

$$CO_{2P-R} = (TA-BA-HA)D - (TA'-BA'-HA')D' - \tfrac{1}{2}\Delta TA, \tag{33}$$

where parameters superscripted with a prime are the initial values.

The change in inorganic carbon concentration can be estimated from:

$$-\Delta CO_2 = \Delta O_2 \cdot Q, \tag{34}$$

where Q is the value of the metabolic quotient. During the day Q is the net photosynthetic quotient (net PQ), whereas during the night Q is the respiratory quotient (RQ). The determination of net PQ and RQ will be described in Section 3. 3.

Substituting oxygen values for carbon dioxide in Eq. (33) gives:

$$\Delta O_2 \cdot Q = (TA-BA-HA)D-(TA'-BA'-HA')D'-\tfrac{1}{2}(TA-TA'). \tag{35}$$

Rearranging to solve for the change in total alkalinity:

$$D \cdot TA-\tfrac{1}{2}TA-D' \cdot TA'+\tfrac{1}{2}TA' = D(BA+HA)-D'(BA'+HA')-\Delta O_2 \cdot Q,$$

adding $D \cdot TA'$ to both sides of the equation:

$$D \cdot TA'+D \cdot TA-\tfrac{1}{2}TA-D' \cdot TA'+\tfrac{1}{2}TA' = D(BA+HA)-D'(BA'+HA')+D \cdot TA'-\Delta O_2 \cdot Q$$

and rearranging:

$$(D-D')TA'+(D-\tfrac{1}{2})TA-(D-\tfrac{1}{2}) = D(BA+HA)-D'(BA'+HA')-\Delta O_2 \cdot Q$$

to:

$$TA-TA' = \frac{-(D-D')TA'+D(BA+HA)-D'(BA'+HA')-\Delta O_2 \cdot Q}{(D-\tfrac{1}{2})}$$

yields:

$$-\Delta TA = \frac{\Delta O_2 \cdot Q+(D-D')TA'-D(BA+HA)+D'(BA'+HA')}{(D-\tfrac{1}{2})} \tag{36}$$

Recapitulating, Eq. (31) states the relationship between total alkalinity and the change in inorganic carbon due to calcification or solution. Thus **Eqs (36)** and **(31)** describe how calcification or solution can be estimated on the basis of sample pH and oxygen measurements in conjunction with knowledge of the initial alkalinity of the seawater, and of the appropriate metabolic quotients (PQ and RQ).

Estimating calcification using the alkalinity anomaly technique assumes that the only significant factors affecting the alkalinity system are photosynthesis, respiration, and calcification. Gaines & Pilson (1972) have noted that interference can arise, for example, from the liberation of ammonia from amino acids, or from the precipitation of nutrient salts. However, Edmond (1970) and Kinsey (1978b) have shown that interference due to nonconservative, non-carbon dioxide species in well-oxygenated water is neglible. Additional concerns regarding the possible significance of contributions to total alkalinity from nitrate, phosphate, and sulphate in coral reef waters have similarly been dispelled by Kinsey (1978b). It should also be stated that the carbonate equilibrium is known to change with pressure (Skirrow 1975). The dissociation constants for carbonic and boric acid therefore change with water depth. However, at a depth of 100 m (10 atm pressure) the values of the dissociation constants alter by only about 1% (calculated from tables provided by Culberson & Pytkowitcz 1968) and, besides, the basis of the alkalinity anomaly technique resides in the measurement of differences and not absolute values. This means that errors in the determination of absolute alkalinity are not important so long as they are consistent throughout all measurements.

In the present study, the change in inorganic carbon resulting from calcification or solution was calculated using Eqs (36) and (31) from measurements of oxygen, pH, initial total alkalinity, and the value of the appropriate metabolic quotient. The calculated change in inorganic carbon concentration between flushings of the chamber was converted into the rate of calcium carbonate precipitation or solution per hour.

Light-saturation curves for calcification

Rates of calcium carbonate precipitation or solution were plotted against irradiance and analysed by non-linear, least squares regression using subroutine BMDP3R of the BMDP statistical package. The data were modelled by the hyperbolic

tangent function. BMDP3R estimated values for the rate of dark calcification (C_{dark}), the initial slope of the light saturation curve (α), the irradiance at which the initial slope intercepted the horizontal asymptote (I_k), and the maximal rate of light-enhanced calcification (C_{light}).

Further analysis of the light-saturation curves for calcification (*C-I* curves) followed the statistical procedures applied to the light saturation curves for *in situ* photosynthesis (see Section 2. 3. 2).

3. 3. DETERMINATION OF METABOLIC QUOTIENTS

3. 3. 1. MATERIALS AND METHODS

Experimental apparatus

A cylindrical sampling bottle with detachable base, three apical nozzles (Fig. 7B, Plate 10A,B,D), and an internal volume of 110 ml was fabricated out of acrylic. The base was grooved and fitted with a circumferential 'o'-ring. Short lengths (*ca* 50 mm) of flexible hose with clamps were attached to each of the nozzles. Two larger nozzles (3 mm internal diam [I.D]) provided an inlet and an outlet for the bottle. A smaller nozzle (1 mm I.D.) was joined by a short length of hose to a horizontal coil of stainless steel tube affixed to the top of the bottle.

Collection of incubation water samples

Towards the conclusion of each of fourteen, 24-hour *in situ* incubations, two sets of water samples were removed from the specimen chamber. One sample was removed following a period of high irradiance (light sample), the other after a period of darkness (dark sample). Light samples were only collected when experiments ended near noon on fairly clear days. The water samples were collected for determinations of the metabolic quotients. Calculation of the daytime calcification rate from measurements of pH and oxygen requires a value for the net photosynthetic quotient (net *PQ*). Net *PQ* can only be accurately estimated when the rate of photosynthesis significantly exceeds the rate of respiration (i.e., at or near saturation). For this reason samples must be collected following periods of near maximal irradiance.

Water samples were obtained from experiments performed on specimens of *Porolithon onkodes* at 0 m (n = 5, where n was the number of specimens), *Neogoniolithon fosliei* at 3 (n = 1) and 6 m (n = 2), *Hydrolithon reinboldii* at 3 (n = 2) and 6 m (n = 1), and *Paragoniolithon conicum* at 6 m (n = 3).

Experimental procedures

The sampling bottle was carried to the experimental site with the hose clamps tightened and the base detached. The bottle was held upright at a depth just below that of the specimen chamber and the water in the bottle was replaced with air from the diver's regulator. The base was fitted to prevent seawater from re-entering the bottle and the hoses on the specimen chamber and sampling bottle were joined together pending removal of the incubation water.

The light sample was collected just prior to the final flushing of the specimen chamber. If cloud cover reduced the available irradiance for a significant proportion of the incubation period the experiment was continued until an extended period of little or no cloud cover was encountered. The datalogging operation was halted, and with the sampling bottle held below the level of the specimen chamber, the clamps at either end of the hose connections were opened. This permitted air within the sampling bottle to travel upwards through one hose into the specimen chamber and incubation water from the specimen chamber to travel downwards through the other into the sampling bottle. As soon as the sampling bottle was filled with water (*ca* 10-15 s) the two clamps on the hoses attached to the sampling bottle were tightened. The electrode chamber was removed from the specimen to release the trapped air, then again positioned over the specimen and the hose clamps adjacent to the inlet and outlet nozzles re-tightened. A large black cloth with weighted margin was placed over the chamber to exclude all sunlight and the datalogging operation was re-commenced. As soon as the specimen chamber was flushed, the time was recorded and the bottle containing the light sample was returned to the boat. Before ascending to the surface, the hoseclamp located between the smaller nozzle and the coil of stainless steel tubing was slackened to allow the small volume (*ca* 1-5 cc) of air still trapped in the bottle to expand during ascent and trickle out through the coil without admitting seawater. The sample was transferred to an acid-washed and seawater (0.45 µm Millipore filtered) acclimatised glass bottle (100 ml). These procedures were repeated for the dark sample following an equivalent incubation period. The water

samples were taken to the laboratory at Lizard Island Research Station, filtered (0.45 µm Millipore filter) and stored with minimal air volume (0-1 ml) in gas-tight, acid-washed and seawater (0.45 µm Millipore filter) acclimatised glass medicine bottles (100 ml) at 4°C in darkness.

The water samples were later transported in ice-filled, insulated containers to the Australian Institute of Marine Science for the determination of total alkalinities. The total alkalinity of each sample was determined using a semi-automated titrator developed at the A.I.M.S. by Dr. D.J. Barnes and Mr. M.J. Devereux (1984). The alkalinity was determined by measuring the pH of the seawater sample after the addition of a precise volume of HCl according to the methods given Smith & Kinsey (1978). The theoretical basis for the method will be provided in the following section (Section 3. 3. 2.).

The titration apparatus consisted of a water bath which was thermostatically controlled by a MGW Lauda Pumping Thermal Control Unit. An automatic pipette fed precise volumes (3 ml) of 0.005N HCl and sample seawater (5 ml) into a mixing chamber. The mixed and acidified sample was then forced, by compressed air, through a capillary tube into another chamber containing the pH electrode. The sample was gently bubbled for 2 min with water-saturated CO_2-free air to drive off free CO_2 (Culberson *et al.* 1970). The pH was then recorded over a period of 20 s. This process was repeated 10 times. Values which differed from the mean value by more than 2 standard deviations (SD) were rejected and replaced with additional measurements. The alkalinity of the samples could thus be determined with a SD of approximately 0.001 pH units (Barnes & Devereux 1984). A Hewlett-Packard (H-P) Data Acquisition/Control Unit (Model 3497A) controlled the operation of the automatic pipette and channelled the measured pH values to a H-P datalogger (Model 3054). The pH of the acidified samples was measured using a Radiometer GK2401C glass pH electrode.

The pH electrode was stabilised first in Radiometer buffer solution S1316 (pH = 4.01 ± 0.01 at 25°C) and then calibrated using the S1316 buffer and Radiometer precision buffer solution S1510 (pH = 7.410 ± 0.005 at 25°C). The electrode chamber was flushed with 90 volumes of acidified seawater to equilibriate the electrode and then 10 alkalinity determinations were performed on a standard

seawater sample to test the stability of the electrode. These procedures were followed on a daily basis.

The incubation seawater samples were brought to temperature in the water bath before determination of their alkalinities. The light and dark incubation samples from each experiment were measured on the same day to avoid errors resulting from different calibration values for the pH electrode. Samples were measured in order of their expected alkalinities such that all light samples were measured together and all dark samples were measured together to avoid large fluctuations in the response of the pH electrode. The drift of the pH electrode was measured over the course of the day by determining the alkalinity of a standard seawater sample at the beginning, middle, and end of the day. Sample alkalinities were corrected for drift.

The total alkalinities of the samples were used in conjunction with the measurements of oxygen, pH, and temperature for calculation of the metabolic quotients.

3. 3. 2. ANALYSIS OF DATA

Calculation of sample alkalinity

Smith & Kinsey (1978) have described an appropriate method for the determination of total alkalinity from pH measurements of acidified seawater samples. Precise volumes of HCl, of known normality, are added to similarly precise volumes of the seawater sample. The volume ratios chosen are naturally dependent on the normality of the acid and on the alkalinity of the samples. Coral reef water typically has an alkalinity of between 2.26 and 2.42 meq l^{-1} (see Skirrow 1975). Smith & Kinsey suggest that a convenient volumetric ratio of 0.01 N HCl to seawater sample is 0.3, to produce a pH for the mixture of between 3.2 and 3.9 pH units. A ratio of 3 ml 0.01 N HCl to 10 ml seawater sample was therefore recommended. However, it was more desirable in this study to use a ratio of 3 ml 0.005 N HCl to 5 ml seawater sample because the sample volumes were small (*ca* 100 ml). Using HCl of half the normality suggested by Smith & Kinsey enabled twice as many determinations to be made of the total alkalinity for the same volume of sample.

The acidified sample should be bubbled with water-saturated, carbon dioxide-free air before measurement of the pH to drive off free carbon dioxide which would otherwise dissociate to replace the carbonate and bicarbonate ions which become neutralised by the acid. Water-saturated air is required to prevent alteration of the sample salinity.

The pH of the acidified sample is converted into hydrogen ion activity, and the total alkalinity is calculated from:

$$TA = \frac{1000}{V_s} V_a N - \frac{1000}{V_s}(V_s + V_a)\frac{a_H}{f_H} , \qquad (37)$$

where a_H is the hydrogen activity (10^{-pH}), V_a is the volume and N the normality of the acid, V_s is the volume of seawater, and f_H is an empirical constant.

Culberson *et al.* (1970) have discussed the determination of the empirical constant (f_H) and its meaning in the context of total alkalinity calculations. Essentially, f_H is the activity coefficient for hydrogen ions in both free and complexed states, and the term a_H/f_H is the excess hydrogen ion concentration over that which is necessary to titrate the anions of weak acids regardless of the hydrogen ion species involved. The empirical constant can be determined from the slope of a_H versus N if volume and alkalinity remain constant since a_H is directly proportional to N under these conditions. Culberson *et al.* calculated that f_H has a value of 0.74 for the salinity range 31- 40°/oo. Kinsey (cited from Smith & Kinsey 1978) has estimated f_H to lie between 0.76 and 0.77, but as Smith & Kinsey (1978) point out, the value for f_H over this range of salinity has little effect on the calculated alkalinity.

Calculation of metabolic quotients

The total alkalinity (TA) of each incubation water sample was calculated using Equation (37). The metabolic quotients (Q) for each specimen were derived from measurements of sample total alkalinity, oxygen flux (ΔO_2), and pH change. Corrections were applied to the oxygen and pH data for small differences between the calibration temperature and the temperature of the incubation seawater during measurement. As discussed in Section 3. 3. 1., the relationship between carbon dioxide flux and oxygen flux during photosynthesis and respiration is:

$$-\Delta CO_2 = \Delta O_2 \cdot Q, \quad (34)$$

and the relationship between the change in total seawater alkalinity and the change in total inorganic carbon resulting from calcification or solution is:

$$\Delta CO_{2Calc} = \tfrac{1}{2}\Delta TA. \quad (31)$$

The total change in pH is the product of the changes in carbonate alkalinity, and hence total inorganic carbon (ΣCO_2), which result from photosynthesis (P), respiration (R), and calcification ($Calc$):

$$\Delta pH = \Delta CO_{2P\text{-}R} + \Delta CO_{2Calc} \quad (38)$$

Combining and rearranging Eqs (34), (31), and (38) gives:

$$\tfrac{1}{2}\Delta TA = \Delta pH + (\Delta O_2 \cdot Q). \quad (39)$$

and rearranging to solve for Q yields:

$$Q = \frac{\tfrac{1}{2}\Delta TA - \Delta pH}{\Delta O_2}. \quad (40)$$

Eq. (40) permitted calculation of the metabolic quotients for the coralline specimens.

3. 4. RESULTS AND DISCUSSION

3. 4. 1. DATA NORMALISATION

Individual rates of calcification were normalised on the bases of projected surface area, real surface area, and total protein content. In general, rates of calcification were less variable (i.e., smaller coefficients of variation) when data were normalised on the basis of total protein content (Table 16). Estimates based on either of the surface area measures produced similar coefficients of variation (Table 16).

The estimates of calcification were roughly twice as variable as the estimates of photosynthesis when the *in situ* data were normalised by projected area and real surface area (compare Table 16 with Table 3). This is not altogether surprising since

Table 16. Coefficients of variation(%*CV*)for estimates of light-enhanced calcification, when data are normalised on the bases of projected surface area, real surface area, and total protein content respectively.

Species	Projected Area %CV	Real Surface Area %CV	Total Protein %CV
Porolithon onkodes	39.2	41.8	22.9
Neogoniolithon fosliei	24.5	28.6	22.9
Hydrolithon reinboldii	28.4	28.2	15.7
Paragoniolithon conicum	35.7	36.6	27.2
Mean *CV*	**32.0**	**33.8**	**22.2**

the estimates of calcification involved limitations in the precision of measurement of both oxygen and pH. Moreover, the changes in pH which result from the biological precipitation of $CaCO_3$ are of an order requiring that pH be measured with a resolution of around 0.001 units (Barnes 1983). In calcifying systems, and particularly those which do so slowly, the changes in pH may be insufficient to register a measurable change over the time interval between individual measurements. This produces scatter in the pH data as a function of "stepping" (Barnes 1983, p. 157). These methodological difficulties no doubt contribute to the variability of calcification data. Even so, there is evidence which suggests that calcification is a naturally variable process and that several external and internal factors, other than light and photosynthesis, contribute to the measured rate (see later discussion, particularly Section 3. 4. 8).

The relationship between light and photosynthesis has already been examined in detail (see Chapter 2 and references given therein). Before saturation is approached, photosynthesis is largely limited by the amount of light which impinges upon the photosynthetic surface. Overall photosynthetic rate is thus crudely correlated with the area of the surface which is exposed to light. At a cellular level, photosynthetic rate is largely dependent upon the size, number, organisation, and effectiveness of the various pigment complexes which channel light energy to the reaction centres. Calcification rate, in contrast, is more highly correlated with biomass than with surface area (Table 16) which suggests that the rate of $CaCO_3$ deposition is more dependent upon the volume of tissue available for precipitation than upon the surface area available for light reception. Later discussion will examine the interrelationships between irradiance, photosynthesis, tissue volume, and calcification.

Section 2. 4. 1 identified endolithic algae as a significant source of error in determination of the chlorophyll *a* content of the coralline tissue of a crust. Endolithic algae provide a similar source of error in the determination of total protein. However, because their rates of organic production are likely to be very low (Kanwisher & Wainwright 1967) due to the extreme reduction in light (Halldal 1968) it seems unlikely that they would have significant biomass. For this reason total protein content is probably a reasonable measure of the amount of coralline tissue.

3. 4. 2. THE MEASUREMENT OF CALCIFICATION

The technique employed in this study was an adaptation of the alkalinity anomaly technique, which permitted the continuous measurement of carbonate flux and avoided the need for repetitive alkalinity determinations. The alkalinity anomaly technique, or adaptations thereof, has not previously been used to specifically estimate rates of carbonate flux in coralline algae. The technique makes several assumptions, the major ones being that the uptake of CO_2 is rapidly balanced by the release of other ions (Borowitzka 1983), and that nutrient fluxes do not give rise to significant changes in pH and total alkalinity (Brewer & Goldman 1976). Kinsey (1978b) has shown that the assumptions of the alkalinity anomaly technique are valid under normal environmental conditions.

With only one exception (Bohm 1978), all previous estimates of coralline algal calcification have been based on radioisotope incorporation data. Most of these studies have used ^{45}Ca incorporation rates to estimate carbonate deposition (see Borowitzka 1983, Table 3). However, since marine carbonates, and particularly those deposited by coralline algae (e.g., Vinogradov 1953; Chave 1954; Furuya 1960; Moberly 1968), often contain significant amounts of magnesium (as $MgCO_3$) (Milliman 1974) it is more appropriate to measure the flux of carbonate than the flux of calcium itself (Kinsey 1978a).

It is also well known that the use of radioisotope techniques for the measurement of biogenic $CaCO_3$ precipitation involves experimental variables which are difficult to control and errors which are difficult to quantify (see Bohm & Goreau 1973; Borowitzka & Larkum 1976a,b; Barnes & Crossland 1977,1982; Chalker 1976; Bohm 1978). The most significant source of error lies in the non-biologically mediated surface exchange of the different isotopic forms of the calcium or carbon (^{45}Ca or ^{14}C). Bohm (1978) and Borowitzka (1979) have documented procedures which partially overcome this difficulty. They advocate the use of serial incubations which permit determination of the amount of radioactive label incorporated purely as a function of isotopic exchange with skeletal components or internal calcium pools. The "true" rate of incorporation can be derived by subtracting this value from the total rate of incorporation. This method is a significant improvement on earlier procedures, which involved single time-point incubations and gave rise to enormous apparent rates of incorporation (particularly for calcareous algae), largely as a function of isotopic

exchange (see also Bohm 1978). However, the method still possesses the following disadvantages.

(i) The use of radioisotopes does not permit the continuous measurement of calcium or carbonate flux since the experimental subjects must be destroyed to establish the rates of incorporation.

(ii) In algae, passive isotopic exchange is often large with respect to biologically mediated incorporation (Barnes & Chalker in press). This produces a large degree of relative error which is compounded by the inherently variable nature of calcification data (see Borowitzka 1983, Table 3). Since isotopic exchange is a physical process which occurs irrespective of biological calcification it is particularly difficult to determine if calcareous algae calcify in the dark. It has been suggested that the positive rates of dark calcification which are commonly found using radioisotopes are methodological artifacts (Chalker 1976). While this does not appear to be true in all cases (e.g., Chalker *et al.* 1985; and see Table 17), certainly radioisotope techniques are incapable of resolving rates of $CaCO_3$ solution, although the use of dead controls may indicate when this has occurred (Borowitzka & Larkum 1976a).

(iii) Apparent rates of incorporation are greatly influenced by the experimental conditions and post-incubation procedures which are employed (Barnes & Crossland 1977, 1982; Crossland & Barnes 1977; Bohm 1978; Borowitzka 1979).

(iv) Radioisotope techniques are both time-consuming and inflexible since only a single measurement can be made for a given set of external conditions (e.g., irradiance and temperature).

(v) Radioisotopes and scintillation cocktails are expensive commodities which can be used only once.

Given the extent of the criticism which can be levelled at the use of radioisotopes for measuring biological calcification it is surprising that they are still used extensively. Borowitzka (1977) suggests that a major drawback of the alkalinity anomaly technique is that it requires large amounts of algal material. However, this study demonstrates that relatively small quantities of material (*ca* 10 cm^2 of living surface) can be used if the electrodes and associated electrical equipment have the required sensitivity.

3. 4. 3. LIGHT SATURATION CURVES

Representative light saturation curves for calcification (*C-I* curves) are presented for each species, at the depth intervals studied, in Figs 28-31. Table 17 contains the parameter estimates, with their 95% confidence intervals, and r^2 value for each *C-I* dataset. All data sets were modelled using the hyperbolic tangent function (Eq. 3). Statistical analyses was performed in the same manner as for *P-I* data using non-linear, least squares regression analyses.

The *C-I* curves in Figs 28-31 are similar in shape to those obtained for the *P-I* data (see Figs 9-12). As was the case for photosynthesis, the *C-I* curves establish that there is often insufficient light for the saturation of calcification in specimens from deeper water (Figs 28C,D, 29E,F, 30E, 31F). The curves in Figs 28B, 29A,B, and 31B, and the I_k values in Table 17 for shallow water specimens generally show that higher irradiance is required for the saturation of calcification than for the saturation of photosynthesis (Table 5). The data in Figs 28B,D, 29A,B,E, 30A,B,C, and 31A,B,F, and data contained in Table 17 show that there is frequently solution of calcium carbonate at night.

3. 4. 4. PHOTOADAPTIVE TRENDS AMONG DESCRIPTIVE PARAMETERS

Photoadaptive trends were observed in the values of α and I_k. The initial slopes (α,[m^{-2} projected surface area]) of the *C-I* curves increased with increasing depth (Table 17), and *ln* α (normalised on the basis of real surface area or total protein content) was inversely proportional to *ln* %SI (Fig. 32A,B,D). The irradiance at which the initial slope intercepted the horizontal asymptote (I_k, m^{-2} projected surface area) decreased with increasing depth (Table 17), and *ln* I_k (normalised on the basis of real surface area or total protein content) was directly proportional to *ln* %SI (Fig. 33B,C,D). No regression was calculated for *Porolithon onkodes* because the general linearity of the *C-I* curves for this species at 2.5 m (='6' m in terms of PPFD) and the consequential inaccuracy of the estimates of I_k yielded only one reliable estimate of I_k at low irradiance levels. The regression between *ln* α (normalised on the basis of real surface area) and *ln* %SI for *Hydrolithon reinboldii* (Fig. 32C) was only marginally non-significant (P=0.051) at the 95% probability

Fig. 28. Representative light-saturation curves for light-dependent calcification in *Porolithon onkodes.*

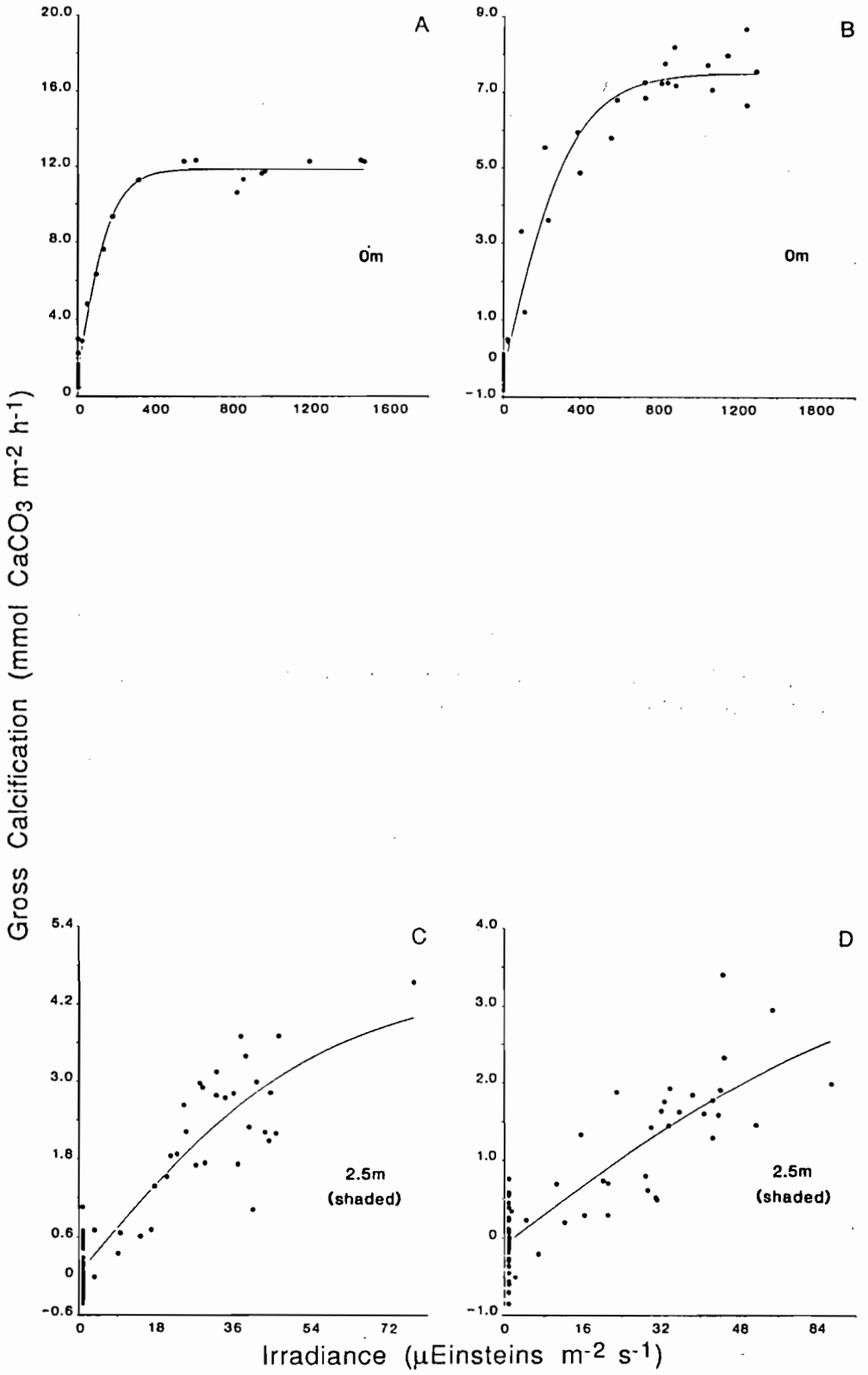
Porolithon onkodes
A
B
C
D
0m
0m
2.5m
(shaded)
2.5m
(shaded)
Gross Calcification (mmol CaCO3 m-2 h-1)
Irradiance (µEinsteins m-2 s-1)

Fig. 29. Representative light-saturation curves for light-dependent calcification in *Neogoniolithon fosliei*.

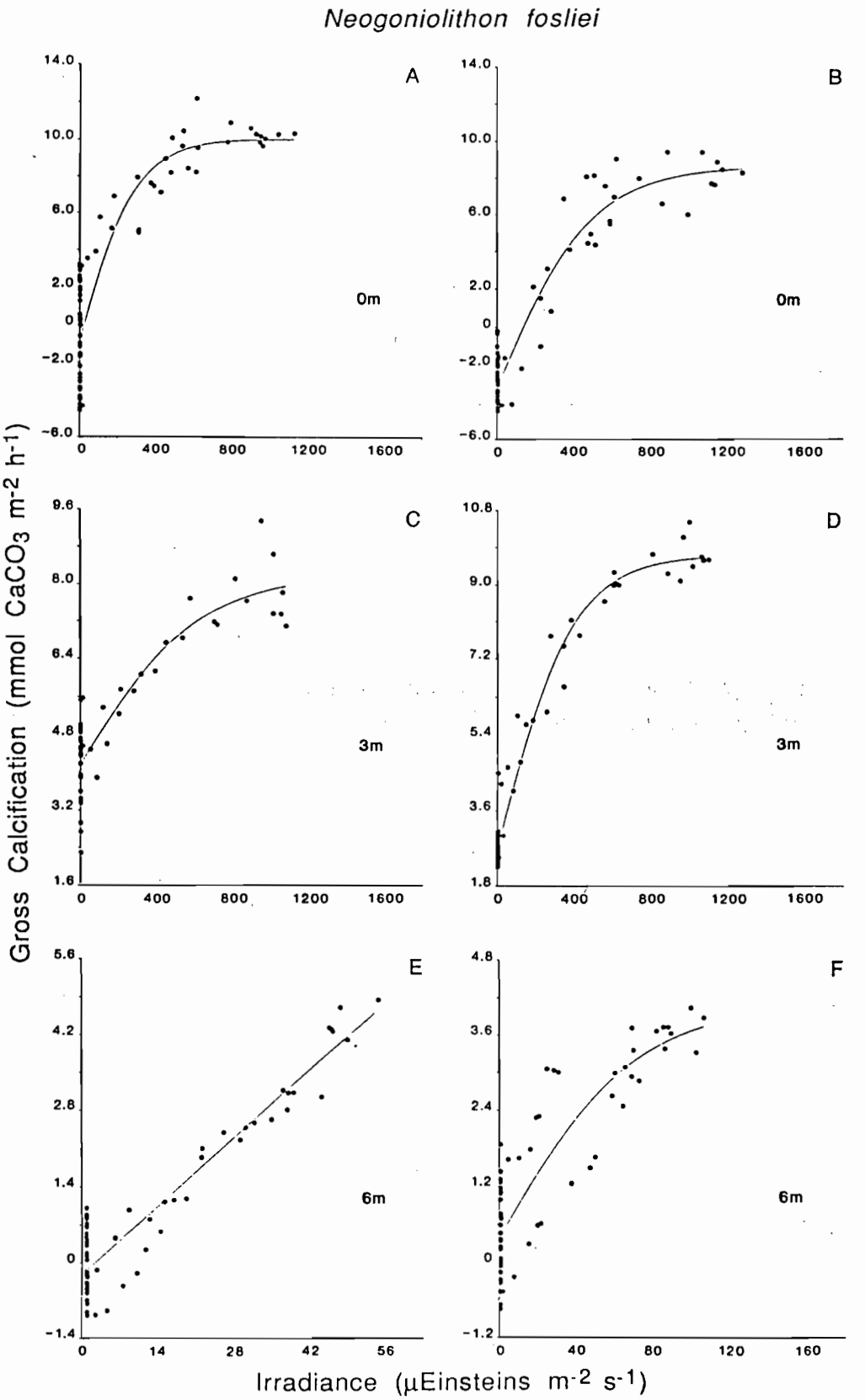
Neogoniolithon fosliei
A
B
C
D
E
F
0m
0m
3m
3m
6m
6m
Gross Calcification (mmol CaCO3 m-2 h-1)
Irradiance (µEinsteins m-2 s-1)

Fig. 30. Representative light-saturation curves for light-dependent calcification in *Hydrolithon reinboldii*.

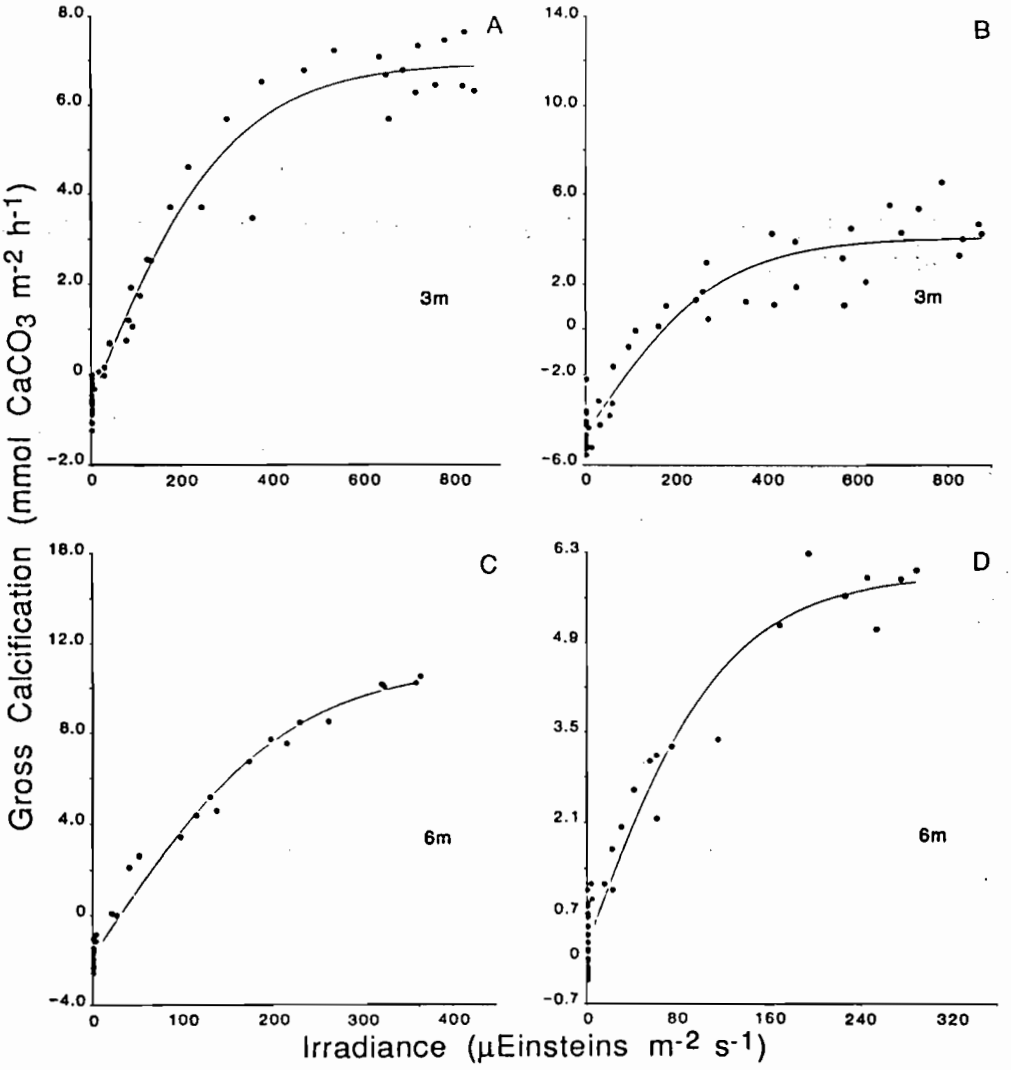
A
B
C
D
3m
3m
6m
6m
Gross Calcification (mmol $CaCO_3$ m^{-2} h^{-1})
Irradiance (μEinsteins m^{-2} s^{-1})
8.0
6.0
4.0
2.0
0
-2.0
14.0
10.0
6.0
2.0
0
-2.0
-6.0
18.0
12.0
8.0
4.0
0
-4.0
6.3
4.9
3.5
2.1
0.7
0
-0.7
0
100
200
300
400
0
80
160
240
320
0
200
400
600
800

Fig. 31. Representative light-saturation curves for light-dependent calcification in *Paragoniolithon conicum.*

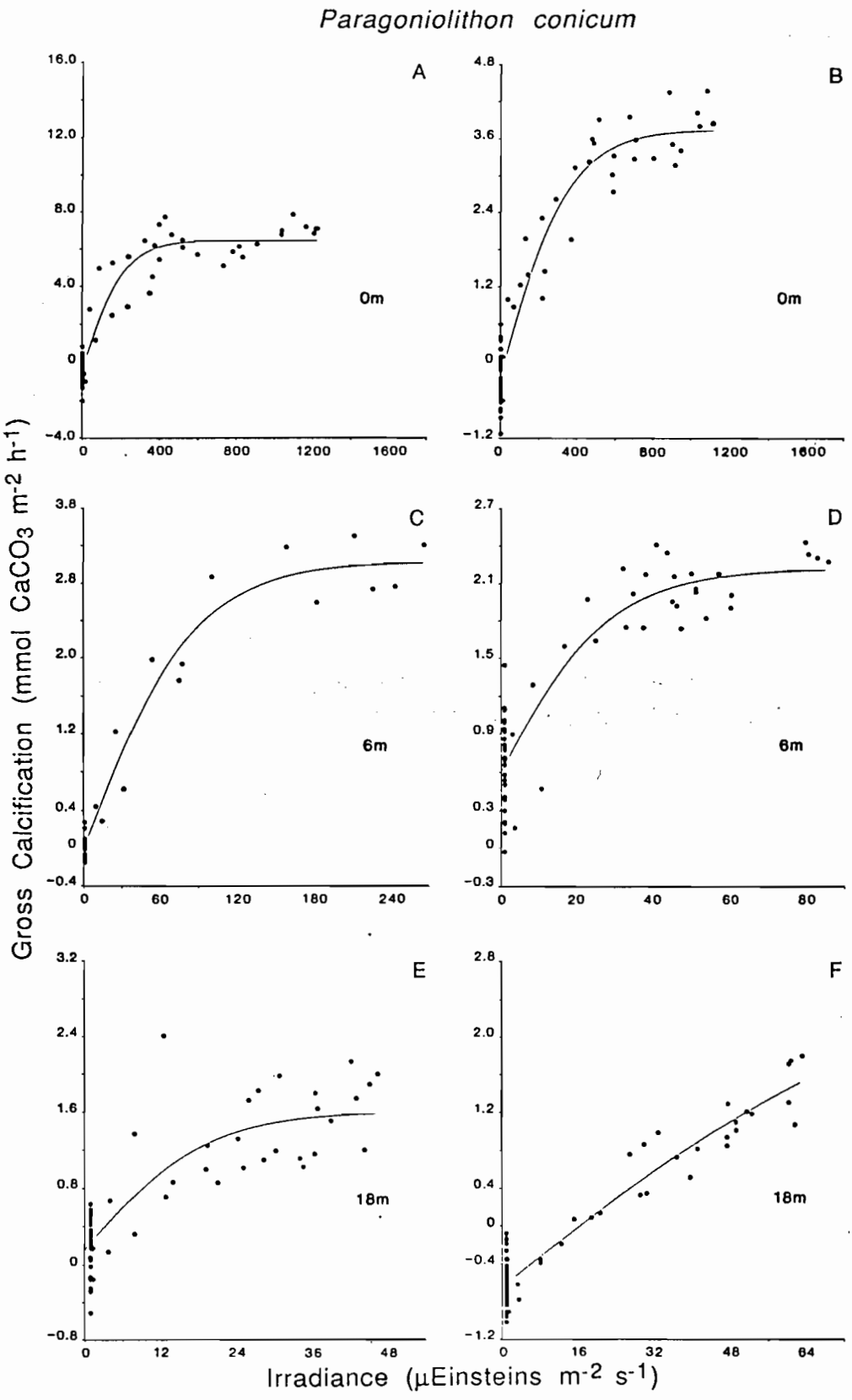
Paragoniolithon conicum
A
B
C
D
E
F
0m
0m
6m
6m
18m
18m
Gross Calcification (mmol CaCO3 m-2 h-1)
Irradiance (µEinsteins m-2 s-1)

Table 17. Parameter estimates, 95% confidence intervals (CI), and r^2 values for light-saturation curves for *in situ* calcification in different species of coralline algae from different depths (see text for parameter definitions). Mean values are given for each set of n (n = sample size) parameter estimates. The modelling function applied to each data set was the hyperbolic tangent (Eq. 3). Values in parentheses were not included in calculations of the means either because the confidence intervals were greater than means or because data were modelled by linear functions in the absence of saturation. Data sets modelled by linear functions are indicated by n/c (denoting values not calculated) in columns for estimates of I_k and $I_{0.95}$.

Species	Depth m	n	Calcification light-enhanced mmol $CaCO_3 m^{-2}$(proj.area)h^{-1}	Calcification dark	∝	I_k	$I_{0.95}$	r^2
			17.1 ± 2.31	-3.03 ±0.43	0.04 ± 0.0065	394 ± 103	721 ± 189	0.969
			10.6 ± 0.46	1.24 ±0.25	0.06 ± 0.0088	181 ± 28.1	332 ± 51	0.985
P. onkodes	0	5	6.49 ± 0.55	0.92 ±0.31	0.03 ± 0.0090	197 ± 58.0	360 ± 106	0.941
			10.1 ± 0.78	-0.62 ±0.46	0.04 ± 0.0107	265 ± 77.5	486 ± 142	0.945
			7.86 ± 0.40	-0.32 ±0.22	0.02 ± 0.0036	365 ± 65.9	669 ± 121	0.977
		x	**10.4**	**-0.36**	**0.04**	**281**	**514**	**0.963**
			10.8 ± 1.49	-0.81 ±0.74	0.04 ± 0.0140	307 ±139	562 ± 255	0.776
			11.8 ± 1.22	-3.17 ±0.44	0.02 ± 0.0042	510 ±123	933 ± 224	0.915
N. fosliei	0	4	8.55 ± 0.68	-0.59 ±0.31	0.02 ± 0.0042	373 ± 78.6	683 ± 144	0.924
			8.15 ± 5.38	2.09 ±0.31	0.01 ± 0.0027	790 ±694	1448 ± 1272	0.735
		x	**9.8**	**-0.62**	**0.02**	**495**	**907**	**0.838**
			6.85 ± 0.52	-0.39 ±0.29	0.03 ± 0.0082	221 ± 62.8	404 ± 115	0.920
			4.35 ± 0.37	1.52 ±0.17	0.02 ± 0.0046	176 ± 38.5	323 ± 71	0.919
P. conicum	0	4	4.00 ± 0.31	-0.23 ±0.14	0.01 ± 0.0021	370 ± 83.4	677 ± 153	0.935
			3.32 ± 0.33	0.59 ±0.21	0.03 ± 0.0149	103 ± 48.1	188 ± 88	0.843
		x	**4.6**	**0.37**	**0.02**	**217**	**398**	**0.904**
			4.06 ± 1.01	4.16 ±0.26	0.01 ± 0.0024	637 ± 352	1167 ± 645	0.779
			7.02 ± 0.38	2.71 ±0.16	0.02 ± 0.0022	402 ± 60.6	736 ± 111	0.971
N. fosliei	3	4	7.34 ± 0.82	0.30 ±0.28	0.03 ± 0.0052	292 ± 79.0	535 ± 145	0.897
			(6.08 ± 0.84)	(-0.44 ±0.44)	0.01 ± 0.0016	n/c	n/c	0.907
		x	**6.1**	**2.39***	**0.02**	**444**	**636**	**0.882**
			6.83 ± 0.47	-0.22 ±0.20	0.03 ± 0.0043	250 ± 46.9	458 ± 86	0.949
			7.51 ± 0.36	-0.54 ±0.15	0.02 ± 0.0028	318 ± 43.2	582 ± 79	0.974
H. reinboldii	3	4	7.92 ± 0.37	-2.75 ±0.20	0.04 ± 0.0061	183 ± 27.3	335 ± 50	0.968
			8.77 ± 0.68	-4.61 ±0.30	0.03 ± 0.0057	297 ± 66.5	544 ± 122	0.933
		x	**7.8**	**-2.03**	**0.03**	**262**	**480**	**0.956**
			(7.35 ± 19.4)	0.77 ±0.22	0.04 ± 0.0136	(182 ± 552)	(333 ± 1061)	0.596
			4.56 ± 1.99	0.05 ±0.09	0.08 ± 0.0070	59 ± 35.2	107 ± 64	0.812
P. onkodes	'6'	4	(3.96 ± 4.85)	-0.09 ±0.16	0.05 ± 0.0141	(84 ± 123)	(153 ± 226)	0.654
			(2.16 ± 0.68)	-0.95 ±0.44	0.08 ± 0.0220	n/c	n/c	0.752
		x		**-0.06**	**0.06**			**0.687**
			2.56 ± 0.43	-0.18 ±0.25	0.07 ± 0.0357	37 ± 20.0	68 ± 37	0.813
			(4.68 ± 0.72)	(-0.21 ±0.32)	0.09 ± 0.0160	n/c	n/c	0.882
N. fosliei	6	4	3.72 ± 1.34	0.38 ±0.23	0.05 ± 0.0194	72 ± 49.3	132 ± 90	0.676
			(9.27 ± 9.58)	2.68 ±0.18	0.07 ± 0.0142	(136 ± 167)	(249 ± 306)	0.921
		x	**3.1***	**0.96**	**0.06**	**55***	**100***	**0.803**
			6.94 ± 0.70	-1.10 ±0.27	0.05 ± 0.0109	140 ± 38.1	257 ± 70	0.958
			13.0 ± 1.09	-1.80 ±0.26	0.06 ± 0.0065	217 ± 37.2	398 ± 68	0.984
H. reinboldii	6	4	5.24 ± 0.99	-1.62 ±0.22	0.07 ± 0.0182	73 ± 29.5	133 ± 54	0.915
			5.75 ± 0.52	0.21 ±0.18	0.05 ± 0.0086	125 ± 29.1	229 ± 53	0.951
		x	**7.7**	**-1.08**	**0.06**	**139**	**254**	**0.952**
			2.85 ± 0.20	-0.77 ±0.12	0.05 ± 0.0137	57 ± 16.5	105 ± 30	0.971
			3.04 ± 0.26	0.00 ±0.12	0.03 ± 0.0069	89 ± 20.3	163 ± 37	0.966
P. conicum	6	4	(8.65 ± 29.4)	1.56 ±0.15	0.07 ± 0.0171	(127 ± 460)	(232 ± 842)	0.828
			1.62 ± 0.25	0.61 ±0.11	0.05 ± 0.0209	30 ± 14.3	55 ± 26	0.805
		x	**2.5***	**0.35**	**0.05**	**59***	**108***	**0.892**
			1.46 ± 0.30	0.16 ±0.14	0.08 ± 0.0397	19 ± 12.0	35 ± 22	0.622
			(2.66 ± 2.62)	-0.77 ±0.23	0.10 ± 0.0534	(28 ± 40.9)	51 ± 75	0.314
P. conicum	18	4	(4.25 ± 13.10)	-0.21 ±0.28	0.05 ± 0.0325	(87 ± 322)	159 ± 589	0.059
			(3.71 ± 3.19)	-0.64 ±0.08	0.04 ± 0.0082	(95 ± 99.7)	174 ± 183	0.903
		x		**-0.20**	**0.06**		**105**	**0.474**

Fig. 32. Double logarithmic plots of alpha (α) (for calcification) against %SI (at the site of measurement) for *in situ* specimens of the different species. r^2 values and significance levels (P) are shown in parentheses for each regression.

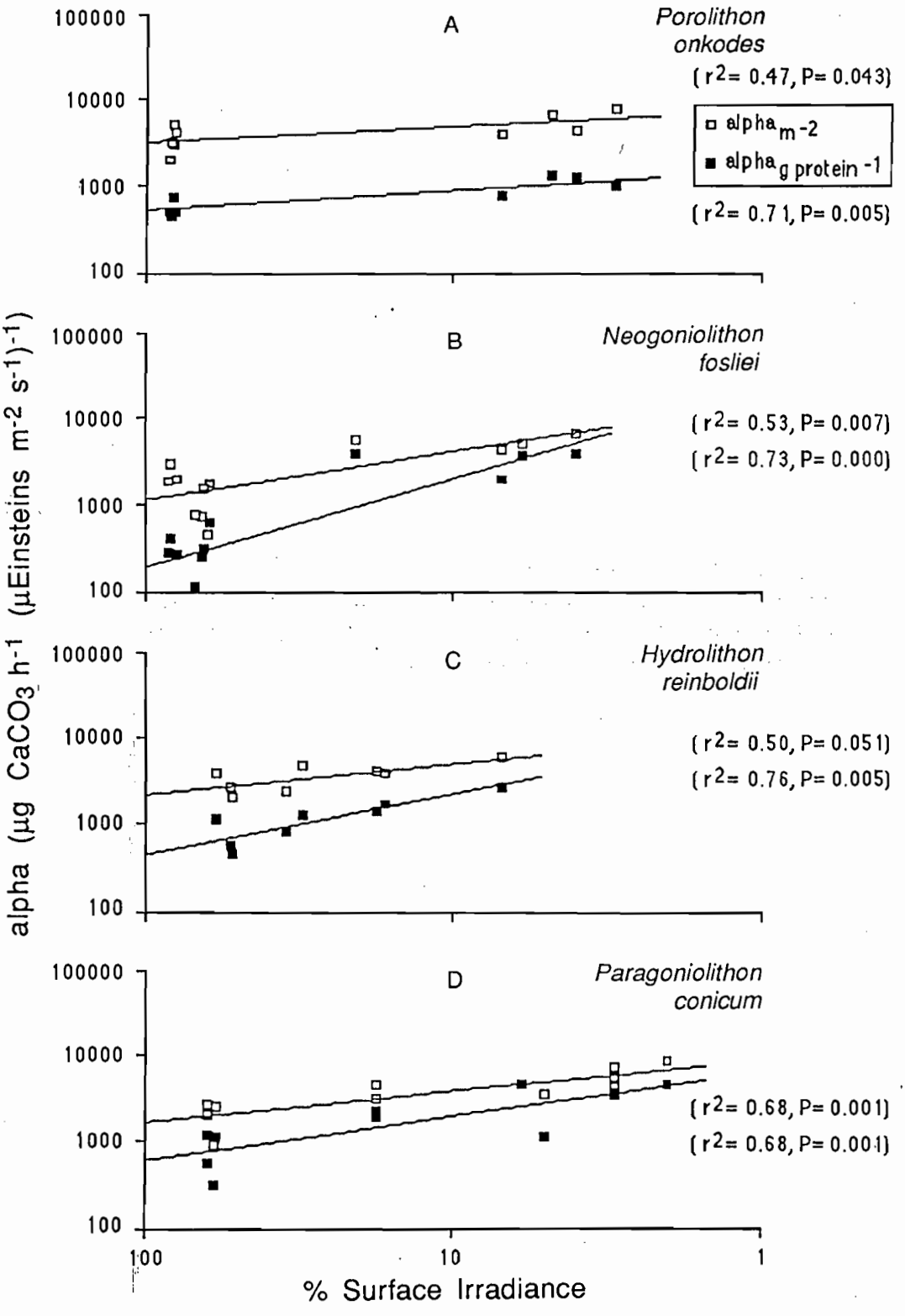
A
Porolithon onkodes
(r2= 0.47, P= 0.043)
alpha m-2
alpha g protein -1
(r2= 0.71, P= 0.005)
B
Neogoniolithon fosliei
(r2= 0.53, P= 0.007)
(r2= 0.73, P= 0.000)
C
Hydrolithon reinboldii
(r2= 0.50, P= 0.051)
(r2= 0.76, P= 0.005)
D
Paragoniolithon conicum
(r2= 0.68, P= 0.001)
(r2= 0.68, P= 0.001)
100000
10000
1000
100
100
10
1
% Surface Irradiance
alpha (µg CaCO3 h-1 (µEinsteins m-2 s-1)-1)

Fig. 33. Double logarithmic plots of I_k (for calcification) against %SI (at the site of measurement) for *in situ* specimens of the different species. r^2 values and significance levels (P) are shown in parentheses for each regression.

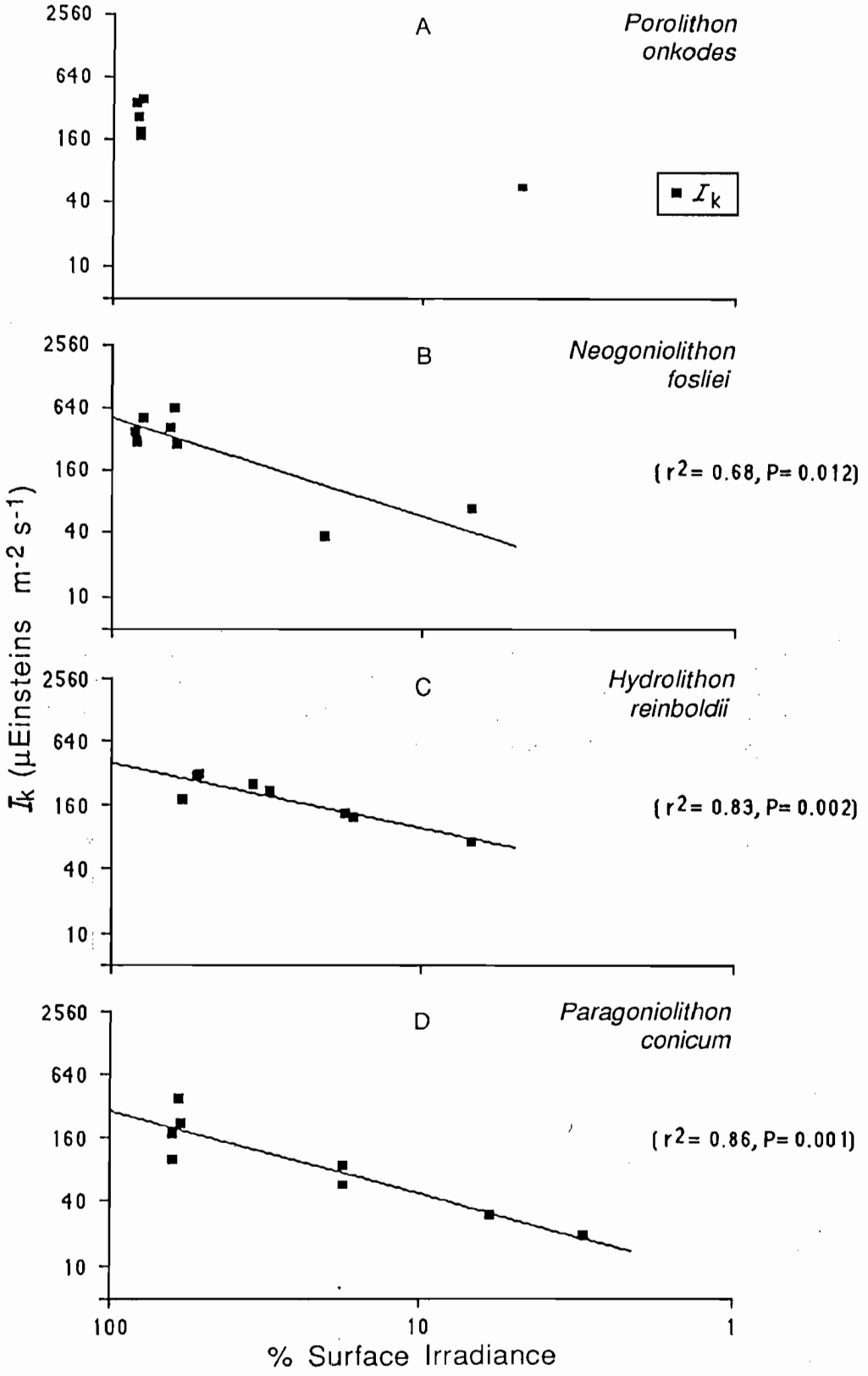
A
Porolithon onkodes
I_k
B
Neogoniolithon fosliei
(r^2= 0.68, P= 0.012)
C
Hydrolithon reinboldii
(r^2= 0.83, P= 0.002)
D
Paragoniolithon conicum
(r^2= 0.86, P= 0.001)
2560
640
160
40
10
I_k (µEinsteins m^{-2} s^{-1})
100
10
1
% Surface Irradiance

level. Regressions were always more highly significant when α was normalised on the basis of protein content rather than real surface area. The photoadaptive trends observed in α and I_k for *C-I* data were the same as those observed in α and I_k for *P-I* data (Section 2. 4. 4).

When data were normalised by surface area the rate of light-enhanced calcification (C_{light}) generally decreased with increasing depth (see Table 17 - based on projected surface areas) and decreasing irradiance (Fig. 34 - based on real surface areas). However, *P. conicum* was the only species to show a significant regression between *ln* C_{light} and *ln* %SI at the 95% probability level (Fig. 34D). *N. fosliei* and *H. reinboldii* both showed significant regressions at the 90% confidence level (Fig. 34B,C). Trends observed in *P-I* data for P^g_m were similar in so far as P^g_m generally decreased with decreasing irradiance but only one double logarithmic plot (Fig. 18B) of P^g_m versus %SI was significant at the 95% probability level. When C_{light} was normalised on the basis of protein content no significant regressions were obtained for *ln* C_{light} vs *ln* %SI (Fig. 35).

The rate of dark calcification (C_{dark}) was highly variable irrespective of the basis chosen for data normalisation (Table 17 - based on projected area; Fig. 34 - based on real surface area; Fig. 35 - based on protein content). No significant correlations were found between the logarithms of the dark calcification (including solution) rates and the percentages of surface irradiance transmitted to the sites at which the algae were growing (Figs 34 & 35).

3. 4. 5. SOURCES OF VARIATION AMONG PHOTOADAPTIVE PARAMETERS

Two-way ANOVAs were performed on the variables I_k and α to determine the major sources of variation. The factors examined were species and depth. ANOVA was performed on estimates of I_k for the species *Neogoniolithon fosliei* and *Paragoniolithon conicum*. Estimates of I_k for *P. onkodes* were omitted from the test because the *C-I* curves yielded only one statistically reliable estimate of I_k at low irradiance (i.e., at '6' m, see Table 17). ANOVAs performed on variable α based on real surface area and protein content included estimates for *Porolithon onkodes*. Parameter estimates for *Hydrolithon reinboldii* were not subjected to ANOVA because

Fig. 34. Double logarithmic plots of maximal light-dependent calcification (C_{light}) and dark calcification or solution (C_{dark}) against %SI (at the site of measurement) for *in situ* specimens of the different species. Calcification is expressed per unit real surface area. Datapoints are offset by 1000 to render all dark values positive. r^2 values and significance levels (P) are shown in parentheses for each regression.

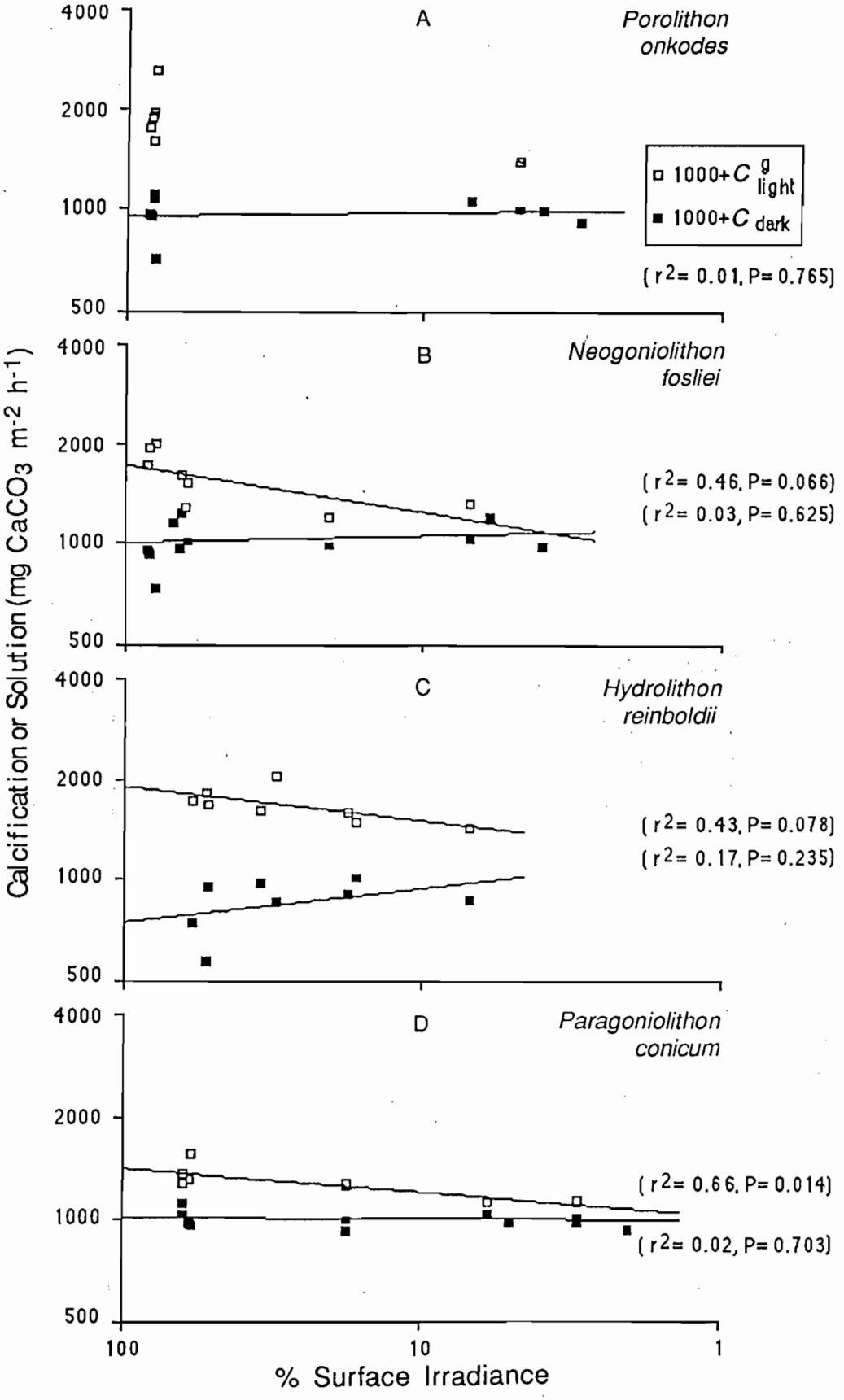
A
Porolithon onkodes
B
Neogoniolithon fosliei
C
Hydrolithon reinboldii
D
Paragoniolithon conicum
4000
2000
1000
500
□ 1000+C g light
■ 1000+C dark
(r2= 0.01, P= 0.765)
(r2= 0.46, P= 0.066)
(r2= 0.03, P= 0.625)
(r2= 0.43, P= 0.078)
(r2= 0.17, P= 0.235)
(r2= 0.66, P= 0.014)
(r2= 0.02, P= 0.703)
Calcification or Solution (mg CaCO3 m-2 h-1)
100
10
1
% Surface Irradiance

Fig. 35. Double logarithmic plots of maximal light-dependent calcification (C_{light}) and dark calcification or solution (C_{dark}) against %SI (at the site of measurement) for *in situ* specimens of the different species. Calcification is expressed per gram of protein. Datapoints are offset by 100 to render all dark values positive. r^2 values and significance levels (P) are shown in parentheses for each regression.

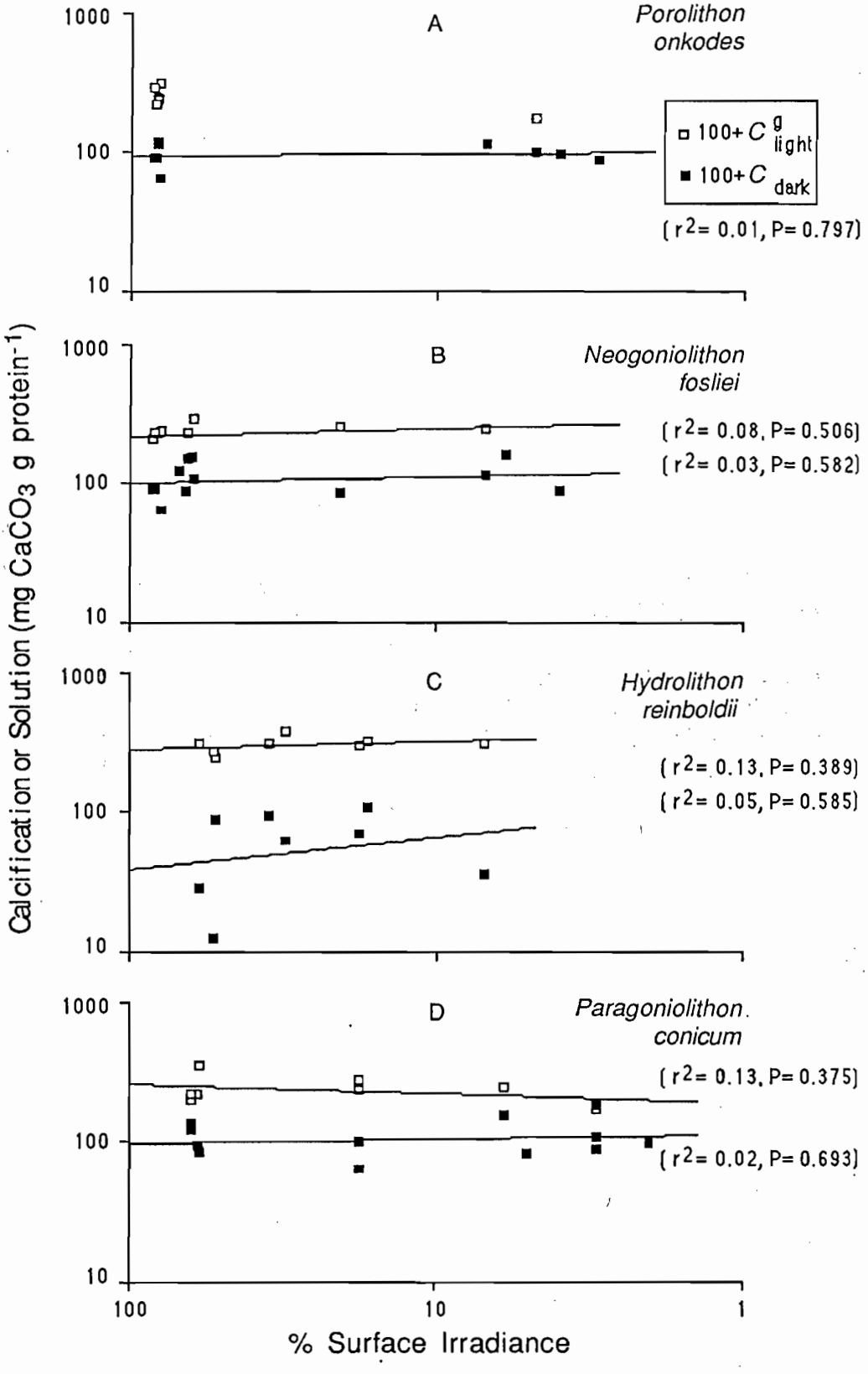
A
Porolithon onkodes
B
Neogoniolithon fosliei
C
Hydrolithon reinboldii
D
Paragoniolithon conicum
1000
100
10
□ 100+C g light
■ 100+C dark
(r2= 0.01, P= 0.797)
(r2= 0.08, P= 0.506)
(r2= 0.03, P= 0.582)
(r2= 0.13, P= 0.389)
(r2= 0.05, P= 0.585)
(r2= 0.13, P= 0.375)
(r2= 0.02, P= 0.693)
Calcification or Solution (mg CaCO3 g protein-1)
100
10
1
% Surface Irradiance

their inclusion would have created an unbalanced design. The depths examined in all cases were 0 and 6 m.

The values of I_k and α (based on protein content) both varied significantly with depth (i.e., irradiance) but not species (Table 18A,C). The value of α (based on real surface area) did not vary significantly with depth or species (Table 18B).

ANOVAs performed on *in situ P-I* data for the same variables (including I_k values for *P. onkodes*) revealed that significant differences in the value of I_k could be attributable to both depth and species effects, and that the value of α (m^{-2} real surface area) varied significantly with depth. Estimates of I_k were highly variable among the data for calcification (Table 17). Either the value of I_k is independent of species, or the wide variation in the estimates of I_k obscured subtle differences which may exist between the species, or species differences are significant at some but not all depths. The latter seems likely since the mean values of I_k for *N. fosliei* and *P. conicum* were very different at 0 but not 6 m (Table 17). It is interesting to note in this context that the mean I_k value for *N. fosliei* was over twice as large as the value for *Paragoniolithon conicum* at 0 m and so was its protein content (Table 6), whereas at 6 m both had similar I_k values and protein contents.

If biomass is a measure of the "thickness" of the living surface then the amount of irradiance required for the onset of saturation (I_k) should be directly related to the biomass (see Section 2. 4. 3). Since I_k is largely inversely related to α, it is not altogether surprising that ANOVAs revealed more significant differences with respect to depth when α was normalised by biomass (Table 18C, $P<0.05$) than when α was normalised by real surface area (Table 18B, $0.05<P<0.1$).

There seems to be growing evidence of a link between the biomass of crustose coralline specimens and aspects of their calcification. The present study demonstrates that the rate of calcification in crustose corallines is greatly enhanced by irradiance (Figs 28, 29, 30, 31) and that the relationship between calcification and irradiance is similar but not identical to the relationship which exists between photosynthesis and irradiance (compare values for I_k in Table 5 with equivalent values in Table 17). Since it is now almost universally accepted that calcification is closely linked to photosynthesis this is an appropriate juncture at which to consider more closely the mechanism of calcification.

Table 18. Results of two-way ANOVAs performed on the parameter estimates of I_k (A), alpha per unit real surface area (α m^{-2})(B), alpha per unit protein content (α g $protein^{-1}$)(C), describing features of the light-saturation curves for calcification in different species from different depths. The factors tested were species and depth. Values show the significance of each factor and of the interaction between the factors in explaining the observed variation.

A

I_k	Species	Depth	Species * Depth
In situ	0.127	**0.005**	0.117

B

α m^{-2}	Species	Depth	Species * Depth
In situ	0.219	0.068	0.418

C

α g prot.$^{-1}$	Species	Depth	Species * Depth
In situ	0.058	**0.000**	**0.001**

3. 4. 6. LIGHT-ENHANCED CALCIFICATION

Light enhances algal and coral calcification (e.g., Goreau 1959, 1963; Goreau & Goreau 1959, 1960a,b; Okazaki *et al.* 1970; Chalker & Taylor 1978; Pentecost 1978; Borowitzka 1979; Chalker 1981; Barnes 1982) in some way which is intimately associated with the photosynthetic process (e.g., Kawaguti & Sakamuto 1948; Goreau 1963; Vandermuelen *et al.* 1972; Bohm & Goreau 1973; Digby 1977a,b; Pearse 1972). However, the precise biochemical mechanism of light-enhanced calcification is still unknown (Chalker 1983), although several theories have been proposed. In principal these theories fall into two categories. Photosynthesis may provide energy for the calcification process or organic materials for the development of an organic matrix, which in some way controls the nucleation and growth of $CaCO_3$ crystals. Alternatively, photosynthesis may remove inorganic substances which inhibit crystal formation from the sites of calcification. These theories are not mutually exclusive and the mechanism of calcification may involve elements of both. Reviews of algal calcification have been provided by Lewin (1962), Darley (1974), Littler (1976), Borowitzka (1977, 1982a,b, 1983), Pentecost (1980), and Barnes & Chalker (in press).

It seems likely that calcification is enhanced by the metabolic removal of CO_2 or HCO_3^- from the sites of calcification during photosynthesis (Goreau 1959; see reviews by Borowitzka 1982a and Barnes & Chalker in press) This would increase the concentration of CO_3^{2-} ions in solution, thus shifting the carbonate equilibrium towards the precipitation of $CaCO_3$. Precipitation will occur when the solubility product of $CaCO_3$ is exceeded. With all such proposed mechanisms the precipitation environment must be effectively isolated from the external medium so that the ionic concentrations necessary for the precipitation of $CaCO_3$ can be maintained against opposing diffusive gradients. This may occur extracellularly, in semi-isolated compartments created by morphological convolutions of the thallus (e.g., *Padina*), or in discrete compartments formed between organic layers and skeletal components (e.g., hermatypic corals), or between appressed filaments (e.g., *Halimeda*). In the most specialised cases, calcification occurs within pre-existing organic structures (e.g., crustose coralline algae, coccolithophorids, and crustacea).

Regardless of the mode of compartmentation, a fundamental consequence of shifting the carbonate equilibrium in favour of the precipitation of $CaCO_3$:

$$H_2O + CO_2 \Leftrightarrow H_2CO_3 \Leftrightarrow HCO_3^- + H^+ \Leftrightarrow \begin{matrix} Ca^{2+} \\ + \\ CO_3^{2-} \\ \Leftrightarrow CaCO_3 \end{matrix} + 2H^+ \qquad (41)$$

is that hydrogen ions (H^+) are generated in the process. In consequence, precipitation could only continue if H^+ ions are simultaneously neutralised or removed from the sites of calcification. For this to occur there would either have to be considerable concentration gradients favouring the outward diffusion of H^+ from the sites of calcification, considerable concentration gradients favouring the inward diffusion of OH^- (or other anions) to the sites of calcification, or active transport mechanisms favouring the movement of H^+ or OH^-, or both. Alternatively Ca^{2+} and CO_3^{2-} may be selectively transported to the sites of calcification without the associated H^+. However, this process would still require that H^+ be in some way neutralised at, or removed from, sites distant to those of calcification.

In *Halimeda*, isolated compartments are created behind the appressed tips (utricles) of the branches which terminate the individual siphons of the algal thallus. Borowitzka & Larkum (1976b,c) propose that CO_2, HCO_3^-, CO_3^{2-}, and Ca^{2+} diffuse into these compartments through the internal or external cell walls. CO_2 is removed from the intercellular compartments during photosynthesis, which raises the pH and concentration of CO_3^{2-} leading to the precipitation of $CaCO_3$ (i.e., Eq. 41) as aragonite. Hydrogen ions are simultaneously exported from the intercellular compartments through the cells to the external environment. It is likely that both the inward movement of HCO_3^- from the seawater and the outward movement of H^+ are both energy requiring processes (Borowitzka 1983).

Borowitzka (1983) pointed out that this model could explain calcification in most other aragonite-depositing algae, with the exception of *Padina*. In fact recent evidence suggests that *Padina* may also calcify by a similar mechanism (Okazaki *et al.* 1986). Nevertheless, the model is problematic in that it does not explain why other algae with similar anatomy do not calcify. An analogous problem exists with models which propose that precipitation can result from the photosynthetic uptake of CO_2 from the surrounding seawater (e.g., Blinks 1951; Smith 1951; Miller 1952; Revelle & Fairbridge 1957). It has been suggested that this may create a sufficiently alkaline environment for the precipitation of $CaCO_3$. However, this does not explain why

fleshy algae which live alongside calcareous algae do not become calcified, nor why calcareous algae only become calcified in certain parts of the thallus (e.g., Stark *et al.* 1969). All of these problems can be overcome if it is found that non-calcifying species (and also articulate calcareous algal species with both non-calcified and calcified regions) secrete, excrete, or concentrate compounds which inhibit the formation of $CaCO_3$ crystals. Such inhibitory substances, or 'crystal poisons', are known to occur (Simkiss 1964a, b; Degens 1976), but it is not known if, or to what extent, these function in the inhibition of biological calcification.

In the freshwater alga *Chara*, calcification results from the localised excretion of OH^- producing a pH shift in certain regions of the thallus leading to the precipitation of $CaCO_3$ (Lucas 1979). In so far as OH^- is strongly implicated in the control of calcification in this alga, there are similarities with the model proposed by Digby (1977a,b, 1979) to explain calcification in coralline algae.

Calcification in coralline algae differs from calcification in aragonite-depositing algae and hermatypic corals in that the $CaCO_3$ crystals are deposited in a pre-existing organic structure (Borowitzka & Vesk 1978, 1979). Crystal growth occurs within both the amorphous and fibrillar regions of the cell wall (Baas-Becking & Galliher 1931; Bailey & Bisalputra 1970; Arnott & Pautard 1971; Flajs 1977; Futterer 1977; Borowitzka & Vesk 1978, 1979). The crystals which form either immediately adjacent to the the outer side of the plasmalemma (e.g., *Corallina officinalis* and *C. cuvierii* - Borowitzka & Vesk 1978) or close to it (e.g., *Lithothrix aspergillum* - Borowitzka & Vesk 1979) are relatively small in size and precisely arranged at right angles to the protoplast surface. The crystals which form in the amorphous region are larger in size and less ordered in arrangement (Borowitzka & Vesk 1978). In some species (e.g., *Lithothrix aspergillum* - Borowitzka & Vesk 1978) the crystals which form at the amorphous junction (sometimes known as the middle lamella) between the cells of neighbouring filaments are arranged parallel to the long axis of the filament.

Both Digby (1977b) and Borowitzka (1983) suggest that calcification in coralline algae involves a higher level of metabolic control than is probably the case for aragonite-depositing algae. Digby emphasises the importance of chemical events controlled by photosynthesis and pH, while Borowitzka attaches greater significance to the organic layers within which the process of calcification occurs.

Borowitzka (1977) proposes that the organic cell wall material either acts to concentrate HCO_3^- and Ca^{2+} at the sites of calcification, or forms a template which controls the nucleation and growth of $CaCO_3$ crystals. Irrespective of the exact mechanism, Borowitzka (1983) maintains that the organic wall material must be responsible for the deposition of calcite and not aragonite. He also suggests that there may be different anion exchange sites on the cellulose and non-cellulose cell wall components since radiotracer studies revealed there to be at least two kinetically distinguishable organic Ca^{2+}-exchanging compartments in coralline algae (Bohm 1978; Borowitzka 1979). Borowitzka drew further conclusions from studies (Smith & Roth 1979; Borowitzka 1981) of the effects of seawater pH and inorganic carbon concentration on coralline calcification. He suggested that precipitation results both from the simple uptake of CO_2 during photosynthesis and from "an active, metabolically controlled carbonate deposition mechanism" (1983, p. 21). The active deposition mechanism may involve Ca^{2+}-dependent ATPase localised on the plasmalemma (Okazaki 1977), and may (Paasche 1964; Ikemori 1970; Borowitzka & Larkum 1976c; Digby 1979) or may not (Ikemori & Nishida 1966, 1968; Bowes 1969; Okazaki 1972; Graham & Smillie 1976) involve carbonic anhydrase.

The extent to which an organic matrix controls calcification in algae and corals is unclear. In coralline algae the organic wall layers may purely influence the structure and organisation of the crystals, or they may be active in the transport and concentration of ions, or in the nucleation and growth of crystals. Lind (1970) concluded from ultrastructural work that the organic matrix at least partially controls the nucleation and orientation of the $CaCO_3$ crystals. She further reported that an organic fraction remained after the skeletal $CaCO_3$ of certain crustose coralline algae (particularly species of the genus *Porolithon*) was dissolved, which possessed the capacity to bind Ca^{2+}, but lost this ability after autoclaving. The extent to which calcium-binding substances are involved in algal calcification is difficult to determine because such substances have been found in some calcareous algae but not in others (see Misonou *et al.* 1980). If there are close parallels with mammalian calcification their existence seems likely. In mammals it is well known that calcium transport and localisation is strongly associated with protein fractions, both in the nervous system and in the bloodstream. Moreover, the calcium pools in the human body exist in a highly dynamic state of equilibrium and calcium may even be removed from precipitated structures, such as bone, if it is required for other physiological processes. When the balance is restored, calcium is rapidly replenished in the depleted areas. A

similar mechanism may also operate in day-night calcification in crustose coralline algae. This point will be raised again at the end of this section.

In *Halimeda opuntia* and *H. discoidea*, Stark *et al.* (1969) postulated that calcification occurs in two stages. They suggested that Ca^{2+} is first absorbed and possibly bound by a mucoprotein and then secondarily precipitated under the action of light. Pearse (1972) accepted that a such a model could explain calcification in the coralline alga *Bossiella orbigniana*, but pointed out that other models could equally apply. She suggested, for example, that Ca^{2+} may be continually exchanged between the organic and mineral phases, but that precipitation only occurs when specific organic substances are produced during photosynthesis which inhibit further exchange and/or bind additional Ca^{2+}. She concluded that much more work was needed before distinctions could be made between these and other models.

However, if as Pearse suggests, Ca^{2+} is rate-limiting then it should have been possible to distinguish at least between the two mechanisms suggested above. Under the same conditions of irradiance, the rates of calcification immediately following periods of dark incubation could have been compared with the rates following periods of light-saturated photosynthesis. If Ca^{2+} is bound or absorbed during darkness, but does not become precipitated until light becomes available, the binding substance should become saturated with Ca^{2+}. When light is first supplied there should be a rapid burst of calcification. On the other hand, if precipitation results from the production of organic substances which inhibit Ca^{2+} exchange then, under the same conditions of irradiance, the precipitation rate should be independent of the time of day or length of interval since darkness. However, if HCO_3^- or CO_3^{2-} and not Ca^{2+} is rate-limiting then it would not be possible by this method to distinguish between the two models.

Pearse (1972) noted great similarities in the patterns of calcification in *Bossiella orbigiana* and the branching reef-coral *Acropora cervicornis* (Goreau & Goreau 1959; Pearse & Muscatine 1971). Both showed decreasing rates of calcification from tip to base and she proposed that similar translocatory mechanisms to those facilitating calcification in *Acropora cervicornis* (Pearse & Muscatine 1971) were probably also operating in *B. orbigiana*. She interpreted the similarity as support for the theory that photosynthesis either increases the supply of free energy for the calcification process (Goreau 1959), or contributes materials for the development of an organic matrix (Wainwright 1963). Pearse concluded that algal calcification rates are

probably not controlled simply by the ionic changes accompanying photosynthesis, but are controlled by the supply of high-energy organic materials which are produced in the process. She further suggested that reserves of these high energy organic materials, possibly phosphates (Paasche 1968), may control calcification in the dark.

The conclusion that high energy organic compounds are involved in the control of calcification in coralline algae is in agreement with the model proposed by Digby (1977b, 1979). Digby proposed that photosynthesis controls a series of chemical reactions which can produce the pH changes and ionic concentrations necessary for the precipitation of $CaCO_3$. His model neither relies upon nor excludes the possibility that an organic matrix is involved in the deposition process. However, it does take account of the fact that coralline algae generally show low rates of organic growth (1977a), which suggests that abundant energy reserves may be available for carbonate deposition (1977b).

In brief, Digby proposed that partial oxidation of the reduced organic products of photosynthesis (e.g., carbohydrate) during respiration results in the production of acid (H^+):

$$CH_2O + O_2 \rightarrow CO_2 + 2H^+ + 2e^-. \quad (42)$$

H^+ ions are then removed from the apices of the terminal cells of the filaments probably by reaction with HCO_3^- in the seawater. Some of the residual electrons ($2e^-$) reduce H^+ formed from the photosynthetic cleavage of water, leaving hydrogen atoms ($H\cdot$) and hydroxyl ions (OH^-):

$$H_2O \Leftrightarrow H^+ + OH^- \quad (43)$$

$$H^+ + e^- \Leftrightarrow H\cdot. \quad (44)$$

Other e^- react with HCO_3^- to form CO_3^{2-}:

$$2HCO_3^- + 2e^- \rightarrow 2H\cdot + 2CO_3^{2-}. \quad (45)$$

The H from Eq. 44 combines with O_2 to produce H_2O:

$$2H + O_2 \rightarrow H_2O \quad (46)$$

while OH^- combines with HCO_3^- in a reaction possibly catalysed by carbonic anhydrase to form CO_3^{2-}:

$$OH^- + HCO_3^- \rightarrow H_2O + CO_3^{2-}. \quad (47)$$

CO_3^{2-} then diffuses out of the cell and into the wall and becomes replaced by inwardly diffusing HCO_3^- from the seawater. Ca^{2+} is simultaneously taken into the cell wall from the surrounding seawater. Some of the CO_3^{2-} in the cell wall reacts with H_2O to form OH^-:

$$2CO_3^{2-} + H_2O \rightarrow 2HCO_3^- + 2OH^- \quad (48)$$

which raises the pH and favours the precipitation of $CaCO_3$:

$$2Ca^{2+} + 2CO_3^{2-} \rightarrow 2CaCO_3. \quad (49)$$

The elegance of the scheme outlined above is that it does not rely upon speculative phenomena such as an "active organic matrix" to explain how CO_3^{2-}, and possibly also Ca^{2+}, may be concentrated to favour $CaCO_3$ precipitation. Most of the reactions can be demonstrated on the basis of simple electrochemical circuits (Digby 1979), assuming that photosynthesis drives the various energy requiring processes. Moreover, the apical excretion of H^+ does explain why the outer surfaces of coralline (and other) algae do not become calcified. Furthermore, the $CaCO_3$ which corallines deposit is enriched with ^{12}C and ^{16}O relative to seawater (cf Borowitzka 1977, 1983), which suggests that a portion of the carbonate is derived from respired CO_2. Since Digby's model involves the respiratory release of CO_2 it is possible that a significant proportion becomes recycled (Ryther 1956) through various pathways which ultimately may lead to the precipitation of $CaCO_3$. However, Borowitzka & Larkum (1976c) propose that respiratory CO_2 release has an inhibitory effect on calcification in *Halimeda*. This need not necessarily be the case under Digby's scheme, since he proposes that OH^- is produced in excess which would tend to counteract a fall in pH due to CO_2, at least so long as rapid photosynthesis is occurring. In fact, since this study revealed that coralline algae frequently dissolve in the dark (Table 17), the argument raised by Borowitzka & Larkum may in fact be in agreement with an expanded version of Digby's model which takes into account chemical changes occurring in the dark.

More interesting still are certain additional observations which have been made on coralline algae and other calcite-depositing aquatic plants which tend to support aspects of Digby's model.

First, various workers have found that a portion of the magnesium which is incorporated into the skeletons of coralline algae is present in the form of $Mg(OH)_2$, or brucite (Weber & Kaufman 1965; Schmalz 1965; Milliman *et al.*1971). However, no workers have so far been able to explain why $Mg(OH)_2$ should be present. If, as Digby suggests, OH^- production is a controlling factor in coralline calcification and that CO_3^{2-} partially reacts with H_2O in the cell wall to produce OH^- (Eq. 48), then his model could explain why $Mg(OH)_2$ is co-precipitated. Circumstantial evidence for this comes from the fact that $Mg(OH)_2$ has generally been found in tropical coralline genera (*Goniolithon*, *Porolithon*, *Neogoniolithon*, & *Amphiroa*), which presumably calcify more rapidly and also incorporate particularly large amounts of magnesium (e.g., Milliman 1974). The kinetics of the reaction between Mg^{2+} and $2OH^-$ presumably would be favoured by high concentrations of both ions.

Second, the models which have been proposed to explain calcification in almost all other calcite-depositing, aquatic plant groups (e.g., coccolithophorids [Paasche 1964, 1969]; charophytes [Lucas & Smith 1973; Lucas 1975a,b, 1976]; aquatic angiosperms [Gessner 1937; Steemann Nielsen 1947]) have strongly implicated OH^- production or excretion as a major controlling factor. However, as Borowitzka (1977) points out, OH^- usually results from the assimilation of HCO_3^- in photosynthesis, but there are many algae which use HCO_3^- and yet do not calcify. Perhaps, as Digby suggests, the control of OH^- production resides in the incomplete oxidation of the reduced organic products of photosynthesis. The availability of O_2 and not OH^- may therefore exert a primary control over calcification.

Third, it has been frequently reported that coralline algae tend to "soften" or show much reduced calcification in culture (Cabioch 1971; Dixon 1973; Littler 1976). Since Digby's model in part relies upon water movement to dissipate the acid excreted from the coralline surface, the small volumes of water and the reduced water movement typical of culture experiments may favour acid accumulation and hence $CaCO_3$ solution. It follows from this that boundary layer effects may also limit rates of calcification. This may help to explain why the coralline algae which calcify most rapidly (e.g., *P. onkodes*, see Table 17) are found in environments of both high irradiance and strong water movement (e.g., Lee 1967; Littler & Doty 1975; Steam *et al.* 1977; Johansen 1981). It would be interesting to determine if the calcification rates of coralline algae are measurably affected by the rate of water motion. This may be one simple way of investigating Digby's hypothesis that

respiratory OH^- production and H^+ excretion controls calcification, since Marsh (1970) and Littler & Doty (1975) found that the rate of water motion did not significantly affect the rate of photosynthesis in *P. onkodes*.

One drawback with Digby's model arises from consideration of the calcification process in the coralline genus *Choreonema*. *Choreonema* is a parasitic alga which does not contain photosynthetic pigments and yet is entirely calcified (Cabioch 1971). On the one hand Digby's model fits in so far as the parasitic alga could obtain the necessary reducing power for calcification from organic products derived from its host. However, unless the parasite has some mechanism other than photosynthesis for cleaving water molecules it is difficult to see how it might generate the required OH^-. Of course the energy for this process might also come from the organic compounds derived from the host, or alternatively, the OH^- step might be eliminated by concentrating CO_3^{2-} or other anions directly from the host.

Finally, how do the results of this study fit in with the various models which have been proposed to explain algal calcification? Borowitzka & Larkum (1976b) have proposed for *Halimeda* that a lag should exist between the onset of photosynthesis and the onset of calcification. They suggest that this threshold would represent the diffusive resistance of the system. However, all models which invoke energy requiring processes, including Digby's model, in principle would require that photosynthesis must first generate energy supplies before calcification can occur. This could also result in threshold phenomena. However, such thresholds may never be seen in experimental data if previously stored products provide the sources of energy. Similarly, animal-plant associations (e.g., reef hermatypic corals) need not show evidence of a photosynthetic threshold before calcification can occur because energy supplies can be generated in the dark by the feeding processes of the animal in addition to the reserve supplies resulting from algal photosynthesis. How then might one discern an energy requiring dependency of calcification on photosynthesis?

Unfortunately, there are only two published comparisons of the light-saturation curves for photosynthesis and calcification in reef organisms and both of these have been concerned with symbiotic hermatypic corals (Chalker & Taylor 1978; Barnes 1982). With the exception of those provided in this thesis, no comparisons have been made for calcareous algae. Nonetheless, the results of the three available comparisons are interesting. Chalker & Taylor found an I_k value of 250 μEinsteins

m^{-2} s^{-1} for photosynthesis and an I_k value of 330 μEinsteins m^{-2} s^{-1} for calcification in the branching reef coral *Acropora cervicornis*. Barnes, in contrast, found virtually no difference between the I_k value for photosynthesis (I_k = 132 μEinsteins m^{-2} s^{-1}) and the I_k value for calcification (I_k = 141 μEinsteins m^{-2} s^{-1}) in *Acropora acuminata*. However, the light intensity response curve for calcification presented by Barnes (Fig. 3, p. 43) appears to be poorly simulated by the hyperbolic tangent function which was the chosen model. Visual inspection of the response curve suggests that a model simulating slower saturation kinetics (e.g., a simple exponent or the right rectangular hyperbola) would have been more appropriate. Had such a model been used the I_k value for calcification would be significantly greater. In consequence, significant differences in the value of I_k for the two processes would have been a common feature of the data presented by Chalker & Taylor and Barnes, and of the data presented for the shallow water coralline specimens in this study (compare the I_k values presented in Tables 5 & 17). Moreover, in all cases the value of I_k would have been significantly greater for calcification than for photosynthesis. This suggests that calcification may lag behind photosynthesis, possibly because the organism satisfies its basic metabolic requirements before there is a "spill-over" of energy, or alternatively there may be a direct controlling of energy supplies for the calcification process.

The fact that the crustose coralline algae examined in this study frequently lost $CaCO_3$ in the dark (Table 17) also suggests that calcification is an energy requiring process. Energy supplies which may not be readily available in the absence of photosynthesis may be needed for the active excretion of acid produced during respiration. Moreover, it may be significant that calcification in shallow water specimens appears to lag further behind photosynthesis than it does in deeper specimens which generally receive less light (compare data presented in Tables 5 & 17). If the alga first satisfies its basic respiratory and growth requirements before releasing energy for processes such as the excretion of H^+, the transport of Ca^{2+}, HCO_3^-, or CO_3^{2-}, and possibly the excretion of OH^- into the cell wall, then the greater respiratory requirements of shallow specimens (Table 5) may result in a longer delay in the availability of free energy, or a sub-optimal rate of supply. Equally, the greater rates of respiration of shallow water specimens may result in greater night-time rates of acid production which in turn may produce larger rates of $CaCO_3$ solution. While no significant relationships were observed between $ln\ C_{dark}$ and ln %SI (Figs 34,35) there was a slight tendency for dark rates of calcification to increase (or dark rates of solution to decrease) with diminishing irradiance (Figs 34A,B,C & Fig. 35). It is

possible that the data for dark calcification, or more appropriately dark solution, are confused by other external factors. These factors will be discussed in the following section.

Finally, if calcification involves the respiratory release of reducing power and/or free energy, the amounts generated will depend upon the reduction level of the products which are consumed. The oxidation of more highly reduced compounds should result in the release of more reducing power, but possibly at the same time more acid. Potentially, this could have both a positive and negative effect on calcification. When free energy is in excess, such as during or after long periods of high irradiance, the oxidation of highly reduced compounds could accelerate calcification, by increasing the concentration of OH^- and by providing more energy for active transport processes. When free energy is limiting, as might occur at night following periods of reduced irradiance or rapid growth, there may be insufficient energy to actively export (or neutralise by the uptake of balancing anions) the acid produced during respiration resulting in $CaCO_3$ solution. In this context, it may be significant that the species which produce the most reduced organic compounds, and thus possess the highest values for *PQ* (Table 10), also show the largest and most variable night-time rates of calcification or solution (Table 17). It is not inconceivable that a link may exist between the value of *PQ* and the erratic nature of dark calcification. This theory will be discussed in more detail in Section 3. 4. 8.

When all is considered, there may be no major disadvantages in allowing a portion of the newly precipitated $CaCO_3$ to dissolve at night, since the arrival of light in the morning rapidly reverses the process (e.g., Figs 28, 29, 30, 31). On the contrary, because calcification occurs within the cell walls in coralline algae, precipitation cannot exceed organic tissue growth. Since it has been suggested that the impregnation of cellular tissues with $CaCO_3$ may restrict nutrient flow and reduce internal light levels (Borowitzka & Vesk 1978; and see Section 2. 4. 3), some level of solution, particularly near the surface of the crust, may actually be an advantage for tissue growth. Moreover, as Borowitzka & Vesk (1979) remarked during discussion of the non-calcified lower regions of the genicular cells of *Lithothrix aspergillum*, cell wall formation and extension in higher plants is often accompanied by localised acidification at the sites of new cell wall growth. The solution of $CaCO_3$ may in fact be both a simple and kinetically favourable way of controlling intracellular pH and promoting cell wall growth.

Conclusions

There are three fundamental requirements before algal and coral calcification may occur:
(i) isolation or compartmentation of the precipitation environment,
(ii) high pH within the precipitation environment, and
(iii) high concentrations of Ca^{2+} and CO_3^{2-}.

It seems likely that light-enhanced calcification is an energy-requiring process which may depend upon photosynthesis for:
(i) shifting the carbonate equilibrium to favour the precipitation of $CaCO_3$,
(ii) the production of high energy organic compounds,
(iii) the production of OH^- ions,
(iv) the supply of energy for active transport processes, and/or
(v) the supply of materials for an organic matrix.

Calcification may or may not involve the active participation of an "organic matrix". Organic materials may influence algal and coral calcification by:
(i) concentrating or binding Ca^{2+} and/or CO_3^{2-} (Bohm 1969, 1973; Lind 1970; Bohm & Goreau 1973; Misonou *et al.* 1980),
(ii) nucleating and favouring the growth of crystals (Borowitzka 1977),
(iii) organising the $CaCO_3$ crystals (Bryan & Hill 1941; Barnes 1970, 1971; Jell 1974; Gladfelter 1982, 1983),
(iv) preventing ionic exchange (Pearse 1972),
(v) controlling the polymorph of $CaCO_3$ precipitated and the form of the crystals (Kitano & Hood 1965; Chave & Suess 1970; Suess & Futterer 1972; Borowitzka & Vesk 1978; Okazaki & Furuya 1985),and
(vi) effectively isolating the precipitation environment from the external medium within pre-existing cellular structures (e.g., coralline algae [Lind 1970; Borowitzka & Vesk 1978, 1979] and coccolithophorids [Paasche 1962]), or by creating long diffusion pathways (e.g., *Halimeda* [Borowitzka & Larkum 1976a,b], and sheath calcification in the Codiaceae [Bohm *et al.* 1978]), or by compartmentation (e.g., bivalve molluscs [Bevelander & Nakahara 1969]).

Calcification appears to be a more highly ordered process in coralline algae than in aragonite-depositing algae. There is ultrastructural and physiological evidence

which suggests that coralline algae exert a considerable level of metabolic control over the precipitation of $CaCO_3$.

3. 4. 7. DARK CALCIFICATION

Attempts to resolve the issue of whether calcareous algae calcify in the dark or not have previously failed. The lack of success can be largely attributed to the continued use of radioisotopes. Isotopic exchange phenomena are known to give rise to large apparent rates of incorporation which have nothing to do with biological precipitation (Bohm & Goreau 1973; Borowitzka & Larkum 1976a; Bohm 1978; Borowitzka 1979). These, and other associated problems (see Section 3. 4. 2), give rise to highly variable estimates of both light-enhanced and dark calcification (see Borowitzka 1983, Table 3). Barnes & Crossland (1982) have demonstrated that it is only just statistically possible to distinguish between the light and dark calcification rates of corals using radioisotopic techniques. Moreover, Barnes & Chalker (in press) consider that the errors associated with the radioisotopic measurement of algal calcification are likely to be even greater as a result of the larger "internal pools of exchangeable calcium" (p. 25) and the less effective isolation of the precipitation environment. It is therefore highly questionable if any significance can be attached to radioisotopic estimates of dark calcification or of light:dark calcification ratios.

Since most of the radioisotopic estimates of coralline algal calcification have been presented on a dry weight basis it is not possible to compare absolute rates with the results of this study. Also, because both positive and negative rates of dark calcification were encountered in this study it is not appropriate to state absolute light:dark ratios. It is only possible to say that a specific dark calcification mechanism seems unlikely. Borowitzka (1981) found that dark calcification in the coralline alga *Amphiroa* was not affected by pH, only by CO_3^{2-} concentration, which suggests that metabolic processes are not involved. He concluded from this and earlier work (Borowitzka 1979) that there may be no dark calcification in coralline algae. The data presented here go one step further and demonstrate that the skeletons of certain coralline algae often actively dissolve at night, thus confirming earlier radiotracer studies on *Halimeda* (Borowitzka & Larkum 1976a). These data and the *C-I* curves shown in Figs. 28, 29, 30, and 31 establish that calcification in coralline algae is highly dependent on light. The reported range in light:dark ratios of 1-4 (Goreau

1963; Okazaki *et al.* 1970; Pearse 1972; Borowitzka 1979) seems, at best, a gross understatement of the importance of light in algal calcification. It may well be that the term "light-enhanced" calcification should be discarded in favour of "light-dependent" calcification.

When crusts are found to dissolve in the dark it is likely that this results from the acid produced during respiration. It is well known that the cell sap of algae is acid during respiration (Blinks 1951). Digby (1977a) has shown that the cell sap of coralline algae is acid in the dark but becomes alkaline after a short period of illumination. In the charophytes *Chara corallina* and *Nitella clavata*, which precipitate calcite, different regions of the cell surface are alternately acid and alkaline in the light (Spear *et al.* 1969; Lucas & Smith 1973; Lucas 1975a,b, 1976). Lucas (1975b) has demonstrated that there is an active, light-stimulated efflux of H^+ and OH^- in *C. corallina*. Where OH^- is extruded calcite is precipitated, and where H^+ is extruded the alga remains uncalcified. Both Bohm & Goreau (1973) and Borowitzka & Larkum (1976a) found that *Halimeda* lost calcium in the dark. Borowitzka & Larkum (1976a,c) and Borowitzka (1982a) concluded that calcification may be inhibited in the dark. Barnes & Chalker (in press) interpret this to mean that respiratory CO_2 release reduces the pH to a value which opposes the precipitation of $CaCO_3$. In short, there is sufficient data to suggest that the night-time rates of $CaCO_3$ solution encountered in this study can be largely explained on the basis of respiratory acid production, although this may not be the only possible explanation.

The surface waters of the sea, particularly in the tropics, are supersaturated with $CaCO_3$, especially with respect to calcite (Wattenberg & Timmerman 1936; Weyl 1961; Cloud 1962; Schmalz & Chave 1963; McIntyre & Platford 1964; Chave & Suess 1967; Pytkowitcz & Fowler 1967; Lyakin 1968; Schmalz & Swanson 1969; Edmond & Gieskes 1970). The activities of calcium and carbonate ions in seawater are decreased by ion-pairing (Garrels & Thompson 1962), but not to below the ionic activity product of calcite (Chave & Schmalz 1966; Chave & Suess 1967). Thus the precipitation of $CaCO_3$ from seawater appears to be dependent on kinetic, rather than thermodynamic, factors as determined by environmental conditions (Skirrow 1975). These considerations suggest that the supersaturated levels of calcium and carbonate ions in seawater are maintained by other factors which oppose the inorganic precipitation of $CaCO_3$. Such factors have been identified as dissolved magnesium or phosphorous (Garrels *et al.* 1961; Simkiss 1964a,b; Pytkowicz 1965) which slow the

rate of $CaCO_3$ crystal nucleus formation, while those nuclei which do form are immediately inactivated by adsorption of dissolved organic materials from the seawater (Chave & Suess 1967, 1970). These arguments tend to discount the possibility that the $CaCO_3$ solution rates encountered in this study could have been caused by physical-chemical factors even though a small area of calcite surrounding each specimen was exposed to the seawater as a result of the core-drilling procedures (see Section 2. 3. 1). This conclusion is supported by the following experimental evidence.

Post-incubation tests were conducted in an aquarium to determine the rate of calcite exchange beween freshly cut surfaces and seawater. A small rate of solution of 0.11 mmol $CaCO_3$ m^{-2}(exposed surface) h^{-1} was determined. Since the experimental material never had a ratio of exposed to living surface greater than 1:3 (usually much less), this rate of solution would have been quite insufficient to explain most of the solution rates reported in Table 17. Moreover, Chave & Suess (1967) observed that the surface adsorption of organics onto crystal nuclei was more rapid than the precipitation of $CaCO_3$ onto the same surfaces. The calcification rates of the coralline specimens used in this study were not determined until 7-10 days after the core-drilling operation (see Section 2. 3. 1). After this period the cut surfaces had noticeably lost their white appearance which indicated coating by organics. Thus it was highly unlikely that any of the bare calcite surfaces around the experimental subjects would have be exposed to solvent action. This is further supported by the fact that there was no correlation between the area of exposed surface around each specimen and the rate of solution. It must be concluded that passive (i.e., aqueous) solution was not responsible for the solution rates determined in this study. However, these arguments do not rule out the possibility of biochemical solution caused by burrowing organisms and perforating algae, which is a valid concern because of the *in situ* nature of the study.

At the termination of each incubation the specimens were examined for the presence of bioeroders. Very few bioeroding animals were found in or beneath the specimens, although the empty channels of previous excavations were often seen. The coralline specimens typically contained relatively small amounts of protein (Table 6), which suggested that significant amounts of animal tissue were not present. Moreover, there was no apparent correlation between the rate of $CaCO_3$ solution and the protein content of the specimens. This leaves the possibility that the $CaCO_3$ might have been dissolved by perforating algae. Bak (1976) considers that perforating algae do not

remove significant amounts of $CaCO_3$ from corals even when these algae are present in high abundance. He and others (e.g., McCloskey 1970) do, however, suggest that the channels made by perforating algae may pave the way for more significant bioerosion by burrowing sponges. Burrowing sponges were seldom seen in the specimens used in this study, and in any case theoretical calculations (Neumann 1966) suggest that even at very high densities their rates of biochemical erosion could not account for the solution rates observed in this study.

The most plausible conclusion is that dark rates of solution are associated with acid production during respiration. The fact that some specimens showed positive rates of calcification in the dark perhaps suggests that energy supplies may be limiting when solution occurs. More work is required before this can be confirmed. Confirmation would be most satisfactorily obtained by investigating the dark carbonate flux of pure coralline specimens. Ideally this would be accomplished by growing the algae in culture, but so far this has proved difficult. A reasonable alternative might be to use largely uncontaminated material grown in the field on glass slides. Glass seems to favour the rapid settlement and growth of crustose coralline algae (personal observations) and for a limited period of time the specimens remain largely free of other algae and bioeroding animals (personal observations).

3. 4. 8. RATES OF CALCIFICATION

Rates of crustose coralline calcification were calculated by subtracting the change in CO_2 resulting from photosynthesis and respiration from the change in CO_2 resulting from calcification. The change in CO_2 due to calcification was calculated from pH data using the methods described in Section 3. 2. 2. Oxygen data were converted into units of inorganic carbon (CO_2) using the metabolic quotients presented in Table 10.

Relative rates of calcification

Mean rates of light and dark calcification per hour for each species are column-graphed in Fig. 36A,B. These data are normalised on the bases of real surface area (Fig. 36A) and total protein content (Fig. 36B). The data graphed in Fig. 36 do not include estimates of C_{light} or C_{dark} when the confidence intervals surrounding the

Fig. 36. Column-graphs of the mean maximal rate of gross calcification, net calcification, and dark calcification or solution, for each species at the depth of measurement.
A. Data normalised by real surface area.
B. Data normalised by total protein content.

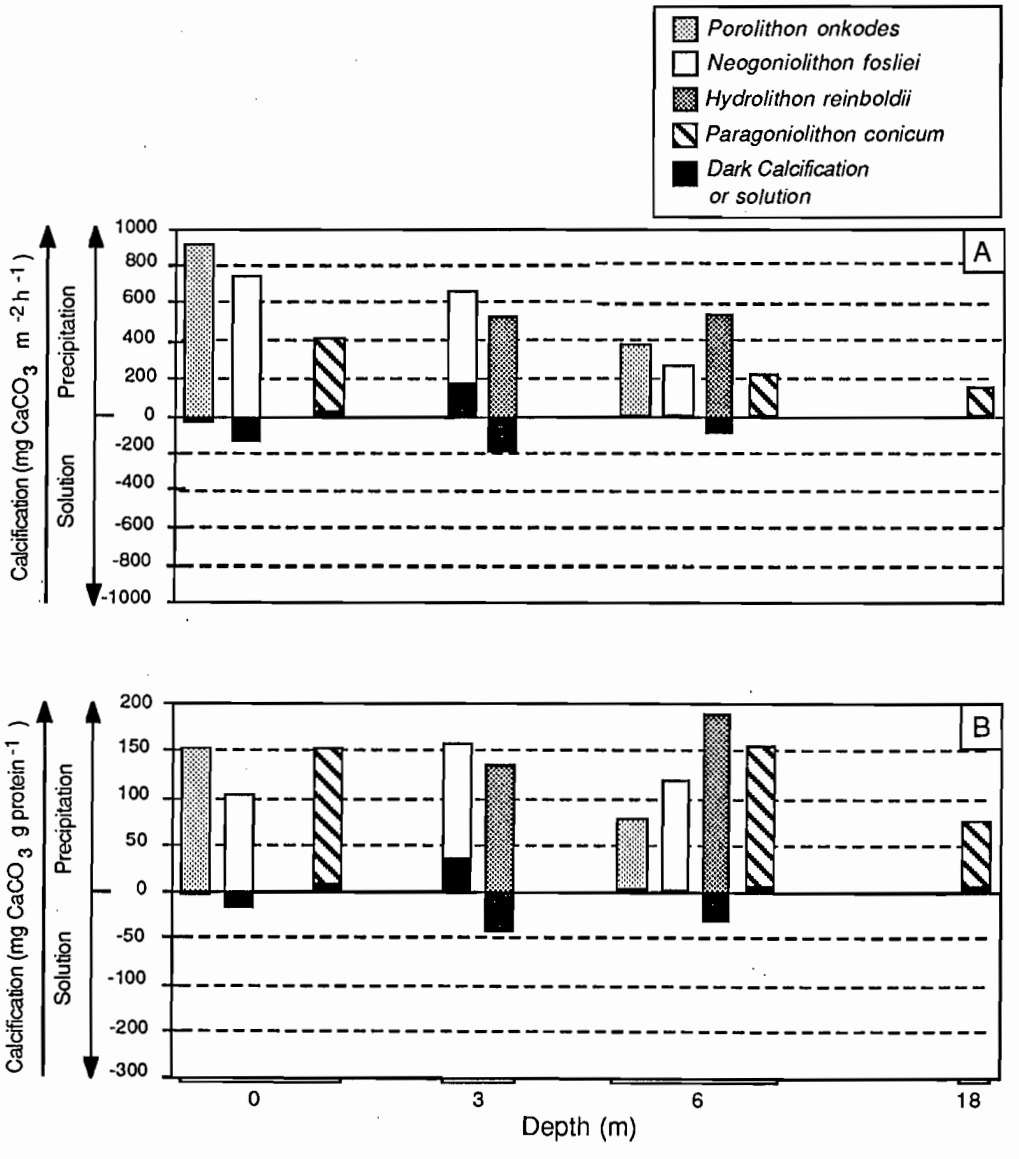
Porolithon onkodes
Neogoniolithon fosliei
Hydrolithon reinboldii
Paragoniolithon conicum
Dark Calcification or solution
A
B
Calcification (mg CaCO3 m-2 h-1)
Calcification (mg CaCO3 g protein-1)
Precipitation
Solution
1000
800
600
400
200
0
-200
-400
-600
-800
-1000
150
100
50
-50
-100
-200
-300
0
3
6
18
Depth (m)

estimates of C_{light} were greater than the estimates themselves. Data shown for *Porolithon onkodes* at 6 m and *Paragoniolithon conicum* at 18 m are therefore based on single estimates of C_{light} and C_{dark} and should not be considered equally reliable.

On a real surface area basis, the mean rate of maximal gross calcification declined with depth for all species. In terms of net deposition, *Porolithon onkodes* showed a faster rate of calcification than *Neogoniolithon fosliei* and *Paragoniolithon conicum* at 0 m, and a rate which was faster than all but *Hydrolithon reinboldii* at 6 m. *N. fosliei* calcified faster than *H. reinboldii* at 3 m, but more slowly at 6 m. *P. conicum* showed the lowest calcification rate of the four species at each depth where comparison was possible.

In the dark, *P. onkodes* showed a low rate of solution at 0 m and virtually no net deposition or solution of $CaCO_3$ at 6 m. *Neogoniolithon fosliei* showed a significant negative dark calcification rate at 0 m, a significant positive dark calcification rate at 3 m, and virtually no dark calcification at 6 m. *H. reinboldii* showed negative dark calcification rates at both 3 and 6 m, but the rate of solution was lower at 6 m. *Paragoniolithon conicum* showed a small positive dark calcification rate at 0 m and almost no dark calcification at 6 and 18 m.

On the basis of protein content, at 0 m *P. onkodes* had a very similar mean maximal rate of calcification to *P. conicum*, and a rate which was considerably higher than that shown by *N. fosliei*. *N. fosliei* calcified somewhat faster than *H. reinboldii* at 3 m, but more slowly at 6 m. At 6 m *H. reinboldii* showed the fastest rate of calcification of the four species, followed in decreasing order of rate by *P. conicum*, *N. fosliei*, and finally *P. onkodes*.

The relationships observed among the dark calcification rates of the four species were the same regardless of whether the data was normalised by surface area or protein content (compare Figs 36A & 36B). In contrast, the relative rates of light-dependent calcification by the four species differed quite significantly with the basis used for data normalisation.

Firstly, the relationships observed in the column-graphed data for calcification in Fig. 36B are rather similar to those observed in the column-graphed data for net primary production (Fig. 22B). The data in Fig. 22B were normalised by

real surface area. A major difference is that at 6 m *P. onkodes* possessed the highest mean maximal rate of net production but the lowest maximal rate of calcification. However, it should be remembered that the value for *P. onkodes* is based on only a single estimate of C_{light}. Even so, further discussion will include the estimate for *P. onkodes* for the purposes of argument.

As has been stated previously, because coralline algae calcify within a pre-existing organic structure their calcification cannot exceed and is probably limited by tissue growth (Barnes & Chalker in press). The rate at which they can produce organic material for new cell growth, especially cell wall components, should thus strongly influence their rates of calcification. The correlations observed in the data graphed in Figs 22B and 36B would suggest this to be the case. However, to a degree calcification may also limit photosynthetic rate and hence tissue growth (see Section 2. 4. 3).

To recapitulate, Borowitzka & Vesk (1978) suggest that the calcareous nature of the thallus in coralline algae probably limits the supply of light and nutrients to cells within the thallus. Since translocatory pathways are likely in coralline algae (Pearse 1972), organic production within the deeper cell layers may be significant for overall tissue growth. If this is the case then photosynthesis and calcification may both limit one another. This possibility is suggested by the data shown in Figs 22B and 36B and the mean protein contents (i.e., tissue biomasses) of the four species shown in Table 6. At 0 m, for example, *P. conicum* has a lower biomass which should result in less tissue shading and smaller barriers to diffusion. As a consequence photosynthesis should be relatively more efficient and calcification could therefore progress at a faster rate. *P. onkodes*, in contrast, has a higher rate of net photosynthesis but a greater biomass, which should be associated with greater tissue shading and increased barriers to diffusion. Because of the higher biomass (i.e., tissue volume) a greater relative amount of $CaCO_3$ should be precipitated per unit surface area of the thallus, and this would increase the attenuation of light and diffusive resistance of the crust. The combined effect would be to significantly reduce the efficiency of photosynthesis and hence reduce the calcification rate. By comparing the data for *P. onkodes* with the data for *P. conicum* in Fig. 36B it may be seen that where the former might have gained on photosynthetic rate it may also have lost on photosynthetic efficiency (a lower value for α and a higher value for I_k in Table 5) and hence calcification rate.

This may explain why *P. conicum* has a lower calcification rate than *P. onkodes* per unit area of thallus but an equivalent rate of calcification per unit of biomass.

N. fosliei has both a lower rate of photosynthesis (Fig. 22B) and a greater biomass (Table 6) than *P. conicum* at 0m. The greater biomass might account for the higher rate of deposition per unit area of thallus (Fig. 36A), while the lower photosynthetic efficiency of *N. fosliei* (compare values for I_k and α in Table 6) might account for the lower rate of deposition per unit of biomass (Fig. 36B). By comparison, the biomass of *N. fosliei* is only slightly greater than the biomass of *P. onkodes* (Table 6) at 0 m and their rates of light-dependent calcification per unit area of thallus are also very similar (compare data in Table 17, or consider gross calcification data by adding dark and light rates in Fig. 36B). However, *P. onkodes* has a higher rate of net photosynthesis (Fig. 22B) and, perhaps as a direct result, a higher rate of calcification per unit of biomass (Fig. 36B).

Ignoring at this stage the anomalous behaviour of *P. onkodes* at 6 m, a similar pattern emerges in the data for the other three species at this depth. The biomass values of the three species are all fairly low (Table 6), which means that the light attenuative properties and diffusive resistances of the thalli should be relatively less significant. However, there are obvious differences in the rates of net photosynthesis by the three species. *H. reinboldii* has the highest rate and shows the fastest rate of calcification. *N. fosliei* has the lowest rate of net photosynthesis and the lowest rate of calcification. *P. conicum* has rates of net photosynthesis and calcification which are intermediate between the two.

With regard to the data for *P. onkodes* at 6 m, this species has a high biomass relative to that of the other 3 species (compare specimen number 2 of *P. onkodes* at 6 m with the mean values for the other three species at this depth in Appendix 2). This should result in a greater rate of calcification per unit area of thallus (Fig. 36A), and in fact the rate is higher than all except *H. reinboldii*. However, its greater biomass should reduce its photosynthetic efficiency and hence its rate of calcification per unit of biomass. The rate of calcification does diminish relative to the other species (Fig. 36B) but its photosynthetic efficiency and apparent rate of net photosynthesis are clearly comparable (compare estimates of I_k, α, and P^n_m for specimen number 2 of *P. onkodes* at 6 m with the estimates for the other three species at this depth in Table 5). It must be emphasized though that the data

presented in Table 5 are maximal rates of photosynthesis assuming light saturation. Fig. 9E shows that photosynthesis in *P. onkodes* at 2.5 m (≡ '6' m in terms of PPFD) is far from saturated under peak noon irradiance. Thus if calcification depends in part upon the supply of free energy, the irradiance available to *P. onkodes* at 6 m may be insufficient for photosynthesis to support both a high biomass and a high rate of calcification. When the biomass is smaller, sub-saturating levels of photosynthesis may be relatively less significant. For example, *N. fosliei* also shows sub-saturated levels of photosynthesis at 6 m (Figs 10F, 21A) but has a biomass less than half of that of *P. onkodes* at the same depth. It is perhaps significant that *H. reinboldii* and *P. conicum*, which show higher rates of calcification per unit of biomass (Fig. 36B), also show greater saturation of photosynthesis (Figs 11E, 12D, 21B,C,D).

The last feature of Fig. 36 which merits discussion is that of the dark rates of $CaCO_3$ solution, particularly for *H. reinboldii* and *N. fosliei*. It is impossible to know without further study why these two species should show large night-time rates of solution while *P. onkodes* and *P. conicum* generally do not (Table 17). It is fairly obvious from Fig. 36 that shallower examples of *N. fosliei* and *H. reinboldii* (i.e., 0 m and 3 m respectively) show more rapid rates of solution than the deeper examples (e.g., 3 or 6 m, and 6 m respectively). If a link does exist between the reduction level of the compounds produced during photosynthesis and the amount of acid produced during respiration (see Section 3. 4. 7), then higher values for *PQ* might indicate a greater potential for night-time $CaCO_3$ solution. However, if there is an excess of stored energy for the export of H^+ or transport of Ca^{2+}, then by generating more reducing power (i.e., e^-), and thus perhaps more OH^-, the rise in pH may favour higher rates of dark calcification (e.g., *N. fosliei* at 3 m in Fig. 36). Since *N. fosliei* and *H. reinboldii* had higher values for *PQ* than *P. onkodes* and *P. conicum* (Table 10), this may provide one possible explanation for the differences in their rates of dark calcification or solution. These processes may also interact with tissue biomass. For example, three of the five *PQ* values for *P. onkodes* at 0 m were below 1.2 and two were between 1.25 and 1.35 (Table 6). Specimen no. 1 (Table 17) had a *PQ* of 1.26 and showed an appreciable rate of dark solution while specimen no. 5 had a *PQ* of 1.34 and showed only a small rate of dark solution (Table 17). However, specimen no. 1 had a biomass which was over twice that of specimen no. 5 (Appendix 2). Thus if more of the photosynthate which was respired at night by specimen no. 1 was required to support the metabolic needs of the living tissue, then conceivably there might have been less residual energy for the maintenance of processes preventing

the solution of $CaCO_3$. This might also explain why the solution rate of *H. reinboldii* was greater at 3 than at 6 m, while the rate of light-dependent calcification was greater at 6 than at 3 m. At 6 m *H. reinboldii* had a biomass which was three-quarters of its value at 3 m. *P. conicum*, which had low values for *PQ* (Table 10), and a relatively low biomass at 0 and 6 m (Table 6 or Appendix 2) showed small positive mean rates of dark calcification at these depths. However, at 18 m *P. conicum* showed sub-saturated levels of photosynthesis (Fig. 12F) and a greater mean biomass than at 6 m (Appendix 2), which might explain why this species exhibited a low mean rate of solution at 18 m but not at 0 and 6 m (Table 5).

While the processes described above may variably influence dark calcification, it is certainly possible that other processes not so far considered may be involved. It is known, for example, that coralline algae decalcify during the formation of reproductive structures (conceptacles) and genicula (Cabioch 1971). *N. fosliei* and *H. reinboldii* do form much larger conceptacles than *P. onkodes* and *P. conicum* (Adey *et al.* 1982; and personal observations). At times these are produced in large numbers over the entire surface of the crust. It is difficult to discount the possibility that solution might have resulted from conceptacle formation because presumably decalcification occurs most rapidly at initiation and not when the conceptacles are fully developed and obvious on the surface of the crust. The crusts were visually inspected after each incubation but there was no apparent correlation between the density of conceptacles and the rate of solution.

Another possibility relates to the observation that *N. fosliei* and *H. reinboldii* both show evidence of epithallial sloughing while *P. onkodes* and *P. conicum* do not. During this process, the upper layer or layers of cells are shed to the surrounding seawater. Although the outer walls of the epithallial cells are uncalcified, the lower walls are impregnated with $CaCO_3$ (Bailey & Bisalputra 1970; Garbary 1978; Borowitzka & Vesk 1978). Presumably, some $CaCO_3$ may be dissolved either passively or actively during the sloughing process. In *N. fosliei* the epithallial cells are shed in large sheets, and it is likely that these layers would have remained in the chamber rather than to have passed out through the small ball-valve controlling the outlet port of the incubation chamber (Fig. 6A) during flushing. This is supported by the fact that on one occasion when the epithallium was sloughed off during incubation by a specimen of *N. fosliei*, the discarded cell-layers were present in the chamber at the time of collection. During this incubation only a slight rate of solution was recorded

(replicate no. 4 at 3 m in Table 17). On no other occasion was it obvious that epithallial sloughing had occurred during incubation. Moreover, *P. onkodes* does not appear to exhibit epithallial sloughing, and yet one specimen still showed a significant rate of dark solution (Table 17, replicate no. 1 at 0 m). Thus it does not seem likely that the solution of $CaCO_3$ in the dark was attributable to processes associated with epithallial sloughing.

Rates of calcification per hour

Rates of light-dependent calcification and dark calcification or solution per hour are presented in Table 19. These estimates are quite variable, particularly with respect to dark calcification or solution. Previous discussion has offered reasons for this variability. It seems that calcification may be affected by several different processes, many of which are not well understood. Also, because of the apparent dependency of calcification on photosynthesis (at least in calcareous algae), some of the variation in calcification data must result from variation in photosynthesis. Moreover, the fact that many calcareous reef organisms, including coralline algae, show rhythmic variations in $CaCO_3$ accretion over the course of a day (e.g., Chalker & Taylor 1978; Agegian 1981), a lunar month (e.g., Buddemeier 1974; Agegian 1981), a year (e.g., Buddemeier 1974; Macintyre & Smith 1974; Stearn *et al.* 1977), with season (e.g., Knutson *et al.* 1972; Dodge & Thompson 1974), and in response to changes in environmental parameters (e.g., Buddemeier 1974; Weber *et al.* 1975) suggests that accretion rates differ naturally from one time to another. The high variability of calcification data may therefore reflect the complexity of controls which govern the process rather than the inadequacies of experimental technique.

The mean maximal calcification rates, per square metre of crust surface, of the coralline algae measured in this study ranged from 396 to 923 mg $CaCO_3$ h^{-1} for *P. onkodes*, from 274 to 761 mg $CaCO_3$ h^{-1} for *N. fosliei*, from 521 to 554 mg $CaCO_3$ h^{-1} for *H. reinboldii*, and from 156 to 420 mg $CaCO_3$ h^{-1} for *P. conicum* (Table 18).

The mean rates of dark calcification, per square metre of crust surface, ranged from -35.0 to -5.0 mg $CaCO_3$ h^{-1} for *P. onkodes*, from -129.7 to

Table 19. Mean rates of net calcification and dark calcification per hour by different species *in situ* at different depths. Data include 95% confidence intervals (CI) and are presented on the bases of projected surface area (PA), real surface area (RA), and total protein content (g protein) respectively. n = number of replicates contributing to each mean value.

Species	Depth m	n	Basis	Maximal Calcification Rate								Dark Calcification Rate							
				mmol Calcium Carbonate per hour				mg Calcium Carbonate per hour				mmol Calcium Carbonate per hour				mg Calcium Carbonate per hour			
				(min)	x	CI	(max)	(min)	x	CI	(max)	(min)	x	CI	(max)	(min)	x	CI	(max)
			sq. m. PA	(7.281)	9.899	±3.789	(13.821)	(728.8)	990.8	±379.3	(1383.4)	(-2.975)	-0.352	±2.226	(1.226)	(-297.7)	-35.3	±222.8	(122.7)
P. onkodes	0	5	sq. m. RA	(6.750)	9.224	±3.747	(13.398)	(675.5)	923.2	±375.0	(1341.0)	(-2.884)	-0.350	±2.126	(1.125)	(-288.6)	-35.0	±212.7	(112.6)
			g Protein	(1.109)	1.542	±0.353	(1.775)	(111.0)	154.4	± 35.4	(177.7)	(-0.362)	-0.029	±0.303	(0.206)	(-36.3)	-2.9	± 30.4	(20.6)
			sq. m. PA	(7.827)	8.721	±1.745	(9.813)	(783.4)	872.9	±174.6	(982.1)	(-3.115)	-1.494	±2.437	(-0.578)	(-311.7)	-149.6	±243.9	(-57.8)
M. fosliei	0	3	sq. m. RA	(6.729)	7.599	±1.751	(8.708)	(673.5)	760.6	±175.3	(871.6)	(-2.689)	-1.296	±2.097	(-0.497)	(-269.1)	-129.7	±209.9	(-49.7)
			g Protein	(0.979)	1.043	±0.168	(1.155)	(98.0)	104.4	± 16.8	(115.6)	(-0.364)	-0.176	±0.282	(-0.072)	(-36.4)	-17.6	± 28.2	(-7.2)
			sq. m. PA	(3.705)	4.916	±2.007	(6.342)	(370.9)	492.0	±200.9	(634.8)	(-0.387)	0.368	±1.297	(1.498)	(-38.8)	36.8	±129.8	(149.9)
P. conicum	0	4	sq. m. RA	(3.107)	4.198	±1.691	(5.340)	(310.9)	420.2	±169.3	(534.4)	(-0.326)	0.323	±1.116	(1.294)	(-32.6)	32.3	±111.6	(129.5)
			g Protein	(1.110)	1.544	±0.804	(2.324)	(111.1)	154.6	± 80.4	(232.6)	(-0.142)	0.088	±0.345	(0.344)	(-14.2)	8.8	± 34.5	(34.4)
			sq. m. PA	(7.510)	8.384	±1.857	(9.563)	(751.6)	839.1	±183.9	(957.2)	(0.298)	2.351	±3.317	(4.089)	(29.8)	235.3	±332.0	(409.3)
M. fosliei	3	3	sq. m. RA	(5.608)	6.669	±2.856	(8.569)	(561.3)	667.5	±285.8	(857.6)	(0.222)	1.854	±2.496	(2.952)	(22.2)	185.6	±249.9	(295.5)
			g Protein	(1.071)	1.602	±0.808	(1.949)	(107.2)	160.3	± 81.0	(195.1)	(0.077)	0.372	±0.444	(0.542)	(7.7)	37.3	± 44.5	(54.3)
			sq. m. PA	(4.091)	5.628	±1.917	(6.846)	(409.4)	563.3	±191.9	(685.2)	(-4.529)	-1.995	+3.030	(-0.214)	(-453.3)	-199.7	±303.2	(-21.4)
H. reinboldii	3	4	sq. m. RA	(3.907)	5.208	±1.604	(6.255)	(391.1)	521.3	±160.5	(626.0)	(-4.321)	-1.887	+2.897	(-0.194)	(-432.4)	-188.8	±289.9	(-19.4)
			g Protein	(0.789)	1.357	±0.716	(1.956)	(79.0)	135.9	± 71.6	(195.8)	(-0.874)	-0.436	+0.618	(-0.064)	(-87.4)	-44.0	± 62.3	(-6.4)
			sq. m. PA		4.480				451.8				0.049				5.0		
P. onkodes	'6'	1	sq. m. RA		3.928				396.1				0.043				4.3		
			g Protein		0.770				77.4				0.008				0.8		
			sq. m. PA	(2.343)	3.186	±2.530	(4.030)	(234.5)	318.9	±253.2	(403.3)	(-0.173)	0.102	±0.825	(0.377)	(-17.3)	10.2	± 82.5	(37.7)
M. fosliei	6	2	sq. m. RA	(1.981)	2.737	±2.269	(3.494)	(198.3)	274.0	±227.1	(349.7)	(-0.146)	0.090	±0.710	(0.327)	(-14.6)	9.1	± 70.9	(32.7)
			g Protein	(1.395)	1.499	±0.312	(1.603)	(100.1)	119.9	± 59.2	(139.6)	(-0.103)	0.024	±0.379	(0.150)	(-13.0)	1.0	± 42.0	(15.0)
			sq. m. PA	(3.549)	6.530	±4.721	(10.974)	(355.2)	653.6	±472.5	(1098.4)	(-1.765)	-1.058	±1.338	(0.207)	(-176.7)	-105.9	±134.0	(20.7)
H. reinboldii	6	4	sq. m. RA	(3.013)	5.532	±3.795	(9.045)	(301.5)	553.7	±379.9	(905.3)	(-1.455)	-0.888	±1.124	(0.182)	(-145.6)	-88.8	±112.5	(18.2)
			g Protein	(1.420)	1.915	±0.697	(2.340)	(142.1)	191.7	± 69.7	(234.2)	(-0.641)	-0.310	±0.447	(0.081)	(-64.1)	-31.0	± 44.7	(8.1)
			sq. m. PA	(2.044)	2.406	±0.884	(2.989)	(204.6)	240.8	± 88.4	(299.2)	(-0.754)	-0.052	±1.173	(0.597)	(-75.5)	-5.2	±117.4	(59.8)
P. conicum	6	3	sq. m. RA	(1.877)	2.249	±0.981	(2.900)	(187.9)	225.1	± 98.2	(290.3)	(-0.726)	-0.070	±1.079	(0.513)	(-72.7)	-7.1	±108.0	(51.4)
			g Protein	(0.973)	1.562	±0.907	(1.974)	(97.4)	156.4	± 90.8	(197.6)	(-0.359)	0.061	±0.783	(0.540)	(-35.1)	6.4	± 77.9	(54.2)
			sq. m. PA		1.594				159.5				0.159				15.9		
P. conicum	18	1	sq. m. RA		1.554				155.5				0.155				15.5		
			g Protein		0.759				75.9				0.074				7.4		

185.6 mg $CaCO_3$ h^{-1} for *N. fosliei*, from -188.8 to -88.8 mg $CaCO_3$ h^{-1} for *H. reinboldii*, and from -33.6 to 32.3 mg $CaCO_3$ h^{-1} for *P. conicum*.

Rates of calcification per day

The potential calcification rate over the course of a cloudless day was calculated by integrating the equation describing the *C-I* curve of a given individual with the changes predicted to occur in irradiance throughout the course of that day (see Section 2. 2. 2). Since the equation describing the *C-I* curve estimates the rate of light-dependent calcification from a baseline set by the dark calcification or solution rate it is appropriate to add, or subtract, the dark rate per hour multiplied by 24 from the daytime estimate of light-dependent calcification. By doing this, the calculated rate of $CaCO_3$ precipitation per day is equivalent to the sum of the measured amounts precipitated during each hour of the day.

From Table 20, *P. onkodes* showed the highest mean rate of $CaCO_3$ deposition per day at 0 m, but the lowest rate at 6 m. *N. fosliei* showed slightly higher mean rates of deposition than *P. conicum* at 0 m, and considerably higher rates than *H. reinboldii* at 3 m. The mean rates of deposition by *N. fosliei* and *H. reinboldii* at 6 m were very similar. *P. conicum* deposited $CaCO_3$ at a slightly lower rate than *N. fosliei* and *H. reinboldii* at 6 m, and showed very little net calcification at 18 m.

Since calcification in crustose coralline algae appears to be highly dependent upon irradiance, it is appropriate to examine the extent to which these two variables may be related. Daily rates of gross calcification (i.e., light-dependent calcification), net calcification ([light-dependent calcification] + [dark calcification or solution x 24]), and dark calcification or solution (x 24) are plotted against the measured peak noon irradiances at the sites where the algae were growing in Figs 37 and 38.

The linear regressions in Figs 37A,D,G,J generally show that gross calcification is directly proportional to irradiance. Figs 37B,K show significant regressions between net calcification and irradiance for *P. onkodes* and *P. conicum* at the 95% probability level. Fig. 37E shows a significant regression at the 90% probability level between net calcification and irradiance for *N. fosliei*. However, there was no significant regression between net calcification and irradiance for *H. reinboldii*

Table 20. Integrated rates of gross calcification, net calcification, and dark calcification or solution per hour for different species at different depths. Peak noon irradiance at the site of measurement and the date of incubation is provided for each of *n* replicates.

Species	Depth	n	Gross Calcification	Net Calcification	Dark Calcification or Solution	Peak Noon Irradiance	Date
				$CaCO_3$ m^{-2}		μEinsteins	
			g d^{-1} (kg y^{-1})	g d^{-1} (kg y^{-1})	g d^{-1} (kg y^{-1})	m^{-2} s^{-1}	
			17.69 (6.456)	10.77 (3.932)	-6.92(-2.524)	1516	30.4.86
			11.15 (4.068)	13.85 (5.056)	2.71 (0.989)	1479	7.5.86
P. onkodes	0	5	6.85 (2.500)	8.85 (3.232)	2.00 (0.731)	1474	8.5.86
			9.70 (3.541)	8.45 (3.083)	-1.25(-0.458)	1445	14.5.86
			8.10 (2.955)	7.38 (2.692)	-0.72(-0.263)	1441	15.5.86
		x	**10.70 (3.904)**	**9.86 (3.599)**	**-0.84(-0.305)**	**1471**	
			10.21 (3.727)	8.53 (3.112)	-1.68(-0.615)	1347	26.6.86
			10.00 (3.652)	3.56 (1.298)	-6.45(-2.354)	1350	1.7.86
N. fosliei	0	4	7.65 (2.791)	6.45 (2.355)	-1.20(-0.438)	1353	3.7.86
			5.32 (1.942)	9.09 (3.317)	3.77 (1.374)	1359	13.7.86
		x	**8.30 (3.028)**	**6.91 (2.521)**	**-1.39(-0.508)**	**1352**	
			6.32 (2.307)	5.53 (2.019)	-0.79(-0.288)	1250	8.7.86
			4.19 (1.531)	7.31 (2.667)	3.11 (1.136)	1252	9.7.86
P. conicum	0	4	3.46 (1.262)	3.02 (1.100)	-0.44(-0.162)	1255	11.7.86
			3.33 (1.217)	4.55 (1.661)	1.22 (0.445)	1257	12.7.86
		x	**4.33 (1.579)**	**5.10 (1.862)**	**0.78 (0.283)**	**1254**	
			2.52 (0.920)	9.61 (3.509)	7.09 (2.589)	1100	20.5.86
			6.28 (2.293)	12.03 (4.390)	5.75 (2.098)	1130	22.5.86
N. fosliei	3	4	5.15 (1.880)	5.69 (2.076)	0.54 (0.196)	650	23.5.86
			4.35 (1.589)	3.52 (1.286)	-0.83(-0.302)	700	26.5.86
		x	**4.58 (1.671)**	**7.71 (2.815)**	**3.14 (1.145)**	**895**	
			5.99 (2.184)	5.53 (2.018)	-0.46(-0.167)	615	24.5.86
			6.90 (2.517)	5.73 (2.092	-1.16(-0.425)	920	27.5.86
H. reinboldii	3	4	8.14 (2.969)	2.03 (0.740)	-6.11(-2.229)	1000	10.6.86
			8.43 (3.077)	-1.95 (-.712)	-10.38(-3.789)	900	11.6.86
		x	**7.37 (2.687)**	**2.84 (1.035)**	**-4.53(-1.653)**	**859**	
			3.12 (1.140)	4.82 (1.761)	1.70 (0.620)	120	30.6.86
			2.87 (1.049)	2.98 (1.087)	0.11 (0.039)	70	4.7.86
P. onkodes	'6'	4	2.13 (0.777)	1.92 (0.700)	-0.21(-0.077)	70	6.7.86
			2.74 (1.000)	0.66 (0.239)	-2.08(-0.761)	50	7.7.86
		x	**2.72 (0.992)**	**2.60 (0.947)**	**-0.12(-0.045)**	**76**	
			2.53 (0.924)	2.19 (0.798)	-0.35(-0.126)	390	27.4.86
			3.59 (1.309)	3.21 (1.170)	-0.38(-0.139)	70	9.6.86
N. fosliei	6	4	2.65 (0.966)	3.44 (1.255)	0.79 (0.289)	115	13.6.86
			3.18 (1.160)	8.07 (2.945)	4.89 (1.785)	87	17.6.86
		x	**2.99 (1.090)**	**4.23 (1.542)**	**1.24 (0.452)**	**166**	
			5.91 (2.157)	3.69 (1.345)	-2.23(-0.812)	350	23.4.86
			10.46 (3.818)	6.96 (2.539)	-3.50(-1.279)	550	16.5.86
H. reinboldii	6	4	3.89 (1.419)	0.62 (0.228)	-3.26(-1.191)	130	18.5.86
			4.86 (1.776)	5.31 (1.937)	0.44 (0.162)	300	19.5.86
		x	**6.28 (2.293)**	**4.15 (1.512)**	**-2.14(-0.780)**	**333**	
			3.14 (1.146)	1.41 (0.512)	-1.74(-0.634)	355	16.4.86
			3.19 (1.163)	3.19 (1.163)	0.00 (0.000)	350	21.4.86
P. conicum	6	4	2.30 (0.840)	5.46 (1.994)	3.16 (1.154)	54	28.5.86
			1.44 (0.524)	2.68 (0.977)	1.24 (0.452)	105	16.6.86
		x	**2.52 (0.918)**	**3.19 (1.162)**	**0.67 (0.243)**	**216**	
			1.39 (0.507)	1.76 (0.643)	0.38 (0.136)	50	18.6.86
			1.66 (0.606)	-0.06 (-.023)	-1.72(-0.628)	30	20.6.86
P. conicum	18	4	1.71 (0.625)	1.25 (0.456)	-0.46(-0.169)	55	21.6.86
			1.94 (0.707)	0.54 (0.196)	-1.40(-0.512)	80	24.6.86
		x	**1.68 (0.611)**	**0.87 (0.318)**	**-0.80(-0.293)**	**54**	

Fig. 37. Plots of mean integrated calcification per day against peak noon irradiance at the sites of measurement. Fitted lines show linear regressions. Equations of the regression lines are shown in boxes. r^2 values and significance levels (P) are shown in parentheses for each regression.
A-C, *Porolithon onkodes*
D-F, *Neogoniolithon fosliei*
G-I, *Hydrolithon reinboldii*
J-L, *Paragoniolithon conicum*

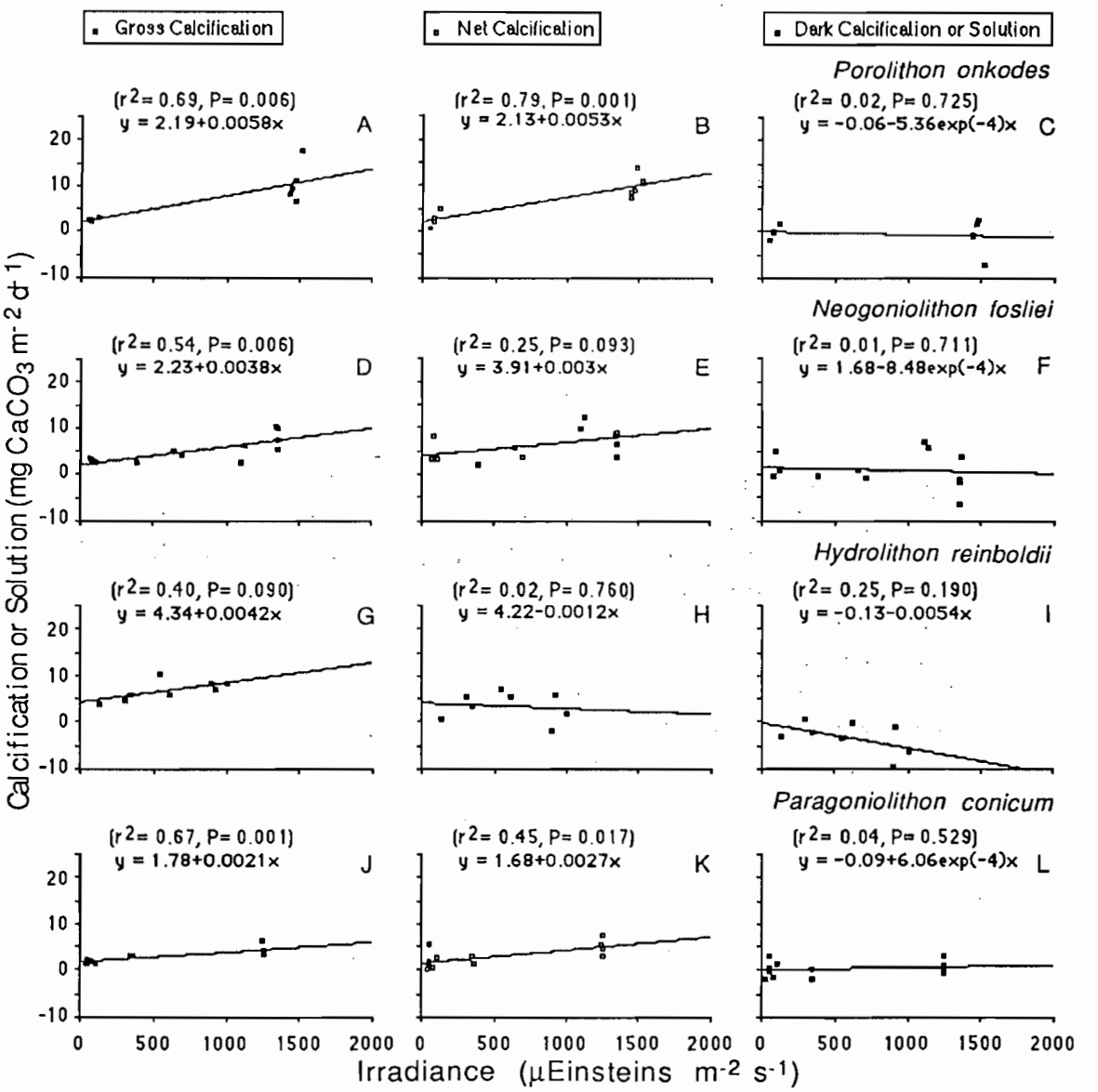
Gross Calcification
Net Calcification
Dark Calcification or Solution
Porolithon onkodes
(r2= 0.69, P= 0.006)
y = 2.19+0.0058x
A
(r2= 0.79, P= 0.001)
y = 2.13+0.0053x
B
(r2= 0.02, P= 0.725)
y = -0.06-5.36exp(-4)x
C
Neogoniolithon fosliei
(r2= 0.54, P= 0.006)
y = 2.23+0.0038x
D
(r2= 0.25, P= 0.093)
y = 3.91+0.003x
E
(r2= 0.01, P= 0.711)
y = 1.68-8.48exp(-4)x
F
Hydrolithon reinboldii
(r2= 0.40, P= 0.090)
y = 4.34+0.0042x
G
(r2= 0.02, P= 0.760)
y = 4.22-0.0012x
H
(r2= 0.25, P= 0.190)
y = -0.13-0.0054x
I
Paragoniolithon conicum
(r2= 0.67, P= 0.001)
y = 1.78+0.0021x
J
(r2= 0.45, P= 0.017)
y = 1.68+0.0027x
K
(r2= 0.04, P= 0.529)
y = -0.09+6.06exp(-4)x
L
Calcification or Solution (mg CaCO3 m-2 d-1)
20
10
0
-10
0
500
1000
1500
2000
Irradiance (µEinsteins m-2 s-1)

Fig. 38. Plots of mean integrated calcification per day against peak noon irradiance at the sites of measurement. Fitted lines show second order polynomial regressions. Equations of the regression lines are shown in boxes. r^2 values and significance levels (P) are shown in parentheses for each regression.
A-C, *Porolithon onkodes*
D-F, *Neogoniolithon fosliei*
G-I, *Hydrolithon reinboldii*

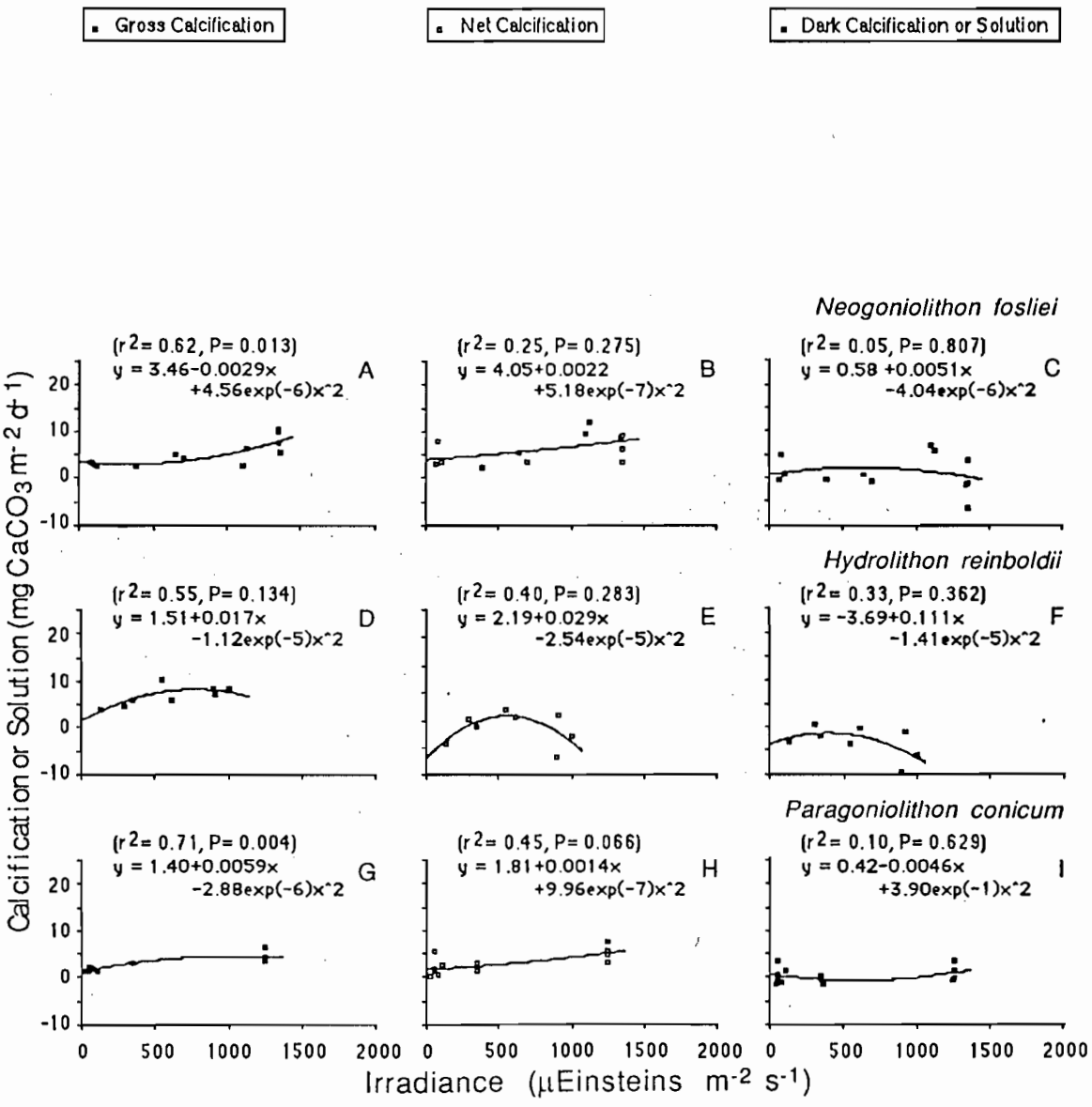
Gross Calcification
Net Calcification
Dark Calcification or Solution
Neogoniolithon fosliei
(r2= 0.62, P= 0.013)
y = 3.46-0.0029x
+4.56exp(-6)x^2
A
(r2= 0.25, P= 0.275)
y = 4.05+0.0022
+5.18exp(-7)x^2
B
(r2= 0.05, P= 0.807)
y = 0.58 +0.0051x
-4.04exp(-6)x^2
C
Hydrolithon reinboldii
(r2= 0.55, P= 0.134)
y = 1.51+0.017x
-1.12exp(-5)x^2
D
(r2= 0.40, P= 0.283)
y = 2.19+0.029x
-2.54exp(-5)x^2
E
(r2= 0.33, P= 0.362)
y = -3.69+0.111x
-1.41exp(-5)x^2
F
Paragoniolithon conicum
(r2= 0.71, P= 0.004)
y = 1.40+0.0059x
-2.88exp(-6)x^2
G
(r2= 0.45, P= 0.066)
y = 1.81+0.0014x
+9.96exp(-7)x^2
H
(r2= 0.10, P= 0.629)
y = 0.42-0.0046x
+3.90exp(-1)x^2
I
Calcification or Solution (mg CaCO3 m-2 d-1)
20
10
0
-10
0
500
1000
1500
2000
Irradiance (μEinsteins m-2 s-1)

(Fig. 37H). There was also no significant relationship between the rate of dark calcification or solution and irradiance (Figs. 37C,F,I,L).

The plots in Fig. 37 indicate that gross calcification, and to a lesser extent net calcification, can be predicted largely on the basis of irradiance. However, large and variable rates of dark solution can interfere with the predictability of light-dependent calcification rates (e.g., *H. reinboldii*, Figs. 37H,I). The equations describing the significant regression lines (at $P<0.05$ or $P<0.1$, given the variable nature of calcification data) can be used to predict the calcification rates of the coralline algae measured in this study for any level of irradiance encountered in the field on a cloudless day.

In most instances when the same data were fitted using second order polynomial rather than linear expressions (Fig. 38), there was little or no improvement in values of the coefficients of determination. Furthermore, the statistical confidence in each result was usually reduced by the greater number of mathematical terms used to describe each regression line. No plots are shown for *P. onkodes* because the absence of data points at intermediate irradiance levels and the spread of the data points caused the fitted lines to run to entirely unrealistic values.

Rates of calcification per year

There is only one published article which estimates the amount of $CaCO_3$ (in units of weight) which can be precipitated over the surface of a coral reef by specific members of the Corallinaceae. Stearn *et al.* (1977) measured the growth rates of four genera of crustose coralline algae using the alizarin dye method. Growth increments were converted into units of weight increase by calculating the bulk density of the coralline skeletons from the specific gravity of calcite minus the volume of the pore space. On a real surface area basis, Stearn *et al.* calculated the mean accretion rate of *Porolithon* to be 2378 g $CaCO_3$ m^{-2} y^{-1}, of *Neogoniolithon* to be 1225 g $CaCO_3$ m^{-2} y^{-1}, of *Lithophyllum* to be 1355 g $CaCO_3$ m^{-2} y^{-1}, and of *Mesophyllum* to be 167 g $CaCO_3$ m^{-2} y^{-1}. These rates of calcification for *Porolithon* and *Neogoniolithon* are somewhat lower than those determined in this study for the same genera (Table 20 - values in parentheses).

The annual estimates of calcification presented in Table 20 were obtained simply by multiplying the rates of net calcification per day by 365. Of course these may be in error if seasonal differences in calcification occur. However, the values published of Stearn *et al.* may have been lower because their measurements were based on young, small (<1 cm^2) crusts which had grown on artificial substrates. When these workers made additional measurements on "fist" sized individuals of *Porolithon* growing on naturally occurring substrates the estimated mean rate of accretion increased to 3120 g $CaCO_3$ m^{-2} y^{-1}, which is within the range of values and not dissimilar to the mean value reported here for *P. onkodes*. It seems likely that the calcification rates of young crusts, which spread outwards rapidly and upwards slowly in the absence of competition for space on clean artificial substrates such as glass or perspex (personal observations), may be controlled by similar processes to those which may be operating in mature crusts of *Paragoniolithon conicum*. The crusts of *P. conicum* were found to possess relatively rapid rates of calcification on a biomass basis (Fig 36B). This may be because the thinner actively photosynthetic layer offers less resistance to the diffusion of nutrients and/or gases and is more efficient in terms of light capture per unit biomass. However, on a surface area basis, shallow water individuals of *P. conicum* had a significantly lower rate of calcification than *P. onkodes* and *N. fosliei*. Possibly the rate of calcification was limited by the amount of organic tissue (total cell wall volume) per unit surface area of the crust. These factors may also have contributed to the lower rates of calcification reported by Stearn *et al.*

Rates of calcification per year as compared with other reef communities

Apart from the data of Stearn *et al.* (1977), all previous estimates of the amount of $CaCO_3$ deposited by coralline algae on a square metre of reef per year have come from community studies using the alkalinity anomaly technique, or adaptations thereof. These data have been summarised by Smith (1983) and Kinsey (1983, 1985). Both authors conclude that the calcification rates of different coral reef communities fall broadly into three categories. A high rate category, comprising 100% coral/algal cover and occupying only 1-2% of the reef, precipitates *ca* 10 kg $CaCO_3$ m^{-2}(projected area) y^{-1} (Kinsey 1979; Smith 1981). An intermediate category, comprising 100% cover of algal encrusted pavement and occupying 4-8% of the reef, precipitates *ca* 4 kg $CaCO_3$ m^{-2}(projected area) y^{-1} (Smith & Kinsey 1976). A low rate category, comprising 100% cover of sand and rubble and occupying 90-95% of the reef,

precipitates only *ca* 0.5-1.0 (Kinsey 1985) or 0.8 (Smith 1983) kg $CaCO_3$ m^{-2}(projected area) y^{-1}.

Since these estimates largely relate to measurements of shallow water reef communities it is most appropriate to compare them with the calcification rates of coralline species which predominate on coral reef flats and crests. In these areas, *Porolithon* spp. (in the GBR mainly *P. onkodes*) typically provide the dominant cover (see review by Johansen 1981). At Lizard Island, *Neogoniolithon foslie* is also abundant in exposed environments although less so than *P. onkodes*.

Stearn *et al.* (1977) estimated that coralline algae covered 41% of a fringing reef on the west coast of Barbados. Of the 41% reef cover, *Porolithon* comprised 40%, *Neogoniolithon* 25%, *Lithophyllum* 20%, and *Mesophyllum* 15% cover. They estimated the relief factor to be 4:1 (real surface area:projected area). If the entire 41% had been comprised of *Porolithon onkodes*, as estimated by Littler & Doty (1975) for the crest and shallow (<10 m) windward slope of the reef at Waikiki, the coralline contribution to reef calcification would have been 5.9 kg $CaCO_3$ m^{-2}(projected area) y^{-1}. If the percentage cover of *P. onkodes* had been 90%, which is not uncommon for reef crests (e.g., Sheveiko 1981; Atkinson & Grigg 1984; and personal observations), particularly on outer barrier reefs and atolls, the contribution by *P. onkodes* would have been 13 kg $CaCO_3$ m^{-2}(projected area) y^{-1}. At Lizard Island, the relief factor on the reef crest was closer to 3:1. If this relief factor is used the contribution of *P. onkodes* would be 9.8 kg $CaCO_3$ m^{-2}(projected area) y^{-1}. This rate would place a monospecific stand of *P. onkodes* with 90% cover in the high rate category as defined by Smith (1983) and Kinsey (1985).

In contrast, if the same data are calculated for monospecific stands of *N. fosliei*, a 41% cover and relief factor of 4:1 would yield a deposition rate of 4.1 kg $CaCO_3$ m^{-2}(projected area) y^{-1}. With 90% cover and a relief factor of 3:1, a rate of 6.8 kg $CaCO_3$ m^{-2}(projected area) y^{-1} would result.

If the mean rates of calcification for all the species included in this study are averaged and a relief factor of 5:1 is assumed for the entire seaward slope (unpublished data; see also Dahl 1973, Wanders 1976, and discussion in Section 2. 3. 7), the contribution to community metabolism by a mixed stand of coralline algae with 41% cover would be 3.5 kg $CaCO_3$ m^{-2}(projected area) y^{-1}. On

outer barrier reefs in the northern GBR, SCUBA surveys reveal that 41% is probably an underestimate of the cover of crustose coralline algae in these high energy environments (unpublished data). In these environments cover of 60% or above is common. If a cover of 60% is combined with a relief factor of 5:1, the total contribution of crustose coralline algae would be 5.2 kg $CaCO_3$ m^{-2}(projected area) y^{-1}. This is probably still a conservative estimate since the cover of crustose coralline algae is often higher than 60%, the dominant coralline is *P. onkodes*, which shows rapid calcification, and significantly more light is available due to the greater clarity of oceanic water.

These calculations suggest that the shallow wave-exposed margins of coral reefs, which typically support very high surface cover of primary reef-frame building crustose coralline algae (especially *Porolithon* spp.), may be areas of extremely high inorganic carbon fixation (*ca* 10 kg $CaCO_3$ m^{-2}(projected area) y^{-1}. In other forereef zones and on reef flats, where the cover of coralline algae may be significantly lower, the amount of inorganic carbon produced by these organisms is likely be of the order of 4 kg $CaCO_3$ m^{-2}(projected area) y^{-1}.

CHAPTER 4

SUMMARY AND CONCLUSIONS

4. 1. SUMMARY

The following sections summarise the data acquired from studies designed to meet the objectives specified in the introductory sections of Chapters 2 and 3.

Primary production

(i) This study describes the development of an underwater respirometer for the simultaneous measurement of *in situ* photosynthesis and calcification by crustose coralline algae.
(ii) *In situ* rates of photosynthesis were determined for four dominant reef-building species of coralline algae on the windward crest and slope of the reef at Lizard Island, in the northern GBR. Rates were determined at depths of between 0 and 18 m, representing a gradient of from 84 to 2% of surface irradiance.
(iii) Also described is the construction of an oxygen electrode cell for the measurement of photosynthesis by crustose coralline algae in the laboratory. Rates of photosynthesis were determined using the cell for specimens sampled from the same field populations as the *in situ* subjects, and experiencing a range of irradiance from 85 to 2% of surface irradiance.
(iv) In all cases except for specimens of *Porolithon onkodes* at 0 m, rates of photosynthesis were lower under laboratory conditions than *in situ* and the difference increased with increasing depth.
(v) Integrated rates of gross primary production per day ranged from 0.932 to 2.408 g C m^{-2} (real surface area) *in situ*, and from 0.686 to 2.308 g C m^{-2} in the laboratory.
(vi) Integrated rates of consumption per day ranged from 0.588 to 1.097 g C m^{-2} (real surface area) *in situ*, and from 0.449 to 1.355g C m^{-2} in the laboratory. When consumption was subtracted from gross production the net rate of primary primary production per day ranged from 0.180 to 1.352 g C m^{-2} (real surface area) *in situ*, and from 0.157 to 1.206 g C m^{-2} in the laboratory.

(vii) Rates of photosynthesis determined in the laboratory tended to underestimate productivity *in situ*, possibly by as much as 30%. It is suggested that failure to adequately simulate the changes occurring in underwater spectral distribution with increasing water depth was the principal cause of the lower rates.
(viii) Differences were observed in the *in situ* rates of photosynthesis of the four species of coralline algae studied.
(ix) Rates of photosynthesis varied with respect to depth and irradiance. *Porolithon onkodes* exhibited the highest rates of maximal gross and net photosynthesis at both 0 and 6 m but the rate of carbon accumulation at '6' m was below that of the other species because of the much reduced irradiance. *Paragoniolithon conicum* exhibited a higher rate of photosynthesis than *Neogoniolithon fosliei* and *Hydrolithon reinboldii* at 0 m but its rates of maximal gross and net photosynthesis declined with increasing depth to values at 6 m which were intermediate to those of *H. reinboldii* and *N. fosliei*. *P. conicum* was the only one of the four species to be found growing below 9 m and at 18 m had a rate of gross carbon production just sufficient to support its respiratory requirements plus a small amount of organic growth. *N. fosliei* exhibited slightly higher rates of maximal gross and net photosynthesis than *H. reinboldii* at 3 m but significantly lower rates at 6 m. Net carbon production per day varied in a similar fashion. Thus, *P. onkodes* appears well adapted to very high irradiance, *N. fosliei* to high to moderate irradiance, and *H. reinboldii* to moderate to low irradiance. *P. conicum* is enigmatic in that it showed maximum productivity under high to moderate irradiance but is generally more abundant where irradiance is low and appears well-adapted to shade.
(x) Integrated rates of primary production and consumption per day were usually significantly related to the peak noon irradiance at the site of measurement or collection. The relationship could be expressed in linear or second order polynomial terms. The equations describing the regression lines between primary production and peak noon irradiance can be used to predict rates of productivity under any given amount of irradiance on a cloudless day.
(xi) Estimates of carbon production, or consumption, based on measurements of oxygen flux can be significantly in error if inappropriate values are chosen for the metabolic quotients. Significant differences were found in the values of the photosynthetic quotients for each species. *P. conicum* had values for *PQ* which approached unity indicating carbohydrate metabolism. Mean values of *PQ* for the other three species were in excess of 1.2 indicating significant production of storage materials (i.e., fats or protein). The lower *PQ* values for *P. conicum* may be to do

with adaptation to low light environments. If low molecular weight carbon compounds are transported to the perimeter of the crust and metabolised more efficiently than larger storage product molecules, this would expedite areal expansion of the crust leading to a thinner more extensive photosynthetic layer with more effective light-harvesting properties.

Photoadaptation

(i) The photosynthetic rates of the four crustose coralline species were measured over the entire range of irradiance levels encountered in the field.
(ii) The relationship between photosynthesis and irradiance *in situ* could be described accurately using the hyperbolic tangent function (Eq. 3). *In situ P-I* curves for specimens existing at the lower limits of their species distributions did not show evidence of saturation. Laboratory studies revealed that different specimens showed *P-I* responses which varied in terms of the rate of transition from light-limited to light-saturated photosynthesis. Specimens living under high irradiance generally showed relatively slow rates of transition and were not entirely saturated at irradiance levels above those occurring in the field. Specimens living under low irradiance revealed more rapid rates of transition from light-limited to light-saturated photosynthesis and showed greater potential for saturation under natural levels of irradiance. The *P-I* responses of specimens measured in the laboratory were accurately described by one of four functions ranging from the right rectangular hyperbola (Eq. 1), in specimens showing the most gradual rates of transition, to the hyperbolic tangent (Eq. 3), in specimens showing the most rapid rates of transition. Intermediate rates of transition were described either in fixed terms by a simple exponential function (Eq. 2), or in variable terms by a general exponential function (Eq. 4).
(iii) Light saturation curves were constructed for *in situ* and laboratory data using non-linear, least squares regression analysis and the most appropriate of the models described above.
(iv) The shapes of the *P-I* curves changed with increasing depth and decreasing irradiance. These changes were interpreted as evidence of photoadaptation, and
(v) they conformed with the changes reported in the literature for other photosynthetic marine plants and plant-animal associations.
(vi) The greatest capacity to adapt to shade (i.e., values for I_k [Steemann Nielsen 1975] and α) was shown by *P. conicum* which is perhaps not surprising since it grows

to more than twice the depth of the other species. However, the photoadaptive capabilities of the other three species were found to be quite similar even though (vii) the field distribution of *P. onkodes* is sharply restricted to water shallower than 3-4 m, whereas *N. fosliei* and *H. reinboldii* both grow to 6 m and sometimes deeper. It is suggested that the restricted distributions of *P. onkodes* to areas of high grazing pressure and water motion, and of *P. conicum* to sharply inclined surfaces and low irradiance environments, may be a product of their relative inabilities to compete successfully with turf algae or to endure prolonged sediment burial. *N. fosliei* and *H. reinboldii*, in contrast, both show evidence of regular epithallial sloughing (especially the former), and both appear capable of growth on flat surfaces under moderate irradiance where there is significant turf cover and sedimentation. It is further suggested that these factors may influence the relative proportions of the four species on outer-barrier as compared with mid-shelf reef environments where the energetics of the systems differ. The lack of saturation observed among the *in situ P-I* curves for specimens existing at the lower limits of their species distributions perhaps indicates that specimens are not capable of "fine tuning" their photosynthetic apparatus at very low light levels, and must ensure maximum photon capture even at the cost of maintaining superfluous apparatus.

Calcification

(i) *In situ* rates of calcification by the four species of crustose coralline algae were measured at depths of between 0 and 18 m, which represented a gradient of from 84 to 2% of surface irradiance. Calcification rates were always considerably higher in the light than in the dark. In fact the were many examples of night-time solution of $CaCO_3$.
(ii) Light-saturation curves were constructed for calcification using non-linear, least squares regression analysis and the hyperbolic tangent function.
(iii) The relationship between calcification and irradiance was significant in all cases. The shapes of the *C-I* curves changed with depth and irradiance. The changes were consistent with the photoadaptive trends observed among the *P-I* data.
(iv) Neither calcification nor photosynthesis were saturated in specimens measured at the lower limits of their species distributions. Comparison of the *C-I* and *P-I* curves showed that both processes responded in a similar fashion to irradiance but that higher irradiance was needed for the saturation of calcification in shallow water specimens than for the saturation of photosynthesis.

(v) This fact may be interpreted as a dependency of calcification on photosynthesis in the first instance to alter the concentration of carbonate ions in solution thus shifting the carbonate equilibrium in favour of the precipitation of $CaCO_3$; in the second for the production and release of energy supplies for the active transport of Ca^{2+}, CO_3^{2-}, and/or OH^- ions, and/or for the export of H^+ ions; and possibly in a third instance for the supply of materials for construction of an organic matrix. Moreover the regular occurrence of night-time $CaCO_3$ solution suggests that calcification may be entirely dependent on photosynthesis and that when calcification occurs in the dark it is the indirect product of daytime photosynthesis. This would imply that calcification does not simply result from ionic shifts accompanying photosynthesis, but also depends upon the supply of free energy. The facts suggest that there is no specific mechanism of dark calcification in crustose coralline algae and that the term "light-enhanced" calcification should be changed to "light-dependent" calcification. The most likely reason for night-time $CaCO_3$ solution would seem to be acidification of the cellular sap during respiration.
(vi) Rates of calcification in the light were integrated against the amount of irradiance over a cloudless day for each specimen. Integrated rates of dark calcification were appropriately added or subtracted to yield estimates of the net rates of $CaCO_3$ deposition. Rates of net accretion per day ranged from 0.87 to 9.86 g $CaCO_3$ m^{-2}.
(vii) Rates of gross calcification (i.e., light-dependent) were generally significantly related to peak noon irradiance at the site of measurement. Two out of four regressions for net calcification against peak noon irradiance were significant at $P<0.05$, and one was significant at $P<0.1$. Rates of dark calcification were not significantly related to peak noon irradiance. Regressions were more significant when the data were fitted with linear rather than second order polynomial functions. The significant regressions can be used to estimate the rates of gross and net calcification for any amount of irradiance on a cloudless day.

4. 2. CONCLUSIONS

(i) Given the great abundance of crustose coralline algae on coral reefs and the rates of *in situ* primary production and calcification measured in this study it is clear that they are very important contributors of organic and inorganic carbon. In fact, according to the schemes proposed by Smith (1983) and Kinsey (1985), the rate of organic production for a windward reef crest dominated by *P. onkodes* is likely be

well within the intermediate category of 5-10 g C m^{-2}(projected surface area) d^{-1}, which occupies 4-8% of the reef surface; and in terms of inorganic carbon production these areas probably fall in the highest rate category of around 10 kg $CaCO_3$ m^{-2}(projected surface area) y^{-1}, which is a rate applicable to only 0.5-1% of the reef surface. Thus it seems the true contribution of coralline algae to reef growth has been seriously underestimated. The fact that little upward reef growth has occurred over the last 4000 years (Buddemeier *et al.* 1975) doubtlessly bears testimony to the great amount of material which is removed from the shallow parts of coral reefs particularly on the windward margin. The maintenance of a wave-resistant front obviously involves considerable cost which is never recognized if estimates of production are based on long term rates of accretion. This study therefore emphasizes the need for detailed *in situ* studies to enable proper assessment of the carbon budgets of coral reef systems.
(ii) As expected, crustose coralline algae do photoadapt to decreasing irradiance. The success with which they do so obviously sets lower limits but does not necessarily determine species distributions. It would appear that competition from turf algae, and frequency and degree of sediment burial more markedly affect the distributions of *P. onkodes* and *P. conicum* than *N. fosliei* and *H. reinboldii*. Thus on outer barrier reefs where these factors are of less significance *P. onkodes* is more widely distributed and in greater abundance in high irradiance environments, and *P. conicum* which shows rapid rates of photosynthesis and extensive areal growth often dominates the shaded but nonetheless fairly well illuminated areas. *N. fosliei* and *H. reinboldii* both grow well at Lizard Island where turf growth and sedimentation are often significant factors and it appears that the ability to regularly shed the outermost layer of cells is of significant advantage in the lower energy environments of mid-shelf reefs.

4. 3. FUTURE RESEARCH

(i) Studies are needed to confirm the importance of spectral distribution on crustose coralline metabolism. If light quality does affect production rate then quantitative correction factors need to be experimentally determined to correct productivity estimates using neutral density filters to simulate light at depth.
(ii) The question of why crustose coralline algae and possibly other calcareous algae (see Borowitzka & Larkum 1976a) dissolve at times in the dark is a most intriguing one because the answer may provide much information on influence of photosynthesis and respiration on calcification and, indeed, of the effects that calcification has on

photosynthesis and organic growth. The reduction in pH associated with respiration seems to be the most likely reason for $CaCO_3$ solution in the dark but this requires confirmation. Productive lines of research may include fine-scale measurements of the pH change accompanying the flux of $CaCO_3$ in the dark, such as those carried out by Digby (1977a). Attempts should be made to determine if solution is correlated with endogenous or exogenous factors. If, as seems likely, calcification is an energy requiring process then starving corallines of light may deplete energy reserves and stimulate dark solution. Alternatively, if a certain level of solution facilitates organic growth then a reversal of the above procedures may stimulate solution in the dark.

(iii) Investigations should be undertaken to determine if coralline algae translocate significant amounts of photosynthate to the sites of active growth, and if so in what form. The low value of *PQ* for *P. conicum*, which appears to prefer shaded conditons and developes large thin crusts, may indicate that low molecular weight carbohydrates (e.g., glucose) are produced and translocated preferentially to the perimeter margin to expedite areal growth of the crust.

(iv) Repetitive measurements of calcification need to be made under controlled experimental conditions on the same biological material to determine if endogenous rhythms occur in calcification rate. Some of the variability commonly encountered with calcification estimates may be attributable to such endogenous factors.

REFERENCES

ADEY, W.H., 1966. The genus *Pseudolithophyllum* (Corallinaceae in the Gulf of Maine). *Hydrobiologia*, Vol. 27, pp. 479-497.

ADEY, W.H., 1971. The sublittoral distribution of corallines on the Norwegian Coast. *Sarsia*, Vol. 46, pp. 41-58.

ADEY, W.H., 1975. The algal ridges and coral reefs of St. Croix their structure and Holocene development. *Atoll Res. Bull.*, Vol. 187, pp. 1-67.

ADEY, W.H., 1978a. Coral reef morphogenesis: a multidimensional model. *Science*, Vol. 202, pp. 831-857.

ADEY, W.H., 1978b. Algal ridges of the Caribbean sea and West Indies. *Phycologia*, Vol. 17, pp. 361-367.

ADEY, W.H. & P.J. ADEY, 1973. Studies on the biosystematics and ecology of the epilithic crustose Corallinaceae of the British Isles. *Br. Phycol. J.*, Vol. 8, pp. 343-407.

ADEY, W.H. & R. BURKE, 1976. Holocene bioherms (algal ridges and bank barrier reefs) of the eastern Caribbean. *Geol. Soc. Am. Bull.*, Vol. 87, pp. 95-109.

ADEY, W.H. & I.G. MACINTYRE, 1973. Crustose coralline algae: a reevaluation in the geological sciences. *Geol. Soc. Am. Bull.*, Vol. 84, pp. 883-904.

ADEY, W.H., R.A. TOWNSEND & W.T. BOYKINS, 1982. The crustose coralline algae (Rhodophyta: Corallinaceae) of the Hawaiian Islands. *Smithson. Contrib. Mar. Sci.*, No. 15, pp. 1-74.

ADEY, W.H. & J.M. VASSAR, 1975. Colonisation, succession and growth rates of tropical crustose coralline algae (Rhodophyta, Cryptonemiales). *Phycologia*, Vol. 14, pp. 55-69.

AGASSIZ, A., 1889. The coral reefs of the Hawaiian Islands. *Bull. Mus. comp. zool. Harv.*, Vol. 17, pp. 121-170.

AGEGIAN, C.R., 1981. Growth of the branched coralline alga, *Porolithon gardineri* (Foslie) in the Hawaiian Archipelago. *Proc. 4th Int. Cor. Reef. Symp., Manila*, edited by E.D. Gomez, C.E. Birkeland, R.W. Buddemeier, R.E. Johannes, J.A. Marsh, Jr. & R.Y. Tsuda, Marine Sciences Centre, Univ. Philippines, Quezon City, Vol. 2, pp. 419-423.

ARNOLD, K.E. & S.N. MURRAY, 1980. Relationships between irradiance and photosynthesis for marine benthic green algae (Chlorophyta) of differing morphologies. *J. Exp. Mar. Biol. Ecol.*, Vol. 43, pp. 183-192.

ARNOTT, H.J. & F.G.E. PAUTARD, 1971. Calcification in plants. In, *Biological calcification*, edited by H. Schraer, North Holland Publishing Co., Amsterdam, pp. 375-446.

ATKINSON, M.J. & R.W. GRIGG, 1984. Model of a coral reef ecosystem. II. Gross and net benthic primary production at French Frigate Shoals, Hawaii. *Coral Reefs*, Vol. 3, pp. 13-22.

BAAS-BECKING, L.G.M. & E.W. GALLIHER, 1931. Wall structure and mineralisation in coralline algae. *J. Phys. Chem.*, Vol. 35, pp. 467-479.

BAILEY, A. & T. BISALPUTRA, 1970. A preliminary account of the application of thin sectioning, freeze etching and scanning electron microscopy to the study of coralline algae. *Phycologia*, Vol. 9, pp. 83-101.

BAK, R.P.M., 1976. The growth of coral colonies and the importance of crustose coralline algae and burrowing sponges in relation with carbon accumulation. *Neth. J. Sea Res.*, Vol. 10, pp. 285-337.

BARNES, D.J., 1970. Coral skeletons: an explanation of their growth and structure. *Science*, Vol. 170, pp. 1305-1308.

BARNES, D.J., 1971. A study of growth, structure and form in modern coral skeletons. *Ph.D. thesis*, Univ. Newcastle, England, 180 pp.

BARNES, D.J., 1982. Light response curve for calcification in the staghorn coral, *Acropora acuminata*. *Comp. Biochem. Physiol.*, Vol. 73A, pp. 41-45.

BARNES, D.J., 1983. Profiling coral reef productivity and calcification using pH and oxygen electrodes. *J. Exp. Mar. Biol. Ecol.*, Vol. 66, pp. 149-161.

BARNES, D.J. & B.E. CHALKER, in press. Calcification and photosynthesis in reef-building corals and algae. In, *Coral reef ecosystems*, edited by Z. Dubinsky, Elsevier, Amsterdam.

BARNES, D.J. & C.J. CROSSLAND, 1977. Coral calcification: sources of error in radioisotope techniques. *Mar. Biol.*, Vol. 42, pp. 119-129.

BARNES, D.J. & C.J. CROSSLAND, 1982. Variability in the calcification rate of *Acropora acuminata* measured with radioisotopes. *Coral Reefs*, Vol. 1, pp. 53-57.

BARNES, D.J. & M.J. DEVEREUX, 1984. Productivity and calcification on a coral reef: a survey using pH and oxygen electrode techniques. *J. Exp. Mar. Biol. Ecol.*, Vol. 79, pp. 213-231.

BARNES, D.J. & D.L. TAYLOR, 1973. *In situ* studies of calcification and photosynthetic carbon fixation in the coral, *Montastrea annularis*. *Helgol. Wiss. Meeresunters*, Vol. 24, pp. 284-291.

BERTHOLD, G., 1882. Uber die Verteilung der Algen in Golf von Neapel nebst einem Verzeichnis der bisher daselbst beobachten Arten. *Mitt. Zool. Sta. Neapel.*, Vol. 3, pp. 393-536.

BEVELANDER, G. & H. NAKAHARA, 1969. An electron microscope study of the formation of the nacreous layer in the shell of certain bivalve molluscs. *Calcif. Tissue. Res.*, Vol. 3, pp. 84-92.

BIO-RAD LABORATORIES, 1979. *Bio-Rad protein assay instruction manual.* Bio-Rad Laboratories, Richmond, California, 17 pp.

BLINKS, L.R., 1951. Physiology and biochemistry of algae. In, *Manual of Phycology*, edited by G.M. Smith, Ronald Press Co., New York, pp. 263-291.

BOHM, E.L., 1969. *Calcification in the calcareous alga Halimeda opuntia (L.)(Chlorophyta, Udoteaceae)*. Ph.D. thesis, Univ. West Indies, Mona, Jamaica, 132 pp.

BOHM, E.L., 1973. Composition and calcium binding properties of the water soluble polysaccharides in the calcareous alga *Halimeda opuntia* (L.)(Chlorophyta, Udoteaceae). *Int. Rev. Gesamten. Hydrobiol.*, Vol. 58, pp. 117-126.

BOHM, E.L., 1978. Application of the ^{45}Ca tracer method for the determination of calcification rates in calcareous algae: effect of calcium exchange and differential saturation of algal calcium pools. *Mar. Biol.*, Vol. 47, pp. 9-14.

BOHM, E.L. & T.F. GOREAU, 1973. Rates of turnover and net accretion of calcium and role of calcium binding polysaccharides during calcification in the calcareous alga *Halimeda opuntia* (L.). *Int. Rev. Gesamten. Hydrobiol.*, Vol. 58, pp. 723-740.

BOHM, L., D. FUTTERER & E. KAMINSKI, 1978. Algal calcification in some Codiaceae (Chlorophyta): ultrastructure and location of skeletal deposits. *J. Phycol.*, Vol. 14, pp. 486-493.

BOROWITZKA, M.A., 1977. Algal calcification. *Oceanogr. Mar. Biol. Annu. Rev.*, Vol. 15, pp. 189-223.

BOROWITZKA, M.A., 1979. Calcium exchange and the measurement of calcification rates in the calcareous coralline red alga *Amphiroa foliacea*. *Mar. Biol.*, Vol. 50, pp. 339-347.

BOROWITZKA, M.A., 1981. Photosynthesis and calcification in the articulated coralline red algae *Amphiroa anceps* and *A. foliacea*. *Mar. Biol.*, Vol. 62, pp. 17-23.

BOROWITZKA, M.A., 1982a. Mechanisms in algal calcification. In, *Progress in phycological research*, edited by F.E. Round & D.J. Chapman, Elsevier, Amsterdam, pp. 137-177.

BOROWITZKA, M.A., 1982b. Morphological and cytological aspects of algal calcification. *Int. Rev. Cytol.*, Vol. 74, pp. 127-162.

BOROWITZKA, M.A., 1983. Calcium carbonate deposition by reef algae: morphological and physiological aspects. In, *Perspectives on coral reefs*, edited by D.J. Barnes, Australian Institute of Marine Science, Townsville, pp. 16-28.

BOROWITZKA, M.A. & A.W.D. LARKUM, 1976a. Calcification in the green alga *Halimeda*. II. The exchange of Ca^{2+} and the occurrence of age gradients in calcification and photosynthesis. *J. Exp. Bot.*, Vol. 27, pp. 864-878.

BOROWITZKA, M.A. & A.W.D. LARKUM, 1976b. Calcification in the green alga *Halimeda*. III. The sources of inorganic carbon for photosynthesis and calcification and a model of the mechanism of calcification. *J. Exp. Bot.*, Vol. 27, pp. 879-893.

BOROWITZKA, M.A. & A.W.D. LARKUM, 1976c. Calcification in the green alga *Halimeda*. I. An ultrastructure study of thallus development. *J. Phycol.* Vol. 13, pp. 6-16.

BOROWITZKA, M.A. & M. VESK, 1978. Ultrastructure of the Corallinaceae (Rhodophyta). I. The vegetative cells of *Corallina officinalis* and *C. cuvierii*. *Mar. Biol.*, Vol. 46, pp. 295-304.

BOROWITZKA, M.A. & M. VESK, 1979. Ultrastructure of the Corallinaceae. II. The vegetative cells of *Lithothrix aspergillum*. *J. Phycol.*, Vol. 15, pp. 146-153.

BOWES, G.W., 1969. Carbonic anhydrase in marine algae. *Plant Physiol.*, Vol. 44, pp. 726-732.

BRADFORD, M.M., 1976. A rapid and sensitive method for the quantitation of microgram quantities of protein utilizing the principle of protein dye binding. *Anal. Biochem.*, Vol. 72, pp. 248-254.

BRANDT, H. & E. RABEN, 1912-1922. Zur Kenntniss der chemischer Zusammensetzung des Planktons und einiger Bodenorganismen. *Wiss. Meeresuntersuch.*, Vol. 19, pp. 175-210.

BROWN, A.H., 1953. The effects of light on respiration using isotopically enriched oxygen. *Am. J. Bot.*, Vol. 40, pp. 719- 729.

BREWER, P.G. & J.C. GOLDMAN, 1976. Alkalinity changes generated by phytoplankton growth. *Limnol. Oceanogr.*, Vol. 21, pp. 108- 117.

BRYAN, W.H. & D. HILL, 1941. Spherulitic crystallization as a mechanism of skeletal growth in hexacorals. *Proc. R. Soc. Queens.*, Vol. 52, pp. 78-91.

BUDDEMEIER, R.W., 1974. Environmental controls over annual and lunar cycles in hermatypic corals. In, *Proc. 2nd Int. Cor. Reef Symp., Brisbane*, Great Barrier Reef Committee, Vol. 2, pp. 259- 267.

BUDDEMEIER, R.W., S.V. SMITH & R.A. KINZIE, III, 1975. Holocene windward reef flat history, Eniwetak Atoll. *Geol. Soc. Am. Bull.*, Vol. 86, pp. 1581-1584.

BUESA, R.J., 1980. Photosynthetic quotient of marine plants. *Photosynthetica*, Vol. 14, pp. 337-342.

CABIOCH, J., 1971. Etude sur les Corallinacees. I. Characteres generaux de la cytologie. *Cah. Biol. Mar.*, Vol. 12, pp. 121- 186.

CARPENTER, J.H., 1966. New measurements of oxygen solubility in pure and natural water. *Limnol. Oceanogr.*, Vol. 11, pp. 264- 277.

CARPENTER, R.C., 1985. Relationships between primary production and irradiance in coral reef algal communities. *Limnol. Oceanogr.*, Vol. 30, pp. 784-793.

CHALKER, B.E., 1976. Calcium transport during skeletogenesis in hermatypic corals. *Comp. Biochem. Physiol.*, Vol. 54A, pp. 455- 459.

CHALKER, B.E., 1980. Modelling light saturation curves for photosynthesis: an exponential function. *J. Theor. Biol.*, Vol. 84, pp. 205-215.

CHALKER, B.E., 1981. Simulating light saturation curves for photosynthesis and calcification by reef-building corals. *Mar. Biol.*, Vol. 63, pp. 135-141.

CHALKER, B.E., 1983. Calcification by corals and other animals on the reef. In, *Perspectives on coral reefs*, edited by D.J. Barnes, Australian Institute of Marine Science, Townsville, pp. 29-45.

CHALKER, B.E. & W.C. DUNLAP, 1982. Extraction and quantitation of endosymbiotic algal pigments from reef-building corals. In, *Proc. 4th Int. Cor. Reef Symp.*, edited by E.D. Gomez *et al.*, Univ. Philippines, Vol. 2, pp. 45-50.

CHALKER, B.E., W.C. DUNLAP & J.K. OLIVER, 1983. Bathymetric adaptations of reef-building corals at Davies Reef, Great Barrier Reef, Australia. II. Light saturation curves for photosynthesis and respiration. *J. Exp. Mar. Biol. Ecol.*, Vol. 73, pp. 37-56.

CHALKER, B.E., K. CARR & E. GILL, 1985. Measurement of primary production and calcification *in situ* on coral reefs using electrode techniques. *Proc. 5th Int. Cor. Reef Congr., Tahiti*, edited by C. Gabrie & B. Salvat, Vol. 6, pp. 167-172.

CHALKER, B.E., T. COX & W.C. DUNLAP, 1984. Seasonal changes in primary production and photoadaptation by the reef-building coral *Acropora granulosa* on the Great Barrier Reef. In, *Marine phytoplankton and productivity*, edited by O. Holm-Hansen, L. Bolis & R. Giles, Springer-Verlag, Berlin, pp. 73-87.

CHALKER, B.E. & D.L. TAYLOR, 1978. Rhythmic variations in calcification and photosynthesis associated with the coral *Acropora cervicornis* (Lamarck). *Proc. R. Soc. Lond. B*, Vol. 201, pp. 179-189.

CHAVE, K.E. 1954. Aspects of the biogeochemistry of magnesium. I. Calcareous marine organisms. *J. Geol.*, Vol. 62, pp. 266-283.

CHAVE, K.E. & R.F. SCHMALZ, 1966. Carbonate-seawater interaction. *Geochim. Cosmochim.*, Acta 30, pp. 1037-1048.

CHAVE, K.E. & E. SUESS, 1967. Suspended minerals in seawater. *Trans. N.Y. Acad. Sci.*, Vol. 29, pp. 991-1000.

CHAVE, K.E. & E. SUESS, 1970. Calcium carbonate saturation in seawater: effects of dissolved organic matter. *Limnol. Oceanogr.*, Vol. 15, pp. 633-637.

CLOUD, P.E., 1952. Facies relationships of organic reefs. *Am. Assoc. Petrol. Geol. Bull.*, Vol. 36, pp. 2125-2149.

CLOUD, P.E., 1962. Environment of calcium carbonate deposition west of Andros Island, Bahamas. *Geol. Surv. (U.S.) Prof. Pap.*, No. 350, 138 pp.

CROSSLAND, C.J. & D.J. BARNES, 1977. Gas exchange studies with the staghorn coral *Acropora acuminata* and its zooxanthellae. *Mar. Biol.*, Vol. 40, pp. 185-194.

CROSSLAND, C.J. & D.J. BARNES, 1977. Calcification in the staghorn coral *Acropora acuminata*: variations in apparent skeletal incorporation of radioisotopes due to different methods of processing. *Mar. Biol.*, Vol. 43, pp. 57-62.

CULBERSON, C. & R.M. PYTKOWICZ, 1968. Effect of pressure on carbonic acid, boric acid, and the pH of seawater. *Limnol. Oceanogr.*, Vol. 13, pp. 403-417.

CULBERSON, C., R.M. PYTKOWICZ & J.E. HAWLEY, 1970. Seawater alkalinity determination by the pH method. *J. Mar. Res.*, Vol. 28, pp. 15-21.

DAHL, A.L., 1973. Surface area in ecological analysis: quantification of benthic coral-reef algae. *Mar. Biol.*, Vol. 23, pp. 239-249.

DAHL, A.L., 1976. Generation of photosynthetic surface by coral reef algae. *Micronesica*, Vol. 12, pp. 43-47.

DARLEY, W., 1974. Silification and calcification. In, *Algal physiology and biochemistry*, edited by W.D.P. Stewart, Blackwell Scientific Publications, Oxford, pp. 655-675.

DARWIN, C., 1842. *Structure and distribution of coral reefs*. Smith, Elder & Co., London, 214 pp.

DAVID, T.W.E., G.H. HALLIGAN & A.E. FINCKH, 1904. Report on dredging at Funafuti Atoll. Section VII. In, *The Atoll of Funafuti*, R. Soc. Lond., pp. 151-159.

DAVIES, P.J., 1983. Reef growth. In, *Perspectives on coral reefs*, edited by D.J. Barnes, Australian Institute of Marine Science, Townsville, pp. 69-106.

DAVIES, P.S., 1977. Carbon budgets and vertical zonation of Atlantic reef corals. In, *Proc. 3rd Int. Cor. Reef Symp.*, edited by D.L. Taylor, Rosenstiel School of Marine and Atmospheric Science, Univ. Miami, Miami, Florida, Vol. 1, pp. 391-396.

DAVIES, P.S., 1980. Respiration in some Atlantic reef corals in relation to vertical distribution and growth form. *Biol. Bull. (Woods Hole)*, Vol. 158, pp. 187-194.

DAWSON, E.Y., 1960. Marine red algae of Pacific Mexico. Part 3. Cryptonemiales, Corallinaceae subfamily Melobesioideae. *Pac. Natur.*, Vol. 2, pp. 1-125.

DAWSON, E.Y., 1961. The rim of the reef: calcareous algae occupy a major role in the growth of atolls. *Nat. Hist.*, Vol. 70, pp. 8-17.

DEGENS, E.T., 1976. Molecular mechanisms of carbonate, phosphate and silica deposition in the living cell. *Top. Curr. Chem.*, Vol. 64, pp. 1-112.

DIGBY, P.S.B., 1977a. Growth and calcification in the coralline algae *Clathromorphum circumscriptum* and *Corallina officinalis*, and the significance of pH in relation to precipitation. *J. Mar. Biol. Assoc. U.K.*, Vol. 57, pp. 1095-1109.

DIGBY, P.S.B., 1977b. Photosynthesis and respiration in the coralline algae *Clathromorphum circumscriptum* and *Corallina officinalis* and the metabolic basis of calcification. *J. Mar. Biol. Assoc. U.K.*, Vol. 57, pp. 1111-1124.

DIGBY, P.S.B., 1979. Reducing activity and the formation of base in the coralline algae: an electrochemical model. *J. Mar. Biol. Assoc. U.K.*, Vol. 59, pp. 455-477.

DIXON, P.S., 1973. *Biology of the Rhodophyta.* Oliver & Boyd, Edinburgh, 285 pp.

DODGE, R.E. & J. THOMPSON, 1974. The natural radiochemical and growth records in contemporary hermatypic corals from the Atlantic and Caribbean. *Earth Plan. Sci. Lett.*, Vol. 23, pp. 313-322.

DONE, T.J., 1983. Coral zonation: its nature and significance. In, *Perspectives on coral reefs*, edited by D.J. Barnes, Australian Institute of Marine Science, Townsville, pp. 107- 147.

DOTY, M.S., 1954. Floristic and ecological notes on Raroia. Part I. *Atoll Res. Bull.*, No. 33, pp. 1-41.

DOTY, M.S., 1962. *Analysis of the productivity data from the September, Honolulu, intercalibration trials.* 23 pp. (Mimeo.) (Cited by Jitts 1963)

DOTY, M.S., 1974. Coral reef roles played by free-living algae. *Proc. 2nd Int. Cor. Reef Symp.*, Brisbane, Great Barrier Reef Committee, Vol. 1, pp. 27-33.

DOTY, M.S. & J.P.E. MORRISON, 1954. Interrelationships of the organisms on Raroia aside from man. *Atoll Res. Bull.*, No. 35, pp. 1-61.

DREW, E.A., 1983. Light. In, *Sublittoral ecology: the ecology of shallow sublittoral benthos*, edited by R. Earll & D.G. Erwin, Clarendon Press, Oxford, pp. 10-57.

DRING, M.J., 1971. Light quality and the photomorphogenesis of algae in marine environments. In, *4th Eur. Mar. Biol. Symp.*, edited by D.J. Crisp, Cambridge Univ. Press, Cambridge, pp. 375-392.

EDMOND, J.M., 1970. High precision determination of titration alkalinity and total carbon dioxide content of seawater by potentiometric titration. *Deep-Sea Res.*, Vol. 17, pp. 737-750.

EDMOND, J.M. & T.M. GIESKES, 1970. On the calculation of the degree of saturation of seawater with respect to calcium carbonate under *in situ* conditions. *Geochim. Cosmochim.*, Acta 34, pp. 1261-1291.

EMERY, K., J. TRACEY & H. LADD, 1954. Geology of Bikini and nearby atolls. *Geol. Surv. (U.S.) Prof. Pap.*, No. 260-A, pp. 1- 265.

FALKOWSKI, P.G., 1980. Light-shade adaptation in marine phytoplankton. In, *Primary productivity in the sea*, edited by P.G. Falkowski, Plenum Press, New York, pp. 99-119.

FALKOWSKI, P.G. & Z. DUBINSKY, 1981. Light-shade adaptation of *Stylophora pistillata*, a hermatypic coral from the Gulf of Eilat. *Nature*, Vol. 289, pp. 172-174.

FALKOWSKI, P.G. & T.G. OWENS, 1978. Effects of light intensity on photosynthesis and dark respiration in six species of marine phytoplankton. *Mar. Biol.*, Vol. 45, pp. 289-295.

FALKOWSKI, P.G. & T.G. OWENS, 1980. Light-shade adaptation. *Plant Physiol.*, Vol. 66, pp. 592-595.

FINCKH, A.E., 1904. Biology of the reef forming organisms at Funafuti Atoll. Section VI. In, *The Atoll of Funafuti*, Report of the Coral Reef Committee, Royal Society, London, pp. 125- 150.

FLAJS, G., 1977. Die Ultrastrukturen des Kalkalgenskeletts. *Palaeontographica B*, Vol. 160, pp. 69-128.

FOGG, G.E., 1968. *Photosynthesis*. English Univ. Press, London, 116 pp.

FORWARD, D.F., 1960. Effect of temperature on respiration. In, *Handbuch der Pflanzenphysiologie*, edited by W. Ruhland, Springer-Verlag, Berlin, Vol. 12, pp. 234-258.

FOSLIE, M.H., 1907. No. X. The Lithothamnia. In, *Reports of the Percy Sladen Trust Expedition to the Indian Ocean in 1905*, edited by J.S. Gardiner, *Trans. Linn. Soc. Lond., Ser. 2*, Vol. 12, pp. 177-192.

FRANZISKET, L., 1968. Zur Okologie der Fadenalgen im Skelett lebender Riffkorallen. *Zool. Jahrb. Abt. Allg. Zool. Physiol. Tiere*, Vol. 74, pp. 246-253.

FRENCH, C.S., H.I. KOHN & P.S. TANG, 1934. Temperature characteristics of the metabolism of *Chlorella*. II. The rate of respiration of *Chlorella pyrenoidosa* as a function of time and temperature. *J. Gen. Physiol.*, Vol. 18, pp. 193-207.

FUGITA, D. & T. MASAKI, 1982. Antifouling mechanism in *Lithophyllum yessoense* (*Rhodophyta, Corallinaceae*). *Jpn. J. Phycol.*, Vol. 30, pp. 97.

FURUYA, K., 1960. Biochemical studies on calcareous algae. I. Major inorganic constituents of some calcareous red algae. *Bot. Mag. Tokyo*, No. 73, pp. 355-359.

FUTTERER, D.K., 1977. *Die Feinfraktion (silt) in marinen Sedimenten des ariden Klimbereiches: quantitative Analysenmethoden, Herkunft und Verbreitung.* Habilitationsschrift Fachbereich Mathematik- Naturwissenschaften, Univ. Kiel, 246 pp.

GAINES, A.G. & M.E.Q. PILSON, 1972. Anoxic water in the Pettaquamscutt River. *Limnol. Oceanogr.*, Vol. 17, pp. 42-49.

GARBARY, D.J., 1978. An introduction to the scanning electron microscopy of red algae. In, *Syst. Assoc. Spec.* Vol. 10, pp. 205-222.

GARDINER, J.S., 1903. The fauna and geography of the Maldive & Laccadive Archipelagoes, Vol. I. *Cambridge University Press, Cambridge*, 471 pp.

GARRELS, R.M. & M.E. THOMPSON, 1962. A chemical model for seawater at 25°C and one atmosphere total pressure. *Am. J. Sci.*, Vol. 260, pp. 57-66.

GARRELS, R.M., M.E. THOMPSON & R. SIEVER, 1961. Control of carbonate solubility by carbonate complexes. *Am. J. Sci.*, Vol. 259, pp. 24-45.

GESSNER, F., 1937. Untersuchungen uber Assimilation Atmung Submerser Nasserpflanzen. *Jb. Wiss. Bot.*, Vol. 85, pp. 267-328.

GINSBURG, R.N. & J.H. SCHROEDER, 1973. Growth and submarine fossilization of algal cup reefs, Bermuda. *Sedimentology*, Vol. 20, pp. 575-614.

GLADFELTER, E.H., 1982. Skeletal development in *Acropora cervicornis*. I. Patterns of calcification in the axial corallite. *Coral Reefs*, Vol. 1, pp. 45-51.

GLADFELTER, E.H., 1983. Skeletal development in *Acropora cervicornis*. II. Diel patterns of calcium carbonate accretion. *Coral Reefs*, Vol. 2, pp. 91-100.

GLOCK, W.S., 1923. Algae as limstone makers and climatic indicators. *Am. J. Sci.*, Vol. 6, pp. 377-408.

GORDON, M.S. & H.M. KELLY, 1962. Primary productivity of a Hawaiian coral reef: a critique of flow respirometry in turbulent waters. *Ecology*, Vol. 43, pp. 473-480.

GOREAU, T.F., 1959. The physiology of skeleton formation in corals. I. A method for measuring the rate of calcium deposition by corals under different conditions. *Biol. Bull. (Woods Hole)*, Vol. 116, pp. 59-75.

GOREAU, T.F., 1963. Calcium carbonate deposition by coralline algae and corals in relation to their roles as reef-builders. *Ann. N.Y. Acad. Sci.*, Vol. 109, pp. 127-167.

GOREAU, T.F. & N.I. GOREAU, 1959. The physiology of skeleton formation in corals. II. Calcium deposition by hermatypic corals under various conditions in the reef. *Biol. Bull. (Woods Hole)*, Vol. 117, pp. 239-250.

GOREAU, T.F. & N.I. GOREAU, 1960a. The physiology of skeleton formation in corals. III. Calcification rate as a function of colony weight and total nitrogen content in the reef coral *Manicina areolata* (Linnaeus). *Biol. Bull. (Woods Hole)*, Vol. 118, pp. 419-429.

GOREAU, T.F. & N.I. GOREAU, 1960b. The physiology of skeleton formation in corals. IV. On isotopic equilibrium exchanges of calcium between corallum and environment in living and dead reef building corals. *Biol. Bull. (Woods Hole)*, Vol. 119, pp. 416-427.

GRAHAM, D. & R.M. SMILLIE, 1976. Carbonate dehydratase in marine organisms of the Great Barrier Reef. *Aust. J. Plant. Physiol.*, Vol. 3, pp. 113-119.

GRAUS, R.R., 1977. Investigation of coral growth adaptations using computer modelling. In, *Proc. 3rd Int. Cor. Reef Symp.*, edited by D.L. Taylor, Rosenstiel School of Marine and Atmospheric Science, Univ. Miami, Miami, Florida, Vol. 2, pp. 463-469.

GRAUS, R.R. & I.G. MACINTYRE, 1976. Light control of growth form in colonial corals: computer simulation. *Science*, Vol. 193, pp. 895-897.

GROSS, M.G., J.D. MILLIMAN, J.I. TRACEY Jnr. & H.S. LADD, 1969. Marine geology of Kure and Midway atolls, Hawaii: A preliminary report. *Pac, Sci.*, Vol. 23, pp. 17-25.

HALLDAL, P., 1968. Photosynthetic capacities and photosynthetic action spectra of endozoic algae of the massive coral *Favia. Biol. Bull. (Woods Hole)*, Vol. 134, pp. 411-424.

HARRIS, G.P., 1978. Photosynthesis, productivity and growth: the physiological ecology of phytoplankton. *Arch. Hydrobiol.*, Vol. 10 (suppl.), pp. 1-171.

HAWKINS, C.M. & J.B. LEWIS, 1982. Benthic primary production on a fringing coral reef in Barbados, West Indies. *Aquat. Bot.*, Vol. 12, pp. 355-363.

HOWE, M.A., 1912. The building of 'coral' reefs. *Science*, Vol. 35, pp. 837-842.

HUBBARD, D.K., R.B. BURKE & I.P. GILL, 1986. Styles of reef accretion along a steep, shelf-edge reef, St. Croix, U.S. Virgin Islands. *J. Sed. Petrol.*, Vol. 56, pp. 848-861.

HUMM, H.J., 1956. Rediscovery of *Anadyomene menziesii*, a deep- water alga from the Gulf of Mexico. *Bull. Mar. Sci.*, Vol. 6, pp. 346-348.

HUNTER, I., 1977. Sediment production by *Diadema antillarum* on a Barbados fringing reef. In, *Proc. 3rd Int. Cor. Reef Symp.*, edited by D.L. Taylor, I.G. MacIntyre, F.R. Fosberg, E.A. Shinn & J.I. Tracey, Jr., Rosenstiel School of Atmospheric Science, Univ. Miami, Miami, Florida, pp. 105-110.

IKEMORI, M., 1970. Relation of calcium uptake to photosynthetic activity as a factor controlling calcification in marine algae. *Bot. Mag. Tokyo,* Vol. 83, pp. 152-162.

IKEMORI, M. & K. NISHIDA, 1966. Inorganic carbon source and the inhibition of Diamox on the photosynthesis of the marine alga - *Ulva pertusa. Ann. Rep. Noro. Mar. Lab.*, No. 7, pp. 1-5.

IKEMORI, M. & K. NISHIDA, 1968. Carbonic anhydrase in the marine alga *Ulva pertusa. Physiologia Pl.*, Vol. 21, pp. 292-297.

JASSBY, A.D. & T. PLATT, 1976. Mathematical formulation of the relationship between photosynthesis and light for phytoplankton. *Limnol. Oceanogr.*, Vol. 21, pp. 540-547.

JEFFREY, S.W., 1980. Algal pigment systems. In, *Primary productivity in the sea*, edited by P.G. Falkowski, Plenum Press, New York, London, pp. 33-58.

JEFFREY, S.W. & G.F. HUMPHREY, 1975. New spectrophotometric equations for determining chlorophylls *a*, *b*, c_1, and c_2 in higher plants, algae, and natural phytoplankton. *Biochem. Physiol. Pflanz.*, Vol. 167, pp. 191-194.

JELL, J.S., 1974. The microstructure of some scleractinian corals. In, *Proc. 2nd Int. Cor. Reef Symp., Brisbane*, Great Barrier Reef Committee, Vol. 2, pp. 301-320.

JERLOV, N.G., 1976. *Marine Optics*. Elsevier, Amsterdam, 231 pp.

JITTS, H.R., 1963. The simulated *in situ* measurement of oceanic primary production. *Aust. J. Mar. Freshwater. Res.*, Vol. 14, pp. 139-147.

JOHANSEN, H.W., 1981. *Coralline algae, a first synthesis*. CRC Press, Florida, 239 pp.

JOHNSON, C.R. & K.H. MANN, 1986. The crustose coralline alga, *Phymatolithon* Foslie, inhibits the overgrowth of seaweeds without relying on herbivores. *J. Exp. Mar. Biol. Ecol.*, Vol. 96, pp. 127-146.

JOKIEL, P.L. & J.I. MORRISSEY, 1986. Influence of size on primary production in the reef coral *Pocillopora damicornis* and the macroalga *Acanthophora spicifera*. *Mar. Biol.*, Vol. 91, pp. 15- 26.

KANWISHER, J.W. & S.A. WAINWRIGHT, 1967. Oxygen balance in some reef corals. *Biol. Bull. (Woods Hole)*, Vol. 133, pp. 378-390.

KAWAGUTI, S., 1937. On the physiology of reef corals. I. On the oxygen exchanges of corals. *Palaeo. Trop. Biol. Stn Stud.*, Vol. 1, pp. 187-198.

KAWAGUTI, S. & D. SAKAMUTO, 1948. The effect of light on the calcium deposition of corals. *Bull. Oceanogr. Inst. Taiwan*, No. 4, pp. 65-70.

KETCHUM, B.H. & A.C. REDFIELD, 1949. Some physical and chemical characteristics of algae in mass cultures. *J. Cell. Comp. Physiol.*, Vol. 33, pp. 281-300.

KING, R.J. & W. SCHRAMM, 1976. Photosynthetic rates of benthic marine algae in relation to light intensity and seasonal variations. *Mar. Biol.*, Vol. 37, pp. 215-222.

KINSEY, D.W., 1972. Preliminary observations on community metabolism and primary productivity of the pseudo-atoll reef at One Tree Island, Great barrier Reef. In, *Proceedings of the Symposium on Corals and Coral Reefs*, edited by C. Mukundan & C.S. Gopinadha Pillai, Mar. Biol. Assoc. of India, Cochin, pp. 13-32.

KINSEY, D.W., 1978a. Productivity and calcification estimates using slack-water periods and field enclosures. In, *Coral reefs: research methods*, edited by D.R. Stoddart & R.E. Johannes, UNESCO, Paris, pp. 439-468.

KINSEY, D.W., 1978b. Alkalinity changes and coral reef calcification. *Limnol. Oceanogr.*, Vol. 23, pp. 989-991.

KINSEY, D.W., 1979. Carbon turnover and accumulation by coral reefs. Ph.D. thesis, Univ. Hawaii, Honolulu, 248 pp.

KINSEY, D.W., 1983. Standards of performance in coral reef primary production and carbon turnover. In, *Perspectives on coral reefs*, edited by D.J. Barnes, Australian Institute of Marine Science, Townsville, pp. 209-220.

KINSEY, D.W., 1985. Metabolism, calcification and carbon production. I. System level processes. In, *Proc. 5th Int. Cor. Reef Congr., Tahiti*, edited by C. Gabrie & B. Salvat, pp. 505- 526.

KIRK, J.T.O., 1983. *Light and photosynthesis in aquatic ecosystems*. Cambridge Univ. Press, Cambridge, 401 pp.

KITANO, Y. & D.W. HOOD, 1965. The influence of organic material on the polymorphic crystallization of calcium carbonate. *Geochim. Cosmochim.*, Acta 29, pp. 29-41.

KNUTSON, D.W., R.W. BUDDEMEIER & S.V. SMITH, 1972. Coral chronometers: seasonal growth bands in reef corals. *Science*, Vol. 177, pp. 270-272.

KOHN, A.J. & P. HELFRICH, 1957. Primary organic productivity of a Hawaiian coral reef. *Limnol. Oceanogr.*, Vol. 2, pp. 241-251.

KRUSKAL, W.H. & W.A. WALLIS, 1952. Use of ranks in one-criterion analysis of variance. *J. Am. Stat. Assoc.*, Vol. 47, pp. 583- 621.

LADD, H.S., 1961. Reef building. *Science*, Vol. 134, pp. 703-715.

LAND, L.S. & T.F. GOREAU, 1970. Submarine lithification of Jamaican reefs. *J. Sediment. Petrol.*, Vol. 40, pp. 457-462.

LARKUM, A.W.D., 1983. The primary productivity of plant communities on coral reefs. In, *Perspectives on coral reefs*, edited by D.J. Barnes, Australian Institute of Marine Science, Townsville, pp. 221-230.

LARKUM, A.W.D. & J. BARRET, 1983. Light-harvesting processes in algae. *Adv. Bot. Res.*, Vol. 10, pp. 1-219.

LEE, R.K.S., 1967. Taxonomy and distribution of the melobesioid algae on Rongelap Atoll, Marshall Islands. *Can. J. Bot.*, Vol. 45, pp. 985-1001.

LELETKIN, V.A. & V.I. ZVALINSKI, 1981. Photosynthesis of coral reef zooxanthellae from different depths. In, *The reef and man: Proc. 4th Int. Cor. Reef Symp.*, Manila, edited by E.D. Gomez, C.E. Birkeland, R.W. Buddemeier, R.E. Johannes, J.A. Marsh, Jr. & R.Y. Tsuda, Marine Sciences Centre, Univ. Philippines, Quezon City, Vol. 2, pp. 33-37.

LEWIN, J.C., 1962. Calcification. In, *Physiology and biochemistry of algae*, edited by R.A. Lewin, Academic Press, London, pp. 457-465.

LEWIS, J.B., 1977. Processes of organic production on coral reefs. *Biol. Rev.*, Vol. 52, pp. 305-347.

LI, B.D. & E.A. TITLYANOV, 1981. Adaptations of benthic plants to light. 3. Content of photosynthetic pigments in marine macrophytes from differently illuminated habitats. *Sov. J. Mar. Biol.*, Vol. 4, pp. 597-604.

LI-COR, 1979. *Radiation measurement.* Li-Cor, inc./Li-Cor, Ltd., Lincoln, Nebraska, 6 pp.

LIND, J.V., 1970. *Processes of calcification in the coralline algae.* Ph.D. thesis, Univ. Hawaii, Honolulu, 310 pp.

LITTLER, M.M., 1972. The crustose Corallinaceae. *Oceanogr. Mar. Biol. Annu. Rev.*, Vol. 10, pp. 311-347.

LITTLER, M.M., 1973a. The population and community structure of Hawaiian fringing-reef crustose Corallinaceae (Rhodophyta, Cryptonemiales). *J. Exp. Mar. Biol. Ecol.*, Vol. 11, pp. 103- 120.

LITTLER, M.M., 1973b. The distribution, abundance, and communities of deep-water Hawaiian crustose Corallinaceae (Rhodophyta, Cryptonemiales). *Pac. Sci.*, Vol. 27, pp. 281-289.

LITTLER, M.M., 1973c. The productivity of Hawaiian fringing-reef crustose Corallinaceae and an experimental evaluation of production methodology. *Limnol. Oceanogr.*, Vol. 18, pp. 946- 952.

LITTLER, M.M., 1976. Calcification and its role among the macroalgae. *Micronesica*, Vol. 12, pp. 27-41.

LITTLER, M.M., 1979. The effects of bottle volume, thallus weight, oxygen saturation levels, and water movement on apparent photosynthetic rates in marine algae. *Aquat. Bot.*, Vol. 7, pp. 21-34.

LITTLER, M.M., 1980. Morphological form and photosynthetic performances of marine macroalgae: tests of a functional/form hypothesis. *Bot. Mar.*, Vol. 22, pp. 161-165.

LITTLER, M.M. & M. DOTY, 1975. Ecological components structuring the seaward edges of tropical Pacific reefs: the distribution, communities and productivity of *Porolithon*. *J. Ecol.*, Vol. 63, pp. 117-129.

LITTLER, M.M. & D.S. LITTLER, 1984. Relationships between macroalgal functional-form groups and substrata stability in a subtropical rocky-intertidal system. *J. Exp. Mar. Biol. Ecol.*, Vol. 74, pp. 13-34.

LITTLER, M.M., D.S. LITTLER, S.M. BLAIR & J.N. NORRIS, 1985. Deepest known plant life discovered on an uncharted seamount. *Science*, Vol. 227, pp. 57- 59.

LITTLER, M.M., D.S. LITTLER, S.M. BLAIR & J.N. NORRIS, 1986. Deep-water plant communities from an uncharted seamount off San Salvador Island, Bahamas: distribution, abundance and primary productivity. *Deep-Sea Res.*, Vol. 33, pp. 881-892.

LITTLER, M.M., D.S. LITTLER & P.R. TAYLOR, 1983. Evolutionary strategies in a tropical barrier reef system: functional form groups of marine macroalgae. *J. Phycol.*, Vol. 19, pp. 229-237.

LITTLER, M.M. & S.N. MURRAY, 1974. The primary productivity of marine macrophytes from a rocky intertidal community. *Mar. Biol.*, Vol. 27, pp. 131-135.

LOWRY, O.H., N.J. ROSENBROUGH, A.L. FARR & R. RANDALL, 1951. Protein measurement with the Folin phenol reagent. *J. Biol. Chem.*, Vol. 193, pp. 265-276.

LUCAS, W.J., 1975a. Photosynthetic fixation of ^{14}carbon by internodal cells of *Chara corallina*. *J. Exp. Biol.*, Vol. 26, pp. 331-346.

LUCAS, W.J., 1975b. The influence of light intensity on the activation and operation of the hydroxyl efflux system of *Chara corallina*. *J. Exp. Biol.*, Vol. 26, pp. 347-360.

LUCAS, W.J., 1976. The influence of Ca^{2+} and K^+ on $H^{14}CO_3^-$ influx in internodal cells of *Chara corallina*. *J. Exp. Bot.*, Vol. 27, pp. 32-42.

LUCAS, W.J., 1979. Alkaline band formation in *Chara corallina*. *Plant Physiol.*, Vol. 63, pp. 248-254.

LUCAS, W.J. & F.A. SMITH, 1973. The formation of alkaline and acid regions at the surface of *Chara corallina* cells. *J. Exp. Bot.*, Vol. 24, pp. 1-14.

LYAKIN, Y.I., 1968. Calcium carbonate saturation of Pacific water. *Oceanology (USSR)*, Vol. 8, pp. 44-53.

MacCAULL, W.A. & T. PLATT, 1977. Diel variation in the photosynthetic parameters of coastal marine phytoplankton. *Limnol. Oceanogr.*, Vol. 22, pp. 723-731.

MacINTYRE, I.G. & S.V. SMITH, 1974. X-radiographic studies of skeletal development in coral colonies. *Proc. 2nd Int. Cor. Reef Symp., Brisbane*, Great Barrier Reef Committee, Vol. 2, pp. 277-287.

MARSH, J.A., Jr., 1970. Primary productivity of reef-building calcareous red algae. *Ecology*, Vol. 51, pp. 255-263.

MARSH, J.A., Jr., & S.V. SMITH, 1978. Productivity measurements of coral reefs in flowing waters. In, *Coral reefs: research methods*, edited by D.R. Stoddart & R.E. Johannes, UNESCO, Paris, pp. 361-378.

MASAKI, T., D. FUJITA & H. AKIOKA, 1981. Observation on the spore germination of *Laminaria japonica* on *Lithophyllum yessoense* (Rhodophyta, Corallinaceae) in culture. *Bull. Fac. Fish., Hokkaido Univ.*, Vol. 32, pp. 349-356.

MASAKI, T., D. FUJITA & N.T. HAGEN, 1984. The surface ultrastructure and epithallium shedding of crustose coralline algae in an 'Isoyake' area of southwestern Hokkaido, Japan. *Hydrobiologia*, Vol. 116, pp. 218-223.

MAXWELL, W.G.H., 1968. *Atlas of the Great Barrier Reef.* Elsevier, Amsterdam, 258 pp.

MAXWELL, W.G.H., 1969. The structure and development of the Great Barrier Reef. In, *Stratigraphy and Palaeontology*, edited by K.S.W. Campbell, Australian National Univ. Press, Canberra, pp. 353-374.

McCLOSKEY, L.R., 1970. The dynamics of the community associated with a marine scleractinian coral. *Int. Rev. Gesamten. Hydrobiol.*, Vol. 55, pp. 13-81.

McCLOSKEY, L.R. & L. MUSCATINE, 1984. Production and respiration in the Red Sea coral *Stylophora pistillata* as a function of depth. *Proc. R. Soc. Lond. B*, Vol. 222, pp. 215-230.

McINTYRE, W.G. & R.F. PLATFORD, 1964. Dissolved $CaCO_3$ in the Labrador Sea. *J. Fish. Res. Board Can.*, Vol. 21, pp. 1475-1480.

MILLER, J.P., 1952. A portion of the system calcium carbonate-carbon dioxide-water, with geological implications. *Am. J. Sci.*, Vol. 250, pp. 161-203.

MILLER, L.S. & S.C. HOLT, 1976. Effect of carbon dioxide on regreening in *Synechococcus lividus*. *Ann. Meet. Am. Soc. Microbiol.*, Vol. 76, 1120, pp. 131 (Abstr.).

MILLIMAN, J.D., 1974. *Marine carbonates*, Springer-Verlag, Berlin, 375 pp.

MILLIMAN, J.D., M. GASTNER & J. MULLER, 1971. Utilization of magnesium in coralline algae. *Geol. Soc. Am. Bull.*, Vol. 82, pp. 573-579.

MISONOU, T., M. OKAZAKI & K. NISIZAWA, 1980. Particular Ca- binding substances in marine macro-algae. 1. Uptake of ^{45}Ca by various algae and extraction of the Ca-binding substances. *Jap. J. Phycol.*, Vol. 28, pp. 31-36.

MOBERLY, R., Jr., 1968. Composition of magnesian calcites of algae and pelecypods by electron microprobe analysis. *Sedimentology*, Vol. 11, pp. 61-82.

MUSCATINE, L., 1967. Glycerol excretion by symbiotic algae from corals and *Tridacna* and its control by the host. *Science*, Vol. 156, pp. 516-519.

MYERS, J. & M. CRAMER, 1948. Nitrate reduction and assimilation in *Chlorella*. *J. Gen. Physiol.*, Vol. 32, pp. 103-110.

NEUMANN, A.C., 1966. Observations on coastal erosion in Bermuda and measurements of the boring rate of the sponge *Cliona lampa*. *Limnol. Oceanogr.*, Vol. 2, pp. 92-108.

ODUM, E.P., 1969. The strategy of ecosystem development. *Science*, Vol. 164, pp. 262-270.

ODUM, H.T., R.R. BURKEHOLDER & J. RIVERO, 1960. Measurement of productivity of turtle grass flats, reefs and the Bahia Fosforescente of southern Puerto Rico. *Publ. Inst. Mar. Sci., Univ. Tex.*, Port Aransas, Texas, Vol. 6, pp. 159-170.

ODUM, H.T. & E.P. ODUM, 1955. Trophic structure and productivity of a windward coral reef community on Eniwetok Atoll. *Ecol. Monogr.*, Vol. 25, pp. 291-320.

OGDEN, J.C. & P.S. LOBEL, 1978. The role of herbivorous fishes and urchins in coral reef communities. *Env. Biol. Fish.*, Vol. 3, pp. 49-63.

OKAZAKI, M., 1972. Carbonic anhydrase in the calcareous red alga, *Serraticardia maxima*. *Bot. Mar.*, Vol. 15, pp. 133-138.

OKAZAKI, M., 1977. Some enzymatic properties of Ca^{2+}-dependent adenosine triphosphatase from a calcareous red alga, *Serraticardia maxima*, and its distribution in marine algae. *Bot. Mar.*, Vol. 20, pp. 347-354.

OKAZAKI, M., T. IKAWA, K. FURUYA, K. NISIZAWA & T. MIWA, 1970. Studies on calcium carbonate deposition of a calcareous red alga, *Serraticardia maxima*. *Bot. Mag. Tokyo*, Vol. 83, pp. 193- 201.

OKAZAKI, M. & K. FURUYA, 1985. Mechanisms in algal calcification. *Jpn. J. Phycol.*, Vol. 33, pp. 328-344.

OKAZAKI, M., P. PENTECOST, Y. TANAKA & M. MIYATA, 1986. A study of calcium carbonate deposition in the genus *Padina* (Phaeophyceae, Dictyotales). *Br. Phycol. J.*, Vol. 21, pp. 217- 224.

PAASCHE, E., 1962. Coccolith formation. *Nature*, Vol. 193, pp. 1094-1095.

PAASCHE, E., 1964. A tracer study of the inorganic carbon uptake during coccolith formation and photosynthesis coccolithophorid *Coccolithus huxleyi*. *Physiol. Planta.*, Vol. 17 (Suppl. 3), pp. 5-82.

PAASCHE, E., 1968. Biology and physiology of coccolithophorids. *Annu. Rev. Microbiol.*, Vol. 22, pp. 71-86.

PAASCHE, E., 1969. Light dependent coccolith formation in the two forms of *Coccolithus pelagicus*. *Arch. Mikrobiol.*, Vol. 67, pp. 199-208.

PARK, P.K., 1969. Oceanic CO_2 systems: an evaluation of 10 methods of investigation. *Limnol. Oceanogr.*, Vol. 14, pp. 179- 186.

PARSONS, T. & M., TAKAHASHI, 1973. *Biological oceanographic processes*, Pergamon Press, 186 pp.

PEARSE, V.B., 1972. Radioisotopic study of calcification in the articulated coralline alga *Bossiella orbigniana*. *J. Phycol.*, Vol. 8, pp. 88-97.

PEARSE, V.B. & L. MUSCATINE, 1971. Role of symbiotic algae (zooxanthellae) in coral calcification. *Biol. Bull. (Woods Hole)*, Vol. 141, pp. 350-363.

PENTECOST, A., 1978. Calcification and photosynthesis in *Corallina officinalis* L. using the $^{14}CO_2$ method. *Br. Phycol. J.* Vol. 13, pp. 383-390.

PENTECOST, A., 1980. Calcification in plants. *Int. Rev. Cytol.*, Vol. 62, pp. 1-27.

PERCHOROWICZ, J.T., D.A. RAYNES & R.G. JENSEN, 1981. Light limitation of photosynthesis and activation of ribulose bisphosphate carboxylase in wheat seedlings. *Proc. Natl. Acad. Sci.*, Vol. 78, pp. 2985-2989.

PLATT, T., C.L. GALLEGOS & W.G. HARRISON, 1980. Photoinhibition of photosynthesis in natural assemblages of marine phytoplankton. *J. Mar. Res.*, Vol. 38, pp. 687-701.

PORTER, J.W., 1980. Primary productivity in the sea: reef corals *in situ*. In, *Primary productivity in the sea*, edited by P.G. Falkowski, Plenum Press, New York, pp. 403-410.

PORTER, J.W., L. MUSCATINE, L. DUBINSKY & P.G. FALKOWSKI, 1984. Primary production and photoadaptation in light- and shade-adapted colonies of the symbiotic coral, *Stylophora pistillata*. *Proc. R. Soc. Lond. B*, Vol. 222, pp. 161-180.

PROVASOLI, L., S.H. HUNTER & A. SCHATZ, 1948. Streptomycin induced chlorophyll-less races of *Euglena*. *Proc. Soc. Exp. Biol. Med.*, Vol. 69, pp. 279-282.

PYTKOWICZ, R.M., 1965. Rates of inorganic calcium carbonate nucleation. *J. Geol.*, Vol. 73, pp. 196-199.

PYTKOWICZ, R.M. & G.M. FOWLER, 1967. Solubility of foraminifera in seawater at high pressures. *Geochim. J.*, Vol. 1, pp. 169- 182.

QASIM, S.Z., P.M.A. Bhattathiri & C.V.G. Reddy, 1972. Primary production of an atoll in the Laccadi. *Proc. Am. Philos. Soc.*, Vol. 65, pp. 136-140.

RABINOWITCH, E.I., 1951. *Photosynthesis and related processes. Vol. II. Pt. I. Spectroscopy and fluorescence of photosynthetic pigments; kinetics of photosynthesis*. Interscience Publications, New York, 1208 pp.

RAMUS, J., S.I. BEALE & D. MAUZERALL, 1976. Correlation of changes in pigment content with photosynthetic capacity of seaweeds as a function of water depth. *Mar. Biol.*, Vol. 37, pp. 231-238.

RAMUS, J. & J.P. VAN der MEER, 1983. A physiological test of the theory of complementary chromatic adaptation. I. Colour mutants of a red seaweed. *J. Phycol.*, Vol. 19, pp. 86-91.

RAVEN, J.A. & S.M. GLIDEWELL, 1975. Photosynthesis, respiration and growth in the shade alga *Hydrodictyon africanum*. *Photosynthetica* Vol. 9, pp. 361-377.

RAVEN, J.A. & F.A. SMITH, 1977. "Sun" and "shade" species of green algae: relation of cell size and environment. *Photosynthetica*, Vol. 11, pp. 48-35.

REVELLE, R. & R.W. FAIRBRIDIGE, 1957. Carbonates and carbon dioxide. *Geol. Soc. Am. Mem.* No. 67, pp. 239-295.

RYTHER, J.H., 1956. The measurement of primary production. *Limnol. Oceanogr.*, Vol. 1, pp. 72-84.

SARGENT, M.C. & T.S. AUSTIN, 1949. Organic productivity of an atoll. *Trans. Am. Geophys. Union*, Vol. 30, pp. 245-249.

SARGENT, M.C. & T.S. AUSTIN, 1954. Biologic economy of coral reefs. *Geol. Surv (U.S.) Prof. Pap.*, No. 260-E, pp. 293-300.

SCHMALZ, R.F. & K.E. CHAVE, 1963. Calcium carbonate: factors affecting saturation in ocean waters off Bermuda. *Science*, Vol. 139, pp. 1206-1207.

SCHMALZ, R.F. & F.J. SWANSON, 1969. Diurnal variations in the carbonate saturation of seawater. *J. Sed. Petrol.*, Vol. 39, pp. 255-267.

SCOTT, B.D. & H.R. JITTS, 1977. Photosynthesis of phytoplankton and zooxanthellae on a coral reef. *Mar. Biol.*, Vol. 41, pp. 307-315.

SETCHELL, W.A., 1926. Phytogeographical notes on Tahiti. II. Marine vegetation. *Univ. Calif. Publ. Bot.*, Vol. 12, pp. 291- 324.

SETCHELL, W.A., 1930. Biotic cementation in coral reefs. *Proc. Natl. Acad. Sci.*, Vol. 16, pp. 781

SHEVEIKO, S.V., 1981. Life forms of coralline algae as an environmental indicator on reefs. *Proc. 4th Int. Cor. Reef. Symp., Manila*, edited by E.D. Gomez, C.E. Birkeland, R.W. Buddemeier, R.E. Johannes, J.A. Marsh, Jr. & R.Y. Tsuda, Marine Sciences Centre, Univ. Philippines, Quezon City, Vol. 2, pp. 461 (Abstr.).

SIMKISS, K., 1964a. Phosphates as crystal poisons of calcification. *Biol. Rev.*, Vol. 39, pp. 487-505.

SIMKISS, K., 1964b. The inhibitory effects of some metabolites on the precipitation of calcium carbonate from artificial and natural seawater. *J. Cons. Int. Explor. Mer*, Vol. 29, pp. 6-18.

SKIRROW, G., 1975. The dissolved gases - carbon dioxide. In, *Chemical oceanography, Vol. 2*, edited by J.P. Riley & G. Skirrow, Academic Press, London, pp. 1-192.

SMITH, G.M., 1951. *Manual of phycology*, Chronica Botanica, Waltham, Mass., 375 pp.

SMITH, S.V., 1973. Carbon dioxide dynamics: a record of organic carbon production, respiration, ans calcification in the Eniwetok reef flat community. *Limnol. Oceanogr.*, Vol. 18, pp. 106-120.

SMITH, S.V., 1981. The Houtman Abrolhos Islands: carbon metabolism of coral reefs at high latitude. *Limnol. Oceanogr.*, Vol. 26, pp. 612-621.

SMITH, S.V., 1983. Coral reef calcification. In, *Perspectives on coral reefs*, edited by D.J. Barnes, Australian Institute of Marine Science, Townsville, pp. 240-247.

SMITH, S.V. & G.S. KEY, 1975. Carbon dioxide and metabolism in marine environments. *Limnol. Oceanogr.*, Vol. 20, pp. 493-495.

SMITH, S.V. & D.W. KINSEY, 1976. Calcium carbonate production, coral reef growth, and sea level change. *Science*, Vol. 194, pp. 937-939.

SMITH, S.V. & D.W. KINSEY, 1978. Calcification and organic carbon metabolism as indicated by carbon dioxide. In, *Coral reefs: research methods*, edited by D.R. Stoddart & R.E. Johannes, UNESCO, Paris, pp. 469-484.

SMITH, A.D. & A.A. ROTH, 1979. Effect of carbon dioxide concentration on calcification in the red coralline alga *Bossiella orbigniana*. *Mar. Biol.*, Vol. 52, pp. 217-225.

SOKAL, R.R. & F.J. ROHLF, 1981. *Biometry*. W.H. Freeman & Company, San Francisco, 776 pp.

SOURNIA, A., 1976. Oxygen metabolism of a fringing reef in French Polynesia. *Helgol. Wiss. Meeresunters*, Vol. 28, pp. 401-410.

SPEAR, D.G., J.K. BARR & C.E. BARR, 1969. Localization of hydrogen ion and chloride ion fluxes in *Nitella*. *J. Gen. Physiol.*, Vol. 54, pp. 397-414.

STARK, L.M., L. ALMODOVAR & R.W. KRAUSS, 1969. Factors affecting the rate of calcification in *Halimeda opuntia* (L.) Lamouroux and *Halimeda discoidea* Descaisne. *J. Phycol.*, Vol. 5, pp. 305-312.

STEARN, C.W., T.P. Scoffin & W. Martindale, 1977. Calcium carbonate budget of a fringing reef on the west coast of Barbados. I - Zonation and productivity. *Bull. Mar. Sci.*, Vol. 27, pp. 479-510.

STEEMANN NIELSEN, E., 1947. Photosynthesis of aquatic plants with special reference to the carbon-sources. *Dan. Bot. Ark.*, Vol. 12(8), pp. 1-71.

STEEMANN NIELSEN, E., 1975. *Marine photosynthesis with special emphasis on the ecological aspects*. Elsevier Scientific Publishing Company, Amsterdam, 141 pp.

STENECK, R.S. & W.H. ADEY, 1976. The role of environment in control of morphology in *Lithophyllum congestum*, a Caribbean algal ridge builder. *Bot. Mar.*, Vol. 19, pp. 197-215.

STODDART, D.R., 1969. Ecology and morphology of recent coral reefs. *Biol. Rev.*, Vol. 44, pp. 433-498.

STRICKLAND, J.D.H., 1960. Measuring the production of marine phytoplankton. *J. Fish. Res. Board Can. Bull.*, No. 122, 172 pp.

STRICKLAND, J.D.H. & T.R. PARSONS, 1972. A practical handbook of seawater analysis. *Bull. Fish. Res. Board Can.*, No. 167, 310 pp.

SUESS, E. & D. FUTTERER, 1972. Aragonitic ooids: experimental precipitation from seawater in the presence of humic acid. *Sedimentology*, Vol. 19, pp. 129-139.

TALLING, J.F., 1957. Photosynthetic characteristics of some freshwater diatoms in relation to underwater radiation. *New Phytol.*, Vol. 56, pp. 29-50.

TALLING, J.F., 1961. Photosynthesis under natural conditions. *Annu. Rev. Plant Physiol.*, Vol. 12, pp. 133-154.

TAYLOR, D.L., 1973. Symbiotic pathways of carbon in coral reef ecosystems. *Helgol. Wiss. Meeresunters.*, Vol. 24, pp. 276-283.

TAYLOR, W.R., 1950. *Plants of Bikini and other northern Marshall Islands.* Univ. Mich. Stud. Scient. Ser. No. 18, 227 pp.

TITLYANOV, E.A., 1981. Adaptation of reef-building corals to low light intensity. In, *The reef and man: Proc. 4th Int. Cor. Reef Symp., Manila, 1981*, edited by E.D. Gomez, C.E. Birkeland, R.W. Buddemeier, R.E. Johannes, J.A. Marsh, Jr. & R.Y. Tsuda, Marine Sciences Centre, Univ. Philippines, Quezon City, Vol. 2, pp. 39-43.

TRACEY, J.I., Jr., H.S. LADD & J.E. HOFFMEISTER, 1948. Reefs of Bikini, Marshall Islands. *Bull. Geol. Soc. Am.*, Vol. 59, pp. 861-878.

VAN den HOEK, C., 1969. Algal vegetation types along the open coasts of Curacao, Netherlands Antilles. I & II. *Proc. K. Ned. Akad. Wet. Ser. C*, Vol. 72, pp. 537-577.

VAN den HOEK, C., A.M. CORTEL-BREEMAN & J.B.W. WANDERS, 1975. Algal zonation in the fringing coral reef of Curacao, Netherlands Antilles, in relation to the zonation of corals and gorgonians. *Aquat. Bot.*, Vol. 1, pp. 269-308.

VAN den HOEK, C., A.M. CORTEL-BREEMAN, R.P.M. BAK & G. VAN BUURT, 1978. The distribution of algae, corals and gorgonians in relation to depth, light attenuation, water movement and grazing pressure in the fringing coral reef of Curacao, Netherlands Antilles. *Aquat. Bot.*, Vol. 5, pp. 1-46.

VANDERMUELEN, J.H., N.D. DAVIS & L. MUSCATINE, 1972. The effect of inhibitors of photosynthesis on zooxanthellae in corals and other marine invertebrates. *Mar. Biol.*, Vol. 16, pp. 185-191.

VINOGRADOV, A.P., 1953. *The elementary chemical composition of marine organisms.* Sears Found. Mar. Res., Mem. 2, 647 pp.

VOOREN, C.M., 1981. Photosynthetic rates of benthic algae from the deep coral reef of Curacao. *Aquat. Bot.*, Vol. 10, pp. 143- 159.

WAINWRIGHT, S.A., 1963. Skeletal organisation in the coral *Pocillopora damicornis. Q. J. Microsc. Sci.*, Vol. 104, pp. 169- 183.

WANDERS, J.B.W., 1976. The role of benthic algae in the shallow reef of Curacao (Netherlands Antilles). I. Primary productivity in the coral reef. *Aquat. Bot.*, Vol. 2, pp. 235-270.

WANDERS, J.B.W., 1977. The role of benthic algae in the shallow reef of Curacao (Netherlands Antilles). III. The significance of grazing. *Aquat. Bot.* , Vol. 3, pp. 357-390.

WATTENBERG, H. & E. TIMMERMAN, 1936. Uber die Sattigung des Seewassers an $CaCO_3$. *Ann. Hydrogr. Mar. Meteorol.*, Vol. 64, pp. 23-31.

WEBER, J.N. & J.W. KAUFMAN, 1965. Brucite in the calcareous alga *Goniolithon*. *Science*, Vol. 149, pp. 996-997.

WEBER, J.N., P. DEINES, E.W. WHITE & P.H. WEBER, 1975. Seasonal high and low density bands in reef coral skeletons. *Nature*, Vol. 255, pp. 697.

WETHEY, D.S. & J.W. PORTER, 1976a. Sun and shade differences in productivity of reef corals. *Nature*, Vol. 262, pp. 281-282.

WETHEY, D.S. & J.W. PORTER, 1976b. Habitat-related patterns of productivity of the foliaceous reef coral, *Pavona praetorta* Dana. In, *Coelenterate ecology and behaviour*, edited by G.O. Mackie, Plenum Publishing, New York, pp. 59-66.

WEYL, P.K., 1961. The carbonate saturometer. *J. Geol.*, Vol. 69, pp. 32-44.

WOELKERLING, Wm.J., 1987. The status and disposition of *Paragoniolithon* (Corallinaceae, Rhodophyta). *Phycologia*, Vol. 26, pp. 144-148.

WOLKEN, J.J., 1956. Molecular morphology of *Euglena gracilis* var. *bacillaris*. *J. Protozool.*, Vol. 3, pp. 211-221.

WRAY, J.L., 1971. Algae in reefs through time. *Proc. North Am. Paleont. Conv.*, Part J, pp. 1358-1373.

YONGE, C.M., 1963. The biology of coral reefs. *Adv. Mar. Biol.*, Vol. 1, pp. 209-260.

ZVALINSKI, V.I., V.A. LELETKIN, E.A. TITLYANOV & M.G. SHAPOSHNIKOVA, 1980. Photosynthesis and adaptation of corals to irradiance. 2. Oxygen exchange. *Photosynthetica*, Vol. 14, pp. 422-430.

Appendix 1. Mean (x) chlorophyll *a* contents of different species of crustose coralline algae, including endolithic fractions, and mean chlorophyll *a* content of endolithic algae remaining after removal of overlying coralline tissue. Confidence intervals (CI) are provided at the 95% probability level.

Species	Depth m	*n*	Total Chlorophyll *a* ug cm-2 (proj. area) x	CI
P. onkodes	0	6	22.4	± 10.3
N. fosliei	0	4	43.4	± 8.1
H. reinboldii	0	5	16.3	± 4.7
P. conicum	0	5	33.4	± 8.9
Endolithic sp.	0	4	18.8	± 11.6

Appendix 2. Protein content of individual specimens of different species of crustose coralline algae from different depths. Mean values (x) are included.

Depth m	Specimen No.	*P. onkodes*	*N. fosliei*	*H. reinboldii*	*P. conicum*
		g protein^{-1} m^{-2}(real surface area)			
	1	7.960	7.541		2.298
	2	7.183	7.387		3.768
0	3	4.080	6.873		2.800
	4	7.310	6.452		2.367
	5	4.037			
	x	6.11	7.06		2.81
	1		5.443	3.010	
3	2		4.799	4.575	
	3		2.877	3.634	
	4		2.842	4.946	
	x		3.99	4.04	
	1	4.876	1.420	3.043	2.024
6	2	5.121	1.571	3.865	1.667
	3	3.673	2.180	2.113	1.552
	4	7.704	3.414	2.256	0.951
	x	5.34	2.15	2.82	1.55
	1				2.048
18	2				2.665
	3				1.703
	4				3.361
	x				2.44